



Universitat Autònoma de Barcelona

ADVERTIMENT. L'accés als continguts d'aquesta tesi queda condicionat a l'acceptació de les condicions d'ús establertes per la següent llicència Creative Commons:  http://cat.creativecommons.org/?page_id=184

ADVERTENCIA. El acceso a los contenidos de esta tesis queda condicionado a la aceptación de las condiciones de uso establecidas por la siguiente licencia Creative Commons:  <http://es.creativecommons.org/blog/licencias/>

WARNING. The access to the contents of this doctoral thesis it is limited to the acceptance of the use conditions set by the following Creative Commons license:  <https://creativecommons.org/licenses/?lang=en>

Urine recycling technologies for a circular future within and beyond terrestrial boundaries

Ir. Jolien De Paepe

Supervisors: Prof. dr. ir. Korneel Rabaey
Prof. dr. ir. Siegfried E. Vlaeminck
Dr. ir. Peter Clauwaert
Prof. dr. Francesc Gòdia Casablanca

Thesis submitted in fulfillment of the requirements for the degree of
Doctor in Bioscience engineering (Ghent University)

Thesis submitted in fulfillment of the requirements for the degree of
Doctor in Biotechnology (Universitat Autònoma de Barcelona)

2020

Promotors:

- Prof. dr. ir. Korneel Rabaey
Center for Microbial Ecology and Technology (CMET)
Department of Biotechnology
Faculty of Bioscience Engineering, Ghent University, Belgium
- Prof. dr. ir. Siegfried E. Vlaeminck
Research group of Sustainable Energy, Air and Water Technology
Department of Bioscience engineering
Faculty of Sciences, University of Antwerp, Belgium
- Dr. ir. Peter Clauwaert
Center for Microbial Ecology and Technology (CMET)
Department of Biotechnology
Faculty of Bioscience Engineering, Ghent University, Belgium
- Prof. dr. Francesc Gòdia Casablanca
Department of Chemical, Biological and Environmental Engineering
School of Engineering, Universitat Autònoma de Barcelona, Spain

Members of the reading committee (International Doctoral Research Component UAB):

- Prof. dr. Mathieu Spérandio
National Institute of Applied Sciences (INSA) of Toulouse, France
- Prof.hon. Max Mergeay
ULB, SCK-CEN, Director of the MELiSSA Foundation

Members of the examination committee:

- Prof. dr. ir. Monica Höfte (Chair)
Department of Crop Protection
Faculty of Bioscience Engineering, Ghent University, Belgium
- Prof. dr. ir. Arne Verliefde
Department of Green Chemistry and Technology
Faculty of Bioscience Engineering, Ghent University, Belgium
- Prof. dr. ir. Eveline Volcke
Department of Green Chemistry and Technology
Faculty of Bioscience Engineering, Ghent University, Ghent, Belgium
- Prof. dr. ir. Albert Guisasola
Department of Chemical, Biological and Environmental Engineering
School of Engineering, Universitat Autònoma de Barcelona, Spain
- Dr. Christophe Lasseur
European Space Research and Technology Centre (ESA-ESTEC),
The Netherlands
- Prof. dr. ir. Kai Udert
Department of Process Engineering, Eawag, Switzerland

Dean Faculty of Bioscience Engineering: Prof. dr. ir. Marc Van Meirvenne

Rector of Ghent University: Prof. dr. ir. Rik Van de Walle

Notation Index

AEM	Anion Exchange Membrane
AMO	Ammonia Mono-oxygenase
AOB	Ammonium Oxidizing Bacteria
AS	Activated Sludge
ATP	Adenosine Triphosphate
BES	Bio-electrochemical System
BPM	Bipolar Membrane
CE	Coulombic efficiency
CEM	Cation Exchange Membrane
CELSS	Controlled Ecological Life Support System
COD	Chemical Oxygen Demand
CR	Cultivation Reactor
CSTR	Continuous Stirred Tank Reactor
DNA	Deoxyribonucleic Acid
DO	Dissolved Oxygen
DW	Dry weight
EC	Electrical Conductivity [$mS\ cm^{-1}$]
ECLSS	Environmental Control and Life Support System
ED	Electrodialysis
ESA	European Space Agency
EVA	Extra Vehicular Activity
FA	Free Ammonia
FAO	Food and Agriculture Organization
FN	Full nitrification
FNA	Free Nitrous Acid
FO	Forward Osmosis
HAO	Hydroxylamine Oxidoreductase
HAP	Hydroxyapatite
HF	Hollow fiber
HOB	Hydrogen Oxidizing Bacteria
HRT	Hydraulic Retention Time
IE	Inhabitant Equivalent
IEM	Ion Exchange Membrane
ISECG	International Space Exploration Coordination Group

ISRU	In-situ Resource Utilization
ISS	International Space Station
LCD	Limiting Current Density
LEO	Low Earth Orbit
LSS	Life Support System
MABR	Membrane Aerated Biofilm Reactor
MBR	Membrane Bioreactor
MBBR	Moving Bed Biofilm Reactor
MEC	Microbial Electrolysis Cell
MELiSSA	Micro-Ecological Life Support System Alternative
MFC	Microbial Fuel Cell
MP	Microbial Protein
NASA	National Aeronautics and Space Administration
NCBI	National Center for Biotechnology Information
NF	Nanofiltration
NOB	Nitrite Oxidizing Bacteria
NOD	Nitrogenous oxygen demand
NOR	Nitrite Oxidoreductase
NU	Nitrified Urine
OD	Optical Density
OTU	Operational Taxonomic Unit
PBR	Photobioreactor
PCoA	Principle Coordinate Analysis
PLC	Programmable Logic Controller
pK_a	Acid Dissociation Constant
PN	Partial Nitrification
PR	Pilot Reactor
PVA	Polyvinyl Alcohol
qPCR	Quantitative Polymerase Chain Reaction
RE	Removal Efficiency
RLSS	Regenerative Life Support System
RNA	Ribonucleic Acid
rRNA	Ribosomal Ribonucleic Acid
RO	Reverse Osmosis
SBR	Sequencing Batch Reactor
SD	Standard Deviation
SDG	Sustainable Development Goal
SRT	Sludge Retention Time
SI	Supplementary Information
TAN	Total Ammonia Nitrogen
TIC	Total Inorganic Carbon

TKN	Total Kjeldahl Nitrogen
TMCS	Transmembrane Chemisorption
TN	Total Nitrogen
TRL	Technology Readiness Level
TSS	Total Suspended Solids
qPCR	Quantitative Polymerase Chain Reaction
OLAND	Oxygen-Limited Autotrophic Nitrification and Denitrification
OTU	Operational Taxonomic Unit
UDDT	Urine Diversion Dehydration Toilet
UF	Ultrafiltration
UPA	Urine Processor Assembly
VCD	Vapor Compression Distillation
VFA	Volatile Fatty Acid
VSS	Volatile Suspended Solids
WHO	World Health Organization
WWTP	Wastewater Treatment Plant
XRD	X-ray Diffraction
XRF	X-ray Fluorescence
ZM	Zarrouk Medium

Contents

Notation Index	i
Abstract	1
Samenvatting	5
1 Introduction	9
1.1 (Extra)terrestrial life	10
1.1.1 Artificial life support systems sustain life in space	10
1.1.2 The natural biosphere sustains life on Earth	13
1.2 Urine, a valuable nutrient resource	18
1.2.1 Urine as an alternative resource for fertilizer production on Earth	18
1.2.2 Urine recycling is of key interest in space life support systems	21
1.3 Urine source separation & treatment	22
1.3.1 Urine diverting toilets	22
1.3.2 Urine characteristics	23
1.3.3 Urine treatment	24
1.4 Urine recycling technologies	34
1.4.1 Nitrification and biological COD oxidation	34
1.4.2 (Bio)-electrochemical methods	40
1.4.3 Valorization of urine-derived products	42
1.5 Research outline	44
2 Refinery and concentration of nutrients from urine with electrodialysis enabled by upstream precipitation and nitrification	47
2.1 Introduction	49
2.2 Materials and methods	51
2.2.1 Automated treatment train	51
2.2.2 Operation	55
2.2.3 Nitrification batch activity tests at different salinities	56
2.2.4 ED batch phosphate transport experiment	58
2.2.5 Analytical methods	58
2.2.6 Microbial community analysis	58
2.3 Results	59
2.3.1 Precipitation on a 20% urine solution	59
2.3.2 Nitrification bioreactor	59
2.3.3 Electrodialysis	65
2.4 Discussion	69

2.4.1	Precipitation and nitrification minimize scaling and biofouling in ED	69
2.4.2	Nitrification and COD oxidation remained unaffected at a decreased urine dilution	70
2.4.3	Shifts in microbial community composition parallel shifts in influent composition	70
2.4.4	Lowering the urine dilution leads to a higher recovery efficiency but a lower concentration factor in ED	71
2.4.5	Strategies to increase nutrient recovery efficiencies	71
2.4.6	Resource reuse possibilities for precipitate, ED concentrate and ED diluate	72
2.5	Conclusion	74
2.6	Supplementary information	75
2.6.1	Supplementary materials and methods	75
2.6.2	Supplementary tables and figures	77
2.7	Acknowledgements	90
3	Bio-electrochemical COD removal for energy-efficient, maximum and robust nitrogen recovery from urine through membrane aerated nitrification	91
3.1	Introduction	93
3.2	Materials and methods	95
3.2.1	Experimental setup	95
3.2.2	Reactor operation	96
3.2.3	Analytical methods	98
3.2.4	Microbial community analysis	100
3.3	Results	101
3.3.1	COD removal, current production, coulombic efficiency and urea hydrolysis in the MEC	101
3.3.2	Nitrification and COD removal in MABR	104
3.3.3	Microbial community composition of MEC and MABR	107
3.4	Discussion	110
3.4.1	The MEC reached high COD removal efficiencies, yet converted only 25-45% of the removed COD to current	110
3.4.2	Upstream bio-anodic COD oxidation effectively prevented denitrification in the MABR	111
3.4.3	Both MEC and MABR showed robustness against fluctuating loading rates and operational conditions	112
3.4.4	MEC-MABR integration not only prevents N losses but also reduces the overall oxygen demand, increases the alkalinity and enables energy efficient COD removal	112
3.4.5	Closing the nitrogen cycle on Earth and in space	113
3.5	Conclusion	114
3.6	Supplementary information	115

3.6.1	MABR setup and operation	115
3.6.2	MEC: influent and effluent composition	116
3.6.3	MEC: COD and TAN concentration in influent and effluent	118
3.6.4	Electron balance	120
3.6.5	MABR: influent and effluent composition	121
3.6.6	Time profile of MABR N and COD load/loading	123
3.6.7	Nitrification activity test	124
3.6.8	Microbial community composition of MEC	125
3.6.9	Microbial community composition of MABR	130
3.6.10	Literature overview of bio-electrochemical systems on real human urine	134
3.7	Acknowledgements	135
4	Electrochemically induced alkalization enables fresh urine stabilization and facilitates source separation	137
4.1	Introduction	139
4.2	Materials and methods	141
4.2.1	Urine collection	141
4.2.2	Electrochemical cell and crystallizer	141
4.2.3	Experimental protocol	142
4.2.4	Assessment of urine stabilization	143
4.2.5	Analytical methods	143
4.3	Results and discussion	144
4.3.1	Configuration specific electromigration	144
4.3.2	pH profile in the crystallizer	146
4.3.3	Precipitation of divalent cations at high pH	147
4.3.4	Urine long-term stabilization	149
4.3.5	Phosphorus recovery from precipitates	151
4.3.6	Implementation & application of electrochemical urine precipitation and stabilization	151
4.4	Supplementary information	154
4.4.1	Experimental setup	154
4.4.2	Electromigration	157
4.4.3	Electric charge and electrode energy consumption	161
4.4.4	Divalent cation removal	163
4.4.5	Long-term stabilization	165
4.4.6	Phosphate removal	166
4.5	Acknowledgements	167
5	Electrochemical in-situ pH control enables chemical-free full urine nitrification with concomitant nitrate extraction	169
5.1	Introduction	171
5.2	Materials and methods	173

5.2.1	Experimental setup	173
5.2.2	Urine collection and alkalization	174
5.2.3	Reactor operation	176
5.2.4	Analytical methods	179
5.3	Results and discussion	180
5.3.1	Two-step urine stabilization: alkalization and subsequent nitrification	180
5.3.2	The extent of nitrification (NO_3^- -N/TAN ratio in the effluent) increases as a function of the influent alkalinity	180
5.3.3	Electrochemical hydroxide production enables full nitrification by dynamically compensating for the associated acidification	182
5.3.4	Configuration 1 enables full nitrate recovery	186
5.3.5	Configuration 2 enables anion extraction and concentration in the middle compartment	187
5.3.6	Configuration 3 enables anion and cation extraction and concentration in the middle compartment	190
5.3.7	COD removal eliminates the risk for downstream biofouling	190
5.3.8	Application of electrochemical in-situ pH control and extraction	191
5.4	Conclusions	193
5.5	Supplementary information	194
5.5.1	Experimental setup and operation	194
5.5.2	Partial nitrification without pH control (PN)	198
5.5.3	Full nitrification with NaOH addition	202
5.5.4	Full nitrification with electrochemical hydroxide addition	206
5.6	Acknowledgements	216
6	Limited supplementation maximizes nitrogen recovery from nitrified urine through continuous cultivation of microalgae	217
6.1	Introduction	219
6.2	Materials and methods	221
6.2.1	Urine pre-treatment through alkalization and biostabilization	221
6.2.2	Batch culture experiments	222
6.2.3	Cultivation in a continuous photobioreactor	224
6.2.4	Analytical methods	224
6.3	Results and discussion	226
6.3.1	Urine dilution is essential to obtain high N conversion efficiencies	226
6.3.2	Nitrified urine sustains <i>Limnospira</i> biomass production, but growth stagnates earlier than on modified Zarrouk medium	227
6.3.3	Supplementing nitrified urine can yield the same biomass production and N uptake as modified Zarrouk medium	230
6.3.4	Identifying the limiting element(s) for <i>Limnospira</i> growth in nitrified urine	230

6.3.5	Long-term continuous <i>Limnospira</i> cultivation in a photobioreactor confirmed the application potential of supplemented nitrified urine as a culture medium	233
6.3.6	Overall concept	234
6.4	Conclusions	237
6.5	Supplementary information	237
6.5.1	Literature overview	237
6.5.2	Supplementary materials and methods	241
6.5.3	Preliminary batch culture experiment with modified Zarrouk medium	241
6.5.4	Optimization of the nitrified urine-based culture medium	242
6.6	Acknowledgements	246
7	General discussion & perspectives	247
7.1	Main research outcomes	248
7.2	Strengths, challenges and potential bottlenecks for technology development and implementation	253
7.2.1	Strengths	253
7.2.2	Practical considerations and potential bottlenecks	255
7.3	On a mission to Mars	260
7.3.1	Optimal urine treatment train	260
7.3.2	Design of a urine treatment train for deep-space missions	263
7.3.3	Readiness towards space	266
7.4	Implementation of urine recycling on Earth	267
7.4.1	Optimal urine treatment train	267
7.4.2	Design of a urine treatment train	268
7.4.3	Barriers for terrestrial urine recycling	269
7.5	Outlook	270
7.5.1	'A journey of a thousand miles begins with a single step' - Chinese proverb	270
7.5.2	Urine source separation can contribute to a more sustainable, circular future on Earth	270
	References	273
	Copyright attribution	286
	Curriculum Vitae	289

Abstract

Human presence in outer space is currently supported by a regular resupply of life support consumables from Earth. Deep-space exploration or space habitation will, however, depend on regenerative life support systems (RLSS) for in-situ oxygen, water and food production and waste management as resupply becomes practically impossible due to the long distance. Urine recycling is of key interest in RLSS to recover water and macro-/micronutrients, which can serve as a fertilizer for plants and microalgae.

Urine source separation and recycling also gains attention on Earth to close and/or shorten the terrestrial nutrient cycles, which play a pivotal role in our food supply, but are currently pushed to their planetary boundaries by extensive synthetic fertilizer production and use. Nutrient recovery from waste streams could i) reduce the need for energy intensive ammonia production using the Haber-Bosch process and mining of non-renewable phosphorus and potassium, and ii) obviate the need for advanced nutrient removal to protect the environment. Amongst other streams, urine is targeted, as it presents the major nutrient source in domestic wastewater and has good fertilizing properties (i.e., contains all macro- and micronutrients required for plant growth). Other benefits stemming from urine source separation and recycling include the reduced water consumption for flushing and the decreased nutrient load and better effluent quality of wastewater treatment plants.

The goal of this PhD thesis was to develop resource-efficient urine recycling technologies that i) can be implemented in RLSS, such as the Micro-Ecological Life Support System Alternative (MELiSSA) from the European Space Agency (ESA) or, ii) used for on-site/decentralized urine treatment on Earth. As resources are scarce in space, the goal was to achieve maximum nutrient recovery with minimum energy expenditure and use of consumables in order to reduce payloads and to minimize the need for resupply. Different urine treatment trains combining biological and physicochemical processes were investigated.

Urine contains many valuable compounds, but the compositional complexity and instability of urine presents a challenge for urine collection, treatment and reuse. Urea, the main nitrogen compound in urine, quickly hydrolyses into ammonia, ammonium and (bi)carbonate, causing nutrient losses, odor nuisance, scaling and clogging by uncontrolled precipitation, and ammonia volatilization. The latter can pose a health risk to the crew in a small space cabin, as ammonia is a toxic gas. Clogging of pipes by the precipitating salts is a common problem in nonwater urinals and urine-diverting toilets, and it is believed to be one of the major barriers for the widespread implementation

of source separation. Therefore, an alkalization step was included to prevent urea hydrolysis during collection and storage and to remove calcium and magnesium by controlled precipitation, thereby minimizing the risk for scaling in the following treatment steps. In Chapter 2 and 3, sodium hydroxide was used to increase the pH of fresh urine, whereas Chapter 4 investigated the use of an electrochemical cell to avoid base consumption, the logistics associated with base storage and dosing, and the associated increase in salinity. Sodium hydroxide addition or electrochemical OH^- addition both yielded $\sim 80\text{-}90\%$ of calcium and magnesium removal. About $\sim 30\%$ to $\sim 80\%$ of the phosphate was captured in the precipitates, which could be valorized as a slow-release P fertilizer in agriculture or as a resource for the phosphate industry. Alkalization, followed by nitrification, also proved to be an effective strategy to safeguard the downstream units from excessive scaling. The alkalized urine could be stored for several months without urea hydrolysis. Yet, urine is only temporarily stabilized by increasing the pH and still contains i) urea, which can easily hydrolyze when the pH is lowered or urease is added, and ii) biodegradable organics, which can cause biofouling. Therefore, the urine was further processed using bacteria, oxidizing COD and urea into CO_2 and nitrate.

Chapter 3 evaluated COD removal in a microbial electrolysis cell (MEC). Up to 85% of the COD was removed at a COD loading rate of $\sim 30 \text{ g COD m}^{-2} \text{ d}^{-1}$ in the MEC, which was dominated by (strictly) anaerobic genera, such as *Geobacter* (electroactive bacteria), *Thiopseudomonas*, a *Lentimicrobiaceae* member, *Alcaligenes* and *Proteiniphilum*. Electroactive bacteria transferred the electrons obtained by COD oxidation to the anode, generating an electric current of 0.5 and 2 A m^{-2} , which was about 27-46% of the current that was expected based on the observed COD removal. Apart from COD removal, urea hydrolysis took place in the MEC, increasing the TAN/TN ratio from $<10\%$ (influent) to $\sim 100\%$ (effluent). Overall, MEC treatment reduces the oxygen demand and limits biomass production in subsequent aerobic treatment, increases the urine alkalinity and can convert the chemical energy contained in organics into electrical energy.

Nitrification was applied to convert instable urea and/or volatile and toxic TAN into non-volatile nitrate in Chapter 2, 3 and 5. Besides nitrification, treatment in the aerobic bioreactor yielded $\sim 90\%$ COD removal in Chapter 2 and 5, whereas almost all biodegradable COD had been removed by a MEC prior to nitrification in Chapter 3. Three different reactors were employed: a pilot scale MBBR (Chapter 2), a bench scale MABR (Chapter 3) and a bench scale MBBR (Chapter 5). MABR reactors have a high oxygen utilization efficiency, compact design and are compatible with the reduced gravity conditions in space, but, due to their counter-diffusional biofilm, there is a higher risk for denitrification. Indeed, feeding the MABR directly with raw urine in Chapter 3 resulted in N loss (18%) due to denitrification, whereas pre-treatment in the MEC allowed to recover all N in the MABR. Full urine nitrification (conversion of all TAN into nitrate) is preferred over partial nitrification because of the higher process stability and safety, but requires additional alkalinity to compensate for the proton release by nitrification.

The alkalization step provided some additional alkalinity, but this was not sufficient to obtain complete TAN conversion (Chapter 5). Therefore, the nitrification reactors in Chapter 2 and 3 were equipped with pH control (NaOH addition). In Chapter 5, the nitrification reactor was coupled to a dynamically controlled electrochemical cell to study in-situ electrochemical hydroxide production as an alternative to base addition, enabling full nitrification. Overall, stable, full urine nitrification was obtained in all nitrification reactors at urine concentrations of 17% to 40% (i.e., urine dilution factors of 6 to 2.5) and maximum loading rates between 200 and 300 mg N L⁻¹ d⁻¹ without substantial N loss.

Nitrified urine can be applied as a fertilizer, but the nutrient concentrations are relatively low compared to synthetic fertilizers. Hence, for terrestrial applications, a concentration step is preferred in order to reduce the storage and transportation volumes. Chapter 2 explored the feasibility of ED to concentrate nutrients. About 70% of the ions were captured in 15% of the initial volume when the pilot installation was operated using a 20% urine solution at a volumetric salt loading rate of 240 mmol NaCl-eq L⁻¹ d⁻¹. Nitrate, phosphate and potassium were concentrated by factors 4.3, 2.6 and 4.6, respectively. Doubling the urine concentration from 20% to 40% further increased the ED recovery efficiency by ~10% and decreased the volume ratio of diluate to concentrate from 5.8 to 4. Besides providing alkalinity to enable full nitrification, the electrochemical cell installed in the bioreactor in Chapter 5 functioned as concentration technology, yielding a clean acidic nitrate-rich side stream and a nitrate-depleted urine stream. Similar to ED, ~70% of the nitrate could be recovered and a concentration factor of ~3 was obtained.

Alternatively, nitrified urine can be valorized as culture medium for microalgae. Chapter 6 provided a proof of concept for *Limnospira indica* cultivation on the nitrified urine produced in Chapter 5. Dilution proved to be important to obtain high N utilization efficiencies, as the N uptake is limited by the biomass concentration which is in turn limited by the light availability. Furthermore, supplementation with chemicals was required to obtain a high yield and N uptake. Nitrified urine supplemented with phosphorus, magnesium, calcium, iron, EDTA and trace elements was as effective as standard synthetic medium in terms of biomass production, nutrient uptake and protein yield. Urine precipitates harvested in the alkalization step could potentially supply enough phosphorus, calcium and magnesium, requiring only external addition of inorganic carbon, iron, EDTA and (possibly) trace elements.

Overall, this research opens opportunities for efficient resource recovery from urine during deep-space missions and for on-site/decentralized treatment on Earth. The process configuration of the treatment train can be tailored, offering versatility for applications on Earth and in space.

Samenvatting

Bemande ruimtemissies worden momenteel regelmatig bevoorrad met water en voedsel vanop Aarde. Voor lange en verdere bemandede ruimtereizen, bijvoorbeeld een reis naar Mars of een permanent bewoonde basis op de Maan of Mars, is dit niet langer mogelijk door de grote afstand. Deze ruimtemissies zijn daarom afhankelijk van een zelfvoorzienend *life support*-systeem (RLSS) om zuurstof, water en voedsel te produceren en afvalstromen te verwerken. Urine is één van deze afvalstromen en een belangrijke bron van water, macro- en micronutriënten, die als meststoffen voor planten en microalgen kunnen dienen.

Het apart collecteren en recycleren van urine kan ook bijdragen tot een duurzame toekomst op Aarde door het sluiten en/of inkorten van de nutriëntencycli, die een belangrijke rol spelen in onze voedselvoorziening, maar die momenteel sterk verstoord worden door het intensieve gebruik van synthetische meststoffen. Door het recupereren van nutriënten uit afvalstromen kan de ammoniakproductie via het energie-intensieve Haber-Bosch proces en de ontginning van fosfor en kalium gereduceerd worden. Urine is een interessante afvalstroom omdat het de voornaamste bron van nutriënten in afvalwater is. Het is ook een goede meststof aangezien het alle vereiste macro- en micronutriënten voor planten bevat. Andere voordelen van het apart collecteren en recycleren van urine zijn, een lager waterverbruik bij het doorspoelen, het minder belasten en een betere effluentkwaliteit van waterzuiveringsinstallaties.

Het doel van deze doctoraatsthesis was het ontwikkelen van efficiënte urine-recyclage technologieën die geïmplementeerd kunnen worden in een RLSS, zoals het Micro-Ecological Life Support System Alternative (MELISSA) van de Europese ruimtevaartorganisatie (ESA) of die gebruikt kunnen worden voor decentrale urine-recyclage op Aarde. Aangezien bevoorrad van verre ruimtemissies beperkt is, werd er gestreefd naar maximale nutriëntenrecuperatie met een minimaal energieverbruik en gebruik van chemicaliën. Verschillende combinaties van biologische en fysisch-chemische technologieën werden onderzocht.

Urine bevat tal van waardevolle componenten, maar de complexe matrix en instabiliteit vormen een uitdaging voor urine collectie, behandeling en hergebruik. Ureum, de belangrijkste stikstofcomponent in urine, hydrolyseert snel tot ammoniak, ammonium en (bi)carbonaat. Dit veroorzaakt een verlies van nutriënten, geurhinder, verstoppingen en neerslag door ongecontroleerde precipitatie en vervluchtiging van ammoniak. Ammoniak is toxisch en vormt dus een risico voor de bemanning in een kleine ruimte. Verstoppingen van leidingen is een veel voorkomend probleem in urine collectiesystemen en blijkt

momenteel de voornaamste barrière voor de implementatie van bronscheiding van urine.

Om ureum hydrolyse tijdens collectie en opslag te vermijden en calcium en magnesium te verwijderen via gecontroleerde precipitatie werd de pH van de urine meteen na collectie verhoogd. In Hoofdstuk 2 en 3 werd hiervoor natriumhydroxide gebruikt. In Hoofdstuk 4 werd de pH verhoogd d.m.v. hydroxide productie aan de kathode van een elektrochemische cel om het gebruik van een base en de logistiek en de stijging van het zoutgehalte die daarmee gepaard gaan, te vermijden. Additie van natriumhydroxide of elektrochemisch geproduceerde hydroxide verwijderde 80-90% van de calcium en magnesium en 30 tot 80% van het fosfaat. Het precipitaat kan gevaloriseerd worden als een fosfor meststof in landbouw of als een grondstof voor de fosfor industrie. De gealkaliseerde urine kon meerdere maanden opgeslagen worden zonder ureum hydrolyse. Urine is echter enkel tijdelijk gestabiliseerd door de pH stijging en bevat nog steeds ureum die kan hydrolyseren als de pH verlaagd wordt of als urease toegevoegd wordt. Ook de biologisch afbreekbare organische verbindingen (COD) in urine kunnen hydrolyseren, wat resulteert in geurhinder door de vrijstelling van vluchtige organische componenten. De urine werd daarom verder behandeld met behulp van bacteriën om de COD en ureum te oxideren tot CO₂ en nitraat.

In Hoofdstuk 3 werd COD verwijderd in een microbiële elektrolysecel (MEC). Tot 85% van de COD werd verwijderd aan een COD belasting van 30 g COD m⁻² d⁻¹. Anaerobe genera, zoals *Geobacter* (elektroactieve bacteriën), *Thiopseudomonas*, een genus van de *Lentimicrobiaceae*, *Alcaligenes* en *Proteiniphilum* waren dominant aanwezig in de MEC. Elektroactieve bacteriën produceerden een elektrische stroom van 0.5 tot 2 A m⁻² door transfer van de elektronen die vrijkomen bij de COD oxidatie naar de anode. Naast de COD verwijdering was er ook ureum hydrolyse in de MEC. Hierdoor steeg de ratio van TAN (som van ammoniak-N en ammonium-N) over totale stikstof van <10% (in het influent) tot ~100% (in het effluent). Het gebruik van een MEC vermindert de zuurstofvraag en biomassaproductie in de daaropvolgende aerobe behandeling, verhoogt de alkaliteit van de urine en kan een deel van de energie in organische verbindingen omzetten tot elektrische energie.

Ureum en vluchtige, toxische ammoniak werden omgezet tot niet-vluchtig nitraat d.m.v. nitrificatie in Hoofdstuk 2, 3 en 5. In Hoofdstuk 2 en 5 werd ook ~90% van de COD verwijderd in de aerobe bioreactor, terwijl in Hoofdstuk 3 alle biologisch afbreekbare COD reeds verwijderd was in de MEC. Twee verschillende reactortypes werden gebruikt: een *moving bed biofilm reactor* (MBBR, Hoofdstuk 2 en 5) en een *membrane-aerated biofilm reactor* (MABR, Hoofdstuk 3). Een MABR heeft een hogere zuurstof efficiëntie en een compact design en is compatibel met de gelimiteerde graviteit in de ruimte. Door de *counter-diffusional* biofilm is er echter een groter risico op stikstofverlies door denitrificatie. Wanneer de MABR gevoed werd met onbehandelde urine was er een stikstofverlies van 18%. Na COD verwijdering in de MEC kon daarentegen alle stikstof gerecupereerd worden. Volledige nitrificatie (omzetting van alle TAN tot nitraat) wordt

verkozen boven partiële nitrificatie vanwege de hogere processtabiliteit en veiligheid, maar er moet extra alkaliteit toegediend worden om de protonen, die vrijkomen tijdens nitrificatie, te compenseren. De extra alkaliteit, toegediend in de alkalisatiestap (om ureum hydrolyse tijdens opslag te vermijden) was onvoldoende om alle TAN om te zetten tot nitraat (Hoofdstuk 5). In Hoofdstuk 2 en 3 werd er extra natriumhydroxide gedoseerd in de reactor. In Hoofdstuk 5 werd een dynamisch gecontroleerde elektrochemische cel ingebouwd in de reactor om hydroxide te produceren. In alle hoofdstukken werd stabiele nitrificatie bereikt op 17-40% urine (verdunningsfactor van 6 tot 2.5) en aan een maximale stikstofbelasting van 200-300 mg N L⁻¹ d⁻¹.

Genitrificeerde urine kan gebruikt worden als meststof, maar de nutriëntenconcentraties zijn relatief laag in vergelijking met synthetische meststoffen. Een concentratiestap is daarom aanbevolen om de opslag- en transportvolumes te beperken. In Hoofdstuk 2 werden de nutriënten m.b.v. elektro-dialyse (ED) geconcentreerd. Ongeveer 70-80% van alle ionen werden geconcentreerd in 15-20% van het initiële volume. De elektrochemische cel voor pH controle in de bioreactor in Hoofdstuk 5 kon ook gebruikt worden als concentratietechnologie en de concentratiefactor en de recuperatie-efficiëntie waren gelijkaardig aan ED.

Genitrificeerde urine kan ook gevaloriseerd worden als medium om microalgen te kweken. Dit werd aangetoond in Hoofdstuk 6 met de microalg *Limnospira indica*. Om een groot deel van de stikstof in het medium om te zetten tot biomassa was verdunning van de genitrificeerde urine noodzakelijk. De stikstofopname is namelijk afhankelijk van de biomassaconcentratie die beperkt wordt door de beschikbaarheid van licht. Genitrificeerde urine, gesupplementeerd met fosfaat, magnesium, calcium, ijzer, EDTA en sporenelementen resulteerde in een zelfde hoeveelheid biomassa en stikstofopname als standaard synthetisch medium. Het precipitaat dat gevormd wordt tijdens de alkalisatiestap bevat in theorie voldoende fosfaat, calcium en magnesium waardoor enkel anorganische koolstof, ijzer, EDTA en sporenelementen extern moeten worden toegevoegd.

Dit onderzoek toonde aan dat de onderzochte en ontwikkelde technologieën geschikt zijn om op een efficiënte manier water en nutriënten te recupereren uit urine. Verscheidene configuraties en toepassingen zijn mogelijk op Aarde en in de ruimte.

Introduction

Mars is there, waiting to be reached
(Buzz Aldrin)

Parts of this chapter are redrafted from:

Clauwaert, P., Muys, M., Alloul, A., De Paepe, J., Luther, A., Sun, X., Ilgrande, C., Christiaens, M.E.R., Hu, X., Zhang, D., Lindeboom, R.E.F., Sas, B., Rabaey, K., Boon, N., Ronsse, F., Geelen, D., Vlaeminck, S.E. Nitrogen cycling in Bioregenerative Life Support Systems: Challenges for waste refinery and food production processes. *Progress in aerospace sciences*, 91 (2017), 87-98.

1

1.1 (Extra)terrestrial life

1.1.1 Artificial life support systems sustain life in space

“Mars is there, waiting to be reached” (Buzz Aldrin)

Since the beginning of mankind, humans have looked up to the stars and dreamed about exploring outer space. Driven by their curiosity, astronomers from the ancient world and the scientific revolution in the 16th century, such as Nicolaus Copernicus and Galileo Galilei, took the first steps in observing and understanding the universe [165]. The development of rockets (intended as weapons) at the end of the World War II paved the way for space exploration [165]. Driven by national prestige, space exploration gained momentum during the Cold War between the United States and the Soviet Union [165]. The Soviets achieved many of the first milestones, including the launch of the first satellite ‘Sputnik 1’, followed by the first animal in space in 1957, the first human spaceflight by Yuri Gagarin in 1961, and the first space walk by Alexei Leonov in 1965. The space race came to an end in 1969, when the American astronaut Neill Armstrong took ‘one giant leap for mankind’ when he set foot on the Moon. This era of competition and rivalry was followed by an era of space collaboration, leading to the establishment of the International Space Station (ISS), a research station in low Earth Orbit (LEO) designed and constructed by many space agencies, led by former enemies US and Russia. In the meantime, numerous satellites, telescopes, orbiters, landers and rovers were successfully launched and discovered deep-space or the atmosphere and surface of nearby planets. After 20 years of continuous occupation and research at the ISS, the National Aeronautics and Space Administration (NASA), in collaboration with other space agencies, is preparing a new space era beyond LEO: the Lunar Gateway (to be launched in 2022-2026) [135, 211]. This small spaceship in orbit around the Moon, outside of Earth’s deep gravity environment, will act as a science outpost for human and robotic lunar exploration [211]. As the conditions are very similar to what astronauts and spaceships will experience in deep-space, the Gateway will also be used to develop and test new technologies, procedures and risk management protocols for future human deep-space missions, laying the groundwork for the ultimate goal, i.e., a manned mission to Mars, our closest neighbour in our solar system, in the 2040s

(Figure 1.1).

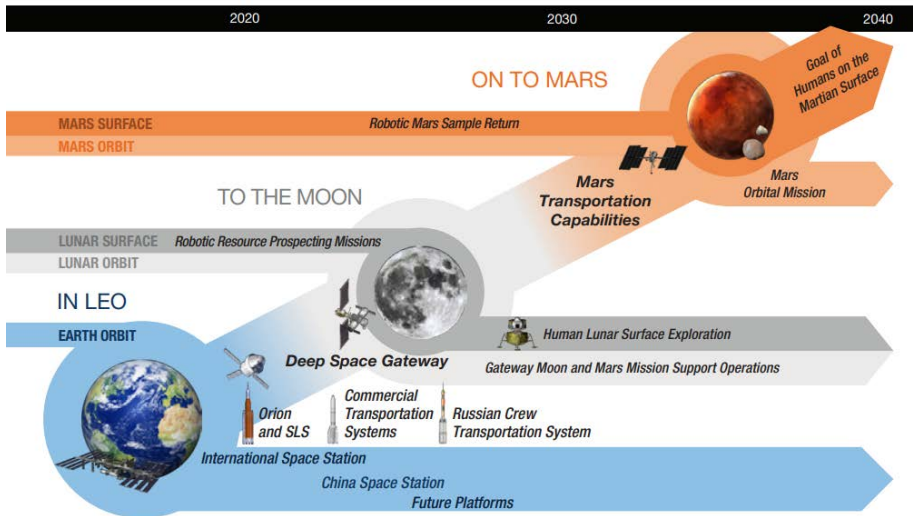


Figure 1.1: **The global exploration roadmap (2018), made by the International Space Exploration Coordination Group (ISECG) [135]. Image: ISECG**

The need for a regenerative life support system

Providing water, food and oxygen for astronauts is one of the major challenges for deep-space exploration and habitation. Also waste management is important, e.g., to prevent toxic levels of CO_2 (exhaled by the astronauts) and NH_3 (from urine degradation). An astronaut needs 0.636-1 kg of oxygen, 0.5-0.863 kg of food (dry ash based) and 4-13 L of water (2.3-3.6 L drinking water and 1.4-9 L of hygienic water) per day, and excretes 0.726-1.226 kg of CO_2 and 1.27-2.27 kg of urine per day [74]. Historically, all life support consumables (air, water and food) were taken on board and the waste was vented or stored and brought back to Earth [74]. This open-loop life support system (LSS) only allows short-term space missions due to payload limitations [74, 122]. Long-term short-distance missions in space, such as the continuously manned ISS, are frequently resupplied by an expensive delivery system (US \$12 600 per kg payload, SpaceX) [20, 122]. For deep-space missions involving several astronauts and long distances, resupply of water and food from Earth is neither technically nor economically feasible [74, 105]. With a minimum requirement of 15 kg of life support consumables per day [122], a crew of six members would require more than 50 tons on a 1.5-year trip to Mars. In comparison, the payload of world's most powerful rocket (Falcon Heavy, SpaceX) amounts to 16.8 tons for a mission to Mars [264]. Hence, to permit deep-space missions or the establishment of manned planetary bases, the development of a closed-loop regenerative life support system (RLSS), which relies on minimal or no resupply, is indispensable. A closed-loop RLSS addresses four main functions to enable human

presence and activity in space: i) atmosphere regeneration for respiration, ii) water recycling, iii) generation of food and iv) waste management [277]. Initially, physico-chemical systems were developed for atmosphere regeneration and water recycling, e.g., the ISS Environmental Control and Life Support System (ECLSS) developed by NASA [74]. Nowadays, various space agencies focus on incorporating biological systems to enable food production to increase the closure of the RLSS [105]. Examples of (ground-based) RLSS include BIOS I-III (Russia), Biosphere 2 (USA), Lunar Palace (China) and MELiSSA (ESA) [310].

Micro-Ecological Life Support System Alternative

The Micro-Ecological Life Support System Alternative (MELiSSA) is the RLSS under development by the European Space Agency (ESA) with the aim to produce food, oxygen and potable water from the mission waste streams by the use of microorganisms and higher plants [105, 163]. The project was started in 1989 and is inspired on a natural lake ecosystem. The MELiSSA loop consists of five compartments, connected in the gas, liquid and solid phase: an anaerobic compartment, a photoheterotrophic compartment, a nitrifying compartment, a photoautotrophic compartment and a crew compartment (Figure 1.2) [164].

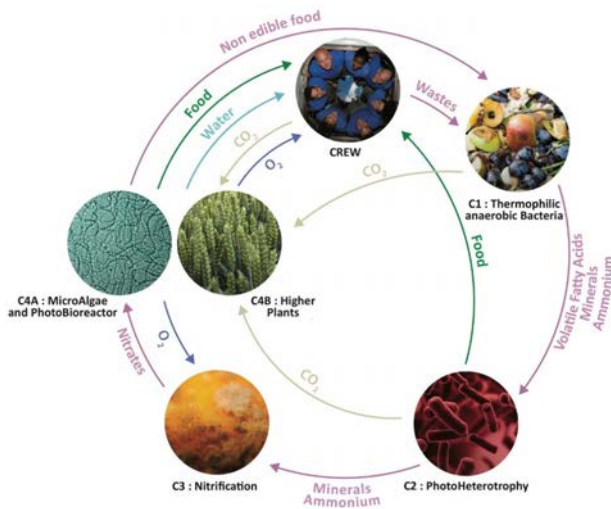


Figure 1.2: MELiSSA loop [190].

Organic waste (including human faeces, toilet paper and inedible crop residues) is first degraded in an anaerobic thermophilic fermenter to volatile fatty acids (VFA) and CO₂ [105]. The VFA are subsequently transformed into edible biomass and CO₂ by anaerobic photoheterotrophic bacteria (*Rhodospirillum rubrus*) in compartment II. The nitrifying compartment converts volatile ammonia into nitrate via biological nitrification. In the fourth compartment, higher plants and cyanobacteria assimilate the nutrients and

CO₂ produced in compartment I, II and V using light as an energy source to produce O₂ for compartment III and V and edible biomass for the crew. Also potable water is recovered from evapotranspiration of higher plants. Initially, all different compartments have been studied individually in great detail (i.e., selection and characterization of microbial strains used in compartment III and IVa). Besides the biological processes, mathematic models and control loops are being developed. All compartments are being integrated and the robustness and stability is being tested in a highly automated and controlled pilot plant located at the Universitat Autònoma de Barcelona [106].

1.1.2 The natural biosphere sustains life on Earth

The Earth biosphere: a bioregenerative life support system

On Earth, the biosphere acts as a global regenerative life support system, providing us with breathable air, water and food [74]. Hundreds of processes involving millions of organisms (e.g., plants, animals and microorganisms) recycle, regulate and control life's necessities [74]. For instance, oxygen gas in our atmosphere is used by amongst others humans, and is constantly replenished by photosynthetic organisms (plants, algae, cyanobacteria...), converting the exhaled CO₂ back into oxygen gas. Also in the biogeochemical cycles, e.g., the water cycle and nutrient cycles (carbon, nitrogen and phosphorus), elements are continuously being recycled between organisms and the environment (Figure 1.3) [74].

Fertilizers feed the world

Food is undoubtedly the least available life support consumable on Earth. The vast majority of our food comes from agriculture. About 10 000 years ago, in the early Holocene, humans started to domesticate plants and animals in order to secure a more predictable, reliable and accessible food supply [282]. This transition away from a nomadic hunter-gathering lifestyle toward a life of farming gave rise to cities, reshaping human civilization. Throughout history, advancements in agriculture (i.e., intensified breeding efforts, the invention of new farming tools such as plows and seed drills, synthetic fertilizers and pesticides) and concomitant increases in productivity were accompanied by population growth. The global population has grown from below 15 million before the appearance of agriculture to 7.7 billion in 2020 [282]. The most spectacular population boom occurred during the past 120 years (from 1.6 billion in 1900 to 7.7 billion in 2020) and was triggered by the invention of the Haber-Bosch process, a process to transform atmospheric nitrogen gas into reactive ammonia, the main constituent of synthetic N fertilizers [116, 184]. Nowadays, agriculture largely depends on the use of these synthetic fertilizers to replenish the nutrients in the soil. More than half of the food consumed in the world is grown using synthetically produced fertilizers [80]. According to the Food and Agriculture Organization of the United Nations (FAO), approximately 110 million tonnes of nitrogen, 45 million tonnes of P₂O₅ and 37

million tonnes of K_2O were used in agriculture in 2017 [93].

It is anticipated that the world population will grow to 9.4-10.1 billion people by 2050 [297]. Together with changes in diet and lifestyle resulting from the increasing income and wealth in developing countries, this is expected to increase the protein demand with 50% [110, 300]. For dairy and meat products increases up to 82% and 102% are forecasted by FAO between 2000 and 2050 [25]. Fertilizers will play a key role in meeting these increasing global food needs [276].

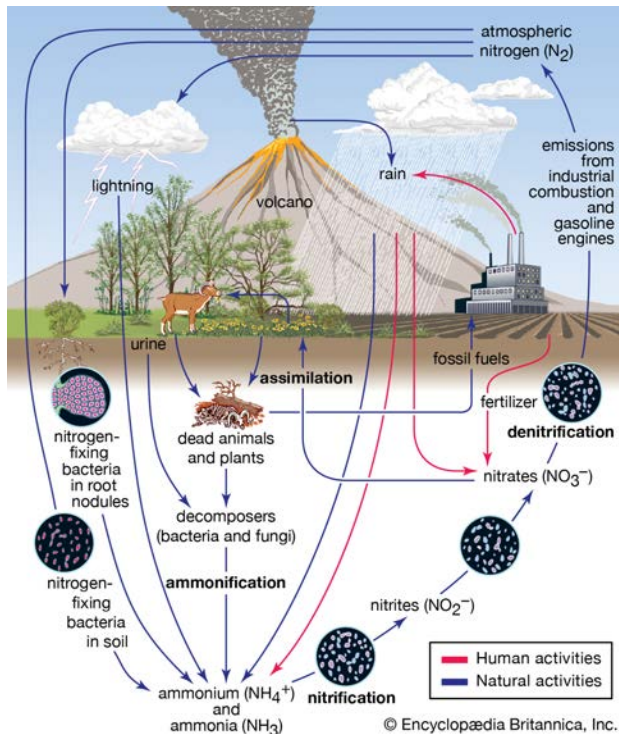


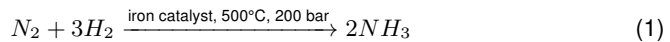
Figure 1.3: **Nitrogen cycle.** From Encyclopædia Britannica [78] Atmospheric nitrogen (N_2) is converted into reactive nitrogen (ammonia) by nitrogen-fixing bacteria in the soil and root nodules of N-fixing plants or by industrial fixation (Haber-Bosch). The fixed nitrogen is transformed into amino acids and oxidized compounds by microorganisms, plants and animals, and finally returns to the atmosphere as N_2 via microbial denitrification in soils and aquatic ecosystems [102].

Present fertilizer production is unsustainable

Nitrogen (N), phosphorus (P) and potassium (K) are the main constituents of synthetic fertilizers, as they are essential elements and often present a limiting factor for the growth of living organisms [79, 116, 153]. As building block of amino acids and nucleic acids, N is present in the proteins, DNA and RNA of all living organisms [153]. P is a

building block of DNA, RNA and ATP and has an essential role in metabolic energy transfer (from ATP to ADP) and the structure of cell walls [57, 124]. K plays a role in the maintenance of the fluid and electrolyte balance and in photosynthesis (regulates CO₂ uptake by plants).

N is very abundant on Earth, as nitrogen gas (N₂) makes up 78% (v/v) of our atmosphere [80]. Yet, N₂ in our atmosphere can only be assimilated by a limited number of N-fixing plants and microorganisms. The Haber-Bosch process allows to convert N₂ into reactive nitrogen, using hydrogen gas (H₂) and iron (as catalyst) at high temperature (~ 500°C) and pressure (~200 bar) (Reaction 1). The ammonia can be used directly as a fertilizer or can be combined with nitric acid (also derived from ammonia) to produce ammonium nitrate, or with liquid CO₂ to produce urea.



The Haber-Bosch process consumes a lot of energy (30-60 MJ kg⁻¹ N depending on which fossil fuel is used) due to the need for H₂ (mostly produced from fossil fuels) and the high pressure/temperature conditions [80, 167]. With a global production of about 120-160 Mt NH₃-N per year (of which 80% is used in fertilizers), the Haber-Bosch process is responsible for an estimated 1-2% of the total global energy consumption and 1% of the global CO₂ footprint (4-8 tons of CO₂-equivalents per ton N fertilizer produced) [184].

In contrast to N which can be industrially produced on a large scale, P and K fertilizers are produced from non-renewable natural resources, i.e., phosphate rock and potash ores, respectively [58, 92]. Because of the high fertilizer demand, the reserves are shrinking at a rapid pace. Several studies estimated that the readily accessible, qualitative phosphate rocks will be depleted in the coming 50-100 years [58]. Furthermore, the supply is controlled by a limited number of countries (i.e., China, US and Morocco) with access to these phosphate mines [58]. As a consequence, phosphate rock has been listed as one of the critical raw materials for the EU since 2013 [300]. Projections based on the K production rates of 2007 indicate that the current potash reserves are sufficient for at least 235 more years [92].

The terrestrial life support system is threatened by increasing pressures

Fertilizer production and use have altered the natural biogeochemical cycles and are pushing the Earth's life support system to its planetary boundaries or even beyond (Figure 1.4) [79, 116, 249, 270]. These planetary boundaries were defined as a 'safe operating space for humanity', within which irreversible and abrupt environmental changes can be avoided [249]. The N-cycle has already transgressed its critical planetary boundary (beyond the zone of uncertainty). Today, as a result of fertilizer application, cultivation of N-fixing crops and fossil fuel burning, more inert N₂ is converted into reactive N anthropogenically than by all of the Earth's natural processes combined [79, 94, 249]. As a consequence, reactive nitrogen accumulates in the soil or ends up

in the atmosphere and aquatic ecosystems. Similarly, mining of phosphate rock and application of P fertilizers on agricultural land resulted in an accumulation of P in the environment. As a consequence, the P-cycle is approaching its critical boundary [249].

Modern agriculture was identified as one of the major causes of environmental pollution [249]. Massive nutrient losses occur in the production-consumption chain of plant and meat protein, resulting in reactive N and P entering and polluting the environment, causing e.g., eutrophication and dead zones (algae blooms) in aqueous ecosystems [57, 80]. Phosphate fertilizer production also generates a radio-active waste by-product phosphor-gypsum [58], whereas nitrogen fertilizer production is responsible for among others global acidification and increasing greenhouse-gas levels (CO_2 and N_2O), thereby contributing to climate change and stratospheric ozone loss [80, 101, 116, 249].

In light of the growing global population and food demand, the shrinking P and K reserves and the intensified environmental pollution, it is evident that we cannot continue business-as-usual. First and foremost, minimizing losses is paramount [59, 80]. Nowadays, most of the nutrients applied on land are lost via run-off, leaching, volatilization and denitrification in agriculture or inefficiencies at the following stages of the food chain (Figure 1.5) [80, 103, 184]. From the 100 million tonnes of N used in global agriculture in 2005, only 17 million tonnes of N was consumed by humans in crop, dairy and meat products [80]. Similarly, about five times the amount of phosphorus that humans are actually consuming in food is mined (Figure 1.5) [58]. Besides optimizing the use of nutrients, recovery and recycling will be key in the future to close/shorten the nutrient cycles [58].

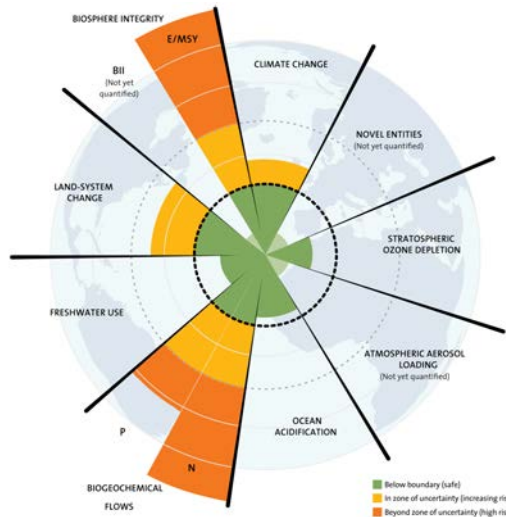


Figure 1.4: **The planetary boundaries.** Credit: J. Lokrantz/Azote based on Steffen et al. 2015 [270].

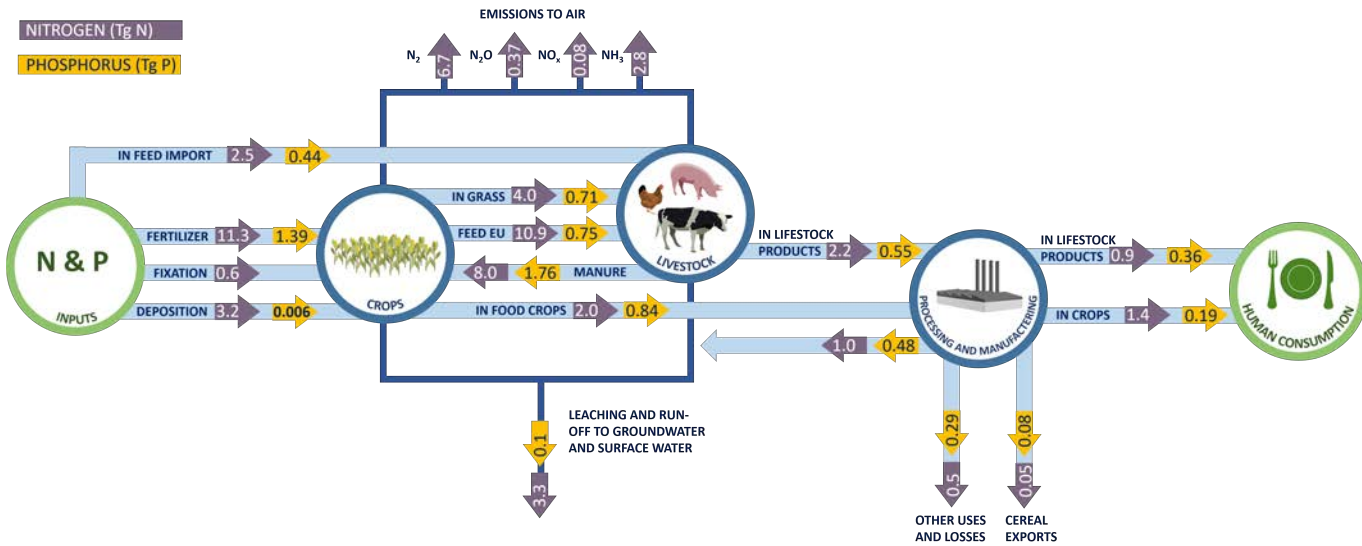


Figure 1.5: **Nitrogen and phosphorus flows (in million tonnes per year) through the agricultural food system in the EU (adapted from an infographic from the European Environmental Agency, 2019).** In the EU, only 20-30% of the total N and P input through fertilizers is embedded in our food.

1.2 Urine, a valuable nutrient resource

1.2.1 Urine as an alternative resource for fertilizer production on Earth

Urine is a widely available, relatively concentrated source of N and P

Depending on the diet, approximately 70-88% of the N, 25-67% of the P and 80-90% of the K in our food is excreted in urine, while the remaining N, P and K is discharged in faeces [140, 193, 301]. Hence, urine presents an interesting, widely available and accessible source of nutrients. Nutrient recovery from urine could shorten the nutrient cycles, thereby reducing the need for energy intensive ammonia production using the Haber-Bosch process and mining of non-renewable P and K. It was estimated that efficient recovery from source-separated urine could yield about 4 kg N, 0.4 kg of P and 1 kg of K per caput per year, covering ~15-20% of the global N and P demand [167, 193, 304]. Moreover, urine is not only rich in macronutrients (in similar proportions as in synthetic fertilizers), but also contains all other micronutrients and trace elements required for plant growth, making urine an adequate plant fertilizer [124, 167, 289].

The fate of urine: from past to present

The potential of urine as a fertilizer was long recognized [29]. Archaeological findings revealed the use of human excreta for land fertilization as early as 3000BC in Mesopotamia [167]. Urine was also a valuable multi-purpose commodity, deployed as a cleaning agent for amongst others wool and clothes, and as a teeth whitener in the ancient Roman Empire [29, 152, 261]. Thereto public urinals were constructed to collect and sell urine (which was even subjected to a special tax). Also complex sewer networks ('cloaca maxima') with holes serving as public toilets were built to drain human excreta and other waste streams away from the living areas [29, 261]. After the collapse of Roman civilization, mankind was condemned to return to 'the bucket era' in Medieval Europe, both for water supply and waste collection. The buckets were emptied on the streets, which were cleaned during the night by dung collectors, who sold on the human waste (known as 'night soil') as fertilizer to farmers [261]. The versatile application potential of urine was further exploited during the pre-industrial time period. In the 16th century, urine was applied as a mordant in the English textile industry, and during the Napoleonic wars, urine from soldiers was put to use to manufacture gunpowder. During the 1850s, French chemists developed a distillation method to produce a pure ammonium sulfate fertilizer from human waste [261]. In the meantime, sewer networks were put in place to flush the human waste from the expanding cities to the surrounding agricultural fields or surface waters. Discharge of human waste into rivers caused numerous outbreaks of waterborne diseases, such as cholera and typhoid, and odor nuisance [261]. The discovery of cheap mineral fertilizers (e.g., superphosphate) in the late 19th century and the lack of arable land to dispose of sewage put an end to widespread sewage farming in Europe [261]. Urine was no longer a valuable commodity. Instead, urine was

dumped with the other waste streams into surface waters, until the establishment of wastewater treatment plants (WWTP) over the course of the 20th century. Worldwide, sewage farming is still carried out in some remote local rural communities, e.g., in China, Vietnam and Japan [167].

Nowadays, in developed countries, most of the urine is flushed down to the sewer system together with other domestic wastewater streams (flush water, water from the kitchen tap, dishwasher, washing machine, shower/bath...) and treated in a WWTP before discharge into the environment in order to prevent environmental pollution. Still, in 2018, 13% of the households in Flanders was not connected to a sewer network, and, hence, discharged all their domestic wastewater (including urine) untreated into the environment [302]. On a global scale, only 31% of the population (2.4 billion people) used private sanitation facilities connected to sewers and WWTP anno 2017 (Figure 1.6) [319]. Many cities in developing countries do not dispose of sewer systems and WWTP and even lack proper sanitation. Providing 'clean water and sanitation for all' was set as one of the 17 sustainable development goals (SDG 6) in 2015 and should be achieved by 2030. Yet, globally, an estimated 4.2 billion people (55% of the global population) are still deprived of safely managed sanitation facilities [296]. 673 million people (mainly in Sub-Saharan Africa and Southern Asia) still practiced open defecation in 2017 [296]. Due to inadequate sanitation, untreated human waste is spreading diseases into water supplies and the food chain (e.g., cholera, diarrhoea, dysentery and intestinal worms), and is causing environmental pollution [319].

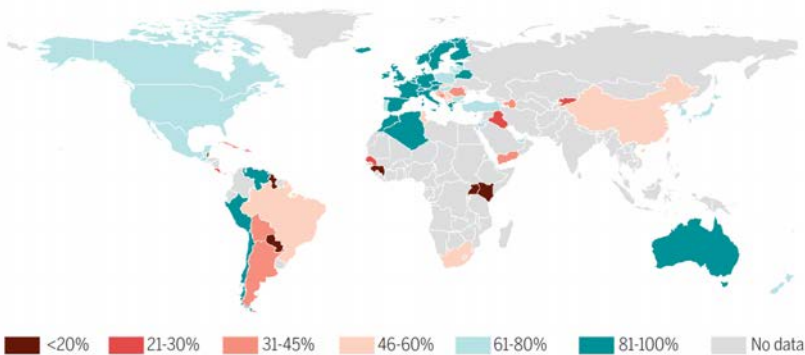


Figure 1.6: **Proportion of population connected to sewers.** From Larsen et al. (2016) [161]. Reprinted with permission from AAAS.

A sustainable future through urine source separation?

For an efficient nutrient recovery from urine, urine should be collected separately, since dilution with other domestic wastewater streams decreases the concentrations of the nutrients, thereby complicating recovery [187, 313]. The separate collection of human urine and faeces at the toilet or urinal is known as urine diversion or source separation.

In the 1990s, several groups in Sweden and Switzerland started working on source separation technologies for urine as a sustainable alternative to the existing end-of-pipe wastewater management [160].

Apart from enabling nutrient recovery, saving water and facilitating wastewater management are two important incentives for urine diversion [171, 313]. In Flanders, on average 20-30 L of water per day is used for toilet flushing, which makes up about 20% of the total household water consumption [302]. Urine diverting toilets or waterless urinals can reduce the water consumption by over 50% compared to conventional modern 3/6 liter dual flush toilets [171].

Conventional WWTP use two-stage nitrification-denitrification to convert reactive nitrogen (predominantly ammonia) into nitrogen gas, whereas P is mostly removed via chemical precipitation with Fe^{3+} or Al^{3+} . Although urine makes up less than 1% of the total volume of domestic wastewater, it contributes to $\sim 80\%$ of the N, 45-56% of the P and 63% of the K load to a WWTP [241, 313]. As N and P are in excess in WWTP influent, ideally 60-75% of the urine should be collected and treated separately in order to achieve a WWTP influent that better meets the cell growth requirements for activated sludge production (i.e., COD:N:P ratio of $\sim 100:5:1$) [313]. This would allow for a complete N and P removal in the WWTP via waste sludge production, obviating the need for nitrification-denitrification and P precipitation [313].

Furthermore, urine diversion could make WWTP energy neutral or even positive, when combined with biogas production from the sludge, as the energy cost for nutrient removal is greatly reduced (nitrification-denitrification and P removal require about 45 MJ kg^{-1} N and 49 MJ kg^{-1} P, respectively) [131, 187, 313].

Another advantage of urine source-separation is the improvement of the quality of the WWTP effluent, and the corresponding positive effect on the water quality of the receiving water bodies. In total, it is estimated that approximately 1.5 million tonnes of P [248] and 7.4 million tonnes of N [298] is discharged by WWTP into surface water each year [241]. Simulations by Wilsenach and van Loosdrecht (2003) [313] showed that the WWTP effluent would contain less than 1 mg L^{-1} of NH_4^+ , NO_3^- and PO_4^{3-} with more than 60% urine separation. Urine diversion would also reduce the concentration of micropollutants in the effluent, as about 60-70% of the micropollutants in wastewater originate from urine [160].

The main bottleneck for urine diversion and reuse is probably the implementation itself. How to retrofit urine diversion into the existing sanitation technology, extended sewer network and centralized WWTP? As it is too expensive to install a second sewer network for urine collection, urine should be treated on-site or transported via trucks to decentralized treatment facilities [160, 241]. This comes with high investment and operational costs. Urine diversion will only be implemented on a large scale, when economically viable and if the treatment technologies are reliable and easy to operate [289].

Developing countries, in contrast, have great potential to implement urine diversion

and reuse. Urine diversion could boost the sanitation coverage, without the need to install expensive sewer systems and centralized WWTP, in addition to providing a cheap source of fertilizer (to increase the crop yields) and reducing environmental pollution (as, currently, most of the urine is discharged without any treatment into the environment) [241]. The ‘reinvent the toilet challenge’ is an initiative funded by the Bill & Melinda Gates Foundation to accelerate the development and implementation of innovative, off-the-grid pro-poor sanitation technologies in developing countries.

1.2.2 Urine recycling is of key interest in space life support systems

Regenerative life support systems almost solely rely on recovery from waste streams for subsistence. Urine is one of the most important waste streams in a RLSS, given its high nutrient and water content [70]. A theoretical nitrogen balance of a RLSS (Figure 1.7) shows that about 78-84% of the nitrogen in the food consumed by an astronaut ends up in urine [52].

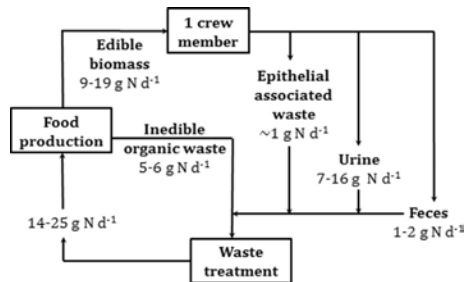


Figure 1.7: **Theoretical nitrogen balance in a RLSS for one crew member [52].**

Even when recovery is not envisaged (e.g., in short-term space missions), urine stabilization is essential since ammonia, originating from urea hydrolysis during storage (Section 1.3.2), can pose a hazard to the crew upon volatilization [52]. Currently, on-board the ISS, urine is treated in the Water Recovery and Management System developed by NASA [38]. This system converts urine, flush water, Sabatier product water and humidity condensate into potable water that can be used for the purpose of drinking, personal hygiene, food preparation, oxygen generation and toilet flushing [38]. First, the urine is pre-treated with chromium trioxide (CrO_3) and sulfuric/phosphoric acid to control the microbial growth and to inhibit urea hydrolysis into volatile and potentially harmful ammonia [38]. Subsequently, water is recovered using vapour compression distillation (VCD), filtration, a catalytic reactor and ion-exchange [38]. This system allows to recover up to 85% of water from urine [39, 122, 201], but the nutrients end up in the brine of the VCD which cannot be reused because it contains toxic chromium trioxide.

1.3 Urine source separation & treatment

1.3.1 Urine diverting toilets

Urine source separation requires a modified toilet design to separate urine and faeces at the point of collection in the toilet [304]. The easiest way to achieve source separation is through waterless urinals, which are primarily designed to collect urine from male users. Urine diversion flush toilets (e.g., NoMix toilets (Figure 1.8A)) are probably the most advanced urine diverting toilets on the market. Urine is collected in the front bowl and drained into a separate tank, whereas faeces are collected at the back and flushed in the same way as conventional toilets. Urine diversion dehydration toilets (UDDTs) have a similar design but collect the faeces without the use of flush water in vaults or buckets located underneath the pedestal or squatting pan [304]. Because of the low cost and simple design (no need for flush water and connection to a sewer system), UDDTs are mainly implemented in developing countries.

Urine collection in a space shuttle/station is a bigger challenge because of the microgravity or reduced gravity. The ISS is equipped with fan-driven air suction toilets (Figure 1.8b). Astronauts urinate in a hose, in which an air flow is created by means of a fan. The urine is transferred to the Urine Processor Assembly (UPA) to recover water. Faeces are collected in a bag in the solid waste container, also by means of an air flow, and are compressed and eventually burned on a cargo ship in space.

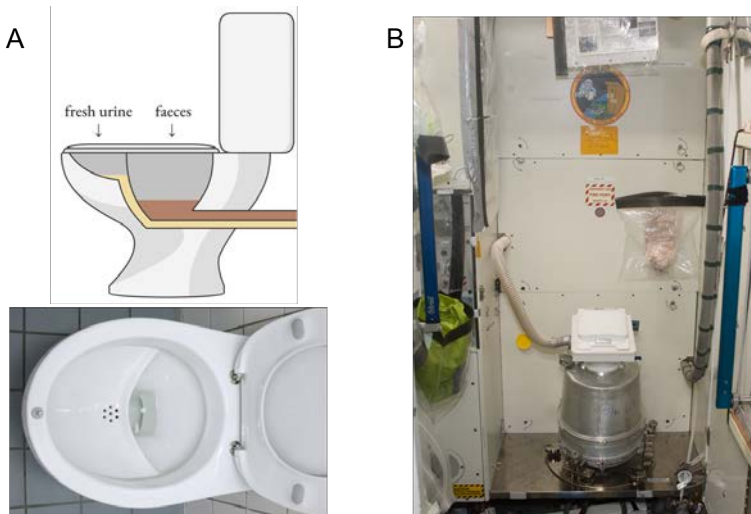


Figure 1.8: **A: NoMix Toilet (Roedinger, Germany), B: Space toilet installed in node 3 of the International Space Station (Google Earth).**

1.3.2 Urine characteristics

Urine composition

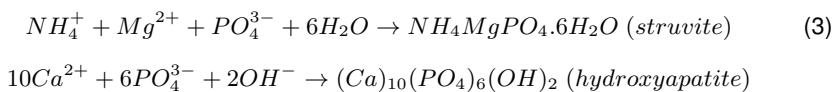
Urine is rich in nitrogen, phosphate and potassium, but mainly consists of water (> 90%) and contains many other compounds. Putnam (1971) reported 158 different chemical constituents, of which 68 components have a concentration >10 mg L⁻¹, thereby accounting for over 99% of the total solutes in urine [234]. The four major categories are i) inorganic salts such as NaCl, KCl, MgSO₄, ii) urea, iii) other organic compounds, e.g., creatinine, uropepsin and glycine and iv) organic ammonium salts, e.g., hippurate, citrate, and urate [234]. The composition of urine varies between and within individuals due to factors such as diet, health, environmental conditions and daily activities [252]. Also space conditions can alter the urine composition. Urine is typically more enriched in calcium due to decalcination of bones in microgravity [199, 311].

Urea hydrolysis

During storage, the composition of urine significantly changes due to enzymatic urea hydrolysis. Urea (CO(NH₂)₂) is hydrolysed by the urease (urea amidohydrolase) enzyme to ammonia (NH₃) and carbamate (NH₂COOH), which spontaneously decomposes into carbonic acid (H₂CO₃) and a second molecule of ammonia. The carbonic acid dissociates and the two ammonia molecules equilibrate with water. The overall reaction (Reaction 2) results in a pH increase from around 6-7 to around 9 [197].



Because of urea hydrolysis, the fraction of organic nitrogen decreases while the total ammonia nitrogen (TAN) increases. The release of ammonia and bicarbonate and the increase in pH also triggers precipitation of salts (Reaction 3), resulting in reduced concentrations of calcium, magnesium and phosphate [292, 293, 294].



Urea hydrolysis is initiated by urease-positive bacteria growing in the pipes of urine collection systems and is usually completed within a few days [292]. Urease-positive bacteria are very abundant and even some eukaryotic and prokaryotic organisms (e.g., some plants and invertebrates) produce urease [197, 292]. Urea amidolyase, an enzyme produced by some yeasts, bacteria and algae, is furthermore known to hydrolyse urea [334].

Urea hydrolysis presents a challenge for an efficient urine collection and recovery. Part of the ammonia can volatilize during collection, storage, treatment, and/or application, resulting in a loss of nitrogen, odor nuisance, and environmental pollution [162, 294]. Moreover, the spontaneous, uncontrolled precipitation of calcium and magnesium salts

leads to clogging of pipes in collection systems and a loss of phosphorus (and to a limited extent also nitrogen) [28, 288, 293]. Clogging of pipes by the precipitating salts is a common problem in nonwater urinals and urine separating toilets, creating odor nuisance, blockages, and leakages and requiring extensive cleaning and maintenance [1, 23, 28, 162, 241, 288]. It is believed that this is currently one of the major barriers for the widespread implementation of source separation [28].

Urea hydrolysis and subsequent precipitation can be prevented by inhibiting the microbial activity and hence the production of urea-degrading enzymes [160]. This can be achieved by, amongst others, addition of acids, caustics, hydrogen peroxide and urease inhibitors (Table 1.1).

Degradation of organics

The high fraction of biodegradable organic compounds also fuels microbial growth in urine during storage [172, 294]. Urine contains up to 10 g COD L⁻¹ (chemical oxygen demand or COD is the amount of oxygen that is required to oxidize all organic material into CO₂), of which ~85% is biodegradable [291, 294]. The main COD compounds in fresh urine are creatinine, hippuric acid, uric acid, amino acids and carbohydrates [241, 294]. During storage, a significant fraction of COD (~50%) is converted into VFA (predominantly acetate) by fermentation [162]. Also sulfate reducing bacteria (using sulfate as electron acceptor) or aerobic bacteria (using oxygen as electron acceptor) can oxidize organics in urine [294]. Organic degradation products are responsible for the characteristic pungent smell of stored urine [289].

1.3.3 Urine treatment

Overview of urine recycling technologies

Although direct urine reuse for fertilizing purposes has been common practice throughout history and is still carried out in some remote rural areas [7, 29], it is not recommended and even prohibited in the European Union, because of the potential spread of pathogens and organic micropollutants [167]. The World Health Organization (WHO) recommends urine storage for >6 months at >20°C to achieve sufficient pathogen inactivation, which is highly impractical in dense urban regions because of the large storage volume requirements [21, 318]. Further concerns that hamper direct urine utilization are degradation of organics and ammonia volatilization during storage, transport and application, resulting in odor nuisance and significant N losses and emissions to the environment, and potential soil salinization by the high salt content of urine [171, 172, 196, 289]. Moreover, the high water content makes the transport to arable land costly [295]. These challenges illustrate the need for urine treatment [171]. To deal with scaling and blockages in urine diverting toilets and pipes, some on-site treatment is recommended, after which the urine can be further processed on-site or transported via trucks to decentralized treatment facilities for nutrient recovery [160, 241]. On-site

and decentralized urine treatment requires a high level of automation, robustness and minimal maintenance [160]. Numerous technologies have been proposed over the years for on-site or decentralized resource recovery or removal from urine. Maurer et al. (2006) [186] identified seven main purposes of urine treatment processes: i) hygienization (to avoid pathogen spreading), ii) volume reduction (to decrease storage volume and transportation costs), iii) stabilization (to prevent degradation of organic matter, ammonia volatilization, and clogging of pipes by precipitation), iv) P-recovery, v) N-recovery, vi) nutrient removal and vii) handling of micropollutants. More recently, also energy recovery using bio-electrochemical systems became one of the purposes of urine treatment. Most technologies attain multiple goals, but, thus far, none of these technologies are all-encompassing [186]. For instance, most of the concentrating techniques only collect some of the elements in the concentrated fraction, e.g., N by ammonia stripping and P by struvite precipitation. Depending on the overall goal of the treatment process, a combination of technologies can be used to meet the requirements [186]. One of the most mature urine recycling technologies at present is the VUNA process, which produces a concentrated liquid fertilizer (Aurin) using partial nitrification, adsorption on activated carbon and distillation [85, 151, 305].

Table 1.1 gives an overview of commonly explored urine treatment technologies. Technologies of interest in this PhD thesis are reviewed in detail in Section 1.4.

Table 1.1: **Overview of urine recovery technologies reported in literature.** The majority has only been tested on lab-scale thus far. For details, we refer to the original publications. This table is not intended to be exhaustive, but rather presents the most commonly explored technologies.

Technology	Input	Product	Principle	References	
Hygienization					
– storage	fresh urine	stored (hydrolysed) urine	Urine is stored for several months to inactivate pathogens. If stored at 20°C for at least 6 months, urine may be considered safe to use as a fertilizer (WHO). During storage, urea hydrolysis results in precipitation of struvite, hydroxyapatite (HAP) and calcite, and potentially some ammonia volatilization [186, 292].	[126]	
Stabilization to prevent urea hydrolysis					
– acidification	fresh urine	stabilized (urea)	urine	Addition of acids such as sulfuric acid, acetic acid, citric acid and vinegar results in a low pH, which affects the protonation states of the active site of the urease enzyme, thereby inhibiting urea hydrolysis [243]	[125, 243, 254]
– alkalization	fresh urine	stabilized (urea)	urine	Addition of caustics, wood ash or biochar results in a high pH, which affects the protonation states of the active site of the urease enzyme, thereby inhibiting urea hydrolysis [243]. The high pH also triggers precipitation.	[240, 262]
– anion exchange	fresh urine	stabilized (urea), low in chloride	urine	Chloride ions are exchanged by OH ⁻ ions by passage through an anion-exchange column. The resulting increase in pH prevents urea hydrolysis.	[263]
– hydrogen peroxide addition	fresh urine	stabilized (urea)	urine	Urease is irreversibly oxidized by hydrogen peroxide	[333]
– electrochemical chlorine addition	fresh urine	stabilized (urea)	urine	Chlorine causes irreversible changes in the conformation of urease, resulting in its inactivation [243]. Chlorine can be produced electrochemically by oxidation of chloride at the anode.	[132]

– addition of sulfuric acid and chromium trioxide	fresh urine	stabilized (urea)	urine	In the urine processor assembly (UPA) of the ISS, urine is stabilized by a combination of sulfuric acid/phosphoric acid and chromium trioxide.	[38]
– addition of urease inhibitors	fresh urine	stabilized (urea)	urine	Many different urease inhibitors have been identified: thiols, boron compounds, fluoride, metals, sulfur compounds, and natural urease inhibitors such as garlic, onion, or cabbage extract. Metals inhibit urea hydrolysis through binding with the functional groups of the urease enzyme which are necessary for the catalytic function of the enzyme, whereas fluoride directly binds with the active nickel site [243].	[243]
– thermal treatment	fresh urine	stabilized (urea)	urine	Urine is stored at 60-70 °C. The high temperature inactivates pathogens and urease-producing bacteria, thereby suppressing urea hydrolysis.	[336]

Volume reduction

– freeze-thaw	urine	nutrient-rich concentrate		During slow ice formation, water molecules are incorporated into ice crystals, whereas ions and other chemical compounds remain concentrated in the liquid part. By freezing urine at a temperature of -14°C, approximately 80% of the nutrients could be concentrated in 25% of the original volume.	[172]
– reverse osmosis (RO)	stored urine	nutrient-rich concentrate		In reverse osmosis (RO), water molecules pass through the RO membrane by applying a pressure to overcome the osmotic pressure. Most salts are retained by the membrane, resulting in a nutrient-rich concentrated solution. By acidifying the stored urine, more TAN can be recovered (since the retention of ammonium is better than ammonia) [186]	[186]
– forward osmosis (FO)	fresh or stored urine	nutrient-rich concentrate		In forward osmosis (FO), water moves across a semipermeable membrane from a low-osmotic-pressure feed solution (urine) to a high osmotic-pressure draw solution (seawater or RO brine) (thus without an externally applied hydraulic pressure).	[332]

Volume reduction & water recovery					
– distillation	stabilized, stored or nitrified urine	– high-quality water – concentrated nutrient-rich product	Vapor compression distillation is used in the Urine Processor Assembly (UPA) on the ISS to evaporate water from stabilized urine. The nutrients are concentrated in the brine, which cannot be recovered because it contains toxic chromium trioxide, used for stabilization/hygienization. Distillation of (partially) nitrified urine allows to concentrate the nutrients with minimal losses of ammonia.	[38, 295]	97,
– membrane distillation (MD)	stored urine	– high-quality water – concentrated nutrient-rich product	Membrane distillation is a relatively new technique for selective water removal using a vapour pressure gradient across a hydrophobic membrane, which results in the transfer of volatile compounds from the liquid phase to the vapor phase through the membrane pores. To prevent ammonia pollution in the recovered water, the urine can be acidified (converting all ammonia into non-volatile ammonium) or stabilized using full nitrification [322].	[71, 322]	287,
Volume reduction & urea recovery					
– dehydration wood ash	in fresh or stabilized urine	dry urea-based fertilizer	Fresh or stabilized urine is added to a bed of wood ash or biochar to dehydrate the urine by ventilation at elevated temperatures (35-60°C). The alkaline bed (pH >12.5) inhibits enzymatic urea hydrolysis during ventilation. Mass balance calculations and experiments demonstrated a volume reduction of >90%, while preserving 70-90% of the N [262, 263]	[262, 263]	
– bio-sorption	fresh urine	MACCS powder	Urea adsorbs onto microwave-activated carbonized coconut shells (MACCS).	[227]	
– evaporation	fresh urine	stabilized concentrated urine (with urea)	Fresh urine is concentrated by water evaporation on a gauze sheet. The accumulation of salts on the gauze sheet and in the concentrated product effectively inhibits urea hydrolysis.	[222]	
– isobutyl-aldehyde-diurea precipitation (IBDU)	fresh urine	isobutylaldehyde-diurea (IBDU)	Urea forms a complex with isobutyraldehyde (IBU), resulting in the precipitation of isobutylaldehydediurea (IBDU), a commercially available slow-release fertilizer.	[18]	

- | | | | | |
|---|---------------------------|----------------------------|---|------------|
| – forward osmosis (FO) and membrane distillation (MD) | fresh or stabilized urine | concentrated urea solution | Urea can be recovered from fresh or stabilized urine by a combination of FO and MD. Urea is first separated from the other urine compounds by FO. Subsequently, MD is used to concentrate the separated urea. | [242, 303] |
|---|---------------------------|----------------------------|---|------------|

Volume reduction & micropollutant removal

- | | | | | |
|-------------------------|---------------------------|--|---|---------------------|
| – electro dialysis (ED) | stored or nitrified urine | concentrated micropollutant-free nutrient solution | ED can be used to selectively extract the nutrients into a concentrated product stream while retaining the micropollutants (pharmaceuticals) in the diluate | [66, 229, 230, 233] |
|-------------------------|---------------------------|--|---|---------------------|

Volume reduction & TAN recovery

- | | | | | |
|--|--------------|--------------------------------|---|--------------|
| – ion exchange | stored urine | concentrated ammonium solution | Driven by the high TAN concentration, ammonium ions replace the counter-ions (e.g., sodium) on the negatively charged functional groups of a cation exchange resin (e.g., clinoptilolite, biochar). Subsequently, the ion exchange resin is regenerated by using concentrated acids (e.g., H_2SO_4) or salts (e.g., Na_2SO_4), exchanging ammonium ions by other cations (e.g., Na^+), creating a concentrated ammonium solution (e.g., $(NH_4)_2SO_4$). | [173, 281] |
| – ammonia stripping/ chemisorption and subsequent absorption | stored urine | concentrated ammonium solution | Ammonia can easily be removed from the liquid phase through air stripping and subsequently be absorbed in sulfuric acid to form ammonium sulfate. An additional pH increase can facilitate ammonia volatilization and hence increase the overall TAN recovery, and can be accomplished by base dosing or water reduction in an electrochemical cell. Liquid-liquid extraction (also called transmembrane chemisorption) employs a hydrophobic membrane with vacuum or gas-filled pores. | [8, 49, 178] |

– (bio)-electrochemical cells	fresh, stabilized or hydrolysed urine	nutrient-rich concentrate or ammonium solution	Different (bio)-electrochemical systems have been applied to produce value-added compounds from urine. The key mechanism is electromigration of nutrients from urine through ion exchange membranes towards another (often more concentrated) solution driven by an electrical field. The electrical field is created by redox reactions occurring at the electrodes (by applying electrical energy) or by electroactive bacteria in bio-electrochemical systems.	[95, 154, 155, 156, 158, 159, 166, 167]
Volume reduction & P recovery				
– (struvite) precipitation	stored urine	precipitate (e.g., struvite)	The pH increase caused by urea hydrolysis triggers precipitation of divalent cations with phosphate. Udert et al. (2003) identified struvite, hydroxyapatite and calcite as the main precipitates in stored urine. However, P recovery is limited by the calcium and magnesium concentration in urine. Addition of a magnesium source (e.g., MgO, Mg(OH) ₂ or MgCl ₂), will promote struvite precipitation, increasing the P recovery [142].	[8, 128, 142, 173, 250, 251, 315]
– ion exchange	stored urine	concentrated phosphate solution	By the use of anion exchange columns, phosphate can be adsorbed and subsequently be recovered.	[218]
Biostabilization (COD removal and N stabilization)				
– treatment in aerobic nitrification reactor	fresh, stabilized or stored urine	nitrate-rich solution, low in organics	Nitrification transforms volatile ammonia into nitrate and ammonium. Due to the limited alkalinity in urine, only about half of the TAN can be converted into nitrate, while the remaining TAN becomes protonated to non-volatile ammonium due to the acidification, yielding a slightly acidic ammonium nitrate solution. With base addition, all TAN can be converted into nitrate. Apart from nitrification, organics are removed by heterotrophic bacteria, reducing the biofouling potential of urine.	[56, 91, 97, 139, 219, 291, 295]

Energy recovery				
– microbial fuel cells (MFC)	fresh, stabilized or stored urine	electricity	Electroactive bacteria oxidize organic compounds in urine and transfer the electrons to the anode, generating a current.	[95, 129, 130]
Micropollutant removal				
– nanofiltration	post-treatment	micropollutant-free nutrient solution	Micropollutants are mostly retained by a nanofiltration membrane, whereas the mineral salts and nutrients can permeate.	[232]
– ozonation and advanced oxidation	post-treatment	micropollutant-free nutrient solution	Micropollutants can be oxidized with chlorine, chlorine dioxide, ozone (O ₃) or OH radicals	[186]
– adsorption on activated carbon or other absorbents	post-treatment	micropollutant-free nutrient solution	Micropollutants are adsorpted on activated carbon	[85]

Challenges for urine recycling in space

Implementation of urine recycling in RLSS for deep-space exploration requires the biology and technology to be compatible with the space conditions. Biological compatibility involves the survival and preserved functional activity of the key players in the recycling technology, for instance nitrifying bacteria, microalgae and higher plants. In space, living organisms are subjected to extreme and hostile conditions including broad ranges of gravity and ionizing radiation, both factors known to have a profound effect on the physiology, morphology and functionality [19, 53, 127, 214]. Without sufficient protection (shielding), radiation can induce random DNA damage and mutations, possibly causing alterations in gene expression, which can be detrimental for the growth and survival of microorganisms and plants [53, 74, 228, 317]. Exposure to variations in gravity, ranging from 'hyper gravity' during vehicle launch (3.2 *g*) and reentry (1.4 *g*), to reduced gravity at the lunar (0.17 *g*) and Martian (0.38 *g*) surface and even microgravity during orbital flight (10^{-6} *g*), brings about mainly indirect effects linked to the altered extracellular fluid properties affecting the nutrient acquisition and waste removal [19, 53, 74, 127, 146, 170, 317]. Flight experiments in LEO have demonstrated that higher plants are able to adapt to microgravity conditions, at least during one generation from seed to seed [228, 299, 317]. Also for microorganisms, the capacity to adapt to microgravity is well-established [170, 179]. Important with respect to urine recycling is the recent finding that the urea hydrolysis, nitrification and denitrification activity of both axenic cultures as mixed nitrifying communities could be restored after exposure to the microgravity and increased radiation conditions during a LEO flight experiment [134, 175].

Technological compatibility involves the adaptation of technology to microgravity or reduced gravity conditions, largely affecting fluid dynamics [53, 61, 74]. The reduced convection and strong cohesion forces in space make efficient gas-liquid interactions no longer possible with major consequences for aeration of bioreactors (Figure 1.9) [53, 61, 244]. Due to the lower diffusion rate of oxygen in water, oxygen transfer might become problematic. Hence, it is necessary to develop reactors with alternative aeration methods that ensure sufficient oxygen supply to the microorganisms to support their viability, growth and functionality such as the removal of TAN. A promising strategy in this regard is to grow the microorganisms in a biofilm based bioreactor with gas-permeable membranes to allow for a continuous replenishment of oxygen rich liquid [244, 279].

Moreover, each system developed for space should eventually comply with the basic rules for space design, including limited volume and mass, low consumable and energy input, a high level of automation to limit the workload of the crew and a high level of robustness, reliability and safety.

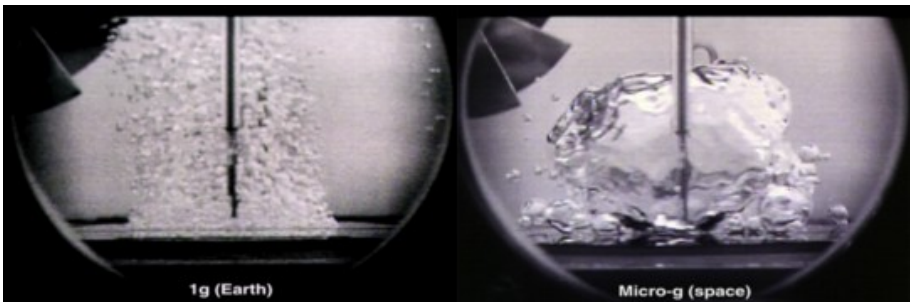


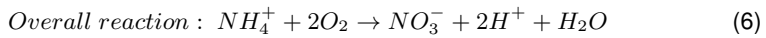
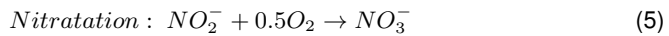
Figure 1.9: **A: aeration on Earth, B: aeration in microgravity. Image courtesy NASA Glenn Research Center.** On earth, small air bubbles are formed, providing a large contact area for oxygen diffusion from the gas phase to the liquid phase. In space, gravity forces are reduced and cohesion forces will dominate resulting in one big bubble. The transfer of oxygen mainly relies on diffusion in space.

1.4 Urine recycling technologies

1.4.1 Nitrification and biological COD oxidation

Nitrification

Nitrification is the two-step biological oxidation of TAN into nitrate (reaction 6), performed by two groups of aerobic chemolithoautotrophic bacteria, i.e., the ammonium oxidizing bacteria (AOB) and the nitrite oxidizing bacteria (NOB). These microorganisms use dissolved CO_2 as a carbon source for cell growth and obtain energy for maintenance and growth from oxidizing inorganic nitrogen compounds [181].



AOB oxidize TAN into nitrite (Reaction 5). This reaction is referred to as nitritation and is usually the rate limiting step in nitrification. The TAN oxidation occurs in two successive steps catalysed by two different enzymes. TAN is first oxidized to hydroxyl-amine (NH_2OH) and water by ammonia mono-oxygenase (AMO). Subsequently, a second key enzyme in AOB, hydroxylamine oxidoreductase (HAO), oxidizes hydroxylamine to nitric oxide, which further reacts with oxygen to nitrite (Figure 1.10) [37, 181]. Besides AOB, some archaea are known to oxidize TAN [148].

NOB are responsible for the oxidation of nitrite into nitrate (Reaction 4). This single step reaction is referred to as nitratation and is catalysed by the enzyme nitrite oxidoreductase (NOR) (Figure 1.10).

In both nitritation and nitratation, oxygen is reduced to water in the cytoplasm. Stoichiometrically, full nitrification to nitrate requires $4.57 \text{ mg O}_2 \text{ mg}^{-1} \text{ N}$. Electrons from the reduced nitrogen compounds enter an electron transport chain where they generate a proton motive force which drives ATP synthesis [181].

Nitrifiers (AOB and NOB) are present in many natural environments such as soils, estuaries, lakes, and marine ecosystems, and play a key role in the nitrogen cycle [181]. Nitrification also plays a pivotal role in WWTP, where it is combined with denitrification (nitrate reduction to N_2) to remove reactive nitrogen from wastewater. Beyond removal, nitrification (without subsequent denitrification) can facilitate nitrogen recovery from urine, by converting volatile ammonia into nitrate, a non-volatile non-toxic compound which can be valorized as a plant fertilizer. However, urine treatment in an aerobic nitrification bioreactor typically results in partial nitrification. This is not an issue, as the remaining ammonia becomes protonated to non-volatile ammonium.

Aerobic treatment also yields removal of organic compounds. COD is used as an energy and carbon source by heterotrophic bacteria. COD oxidation, using oxygen as electron acceptor, generates CO_2 and H_2O . Besides oxidation, part of the COD is assimilated into microbial biomass.

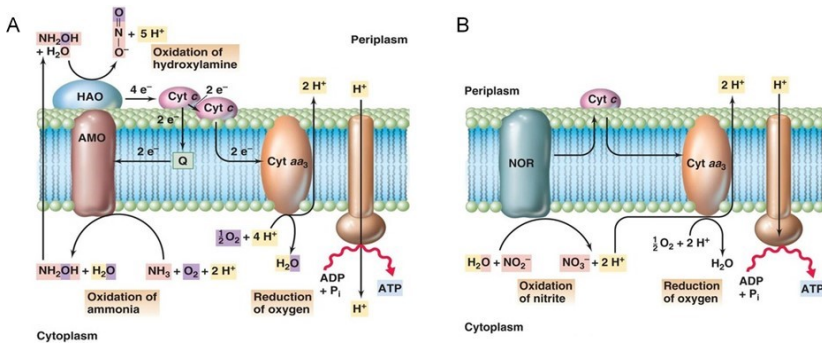


Figure 1.10: **A: Nitritation and electron flow in AOB. B: nitritation and electron flow in NOB.** Credit: Brock Biology of Microorganisms: International Edition, 12th ©2009 [181]. Reprinted by permission of Pearson Education, Inc. AMO: ammonia mono-oxygenase, HAO: hydroxylamine oxidoreductase, NOR: nitrite oxidoreductase.

Challenges for urine nitrification

The unique properties of urine present particular challenges for nitrification and influence the reactor design and operation (Table 1.2). The variable urine flow and composition, the high nitrogen concentration and salinity, and the limited alkalinity make urine nitrification prone to instabilities [83]. Carefully controlling the loading is key in preventing process upsets or failures. A sudden increase in N loading, for instance, often results in nitrite accumulation, as NOB cannot keep pace with the increased AOB activity (resulting from the higher substrate availability). Nitrite accumulation further inhibits AOB and NOB, especially at low pH, because of the increased fraction of free nitrous acid (FNA, i.e., HNO_2 , causing substrate inhibition in NOB and product inhibition in AOB) [83, 289]. Hence, overloading yields NH_4NO_2 instead of NH_4NO_3 [97, 274, 275, 291, 295]. Too low N loading rates, on the other hand, can promote the growth of acid-tolerant AOB, resulting in the production of harmful nitrogen oxide gases through chemical decomposition of nitrite [96]. The variable urine composition can also cause pH fluctuations in reactors without pH control. pH is an important process parameter in nitrification, as it directly affects the nitrification rates and determines the $\text{NH}_3/\text{NH}_4^+$ and $\text{HNO}_2/\text{NO}_2^-$ equilibria. Small changes in reactor pH can destabilize the sensitive balance between AOB and NOB, resulting in nitrite accumulation (as NOB are generally more sensitive to FA (Free Ammonia) and FNA accumulation) [289]. Hence, reliable pH control is essential. Carefully adjusting the influent flow rate based on the pH allows to control the pH and to adapt the loading based on the AOB activity [295]. The reactor receives a pulse of influent (hydrolysed urine) when the pH drops below a given set-point. The pH rapidly increases due to the alkalinity in the influent (influent pH ~ 9.2) and gradually decreases due to the proton release by AOB, until the next pulse of influent. Alternatively, the pH can be controlled in a narrow range with acid/base addition, enabling full nitrification.

Table 1.2: Overview of urine challenges and specificities, consequences for urine nitrification and potential solutions.

Urine challenge	Consequence	Solution
Variable flow	discontinuous influent supply → peak loading, likely resulting in TAN or nitrite accumulation	A buffer (equalization) tank can average out fluctuations in urine composition over time and donor, providing a constant influent flow with a more stable composition.
Variable composition	variable N concentration and alkalinity → fluctuations in N loading and pH, likely resulting in TAN or nitrite accumulation	A high hydraulic residence time (HRT) in the reactor can also help to minimize fluctuations (given the equalization by the reactor content) [83]
Urea hydrolysis	uncontrolled precipitation (P loss and scaling issues), NH ₃ volatilization (N loss), odor nuisance during collection/ storage → reduced recovery potential	Acid or base addition before storage can prevent urea hydrolysis. In combination with nitrification, base addition is more appropriate because of the alkalinity demand for nitrification in a later stage. Base addition will result in precipitation, and also increases the salinity of the urine. Alternatively, hydrolysed urine can be dosed to a nitrification reactor.
High N concentration (4-9 g N L ⁻¹ urine ⇔ ~40 mg N L ⁻¹ domestic wastewater)	<ul style="list-style-type: none"> – risk for rapid FA accumulation and subsequent AOB and NOB inhibition – high TAN concentrations are also known to reduce the growth rate of AOB [291] – overloading causes a TAN and pH increase, resulting in nitrite accumulation due to NOB inhibition by FA [44, 97, 291, 295]. 	As the maximum volumetric loading is defined by the nitrifying biomass concentration, a high HRT or dilution is required to avoid overloading, given the high N concentration. Dilution directly reduces the influent nitrogen concentration (and concentration of other compounds such as salts), whereas applying a high HRT (by feeding a small influent flow or by the use of a high reactor volume) results in a low N concentration in the reactor due to dilution by the reactor content (while the concentration of other compounds is not affected).

High salinity (urine matrix & due to caustic addition to prevent urea hydrolysis during storage or to obtain full nitrification)	<ul style="list-style-type: none"> – salt directly affects the growth rates of AOB and NOB, and hence the nitrification activity and the population structures/diversity [200, 291] – salt affects the maximum solubility of oxygen, which can lead to limited oxygen availability and hence indirectly influence the nitrification performance [200]. 	<p>Several studies showed that nitrifiers can adapt to high salinities, and that the best strategy is to gradually increase the salinity (e.g., by lowering the dilution) [15, 16]. Coppens et al. (2016) demonstrated that selection of a halotolerant inoculum can shorten the start-up time of a urine nitrification reactor with 54% compared to municipal activated sludge. The salinity can be lowered by dilution.</p>
Low alkalinity/N ratio	<p>Alkalinity is needed to counteract the proton release by nitritation (2 mol alkalinity per mol TAN) [295]. Urea hydrolysis releases 1 mol alkalinity per mol TAN [295]. Hence, without base addition, only ~50% of the TAN can be nitrified to nitrate. About 50% of the N remains present as TAN, which can cause FA inhibition when the pH suddenly increases (e.g., due to an increased N loading).</p>	<ul style="list-style-type: none"> – Full nitrification with base addition: Base can be added to provide additional alkalinity, enabling full nitrification (~1 mol OH⁻/mol N). This facilitates reactor operation (stable pH), but increases the salinity and implicates an additional cost and logistic requirements (base storage and dosing). – Partial nitrification without base addition: Without base addition, only ~50% of the TAN is nitrified to nitrate, yielding an ammonium nitrate solution [91, 291]. The remaining TAN can not volatilize due to the low pH. Because of the low pH and the TAN accumulation in the reactor, partial nitrification is more prone to instabilities.
Low COD/N ratio	<p>Urine has a high COD concentration (up to 10 g COD L⁻¹), but a low COD/N ratio because of the high N concentration (~1 g COD g⁻¹ N compared to > 10 g COD g⁻¹ N for domestic wastewater). Heterotrophic bacteria oxidize the biodegradable COD to CO₂ and compete with nitrifiers for oxygen (electron acceptor in nitrification and COD oxidation) [162]. Changes in COD and/or N concentration can disturb the balance between the autotrophic and heterotrophic reactor community. Oxygen limitation can result in TAN and/or nitrite accumulation.</p>	<p>Carefully monitor and control the dissolved oxygen concentration in the reactor to prevent oxygen limitation.</p>

Table 1.3: **Overview of urine nitrification reactors tested in literature.** CSTR: continuous stirred tank reactor, SBR: sequencing batch reactor, MBBR: moving bed biofilm reactor, MBR: membrane bioreactor, MABR: membrane aerated nitrification reactor. AS: activated sludge

Reactor type	CSTR		SBR					
Reference	Udert et al. 2003 [291]	Oosterhuis et al. 2009 ^a [219]	Udert et al. 2003 [291]	Jiang et al. 2011 [139]	Sun et al. 2012 [274]	Sun et al. 2012 [275]	Mackey et al. (2016) [180]	Chen et al. (2017) [44]
Endproduct	NH ₄ NO ₂ (1:1)	NaNO ₃	NH ₄ NO ₂ (1:1)	NaNO ₃	NH ₄ NO ₂ (1:1)	NH ₄ NO ₂ (0.1:0.9)	NaNO ₂	NH ₄ NO ₂ (1:1.24)
Inoculum	AS from nitrification experiment	AS from WWTP	AS from a denitrifying WWTP	preadapted AS from leachate treatment plant	mix of AS from WWTP and nitrifying AS enriched in lab	aerobic granules	sludge from secondary sewage treatment plant	AS from municipal WWTP
Chemical input	-	NaOH	-	Na ₂ CO ₃	-	-	NaHCO ₃	-
Volume [L]	2.8	2500	7.5	3	4.5	3.7	3.2	3.6
HRT [d]	4.8	17.5	4	1.25	-	-	0.25	1.5
SRT [d]	4.8	-	30-100	-	450 ± 50	-	-	20
Temperature [°C]	30.0 ± 0.4	15 - 25	24.5 ± 0.5	25	25	20 - 22	22 ± 2	-
DO [mg O ₂ L ⁻¹]	2.5 - 4	>2	2 - 4.5	>1.5	~ 2	2 - 5	>4	0 - 3
Influent	stored urine + NH ₃ & NH ₄ HCO ₃	stored urine	stored urine + NH ₃ & NH ₄ HCO ₃	stored urine (29%)	stored urine	stored urine (20%)	stored urine (>80% TAN/TN)	stored urine after P precipitation
TN [g N L ⁻¹]	7.3 ± 0.4	1	2.2 ± 0.1	1.5	2.5 ± 0.1	0.25	-	1800 - 3500
Effluent TAN [g N L ⁻¹]	3.9 ± 0.1	<0.1	1.1 ± 0.1	-	1.2	~0.05	-	0.68 ± 0.12
Effluent NO ₂ ⁻ [g N L ⁻¹]	3.9 ± 0.1	0	1.2 ± 0.1	-	1.3	0.15 - 0.25	-	0.82 ± 0.11
Effluent NO ₃ ⁻ [g N L ⁻¹]	0.06 ± 0.03	~1	0.03 ± 0.00	-	< 0.05	< 0.01	-	-
pH	6.9 ± 0.05	7	6.1 ± 0.05	7.3-7.6	6.4	-	7	6.8 ± 0.3
N loading rate [mg N L ⁻¹ d ⁻¹]	1580 ± 30	57	560 ± 30	1100	1250 ± 50	500	1002	1860
Nitrification (nitrification) rate [mg N L ⁻¹ d ⁻¹]	790 ± 20	56	280 ± 20	1096	625	450	-	1395
Nitrification efficiency [%]	50	98	50	99.6 ± 0.2	50	90 ± 7	93	75 ± 3
COD removal efficiency [%]	82 ± 5	-	82 ± 5	89.2 ± 1.1	75	74 ± 1	77 ± 12 (BOD)	85 - 90

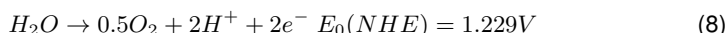
Reactor type	Packed bed	MBBR			MBR	submerged MBR		MABR
Reference	Feng et al. (2008) [91]	Udert et al. (2003) [291]	Etter et al. (2013) [83]	Bischel et al. (2015) [22]	Fumasoli et al. (2016) [97]	Sun et al. 2012 [274]	Coppens et al. (2016) [56]	Udert and Wächter (2012) [295]
Endproduct	NaNO ₃	NH ₄ NO ₃ (1:1)	NH ₄ NO ₃ (1:1)	NH ₄ NO ₃ (1:1)	NH ₄ NO ₃	NH ₄ NO ₂ (1:1)	NaNO ₃	NH ₄ NO ₃ (1:1.15)
Reactor specifications	26%v/v porous ceramic rings	50%v/v Kaldness	60%v/v Kaldness	50%v/v Kaldness, 1.63 m ²	60%v/v Kaldness	polyethylene HF	PVDF sheet	flat
Inoculum	commercially available nitrification product	colonized carriers from another nitrification Reactor	AS from the Eawag experimental WWTP	nitrified urine and carriers from urine nitrification reactor			AS from WWTP	from Eawag experimental WWTP
Chemical input	Na ₂ CO ₃	-	-	-	-	-	NaOH/HCl	-
Volume [L]	7.6	2.8	120	6.5	120	10	8	2.6
HRT [d]	14	9.5	2	20.7 ± 8.2	17	2	21	0.06
SRT [d]						300 ± 50		
Temperature [°C]	27	25.3 ± 0.5		19.1 ± 1.1	22.5 ± 0.6	35		23 ± 2
DO [mg O ₂ L ⁻¹]	4.2 - 5.1	3 - 5.2	6	>8	7	> 3	> 6	5.5 ± 0.5
Influent	fresh urine (10%)	stored urine + NH ₃ & NH ₄ HCO ₃	stored urine	stored urine	stored urine	(partly hydrolysed) urine	urine	stored urine
TN [g N L ⁻¹]	0.65	7.1 ± 0.1	1.8 ± 0.2	3.7 ± 0.2	4.1 ± 0.5	1 ± 0.2	6.3	2.4 ± 0.3
Effluent TAN [g N L ⁻¹]	0.03	3.75 ± 0.02	0.9 ± 0.1	2 ± 0.1	-	0.5	-	-
Effluent NO ₂ ⁻ [g N L ⁻¹]	-	<0.1	0.001	0.001	-	0.5	-	0.005
Effluent NO ₃ ⁻ [g N L ⁻¹]	0.6	3.73 ± 0.06	0.9 ± 0.2	6.1	6.0 ± 0.1	6.3	6.9 - 7.1	6.2 ± 0.1
pH	6.7 ± 0.1	6.3 ± 0.05	5.7 - 6.5					
N loading rate [mg N L ⁻¹ d ⁻¹]	46.5	750 ± 50	746	140 ± 30	239	500 ± 100	225 ± 33	134 ± 30
Nitrification (nitrification) rate [mg N L ⁻¹ d ⁻¹]	44.2	380 ± 30	420	70	120 ± 50	250	214	
Nitrification efficiency [%]	94.9 ± 1	50	50	50	50	50	95	
COD removal efficiency [%]		82 ± 5	90	89		75 ± 5	96	89 ± 27

1.4.2 (Bio)-electrochemical methods

Different (bio)-electrochemical systems have been applied to produce value-added compounds from urine. The key mechanism is electromigration of nutrients from urine through ion exchange membranes towards another (often more concentrated) solution driven by an electrical field.

Electrochemical cells

In electrochemical cells, the electrical field is created by applying electrical energy to establish redox reactions at the anode (positively charged electrode) and cathode (negatively charged electrode). Typically, water oxidation occurs at the anode producing O_2 and protons while water reduction at the cathode generates hydroxide ions and H_2 .



The electrode compartments can be separated by an ion exchange membrane (IEM). The electron flow induces ion migration through the IEM to ensure the charge balance. The transport through IEM is based on the Donnan exclusion mechanism [202]. Anion exchange membranes (AEM) consist of positively charged functional groups, often quaternary ammonium salts, attached to a crosslinked polymer, such as polystyrene-divinylbenzene. The fixed positive charge excludes positively charged ions (cations) and allows the passage of negatively charged ions (anions). The functional groups of cation exchange membranes (CEM) are usually sulfonic or carboxylic acid groups. Hence, these membranes are negatively charged and only cations can pass.

Electrochemical cells are mainly employed for TAN recovery from urine. The urine is fed to the anodic compartment, which is separated from the cathodic compartment by a CEM. Driven by the electrical field, ammonium (and other cations) migrate over the CEM towards the cathodic compartment, where ammonium is deprotonated to ammonia by the hydroxide ions produced at the cathode, allowing for ammonia stripping or chemisorption (Figure 1.11) [157]. The catholyte can be recirculated over stripping and absorption columns (containing sulfuric acid) to recover ammonia as ammonium sulfate [155, 178]. Alternatively, transmembrane chemisorption units (TMCS) for direct liquid-liquid extraction can be used to transfer ammonia from the catholyte to an acidic absorbant.

Besides TAN recovery, electrochemical cells can be used for in situ acid and base production, thereby obviating the need for acid/base dosing and storage (Chapter 4 and 5).

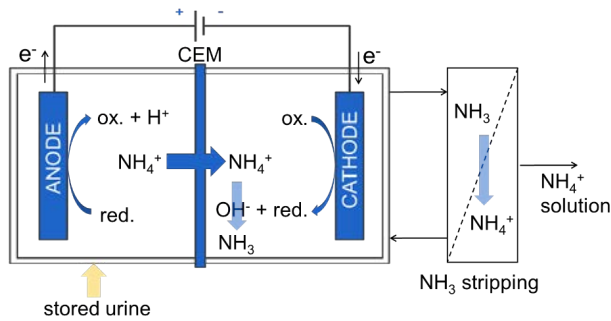


Figure 1.11: **Electrochemical cell for TAN recovery from urine.**

Bio-electrochemical systems

In bio-electrochemical systems, a current is generated by means of electroactive bacteria. In bio-anodes, electroactive bacteria oxidize organic substrates (COD) and transfer the electrons to the anode by direct contact (via membrane-bound cytochromes or nanowires) or by means of electron shuttles [238]. In microbial fuel cells (MFC), COD oxidation at the anode is coupled to the reduction of an electron acceptor with a higher electrode potential at the cathode (e.g., O_2 reduction), resulting in power production [238]. Microbial electrolysis cells (MEC), in contrast, generate hydrogen gas at the cathode (water reduction) by applying a small potential with an external power supply [238].

Similar to electrochemical cells, the electrical current induces ion migration, allowing for TAN extraction or nutrient concentration. In recent years, a large number of studies on bio-electrochemical treatment (MEC and MFC) of (synthetic) urine were published with the purpose of TAN recovery [95, 154, 158, 159, 167, 327] or energy recovery [50, 129, 130, 191, 256, 306, 326]

Electrodialysis

Electrodialysis (ED) is an electrochemical membrane separation process with an electrical potential gradient as the driving force to separate charged ions from an aqueous solution. An electrical current is created through electrochemical reactions occurring at the two electrode surfaces, which drives charged ions to the oppositely charged electrode. This transport is facilitated by IEM which act as a selective barrier. An ED unit or 'stack' consists of multiple AEM and CEM in an alternating pattern between the two electrodes (Figure 1.12). Due to the electrical field, the red cation in Figure 1.12 is attracted to the cathode and will pass through the CEM on the right hand side. Since the cation cannot migrate through the AEM, it is trapped in that compartment. The blue anion in Figure 1.12 will migrate through the AEM towards the anode but is retained by the following CEM. As a consequence, ions will be depleted in alternating compartments resulting in a diluted stream, 'the diluate', whereas ions will accumulate

in the neighbouring compartments forming the 'concentrate'. Uncharged molecules are not attracted to the electrodes and thus stay in the feed stream [202, 271].

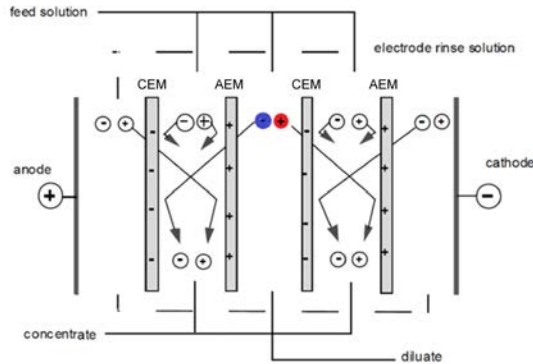


Figure 1.12: **Principle of electrodialysis. Adapted from Mulder (1996).**

ED has been implemented at large scale ($>20\,000\text{ m}^3\text{ d}^{-1}$), mostly for desalination of brackish water and demineralization of industrial process water [271]. A few studies report on urine treatment with ED for the purpose of i) water recovery [31] or NaCl recovery [10, 11] in space life support systems, ii) micropollutants removal [82] and iii) nutrient recovery and concentration for use as a fertilizer [229, 230, 233]. The dense nature of the ED membranes typically results in a high retention of pathogens and micropollutants in the diluate or on the membrane [82, 229, 231], whereas nutrients are captured and concentrated in the concentrate (achieving concentration factors of up to 4) [233]. Pronk et al. (2006) [230] combined an ED unit with bipolar membranes with an ammonia column or membrane stripping unit to capture TAN in an acidic stream. By the use of BPM, an acidic concentrate rich in carbonate and phosphate and an alkaline concentrate rich in TAN and potassium were produced in the ED unit. Subsequently, ammonia was stripped from the alkaline concentrate using a recirculating gas stream or a gas-transfer membrane and dissolved in the acidic concentrate, resulting in an acidic ammonium phosphate rich concentrate. However, the low pH could only be maintained at low TAN recoveries [230]. Tice and colleagues used a combination of a MEC and ED membrane stack to achieve energy-efficient nutrient concentration [283]. COD oxidation at the anode provided the electrical current, while multiple cell pairs (AEM-CEM) increased the rate and degree of ionic separation [283].

1.4.3 Valorization of urine-derived products

Urine derived fertilizers for plant production

Depending on the processing technology, nutrients (e.g., N and/or P) are extracted from urine and can be used as a raw material for fertilizer production, or urine is turned into a stable (concentrated) fertilizer solution, containing macronutrients and other elements

essential to plant growth. Aurin is currently the only commercially available urine-based fertilizer (developed and commercialised by VUNA, Switzerland). It is produced by partial nitrification, activated carbon adsorption and distillation and is approved by the Swiss Federal Office for Agriculture as a universal plant fertilizer. Urine precipitates, such as hydroxyapatite and struvite, are also believed to be good slow-release fertilizers, especially on acidic soils [294].

Microbial protein production

Besides the use of urine-derived fertilizers for plant production, urine can be valorized as a nutrient source for microbial protein (MP) production [49, 56, 89]. In recent years, MP, i.e., the protein-rich biomass of cultivated microorganisms including fungi (yeasts and others), bacteria and microalgae, has gained great interest as a more sustainable alternative to plant and animal protein [226]. In contrast to plants and animals, microorganisms can be highly efficient in their nutrient conversions and can be cultured in fully controlled bioreactors at high volumetric biomass production rates, enabling near full nutrient recycling from a recovered stream with a minimal land usage [52, 87, 300]. Microbial biomass has the highest protein content among organisms (50-70% of their cell dry weight) and is furthermore rich in vitamins, minerals and potentially prebiotic compounds [210]. After cell growth, the biomass is harvested and undergoes some downstream processing such as washing, extraction, purification and/or concentration [9, 210]. Depending on the production process and the final quality, MP may be used as food, feed for livestock or as slow release organic fertilizer (providing organic nitrogen and carbon to arable land) [225]. Examples of commercial MP include QuornTM (fungi *Fusarium venenatum*) and *Spirulina* (members of the genera *Arthrospira*, or, as recently proposed by Nowicka-Krawczyk et al. (2019), *Limnospira*).

Microalgae use light as an energy source and inorganic CO₂ and nutrients to produce organic compounds via photosynthesis. The most widely-produced microalgae is *Spirulina*, filamentous cyanobacteria, rich in protein (46-71% protein on a dry weight basis), vitamins, minerals, β -carotene, essential fatty acids and antioxidants. *Spirulina* has been cultivated for centuries as a food supplement by tribes in Africa and in Mexico. *Spirulina* also plays a key role in the photosynthetic compartment (IVa) of the MELiSSA loop, where O₂ and microbial biomass are produced from nitrate (effluent CIII) and CO₂ (produced by the crew and other compartments). Several studies reported successful growth of *Spirulina* on highly diluted (nitrified) urine [41, 56, 89, 90, 323]. Batch culture experiments by Feng et al. (2007) and Coppens et al. (2016) demonstrated that nitrified urine is a better growth medium compared to fresh or stored urine. Besides *Spirulina*, *Chlorella* species have been cultivated on urine [284, 285].

Source-separated urine has also been used as a nitrogen source for the cultivation of chemolithoautotrophic bacteria, such as hydrogen oxidizing bacteria (HOB) [49]. HOB grow on inorganic CO₂ as carbon source, H₂ as energy source and mostly TAN as N source.

1.5 Research outline

Besides optimizing the use of nutrients in agriculture, recovery and recycling will be key in the future to catch up with the growing food demand as current fertilizer production is pushing the Earth's life support system to its planetary boundaries. Nutrient recovery from 'waste streams' could shorten the nutrient cycles, thereby reducing the need for energy intensive ammonia production using the Haber-Bosch process and mining of non-renewable P and K. Urine is one of the targeted waste streams, as it presents the major nutrient source in domestic wastewater and has good fertilizing properties. Urine recycling is also of key interest for the purpose of nutrient and water recovery in regenerative life support systems for deep-space exploration.

Urine collection, treatment and reuse is challenged by the instability of urine. Urea, the main nitrogen compound in urine, quickly hydrolyses into ammonia, ammonium and (bi)carbonate, causing nutrient losses, odor nuisance, scaling and clogging by uncontrolled precipitation, and ammonia volatilization. The latter can pose a health risk to the crew in a small space cabin, as ammonia is a toxic gas. Clogging of pipes by the precipitating salts is a common problem in nonwater urinals and urine-diverting toilets, and it is believed to be one of the major barriers for the widespread implementation of source separation. The presence of calcium and magnesium can also cause problems during further downstream urine treatment, e.g., through scaling on membranes (used in electrodialysis, (bio)-electrochemical systems...). The biofouling potential, caused by the presence of biodegradable organics in urine, further challenges urine treatment and reuse.

The aim of this PhD thesis was to develop resource-efficient urine recycling technologies that can be implemented in MELiSSA or used for on-site/decentralized urine treatment on Earth. As resources are scarce in space, the goal was to achieve maximum nitrogen recovery with minimum energy expenditure and use of consumables in order to minimize the need for resupply. Different urine treatment trains combining biological and physicochemical processes were investigated. A nitrification bioreactor was the core process in all urine treatment trains, yielding a stable nitrate-rich urine solution low in organics, while preserving the nutrient content. Given the discontinuous nature of urine supplies, the high variability in composition and the fact that nitrifiers are very susceptible to peak loadings, storage in an equalization tank is important in order to provide a constant influent flow and loading to the bioreactor. To prevent urea hydrolysis during storage, alkalization (OH^- addition to increase the pH to 12) is an essential step. The pH increase also yields precipitation of divalent cations, minimizing the scaling potential during downstream processing. The nitrified urine can be valorized as a fertilizer in agriculture, as a culture medium for microalgae or as a raw material in the fertilizer industry. An additional concentration step can be included to decrease the volume and hence the transportation costs.

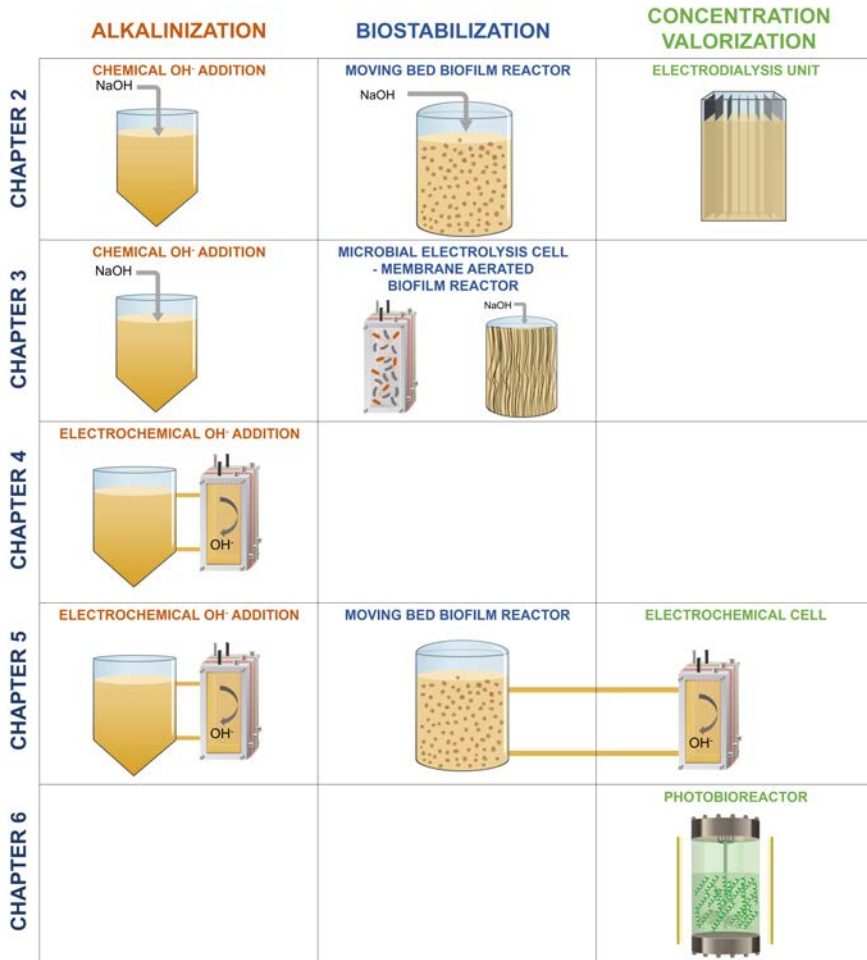


Figure 1.13: Overview of the different PhD chapters.

In **Chapter 2**, alkalization and a nitrification bioreactor were combined with electro-dialysis (ED) to capture the nutrients in a concentrated product. A pilot installation was operated at two different urine dilution factors to study the effect of a lower urine dilution and thus a higher salinity on the nitrification and ED.

Chapter 3 investigates the use of a hollow fiber membrane-aerated biofilm reactor (MABR) for urine nitrification, given its high oxygen utilization efficiency, compact design and compatibility with the reduced gravity conditions in space. In order to maximize the nitrogen recovery at minimum energy expenditure, the COD was removed in a microbial electrolysis cell (MEC) prior to the MABR. Two MEC configurations were evaluated in terms of COD removal, current production and nitrogen recovery, at a range of hydraulic residence times and COD loads. The performance of the MABR was evaluated with

and without MEC pre-treatment.

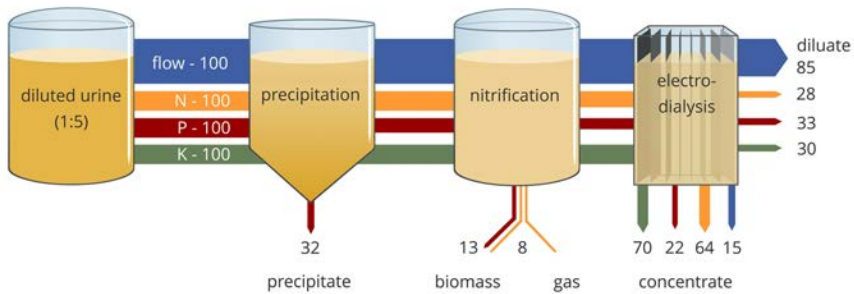
In **Chapter 4**, a chemical-free electrochemical alternative to base addition for alkalinization was evaluated. Four different configurations of an electrochemical cell were compared in terms of pH increase, energy requirement, divalent cation and phosphate removal, and ion migration. Stabilization was assessed by storing the effluent (at pH 11 and pH 12) and measuring the pH, electrical conductivity and TAN concentration over time.

Full urine nitrification (conversion of all TAN into nitrate) is preferred over partial nitrification because of the higher process stability and safety (ammonium nitrate is thermally instable), but requires base addition to compensate for the proton release by nitrification. An electrochemical cell was coupled to a nitrification reactor in **Chapter 5** to study in-situ electrochemical hydroxide production as an alternative to base addition, enabling full nitrification while avoiding the use of chemicals (bases), the logistics associated with base storage and dosing, and the associated increase in salinity. Moreover, concentration and extraction of the produced nitrate by means of migration through the ion exchange membrane separating the different compartments and flows of the electrochemical cell was explored. Three different configurations were tested at different pH set points and/or concentration factors.

The nitrified urine produced in chapter 5 was used in **Chapter 6** as a growth medium for *Limnospira*, a cyanobacterium that can be used as slow-release fertilizer, feed or food. The growth of *Limnospira* on nitrified urine was first compared to the growth on standard synthetic medium in a batch culture experiment, by monitoring the optical density, dry weight, nitrate and phosphate uptake, and protein content of the biomass. In order to improve the nitrogen utilization efficiency, the nitrified urine was supplemented with, amongst others, phosphate, calcium, magnesium and iron. Different mixtures were composed and evaluated in batch culture experiments in order to identify the limiting compound(s) in the nitrified urine. Subsequently, the growth on the optimized nitrified urine solution was evaluated in a continuous photobioreactor.

Chapter 7 summarizes the main research outcomes and identifies the strengths, future challenges and potential bottlenecks of the explored technologies. For both terrestrial decentralized urine treatment and urine recycling in a RLSS, the most optimal combination of technologies is identified. Furthermore, a concrete design is presented in a case study on Earth and in space. The chapter also provides an outlook with future optimization strategies and remaining challenges.

Refinery and concentration of nutrients from urine with electro dialysis enabled by upstream precipitation and nitrification



This chapter has been redrafted after:

De Paepe, J., Lindeboom, R.E.F., Vanoppen, M., De Paepe, K., Demey, D., Coessens, W., Lamaze, B., Verliefe, A.R.D., Clauwaert, P. and Vlaeminck, S.E. Refinery and concentration of nutrients from urine with electro dialysis enabled by upstream precipitation and nitrification. *Water Research* 144 (2018), 76-86.

2

Refinery and concentration of nutrients from urine with electro dialysis enabled by upstream precipitation and nitrification

Abstract

Human urine is a valuable resource for nutrient recovery, given its high levels of nitrogen, phosphorus and potassium, but the compositional complexity of urine presents a challenge for an energy-efficient concentration and refinery of nutrients. In this study, a pilot installation combining precipitation, nitrification and electro dialysis (ED), designed for one person equivalent (1.2 L of urine d⁻¹), was continuously operated for ~7 months. First, NaOH addition yielded calcium and magnesium precipitation, preventing scaling in ED. Second, a moving bed biofilm reactor oxidized organics, preventing downstream biofouling, and yielded complete nitrification on diluted urine (20-40%, i.e. dilution factors 5 and 2.5) at an average loading rate of 215 mg N L⁻¹ d⁻¹. Batch tests demonstrated the halotolerance of the nitrifying community, with nitrification rates not affected up to an electrical conductivity of 40 mS cm⁻¹ and gradually decreasing, yet ongoing, activity up to 96 mS cm⁻¹ at 18% of the maximum rate. Next-generation 16S rRNA gene amplicon sequencing revealed that switching from a synthetic influent to real urine induced a profound shift in microbial community and that the AOB community was dominated by halophilic species closely related to *Nitrosomonas aestuarii* and *Nitrosomonas marina*. Third, nitrate, phosphate and potassium in the filtered (0.1 μm) bioreactor effluent were concentrated by factors 4.3, 2.6 and 4.6, respectively, with ED. Doubling the urine concentration from 20% to 40% further increased the ED recovery efficiency by ~10%. Batch experiments at pH 6, 7 and 8 indicated a more efficient phosphate transport to the concentrate at pH 7. The newly proposed three-stage strategy opens opportunities for energy- and chemical-efficient nutrient recovery from urine. Precipitation and nitrification enabled the long-term continuous operation of ED on fresh urine requiring minimal maintenance, which has, to the best of our knowledge, never been achieved before.

2.1 Introduction

Fertilizers are pivotal in meeting the global food demand. At present, fertilizer production mainly relies on the use of non-renewable energy (to produce ammonia) and finite natural resources, such as phosphate rock and potassium minerals [167]. The growing world population, the limited resources and the environmental burden of eutrophication demand a paradigm shift towards recovery and reuse of nutrients [300]. Recently, source-separated urine has gained great interest as a valuable resource of nutrients, given its relatively high concentration in macronutrients ($\sim 9 \text{ g N L}^{-1}$, 0.7 g P L^{-1} and 2 g K L^{-1}) [294]. Efficient nutrient recovery from source-separated urine could provide an estimated 20% of the nitrogen, phosphorus and potassium for the current fertilizer production in the EU [153, 167]. Since urine is often diluted with flushing water, it is important to concentrate the nutrients in order to reduce transport and storage volumes and to facilitate the recovery of nutrients [186]. Numerous technologies have been proposed to separate and/or concentrate nutrients from urine. However, none of these technologies are capable of capturing the broad urine nutrient spectrum in a micropollutant-free fertilizer in a scalable, energy- and chemical-efficient manner. Evaporation, reverse osmosis, freeze-thawing and nitrification-distillation are energy-intensive, microbial fuel cells are difficult to scale up, whereas struvite precipitation, NH_3 stripping and ion exchange only target specific nutrients (i.e., N or P) [167, 186, 283, 295]. In order to fill this gap, electrodialysis (ED) was selected in the present study.

ED is a membrane separation process with an electric potential gradient as the driving force to separate charged ions from an aqueous solution. Anion and cation exchange membranes compartmentalise the system, producing two effluent streams, an ion-depleted diluate and ion-accumulating concentrate stream. ED has been implemented at large scale ($>20\,000 \text{ m}^3 \text{ d}^{-1}$), mostly for desalination of brackish water and demineralization of industrial process water [271]. A few studies report on urine treatment with ED for the purpose of i) water recovery [31] or urine desalination [11] in space life support systems, ii) micropollutant removal [82] and iii) nutrient recovery [229, 230, 233]. Operating an ED stack on urine is challenging due to the high calcium and magnesium concentration and the high organic load, which can cause scaling and biofouling on the membranes, and clogging of spacers and tubing. As a consequence, the reduced flux and increasing resistance in the stack are limiting factors in achieving high efficiencies [194]. Thus far, autoclaved, filtered urine [11] or urine pre-treated with charcoal adsorption [31] or microfiltration [229, 230] has been used in short-term ED experiments. Only one study addressed the long-term (>3 months), interrupted operation (short operation times of 1-2 weeks) of an ED stack on real, hydrolysed urine [233]. The desalination rate, however, decreased with approximately 50% over a period of 195 days due to fouling [233].

Disadvantages of using hydrolysed urine include uncontrolled precipitation of phosphorus and volatilization of ammonia during storage, leading to phosphorus and nitrogen losses and malodor [186, 292, 293]. Enzymatic urea hydrolysis can be prevented during

storage through addition of acids, metals, caustics... [240, 243]. In the present study, fresh urine was used and scaling and biofouling were prevented by a combination of precipitation and an aerobic bioreactor. Calcium and magnesium were removed in a precipitation reactor in which NaOH was dosed to increase the pH to 11, shifting the speciation of phosphate and carbonate ions, causing supersaturation and thus triggering precipitation. Subsequently, the urine was treated in an aerobic bioreactor. The purpose of the bioreactor was to i) convert biodegradable organics into CO₂ and sludge by heterotrophic bacteria, thereby reducing the biofouling potential in ED, and ii) to convert urea (~85% of the nitrogen in fresh urine) into nitrate through ammonification followed by nitrification. In addition, nitrification decreases the pH, leading to undersaturation, thereby preventing further precipitation in ED.

Ammonification, or the hydrolysis of urea to bicarbonate and total ammonia nitrogen (ammonium-N and ammonia-N), is initiated by the urease enzyme, produced by many heterotrophic bacteria and some nitrifiers [68, 149, 197]. The nitrification process consists of ammonium oxidizing bacteria (AOB) converting ammonium into nitrite ('nitritation') followed by the oxidation of the nitrite into nitrate ('nitrataion') by nitrite oxidizing bacteria (NOB). Nitrification is a well-documented stabilization method of urine as nitrate is a stable molecule, in contrast to ammonia, which upon volatilization causes significant malodor and nitrogen losses [56, 91, 291, 295]. Additionally, nitrate is the preferred nitrogen species for recovery as it is a charged molecule which can be captured in the ED concentrate, and, in a lot of cases, the preferred nitrogen fertilizer for plants [182].

The integration of precipitation, nitrification and ED to refine and concentrate nutrients from fresh urine of one person equivalent was, for the first time, evaluated in an automated pilot-scale installation during four months on a 20% urine solution (i.e., dilution factor of 5). As upstream precipitation and nitrification enable ED to act as a key recovery stage, all units are considered equally important. The installation was operated for another 40 days on a 40% urine solution (i.e., dilution factor of 2.5) to study the effect of a lower urine dilution and thus a higher salinity on the nitrification and ED. The microbial community on the biofilm carriers of the nitrification reactor was followed up over time through next-generation amplicon sequencing of the 16S rRNA gene. To study the impact of salinity on the maximum nitritation and nitrataion rates of the biofilm, batch experiments were performed in which carriers were exposed to salinities between 20 and 96 mS cm⁻¹. Furthermore, a batch experiment was carried out on ED to investigate whether the phosphate recovery in ED was influenced by the pH of the ED feed stream. Three different pH values (in the pH range of nitrification) were tested: pH 6, 7 and 8.

2.2 Materials and methods

2.2.1 Automated treatment train

Precipitation reactor

Diluted human urine was dosed to the precipitation reactor (Figure 2.1) based on a level control PLC (programmable logic controller, Siemens Simatic HMI) feedback loop, in which detection of low level initiated pumping and high level stopped pumping. The pH was controlled at 11 by dosing 2M NaOH and the temperature was controlled at 40°C by means of a heating and stirring plate. The content of the reactor was continuously recycled (3 L h^{-1}) by a peristaltic pump to enhance the formation and growth of crystals. To prevent precipitate from entering the bioreactor, urine was passed through a dead-end filter basket with glass fiber cloth and two filters ($10 \mu\text{m}$ and $0.2 \mu\text{m}$).

Nitrification bioreactor

Nitrification and COD oxidation occurred in a moving bed biofilm reactor (MBBR) filled for 20% (v/v) with polyvinyl alcohol beads and integrated in a membrane bioreactor (MBR) with an external ultrafiltration (UF) module (Figure 2.2). The reactor received effluent from the precipitation reactor when the level dropped below 30.7 L. The pH was controlled between 6.7 and 6.8 by dosing 2M NaOH or 1M HCl. Aeration (dissolved oxygen (DO) level $> 2 \text{ mg O}_2 \text{ L}^{-1}$) and mixing were provided by injection of pressurized ambient air. The UF module consisted of three $0.1 \mu\text{m}$ sidestream tubular $\alpha\text{-Al}_2\text{O}_3$ membranes with a total surface area of 0.057 m^2 placed inside a stainless steel module and was operated at a crossflow velocity of 0.5 m s^{-1} . The UF filtrate was dosed to the diluate tank of the ED unit, the UF retentate was recirculated to the bioreactor. When the pressure over the UF membrane increased ($> 1 \text{ bar}$), the filtration module was disconnected and cleaned by recirculating a 1% P110 (alkaline) and a 1% P73 (acid) ultrasil solution (Ecolab, MN, USA).

Electrodialysis unit

The ED unit (Figure 2.3) contained electrolyte, diluate and concentrate tanks next to a PCCell ED 64004 stack (PCA GmbH, Heusweiler, Germany). The stack comprised 10 cell pairs with standard PC SA anion and PC SK cation exchange membranes with an active membrane area of 64 cm^2 and 0.45 mm thick silicone/polyethylene spacers (PCA GmbH, Heusweiler, Germany). The electrodes were stretched titanium, coated with a mixed metal oxide platinum/iridium coating for the cathode/anode, respectively (PCA GmbH, Heusweiler, Germany). A 1M NaNO_3 electrode rinsing solution was circulated in the electrode compartments over the electrolyte tank. The diluate and concentrate were circulated at a constant flow rate (1 L min^{-1}) between the tank and stack. The concentrate was drained when the level or the conductivity in the concentrate tank exceeded the threshold (2 L or 70 mS cm^{-1} , respectively). The diluate tank was

continuously filled with the filtrate of the bioreactor and partially drained when the level in the tank exceeded 2.1 L. The current of the power supply was controlled at 80-90% of the limiting current density (LCD). The LCD was determined according to the method described by Mulder (1996) [202] using the electrical conductivity (EC) of the ED diluate. When the potential difference surmounted 10 V (about three times the nominal value), the stack was cleaned in place by recirculating a 0.1% oxonia solution and a 0.01 M HCl solution through the diluate and concentrate compartments.

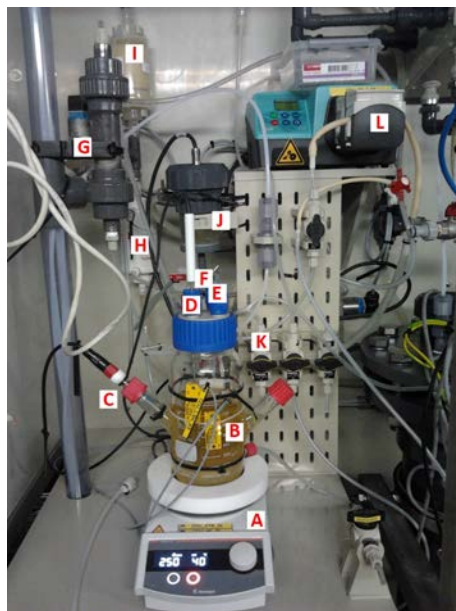


Figure 2.1: **Precipitation reactor.**

A: magnetic stirring and heating plate (MR Hei-Tec, Heidolf, Schwabach, Germany)

B: level sensor (BC10-QF5,5-AP6X2, Turck, Mülheim an der Ruhr, Germany)

C: pH sensor (pH electrode 5334T w/ Pt1000, Hach, CO, USA)

D: temperature sensor

E: influent inlet

F: NaOH dosage with electromagnetic metering pump (EWN-B11 CER, Iwaki Co, Ltd., Tokyo, Japan (not shown))

G: filter basket with glass fiber cloth

H: filter (Kleenpak KA3J100P6 (10 μm), Pall Corporation, NY, USA)

I: filter (Kleenpak KA3NFP6S (0.2 μm), Pall Corporation, NY, USA)

J: dead-end filter basket with electrical conductivity probe (Cond cell 5396, Hach, CO, USA)

K: sample point

L: recycle and feed pump (Model 323E/D, Watson Marlow, MA, USA)

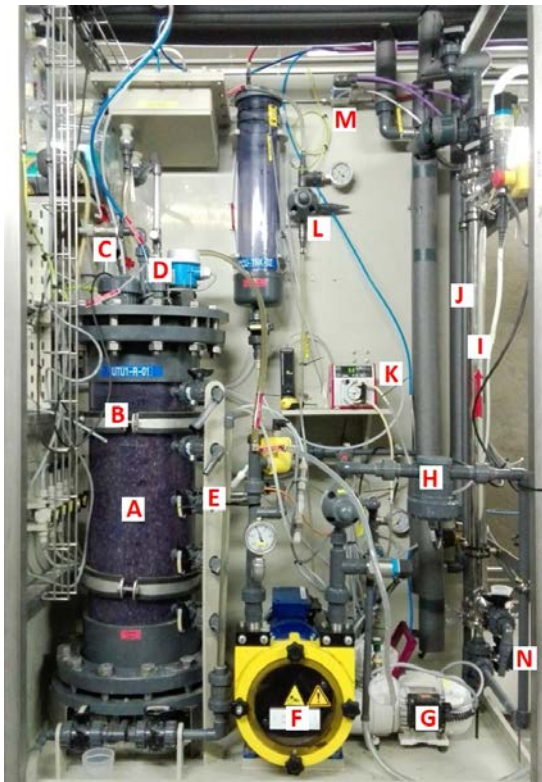


Figure 2.2: **Moving bed biofilm reactor.**

- A: bioreactor with polyvinyl alcohol beads (Kuraray Aqua Co, Ltd., Tokyo, Japan)
- B: pH sensor (Polymetron 8350 series, Hach, CO, USA)
- C: influent inlet (effluent of precipitation reactor)
- D: NaOH dosage with electromagnetic metering pump (EWN-B11 CER, Iwaki Co, Ltd., Tokyo, Japan (not shown))
- E: sample point
- F: recirculation pump (Peristaltic pump AMP Series, Boyser pumps, Barcelona, Spain)
- G: compressor aerator (KNF N035AN.18, KNF, Freiburg, Germany)
- H: EC sensor (Cond cell 5396, Hach, CO, USA) in recirculation loop
- I: ultrafiltration (UF) membrane module (type 1/6, ATech-Innovations GmbH, Gladbeck, Germany)
- J: bypass
- K: filtration pump (120U/D1, Watson Marlow, MA, USA)
- L: pressure relief valve (V185, Frank GmbH, Hessen, Germany)
- M: mass flow meter and controller (LIQUI-FLOW, Bronkhorst, Ruurlo, The Netherlands)
- N: sample point UF filtrate

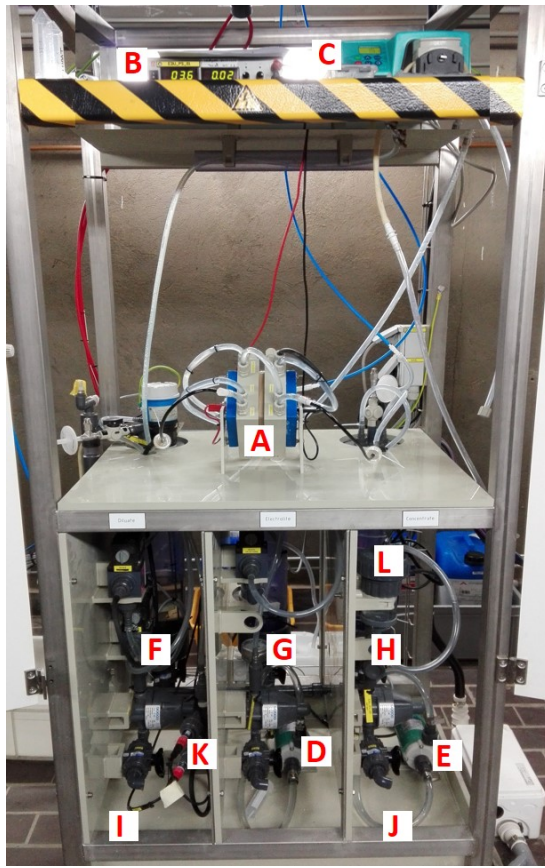


Figure 2.3: **Electrodialysis (ED) unit.**

- A: ED stack (PCCell ED 64004, PCA GmbH, Heusweiler, Germany)
- B: power supply (Type ES300, Delta elektronika BV, Zierikzee, The Netherlands)
- C: recirculation pump diluate (Model 323E/D, Watson Marlow, MA, USA)
- D: recirculation pump electrolyte (MD-15RM-230GS, Iwaki Co, Ltd., Tokyo, Japan)
- E: recirculation pump concentrate (MD-15RM-230GS, Iwaki Co, Ltd., Tokyo, Japan)
- F: diluate tank
- G: electrolyte tank
- H: concentrate tank
- I: sample point diluate
- J: sample point concentrate
- K: pH and EC sensor diluate (pH electrode 5334T w/ Pt1000 and Cond cell 5396, Hach, CO, USA)
- L: EC probe concentrate (Cond cell 5396, Hach, CO, USA)

2.2.2 Operation

Urine collection

Urine from male donors not taking medication, was collected in a nonwater urinal and stored in a freezer (-20°C). Urine collection was approved by the Ethical committee of Ghent University hospital under registration number B670201523246. Before feeding to the precipitation reactor, the urine was thawed and preserved at 4°C. Demineralized water was added to simulate dilutions that would be obtained with flush water. The installation was operated during four months on a 20% urine solution. Daily, 1.2 L of urine and 4.6 L of demineralized water were separately fed into the system and mixed in the precipitation reactor. To study the effect of a higher salinity on the nitrification and the recovery efficiencies and concentration factors of the ED, the installation was operated using a 40% urine solution (1.3 L d⁻¹ of urine mixed with 2.2 L d⁻¹ of demineralized water) for two months.

Reactor inoculation

Based on the inoculum screening described by Coppens et al. (2016) [56], three inoculum sources (urine nitrification, OLAND and commercial aquaculture inoculum) were selected to inoculate a cultivation reactor, used to establish a nitrifying biofilm on the beads. The cultivation reactor (22L) was operated as an MBBR and received a synthetic influent with a salinity around 10 mS cm⁻¹ consisting of 0.7 g N L⁻¹ (as (NH₄)₂SO₄), 7.6 g NaHCO₃ L⁻¹, 25 mg P L⁻¹ (as KH₂PO₄), 27 mg N L⁻¹ (as NaNO₂), 104 mg COD L⁻¹ (as sodium acetate) and 2.5 g NaCl L⁻¹, dissolved in tap water. Prior to operating as MBBR, the cultivation reactor was operated for several months as a sequencing batch reactor (SBR). The initial influent composition was based on the information provided by the suppliers of the inoculum and gradually tuned, also using batch assays, towards maximizing nitrification and nitrification rates, while maintaining the cultures' functionality for ureolysis and COD removal at slightly saline conditions. The additional nitrite was used to create a slight overcapacity in nitrification compared to nitrification to minimize nitrite toxicity risks during start up. The volumetric nitrogen loading rate amounted to 165 mg N L⁻¹ d⁻¹. The pH was between pH 6.5-8.0 (NaHCO₃ buffer) and oxygen was continuously supplied with an aquarium pump (DO > 2 mg O₂ L⁻¹). An average hydraulic retention time (HRT) of 4.4 days was applied to ensure sufficient selective pressure for biofilm growth by washing out the suspended biomass. The bioreactor of the pilot installation was inoculated with beads from the cultivation reactor.

Automation, operation and sampling

The pilot installation was equipped with pH, DO and EC electrodes connected to an SC1000 controller (Hach, CO, USA). An online TAN analyser (AMTAX sc, Hach, CO, USA) continuously monitored the TAN concentration in the UF filtrate of the bioreactor.

The process parameters were automatically logged and controlled by a PLC (Siemens Simatic HMI), allowing an automated operation of the installation. Additionally, samples were taken daily at different positions in the installation through sampling ports, filtered over a 0.20 μm Chromafil Xtra filter (Macherey-Nagel, PA, USA) and stored in the fridge (4°C) prior to analysis. The operational conditions during the tests on a 20% and 40% urine solution are presented in Table 2.1.

2.2.3 Nitrification batch activity tests at different salinities

To determine the salt tolerance of ureolytic bacteria, AOB and NOB on the beads, Erlenmeyer flasks were filled with 200 mL beads and 300 mL mixed liquor from the bioreactor (operated using a 40% urine solution and an EC around 20 mS cm^{-1}). The EC was increased by adding a salt mix (1/5 NaCl and 4/5 NaNO_3 on a mass basis) to the Erlenmeyer flasks. Five different salt additions were tested: 0, 20, 40, 60 and 80 g salt L^{-1} mixed liquor resulting in an EC of 20, 39, 58, 77 and 96 mS cm^{-1} . The ureolysis rate was determined by adding urea (50 mg N L^{-1}) and allylthiourea (250 mg L^{-1} , to inhibit TAN oxidation) to the Erlenmeyer flasks. AOB activity was analysed by adding 2.5 mL of urine and 0.5 g $\text{NaHCO}_3 \text{ L}^{-1}$. NOB activity was determined by spiking the flasks with NaNO_2 (50 mg N L^{-1}). The tests were performed in triplicate in a room controlled at 28°C. The flasks were covered with parafilm to prevent evaporation and shaken at 130 rpm using an orbital shaker (Innova 2300, New Brunswick, The Netherlands) to provide aeration. Samples were taken at a 30 minute time interval. Afterwards, they were filtered (0.20 μm Chromafil Xtra filter, Macherey-Nagel, PA, USA) and stored in the fridge. TAN and nitrite concentrations were determined spectrophotometrically with a Tecan infinite plate reader (Infinite F50 Absorbance Microplate Reader, Tecan Trading AG, Männedorf, Switzerland) according to the Berthelot reaction (at 690 nm) and Montgomery reaction (at 540 nm), respectively [32, 198]. The experiments lasted between 3h (at low salinity) and 24h (at high salinity). Activity rates were derived from the slope of the TAN (ureolytic and AOB activity) or nitrite concentration (NOB activity) in function of time. A linear model was fitted to the data in R using the 'stats' package (version 3.4.0) [236]. Prior to formal hypothesis testing, the assumptions of homoscedasticity and normality of the residuals were visually assessed and confirmed with the Bartlett test and Shapiro test in R.

Table 2.1: **Operational conditions for the precipitation reactor, nitrification bioreactor and electro dialysis (ED) unit during operation using a 20% and 40% urine solutions.** Average values and standard deviations are based on a period of 100 days operating using a 20% urine solution and 40 days operating using a 40% urine solution. HRT: hydraulic retention time; EC: electrical conductivity; DO: dissolved oxygen.

	precipitation reactor		nitrification reactor		ED diluate		ED concentrate	
urine solution [vol%]	20%	40%	20%	40%	20%	40%	20%	40%
Volume [L]	0.8-1		30		1.8-2.1		0.5-2	
Flow rate [$L d^{-1}$]	5.8	3.5	5.8	3.5	5.1	2.8	0.7	0.7
HRT [h or d]	4 h	6.8 h	5 d	8.6 d	8 h	14 h	2 - 3 d	2 - 3 d
pH [-]	10.8 ± 0.6	10.9 ± 0.2	6.7 ± 0.4	6.8 ± 0.1	6.2 ± 0.3	6.9 ± 0.2		
EC [$mS cm^{-1}$]	7.6 ± 2.4	14.6 ± 2.5	10.5 ± 1.2	17.3 ± 1.1	5.1 ± 1.8	5.5 ± 0.4	43.4 ± 9.5	59.6 ± 5.8
DO [$mg O_2 L^{-1}$]			6.3 ± 2.0	5.6 ± 1.8				
Temperature [°C]	39.8 ± 6.1	40.2 ± 5.7	20.8 ± 1.3	22.3 ± 1.4	22.7 ± 2.3	22.6 ± 1.8		
Potential [V]					4.1 ± 2.1	3.9 ± 0.6		
Current [A]					0.05 ± 0.03	0.06 ± 0.01		

2.2.4 ED batch phosphate transport experiment

A batch experiment on the ED unit was performed in order to investigate the influence of the diluate pH on the phosphate transport to the concentrate. The diluate tank was filled with 2 L of UF filtrate with an EC around 20 mS cm^{-1} at the start of each experiment and the pH was adapted with HCl or NaOH to a pH of 6, 7 or 8. The concentrate tank was filled with 1.5 L of demineralized water. The current of the power supply was automatically controlled at 90% of the LCD based on the EC of the diluate. The current, voltage, pH of the diluate and EC of the diluate and concentrate were continuously monitored throughout the experiment. Samples were taken at a 30 or 60 minute time interval, at the beginning and end of the batch experiment, respectively. Afterwards, they were filtered ($0.20 \mu\text{m}$ Chromafil Xtra filter, Macherey-Nagel, PA, USA) and stored in the fridge (4°C) prior to analysis. The experiments were ended after 7h (EC diluate $< 2.3 \text{ mS cm}^{-1}$).

2.2.5 Analytical methods

Chloride, nitrite, nitrate, sulfate and phosphate were analysed with anion chromatography (930 Compact IC Flex with Metrosep A supp 5-150/4.0 column and conductivity detector, Metrohm, Herisau, Switzerland). Sodium, TAN and potassium were measured using cation chromatography (761 Compact IC with Metrosep C6-250/4.0 column and conductivity detector, Metrohm, Herisau, Switzerland). Calcium and magnesium concentrations were analysed by means of flame atomic absorption spectrometry (Shimadzu AA-6300, Shimadzu, Kyoto, Japan). The samples were diluted and acidified with 1% nitric acid and 2% of lanthanum solution. COD was determined with Nanocolor test tubes (Nanocolor COD 15000, Macherey-Nagel, PA, USA) in unfiltered samples. Total Kjeldahl nitrogen (TKN) was analysed according to standard methods [115].

2.2.6 Microbial community analysis

Samples of the biofilm carriers from the cultivation reactor and pilot reactor were collected throughout the experiment for microbial community analysis. A distinction was made between 'young' yellowish beads and 'mature' brownish beads based on a visual colour difference. The 'young' beads developed their colour under the autotrophic conditions of the cultivation reactor and this colour typically matured into brownish upon several weeks exposure to the heterotrophic real urine conditions in the pilot reactor (Figure S2.1). The beads were stored at -80°C . For each sampling time point, three beads were pooled for DNA extraction using the method described by De Paepe et al. (2017) [67]. DNA extracts were sent out to LGC Genomics (Teddington, UK) for library preparation and sequencing of the V3-V4 region of the 16S rRNA gene on an Illumina Miseq platform. The sequence data are deposited at the NCBI (National Center for Biotechnology Information) database under accession number SRP111125. The data was processed using the mothur software package (v.1.38.0) [259] as outlined by

De Paepe et al. (2017) [67] and described in SI Section 2.6.1.

2.3 Results

2.3.1 Precipitation on a 20% urine solution

To prevent scaling in the ED stack, removal of calcium and magnesium was targeted in the precipitation reactor. The fivefold dilution (20% urine solution) resulted in influent concentrations of $31 \pm 10 \text{ mg Ca}^{2+} \text{ L}^{-1}$ and $11 \pm 5 \text{ mg Mg}^{2+} \text{ L}^{-1}$. Precipitation lowered the concentrations to $1.9 \pm 1.0 \text{ mg Ca}^{2+} \text{ L}^{-1}$ (94% reduction) and $1.6 \pm 0.4 \text{ mg Mg}^{2+} \text{ L}^{-1}$ (84% reduction). Concomitantly, 32% of the phosphate and 17% of the sulfate was precipitated. The sodium concentration increased threefold due to the dosage of NaOH to increase the pH. The TAN concentration increased by a factor of 2.4, indicating that some ureolysis occurred in the influent tubing or in the precipitation reactor despite the high pH.

2.3.2 Nitrification bioreactor

Operation using a 20% urine solution

In the bioreactor, organic nitrogen and TAN were converted into nitrate in order to stabilize the urine and to be able to capture the nitrogen in a non-volatile form in ED. On average, 1.2 L d^{-1} of urine with an average TKN concentration of 5.4 g N L^{-1} (before dilution) was treated, which corresponded to a volumetric nitrogen loading rate of $214 \pm 85 \text{ mg N L}^{-1} \text{ d}^{-1}$. Approximately one third of the TKN was already hydrolysed to TAN before the urine entered the bioreactor (Figure 2.4A+B). On average 92% of the nitrogen present in the influent was converted into nitrate (Figure 2.4A+D). Some nitrogen (<1%) was not fully nitrified and was still present under the form of TAN or nitrite in the effluent (Figure 2.4B+C). The missing nitrogen (<8%) was most likely lost in the precipitation reactor and the bioreactor due to struvite precipitation, ammonia stripping and assimilation by the biomass, and also denitrification or N_2O production could not be excluded. The time series data, presented in SI Figure S2.3, showed effluent concentrations below $0.5 \text{ mg TAN L}^{-1}$ during 55% of the operation time and below 5 mg TAN L^{-1} during 80% of the time. Only during reactor upsets (pH control failure or influent dosing problems), the concentration increased above 20 mg TAN L^{-1} . Another purpose of the bioreactor was to remove the organic matter in order to prevent biofouling in ED. The chemical oxygen demand (COD) in the influent and effluent of the bioreactor was $818 \pm 214 \text{ mg COD L}^{-1}$ and $65 \pm 13 \text{ mg COD L}^{-1}$, respectively, which corresponds to a removal percentage of 92%.

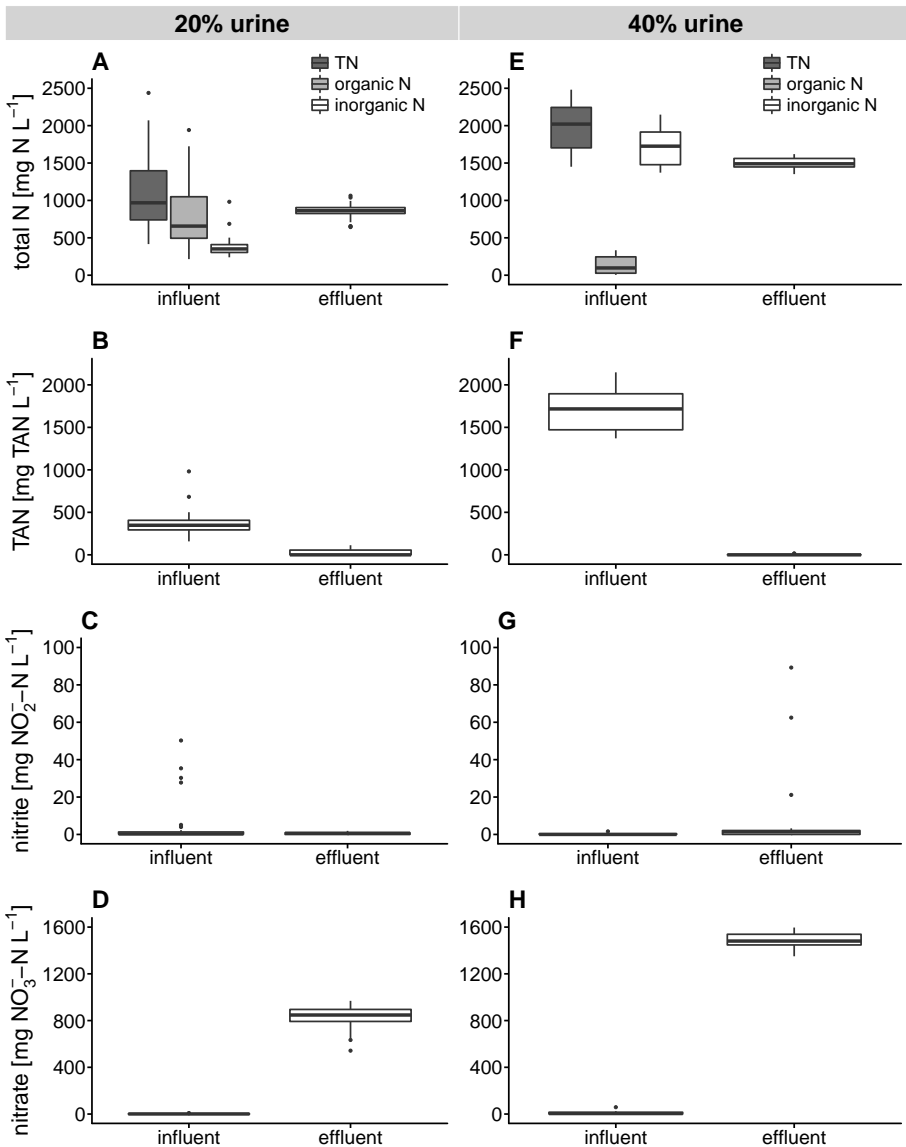


Figure 2.4: Nitrogen concentrations in the influent and effluent of the bioreactor on 20% and 40% urine solutions. Total nitrogen (TN) is calculated as the sum of total Kjeldahl nitrogen (TKN), $\text{NO}_2^- \text{-N}$ and $\text{NO}_3^- \text{-N}$. Organic N is calculated by subtracting total ammonia nitrogen (TAN) from TKN. Inorganic N equals the sum of TAN, $\text{NO}_2^- \text{-N}$ and $\text{NO}_3^- \text{-N}$. Samples were analysed over a period of 100 days on a 20% urine solution ($n=35$) and over a period of 40 days on a 40% urine solution ($n=16$). The box-and-whisker plots depict the minimum, first quartile, median, third quartile, maximum and outlying points ($>1.5 \times$ interquartile range).

Operation using a 40% urine solution

The bioreactor was operated using a 40% urine solution to study the effect of a higher salinity on the nitrification. To maintain the same nitrogen loading rate of $215 \text{ mg N L}^{-1} \text{ d}^{-1}$, the total influent rate was decreased from 5.8 to 3.5 L d^{-1} . As a consequence, the HRT increased from 5.0 to 8.6 days and the influent concentrations of the different ions doubled compared to the test on a 20% urine solution, increasing the EC in the bioreactor to $17.3 \pm 1.1 \text{ mS cm}^{-1}$ (compared to $10.5 \pm 1.2 \text{ mS cm}^{-1}$ in the test on a 20% urine solution). The fraction of organic nitrogen in the influent was considerably lower compared to the period on a 20% urine solution (Figure 2.4E), which is probably due to ureolysis as a result of the longer residence time in the influent line or in the precipitation reactor. No residual TAN or nitrite were detected in the effluent of the bioreactor (Figure 2.4F+G), apart from accumulations on day 16 ($21 \text{ mg NO}_2^- \text{-N L}^{-1}$), day 27 ($62 \text{ mg NO}_2^- \text{-N L}^{-1}$) and day 28 (16 mg TAN L^{-1} and $89 \text{ mg NO}_2^- \text{-N L}^{-1}$) resulting from technical upsets. The nitrate concentration in the effluent reached $1477 \pm 81 \text{ mg NO}_3^- \text{-N L}^{-1}$ (almost double compared to the test on a 20% urine solution) (Figure 2.4H). Again, 91% of the COD was removed but due to the higher influent concentration, the average COD in the effluent was more than twice higher ($158 \text{ mg COD L}^{-1}$ instead of 65 mg COD L^{-1}) compared to the period on a 20% urine solution.

Halotolerance of the nitrifying biofilm

The short-term effect of a higher EC on the maximum ureolysis, nitrification and nitrification rates was investigated in a batch experiment in which the beads were exposed to short-term salt stress by adding a salt mix of NaCl and NaNO_3 . The ureolysis rate decreased by 52% from $1249 \text{ mg N L}^{-1} \text{ d}^{-1}$ at an EC of 20 mS cm^{-1} to $600 \text{ mg N L}^{-1} \text{ d}^{-1}$ at an EC of 96 mS cm^{-1} (Figure 2.5). The nitrification rate was barely affected at low EC ($<58 \text{ mS cm}^{-1}$) but decreased with 77% between an EC of 58 mS cm^{-1} and 96 mS cm^{-1} . The nitrification activity decreased almost linearly ($p=3\text{e-}8$, R^2 of 0.91) with more than 96% between 20 and 96 mS cm^{-1} . The ureolysis/nitrification ratio increased whereas the nitrification/nitrification ratio decreased at higher salt concentrations. Although the NOB activity was most severely affected at high EC, nitrification remained the rate limiting process at high EC.

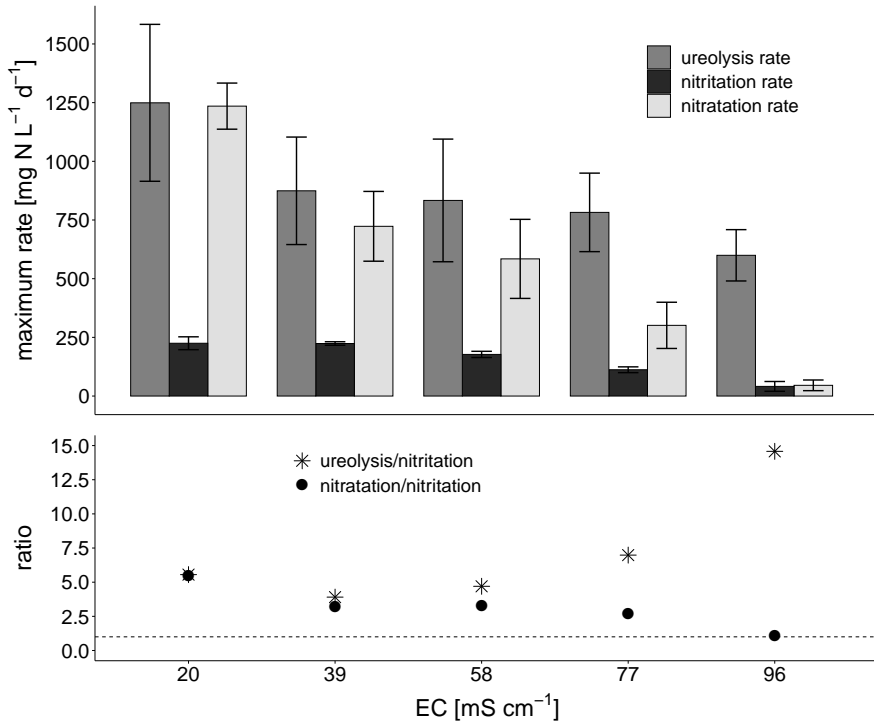


Figure 2.5: **Maximum ureolysis, nitritation and nitratation rates and ratios as a function of electrical conductivity (EC).** The error bars display the standard deviation ($n=3$).

Microbial community composition

The microbial community colonizing the beads in the cultivation reactor and pilot reactor was followed up over time through next-generation 16S rRNA gene amplicon sequencing to track the influence of a synthetic urine solution versus the complex urine matrix. The microbial community at phylum level was dominated by *Proteobacteria* ($70 \pm 10\%$) and *Bacteroidetes* ($23 \pm 9\%$), while *Acidobacteria* gradually increased over time (up to 15% in the pilot reactor) (SI Figure S2.4). The most abundant families were *Moraxellaceae*, *Comamonadaceae*, *Xanthomonadaceae*, *Chitinophagaceae* and the most prevalent genera included *Acinetobacter*, *Luteimonas*, *Nitrosomonas* and *Comamonas* (SI Figures S2.5-S2.6). Approximately 30% of the community could not be classified at the genus level. The most dominant OTUs (Operational Taxonomic Unit) were related to *Acinetobacter venetianus* (OTU1), *Comamonas* sp. (OTU2), *Luteimonas aquatica* (OTU3) and *Nitrosomonas* sp. (OTU4) (SI Table S2.2, SI Figure S2.7).

A principle coordinate analysis (PCoA) of the microbial community on the beads of the cultivation reactor and pilot reactor at the OTU level (Figure 2.6) revealed how the reactor-specific microbial community developed over time. After start-up and

stabilization, samples originating from the same reactor (cultivation reactor or pilot reactor) are clustered together. The cultivation reactor, operated using a synthetic influent, was characterized by the dominance of *Acinetobacter*. On the other hand, *Comamonas*, *Luteimonas* and *Ferruginibacter* were more characteristic for the pilot reactor (SI Figure S2.6). Samples of the pilot reactor were more scattered and the observed shifts coincided with shifts in the influent composition, as demonstrated by the arrows in Figure 2.6. *Acinetobacter*, *Comamonas* and *Ferruginibacter* became more established on the beads when the influent was shifted from the urea solution to real urine, whereas *Azoarcus* and *Dokdonella* disappeared. During operation using a 20% urine solution, the relative abundance of *Luteimonas* and *Nitrosomonas* gradually increased. Changing the influent back to a synthetic ammonium sulfate solution between the two experiments (to maintain the microbial culture), resulted in a decreased relative abundance of *Acinetobacter* and further increased abundance of *Luteimonas*. Feeding the pilot reactor with a 40% urine solution afterwards, led to an increased enrichment of *Comamonas* on the beads.

Nitrosomonas was the sole known AOB genus present in the cultivation reactor and pilot reactor, with a total relative abundance around 7%. Further classification using NCBI BLAST, RDP SeqMatch and a maximum likelihood phylogenetic tree indicated that the key players in the AOB community were closely related to *N. aestuarii*, *N. marina*, *N. europaea* and *N. ureae* (SI Table S2.2, SI Figures S2.8-S2.9). OTU4, which showed the highest sequence identity to *N. aestuarii/marina*, was the most abundant AOB with relative abundances reaching up to 90% in some samples. Interestingly, OTU24, most similar to *N. europaea*, which is only moderately halotolerant, was replaced by more halophilic *N. aestuarii/marina/ureae*-like organisms in the pilot reactor when the influent was shifted from a synthetic influent to real urine. When the influent was changed back to a synthetic ammonium sulfate solution, OTU81 and OTU91 (most similar to *N. halophila* and *N. ureae*, respectively) proportionally increased but disappeared when the reactor was operated again on real urine (40%). 158 *Bradyrhizobiaceae* (family including NOB) related OTUs were found in the microbial community, but individual OTUs were <1% of the sequenced community (SI Figure S2.5). Neither qPCR gave sufficient results to draw conclusions from.

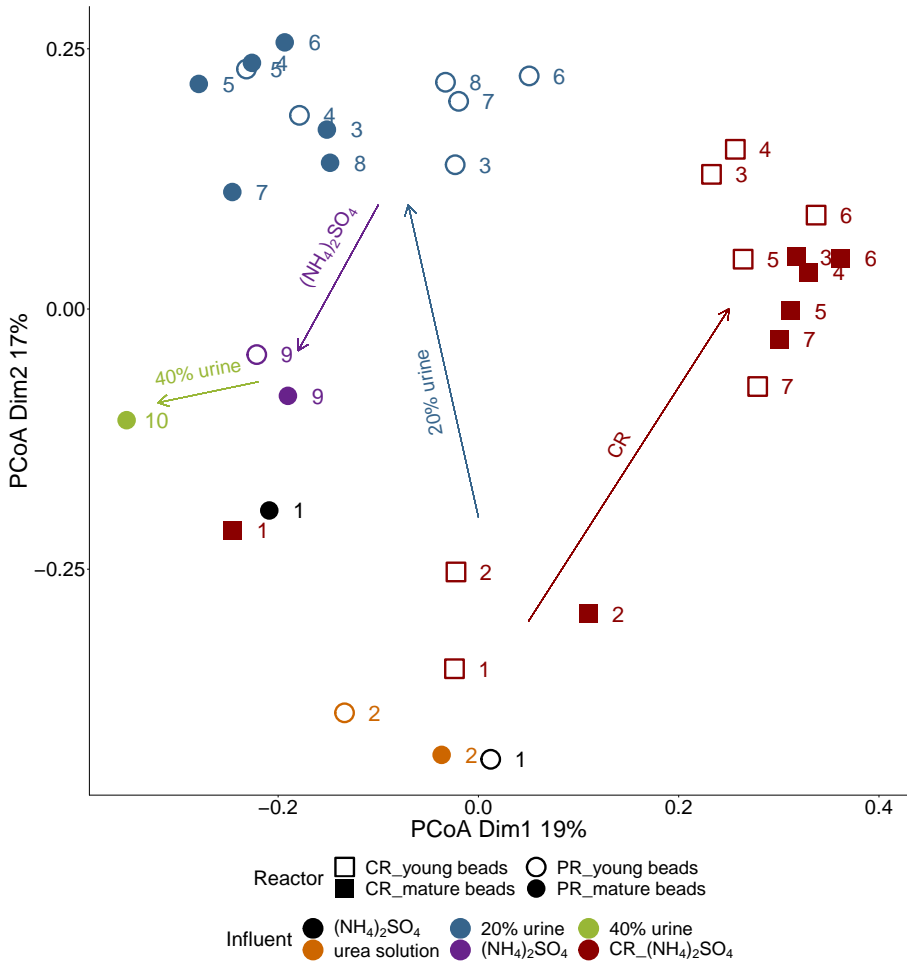


Figure 2.6: Principle coordinate analysis (PCoA) biplot of the microbial community composition on the beads in the cultivation reactor (CR) and pilot reactor (PR) at the OTU level, based on the Jaccard distances as determined by next-generation 16S rRNA gene amplicon sequencing. Each sample is indicated by a symbol with a shape according to the reactor and bead and a colour according to the influent composition. A visual distinction was made between mature and young beads based on the difference in colour of the beads (Figure S2.1). The numbers (1-10) correspond to the sampling day (day 1, 37, 72, 86, 100, 114, 135, 156, 218 and 259). Day 1 refers to the day of the first sample, corresponding to, respectively, 150 days and 1 day after start-up of the cultivation reactor and pilot reactor.

2.3.3 Electrodialysis

Operation using a 20% urine solution

The effluent of the bioreactor, with an EC of $10.5 \pm 1.2 \text{ mS cm}^{-1}$, was fed into the ED to concentrate the nutrients. The predominant ions in the feed stream of the ED were sodium (of which $>75\%$ originated from the NaOH dosage in the precipitation reactor and nitrification reactor), nitrate (due to nitrification), chloride and potassium (Figure 2.7A). By applying an electric field, on average 4.1 L d^{-1} of diluate with an EC of $5.1 \pm 1.8 \text{ mS cm}^{-1}$ and 0.7 L d^{-1} of concentrate with an EC around 50 mS cm^{-1} was produced. The average recovery efficiencies (Figure 2.7C) varied between 40% and 74% with the highest efficiency for sulfate (74%), followed by potassium (71%) and nitrate (70%). Only 40% of the phosphate in the feed stream was transported to the concentrate stream. Sodium and nitrate made up the largest fraction of the transported ions, corresponding to respectively 47% and 35% of the total molar transport, whereas phosphate and sulfate contributed less than 1% to the absolute molar transport. In general, the concentrations in the concentrate were 4-5 times higher than the concentrations in the feed stream (Figure 2.7D), while only phosphate had a lower concentration factor (2.6).

Operation using a 40% urine solution

Increasing the urine concentration from a 20% to 40% urine solution, almost doubled the ion concentrations and the EC of the feed stream to the ED, but the volumetric salt loading rate remained the same (Figure 2.7B, SI Table S2.3). ED produced on average 2.8 L d^{-1} diluate and 0.7 L d^{-1} concentrate with an EC value of around 5.5 mS cm^{-1} and 60 mS cm^{-1} , respectively. The recovery efficiencies increased by 7% to 14% but the concentration factors of each ion decreased (Figure 2.7C+D). The coulombic efficiency is compared in SI Table S2.3.

Influence of pH on phosphate transport in ED

The recovery efficiency of phosphate in ED was significantly lower compared to the other ions. Transfer of phosphate through membranes is challenging due to its large size (high molecular mass and large hydration shell resulting in a high Stokes radius) and low diffusion rate in water (SI Table S2.5). It was hypothesized that the phosphate transfer to the concentrate could be enhanced by increasing the pH in the diluate since the dominant phosphate species shifts from H_2PO_4^- to HPO_4^{2-} between a pH of 6 and 8 (SI Table S2.6). Generally, the higher the charge of an ion, the more the ion is susceptible to the electric field and thus the larger the driving force in the bulk solution (Nernst-Planck). This hypothesis was addressed in a batch experiment in which three different pH values were tested. Since nitrate and chloride removal should not be pH dependent, these ions were used as a reference to confirm whether the difference in recovery efficiency of phosphate could be attributed to the pH difference and not to technical variability between the tests. Phosphate transfer was clearly influenced by the pH as opposed to

nitrate and chloride transfer (Figure 2.8, SI Figure S2.10). After an electric charge of 2500 Coulomb (C) had passed through the ED, 29%, 54% and 31% of phosphate was removed from the diluate at a pH of 6, 7 and 8, respectively, yielding pH 7 as optimum.

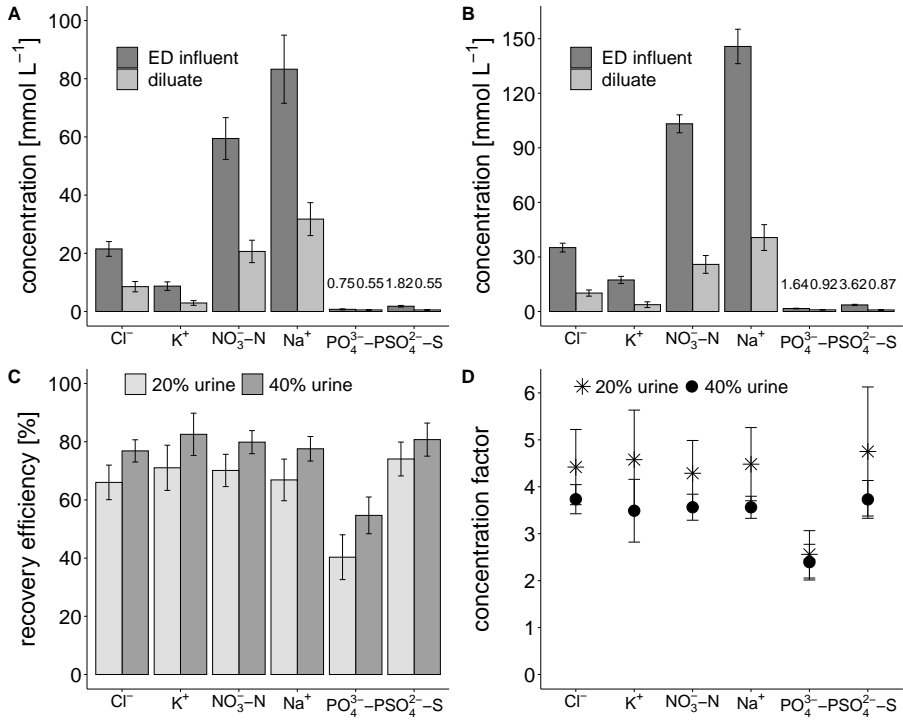


Figure 2.7: **Performance of the electro dialysis (ED) unit on 20% and 40% urine solutions.** Each plot displays average values and standard deviations, based on 35 samples over 100 days using a 20% urine solution and 16 samples over 40 days operating using a 40% urine solution.

A) Concentration in the ED influent and diluate during operation using a 20% urine solution.

B) Concentration in the ED influent and diluate during operation using a 40% urine solution.

C) Recovery efficiency, calculated by dividing the difference in mass of an ion between the feed stream (ED influent) and diluate by the mass of the ion in the feed stream.

D) Concentration factor, calculated by dividing the ion concentration in the concentrate stream by the concentration in the feed stream (ED influent).

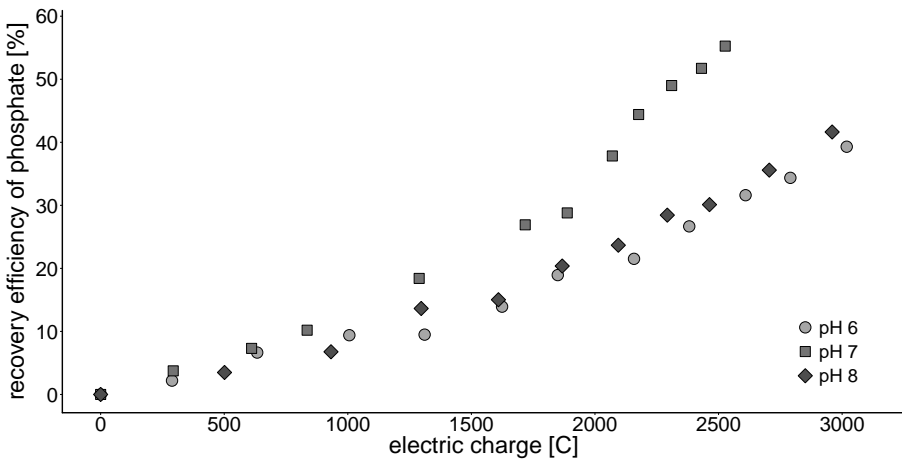


Figure 2.8: **Recovery efficiency of phosphate in function of the cumulative electric charge that passed through the stack in the ED batch experiment at pH 6, 7 and 8.** The cumulative electric charge (in Coulomb) was calculated by multiplying the applied current and time ($Q_{i+1}=Q_i + I_{i+1} \times (t_{i+1}-t_i)$). The recovery efficiency was calculated by dividing the difference in phosphate concentration in the diluate at time t and t_0 by the phosphate concentration at t_0 .

Recovery of N, P and K

The aim of this study was to determine the recovery potential of the nutrients in urine based on the performance of the pilot installation. During operation using a 20% urine solution, on average 32% of the phosphate-P was captured in precipitates. In total, 64% of the nitrogen, 22% of the phosphorus and 70% of the potassium were captured in the concentrate. On average, 29% of the nitrogen, 33% of the phosphorus and 30% of the potassium remained in the diluate (Figure 2.9A-C). About 8% of the nitrogen was not recovered, as mentioned in Section 2.3.2. The concentrate contained on average 3.7 g $\text{NO}_3^- \text{-N L}^{-1}$, 1.5 g $\text{K}^+ \text{L}^{-1}$ and 0.06 g $\text{PO}_4^{3-} \text{-P L}^{-1}$. On a 40% urine solution, 29% of the phosphate-P was captured in precipitates. In total, 70% of the nitrogen, 38% of the phosphate-P and 83% of the potassium were captured in the concentrate. On average, 17% of the nitrogen, 32% of the phosphate-P and 17% of the potassium remained in the diluate (Figure 2.9D-F). About 13% of the nitrogen was lost. The concentrate contained on average 5.1 g $\text{NO}_3^- \text{-N L}^{-1}$, 2.3 g $\text{K}^+ \text{L}^{-1}$ and 0.06 g $\text{PO}_4^{3-} \text{-P L}^{-1}$.

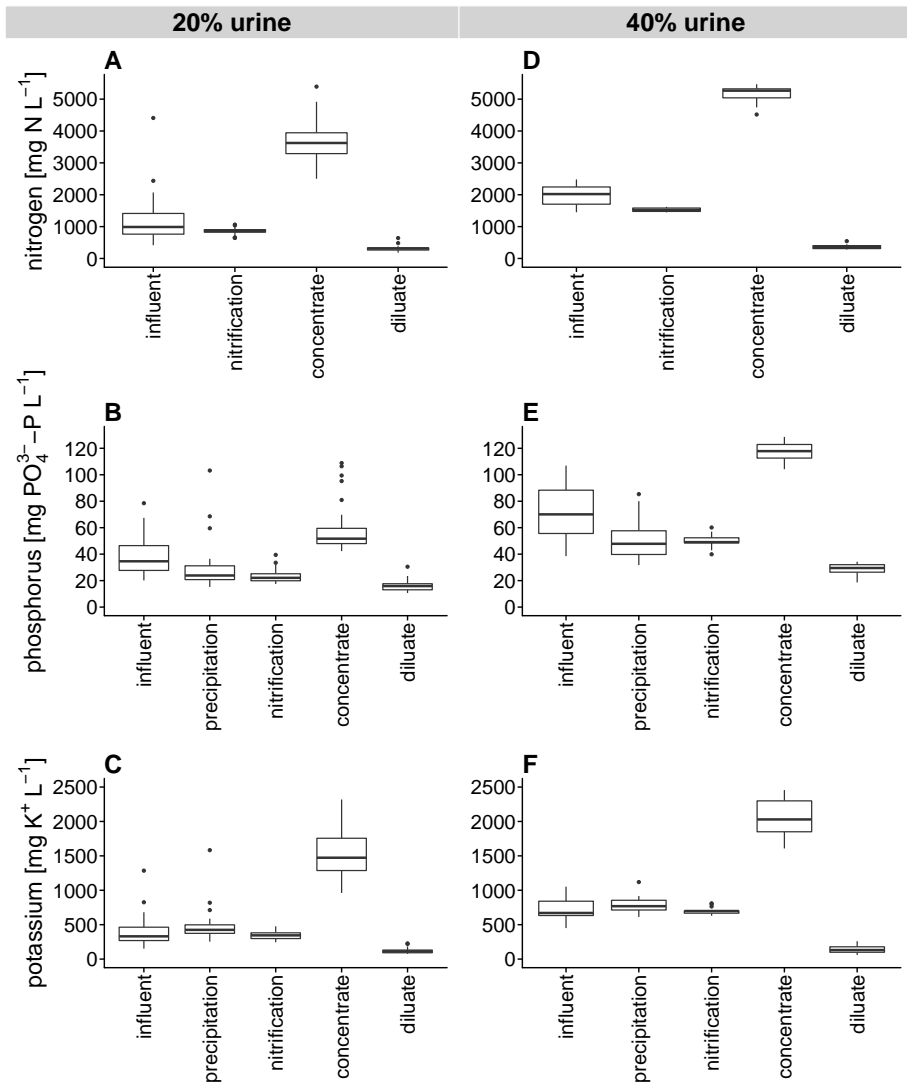


Figure 2.9: **Nitrogen, phosphorus and potassium concentration in the different stages of the pilot installation during operation using 20% and 40% urine solutions.** Samples were analysed over a period of 100 days on a 20% urine solution ($n=35$) and over a period of 40 days on a 40% urine solution ($n=16$). The nitrogen concentration in the influent is calculated as the sum of total Kjeldahl nitrogen (TKN), NO_2^- -N and NO_3^- -N concentrations. The nitrogen concentration after nitrification, in the diluate and concentrate is the sum of TAN, NO_2^- -N and NO_3^- -N.

2.4 Discussion

2.4.1 Precipitation and nitrification minimize scaling and biofouling in ED

In this study, an integrated system combining precipitation, nitrification and ED was evaluated to refine and concentrate nutrients from fresh urine. Operation of this three-stage system was successfully demonstrated in a relevant environment, corresponding to level 6 on the technology readiness level (TRL) scale. The use of a precipitation reactor proved to be an effective strategy to safeguard the ED from excessive scaling. More than 90% of the calcium and 80% of the magnesium was precipitated. Both the precipitation and nitrification reactor require base addition. In the precipitation reactor, approximately 215 mmol NaOH L⁻¹ urine was dosed to increase the pH to 11. In the nitrification reactor, base is needed to counteract the acidification caused by nitrification. Without base addition, maximally ~50% of the nitrogen in urine can be converted into nitrate [291]. In principle, base addition in the precipitation reactor does not increase the total base consumption, as a more alkaline influent entering the bioreactor reduces the amount of alkaline equivalents required in the bioreactor to counteract the acidification. In total, about 300 mmol NaOH L⁻¹ urine was needed to convert all urea into nitrate, of which only one third was dosed in the nitrification reactor.

The use of a bioreactor proved to be an effective strategy to limit biofouling in ED by oxidizing the COD. Moreover, uncharged urea was converted into nitrate in order to stabilize the urine and to capture the nitrogen in a non-volatile form in ED. Although the total nitrogen concentration in the influent fluctuated due to the variable composition of urine, stable nitrification was achieved in the bioreactor with an average volumetric nitrogen loading rate of 215 mg N L⁻¹ reactor d⁻¹, and a salinity of 10.5 mS cm⁻¹. Only after reactor disturbances (due to failure of the pH control or influent dosing problems), TAN was detected in the bioreactor effluent. Nitrifiers quickly recovered once the optimal conditions were restored. Bacteria grown in a biofilm are generally more protected to transient stressors, such as a low pH and high free ammonia concentration due to diffusion limitations [133]. Moreover, nitritation, which causes the acidification, is generally hampered by a low pH, presumably due to a limited ATP generation [98]. Besides precipitation and protection of the subsequent ED, the precipitation reactor was also used to increase the alkalinity of the nitrification reactor influent. As a consequence, we never observed the pH dropping below 5.5, in case of pH control failure.

ED was used to concentrate nutrients in an energy-efficient manner. The concentrate flow was generated by osmotic and electro-osmotic water transport across the membrane and contained about 70% of the ions of the feed stream. The increase in concentrate EC and obtained concentration factors of 3-5 are in line with results obtained by Pronk et al. (2007) [233]. Periodic cleaning in place (~once a month) with an acid and alkaline solution was sufficient to keep the ED stack operational >7 months with the same membranes and a stable performance. Such cleaning can easily be automated. The

anion exchange membranes turned brown (SI Figure S2.11), which was also reported by Aponte and Colon (2001) [11]. This is probably due to irreversible adsorption of negatively charged organic molecules [11].

2.4.2 Nitrification and COD oxidation remained unaffected at a decreased urine dilution

The high salt content of urine and base addition leads to a high EC in the bioreactor. Living in a salty environment is an energetically costly process for bacteria since more energy is required to balance the cell osmotic pressure [220]. This limits the energy available for nitrification, which typically results in lower activity rates at high EC. The salt tolerance of the nitrifying community on the beads was assessed in a batch experiment in which beads were exposed to a short-term salt shock. The maximum ureolysis, nitritation and nitratation rates of the beads decreased with 52%, 82% and 96%, respectively, when the EC was increased from 20 mS cm⁻¹ to 96 mS cm⁻¹. Interestingly, the rate limiting nitritation and hence, the overall nitrification rate, remained unaffected up to 40 mS cm⁻¹. This also explains why nitrification was not affected during continuous operation using a 40% urine solution, despite the higher EC (17.3 mS cm⁻¹ instead of 10.5 mS cm⁻¹). The results of the batch experiment suggest that the bioreactor can operate on undiluted urine (expected EC between 45-60 mS cm⁻¹) but at a lower volumetric rate, although this should be tested on the long-term. The relatively high salt resistance of the beads is probably a result of the inoculum selection [56]. The higher drop in nitratation rate indicates that the NOB on the beads were more sensitive to the short-term salt stress than the AOB. Literature is inconclusive concerning the salt tolerance of AOB versus NOB, due to differences in experimental set-up, operational conditions and test duration, salt dosage and AOB and NOB community composition [200]. Moussa et al. (2006) and Coppens et al. (2016) reported that AOB were more sensitive to salt stress. On the other hand, Bassin et al. (2011) [16], Dincer and Kargi (1999) [72], Cui et al. (2009) [64] and Cortes-Lorenzo et al. (2015) [60] concluded, based on the accumulation of nitrite in their experiments, that NOB were more affected by salinity.

2.4.3 Shifts in microbial community composition parallel shifts in influent composition

The shifts in microbial community composition in the pilot reactor coincided with changes in the influent composition, as shown by PCoA analysis (Figure 2.6) and may be attributed to the nature of the organic fraction in the influent (acetate in synthetic medium versus complex COD matrix in urine). In addition, salinity is known to affect the microbial community composition in nitrification reactors [15, 56, 60, 112, 200]. Classification using NCBI BLAST, RDP SeqMatch and a maximum likelihood phylogenetic tree indicated that the AOB community was dominated by species closely related to *N.*

aestuarii or *N. marina*. Both species are obligate halophilic and described in marine environments [149]. *N. aestuarii* was also found to be the dominating AOB species in reactors operated on seawater [112, 272]. The presence of these halophilic AOB species can also explain why the nitrification activity was so well preserved at high EC in the batch experiment. Besides salinity, the shifts in the AOB community in the pilot reactor corresponded to the nitrogen source (urea-N or TAN). OTUs related to the urease-negative *N. europaea* and *N. halophila* [149], only thrived when the reactor was operated using a synthetic ammonium sulfate solution.

2.4.4 Lowering the urine dilution leads to a higher recovery efficiency but a lower concentration factor in ED

Increasing the urine concentration (from 20% to 40%), decreased the volume ratio of diluate to concentrate from 5.8 to 4. Due to the higher EC gradient between the diluate and concentrate and the increased transport of ions from diluate to concentrate, the osmotic and electro-osmotic water transport increased. Hence, relatively more concentrate was produced on a 40% urine solution. Depending on the ion, the recovery efficiency increased by 7% to 14%, which is probably due to the higher residence time in the diluate tank (14h instead of 8h). Despite the higher end concentrations and overall EC of the concentrate on a 40% urine solution, the concentration factors decreased, as a result of the higher ion concentrations in the feed stream. To conclude, more nutrients were captured in the concentrate, but in a comparatively larger concentrate volume.

2.4.5 Strategies to increase nutrient recovery efficiencies

Respectively 70% and 80% of the ions were captured in 15% and 20% of the initial volume when the pilot installation was operated using a 20% or 40% urine solution. It is almost impossible to capture all nutrients in the concentrate. As a result of the equilibrium established between the diluate and concentrate stream, part of the nutrients remain in the diluate. Additionally, relatively low concentration factors (ion concentration in the concentrate stream divided by the concentration in the feed stream) present a second limitation inherent to ED due to the osmotic and electro-osmotic water transport. A high concentration gradient between the diluate and the concentrate, leads to increased osmotic water transport from diluate to concentrate and back diffusion of ions from concentrate to diluate, which in turn limits the maximum achievable concentration factor.

In case of phosphate, the large size and low diffusion rate of the ion limits the recovery efficiency to 40%, as opposed to 70%-75% for all other ions, corresponding to a concentration factor of only 2.6. It was hypothesized that the phosphate transport would increase by increasing the pH in the diluate since more phosphate ions are dissociated at a higher pH, which could facilitate the transport, as the ions are more susceptible to the electric field. The recovery efficiency of phosphate in the batch test at pH 7 was indeed higher compared to pH 6. The slower phosphate transport at pH 8 compared to pH 7 can possibly be attributed to competition in migration with carbonate

ions. Like phosphate, the charge of carbonate depends on the pH. Most of the carbonate is uncharged (H_2CO_3) at pH 6 while more than 90% of the carbonate species have a charge of -1 (HCO_3^-) at pH 8 (SI Table S2.7). Further research is needed to confirm the hypothesis of reduced phosphorus transport due to carbonate competition at elevated pH.

Another way to recover more phosphorus, is to precipitate all the phosphorus in the precipitation reactor. Phosphorus precipitation is limited by calcium and magnesium due to the excess of anions (phosphate, sulfate and carbonate) in urine. By substituting NaOH by $\text{Ca}(\text{OH})_2$ or $\text{Mg}(\text{OH})_2$ to increase the pH in the precipitation reactor or adding another calcium or magnesium source, up to 90% of the phosphate can be precipitated [84]. However, excess calcium or magnesium dosage should be avoided to prevent scaling issues in the ED unit.

Decreasing the concentrate volume by means of distillation is an option to concentrate the nutrients in a smaller volume. Distillation was already applied by Udert and Wächter (2012) [295] in combination with nitrification to concentrate nutrients in urine. All nutrients were recovered in a dry solid. However, the high energy demand of distillation (~ 700 Wh primary energy L^{-1} urine) presents a major drawback of the process. The energy consumption of ED is significantly lower. The electrode power consumption of ED in this study equalled only 4.3 Wh electrical energy L^{-1} urine or 14 Wh primary energy L^{-1} urine (SI Table S2.4). However, ED removed only $\sim 85\%$ of the water, whereas distillation can remove almost all water. Udert and Wächter (2012) [295] suggested that the energy demand could be significantly reduced by first removing 80% of the water with reverse osmosis and subsequently operating distillation with vapor compression (~ 100 Wh L^{-1} urine). Alternatively, the required 80% water removal could be obtained by ED instead of RO, as demonstrated in this study. To conclude, a combination of precipitation, nitrification, ED and distillation could offer a maximal concentration of nutrients with a minimal input of energy.

2.4.6 Resource reuse possibilities for precipitate, ED concentrate and ED diluate

The output of the integrated system consists of the precipitates formed in the precipitation reactor and the diluate and concentrate stream of the ED unit. The precipitates could be used as a solid phosphorus fertilizer in agriculture. About 30% of the phosphate in urine was incorporated in the precipitates, which corresponds to values reported in literature [294]. The use of urine derived precipitates as fertilizer has been demonstrated by Bonvin et al. (2015) [27]. Moreover, it was reported by Escher et al. (2006) [82] and Ronteltap et al. (2007) [250] that urine precipitates were clean and safe fertilizers since the micropollutants in urine (pharmaceuticals, hormones...) mainly remained in the liquid phase.

The ED concentrate is rich in nutrients, predominantly nitrogen (NPK = 85.9/0.7/13.4 mol%), which is present under the form of nitrate. Nitrate, in contrast to urea,

ammonia or ammonium nitrate, is a thermally stable, non-volatile molecule and, in a lot of cases, the preferred nitrogen source for plants [182, 295]. Besides nitrogen, plant growth requirements are also met for potassium whereas phosphorus will be the limiting macronutrient in the ED concentrate due to the partial incorporation in the precipitates [162]. The excessive salt concentration, particularly sodium, resulting from the NaOH demand by precipitation and nitrification, might present another barrier for fertilizer application. In this regards, partial nitrification is a promising new lead to reduce the sodium load, simultaneously saving chemicals [295]. The dense nature of the ED membranes typically results in a high retention of pathogens and micropollutants in the diluate [82, 230, 231]. However, Pronk et al. (2006) [229] showed that breakthrough of certain micropollutants (e.g., propranolol and ibuprofen) can occur over time. To guarantee a micropollutant-free product, a post-treatment, such as ozonation or adsorption on activated carbon, can be included to remove the residual micropollutants in the concentrate [73, 162, 233, 290]. Ozonation is even more effective in combination with a nitrate based, COD low stream given the ozone scavenging potential of ammonium and competition between COD and micropollutants for the chemical oxidant [162, 233].

Finally, the ED diluate is low in nutrients and salts, which makes it a suitable stream for water recovery through membrane filtration, as particularly relevant for regenerative life support systems for human space exploration [52, 174].

2.5 Conclusion

- An electro dialysis (ED) stack was operated for ~7 months on real, diluted urine. The use of a precipitation reactor and aerobic bioreactor proved to be an effective strategy to minimize scaling and biofouling in ED.
- More than 90% and 95% of incoming COD and urea were converted in the bioreactor at salinities of 10 to 20 mS cm⁻¹. Shifts in the microbial community coincided with changes in the influent composition of the bioreactor. The AOB community was dominated by species closely related to *Nitrosomonas aestuarii* and *Nitrosomonas marina*.
- Respectively 70% and 80% of the ions were captured in 15% and 20% of the initial volume when the pilot installation was operated using a 20% or 40% urine solution.
- The P-rich precipitates and N+K-rich ED concentrate can be valorized as fertilizers, whereas water can be recovered from the ED diluate. Further research on the fate of micropollutants and pathogens in the three-stage system is necessary to valorize the recovered fertilizers

2.6 Supplementary information

2.6.1 Supplementary materials and methods

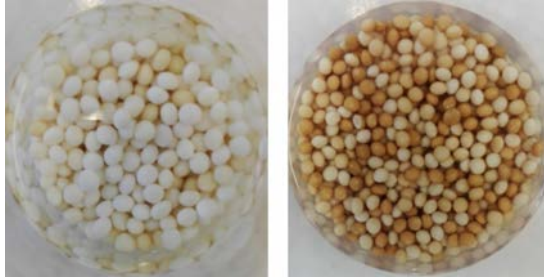


Figure S2.1: **Beads of cultivation reactor (left) and pilot reactor (right).** Fresh carriers were frequently added to the cultivation reactor and covered by microbial biofilms derived from the older beads ensuring continuous and stable inoculum (inoculated beads) for the pilot reactor. Mature beads, present for a long time in the reactor, had a darker colour compared to the young beads, which were more recently added to the reactor. The biofilm present on the beads from the cultivation reactor grew darker upon long term exposure to reactor conditions and real urine in the pilot reactor.

Bioinformatics analysis of next generation 16S rRNA gene amplicon sequencing data (after De Paepe et al. (2017) [67])

The 16S rRNA gene amplicon sequencing data was processed with the mothur software package v.1.38.0 [150, 259]. Forward and reverse reads were binned into contigs using a heuristic approach based on Phred quality scores. After removing contigs with any ambiguous base calls or unsatisfying overlap, 747937 of 1337129 sequences were withheld. The remaining contigs were aligned to the mothur formatted silva_seed release 123 alignment database and trimmed between positions 6428 and 23440 to be compatible with the 341F-785R primers [235]. 12977 sequences, not aligning within this region or containing homopolymer stretches of more than 12 bases, were culled out. Subsequently, sequences with up to four differences were pre-clustered. After performing a chimera check using UCHIME [75], the remaining 602841 reads were classified by means of a naive Bayesian classifier, against the RDP 16S rRNA gene training set, version 14 with an 80% cut-off for the pseudo bootstrap confidence score. Sequences classified as unknown, Chloroplast, Mitochondria, Archaea or Eukaryota at the kingdom level were removed. A total of 602693 sequences were withheld (45% of the data). In a next step, sequences were binned into Operational Taxonomic Units (OTUs) within each order identified by the preceding classification step, using average neighbor clustering with a cut-off set at 0.15 [46, 258, 259]. The 3% dissimilarity level shared file was selected for further analysis. Hence, an OTU is defined in this study as

a collection of sequences with a length between 402 and 427 nucleotides that are found to be more than 97% similar to one another in the V3-V4 region of their 16S rRNA gene [46, 258, 259]. To verify if the samples were sequenced in sufficient depth, rarefaction curves were constructed (Figure S2.2). The resulting 15200 OTUs were identified by means of the RDP version 14 and silva.nr_v123 database [55, 235, 308]. The shared file, containing the number of reads observed for each OTU in each sample and the taxonomy files, were loaded into R version 3.3.3 (2017-03-06) [236]. After removing reads occurring only once in all samples (singletons) and applying additional filtering according to the arbitrary cut-offs proposed by McMurdie and Holmes (2014) [189], 412 OTUs were withheld. A Jaccard dissimilarity matrix (package vegan 2.4-2) was calculated based on the normalized proportional counts at OTU level and was used to perform a Principle Coordinate Analysis (PCoA; package stats4_3.3.3) [114, 215, 239]. The closest sequence match at species level of the most abundant OTUs was obtained by NCBI BLAST, selecting only type material optimized for highly similar sequences in the 16S rRNA gene database, and the RDP Sequence Match tool, restricting the database search to type strains with only near-full-length, good quality sequences.

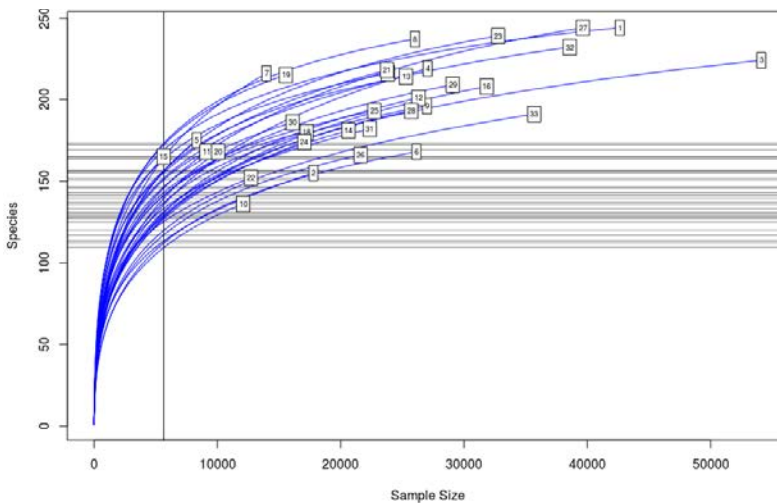


Figure S2.2: **Rarefaction curves of the non-normalized data after removing singletons and applying cut-offs for data filtering described by McMurdie and Holmes (2014) [189].** The number on each curve refers to the sample name which can be looked up in the NCBI submission with accession code SRP111125.

2.6.2 Supplementary tables and figures

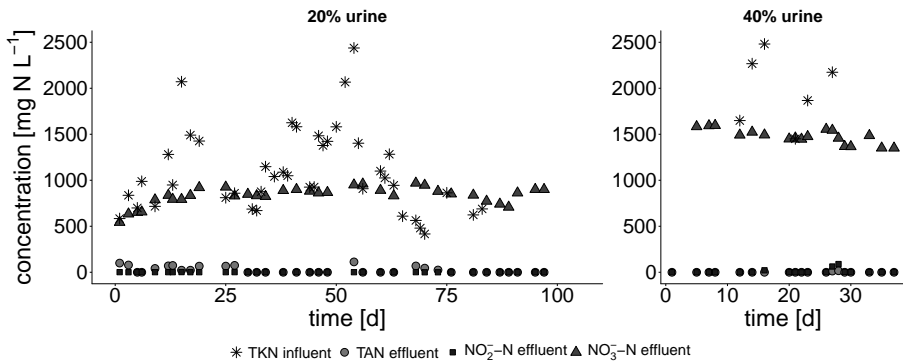


Figure S2.3: Time series data of the total Kjeldahl nitrogen (TKN) in the influent and the total ammonia nitrogen (TAN), NO₂⁻-N and NO₃⁻-N concentration in the effluent during pilot operation on a 20% and 40% urine solution.

Table S2.1: **Average concentration and standard deviation in all stages of the pilot installation.** Values are based on 35 samples over a period of 100 days on a 20% urine solution and 16 samples over a period of 40 days on a 40% urine solution. The average urine composition was in line with values reported in literature. The high standard deviation in the influent is caused by the variability in the collected urine (composition varies between and within individuals due to factors such as health, time, diet and daily activities)

	influent	after precipitation	after nitrification	ED diluate	ED concentrate
20% urine					
TN [$g N L^{-1}$]	1073 ± 170				
TAN [$g N L^{-1}$]	151 ± 82	368 ± 145	25 ± 35	13 ± 13	158 ± 168
N-NO ₃ ⁻ [$g N L^{-1}$]	0.4 ± 0.6	1.5 ± 1.9	832 ± 98	299 ± 76	3528 ± 625
P-PO ₄ ³⁻ [$g P L^{-1}$]	42 ± 26	29 ± 18	23 ± 5	16 ± 4	59 ± 18
K ⁺ [$g L^{-1}$]	401 ± 218	474 ± 227	340 ± 56	117 ± 37	1527 ± 349
Ca ²⁺ [$g L^{-1}$]	31 ± 10	1.9 ± 1.0		0.19 ± 0.09	
Mg ²⁺ [$g L^{-1}$]	11 ± 5	1.6 ± 0.4		0.22 ± 0.13	
Na ⁺ [$g L^{-1}$]	449 ± 259	1444 ± 372	1914 ± 262	755 ± 193	8452 ± 1366
Cl ⁻ [$g L^{-1}$]	753 ± 398	792 ± 347	780 ± 115	322 ± 127	3363 ± 694
S-SO ₄ ²⁻ [$g S L^{-1}$]	14 ± 22	11 ± 14	59 ± 9	19 ± 9	283 ± 65
pH		10.8 ± 0.6	6.7 ± 0.4	6.2 ± 0.3	
EC [$mS cm^{-1}$]		7.6 ± 2.4	10.5 ± 1.2	5.1 ± 1.8	43.4 ± 9.5
40% urine					
TN [$g N L^{-1}$]	1705 ± 814				
TAN [$g N L^{-1}$]	376 ± 179	1713 ± 272	1.6 ± 4.7	0 ± 0	0 ± 0
N-NO ₃ ⁻ [$g N L^{-1}$]	8 ± 10	10 ± 15	1477 ± 81	363 ± 68	5128 ± 280
P-PO ₄ ³⁻ [$g P L^{-1}$]	72 ± 20	52 ± 17	50 ± 5	26 ± 4	120 ± 9
K ⁺ [$g L^{-1}$]	735 ± 174	794 ± 125	677 ± 66	147 ± 61	2335 ± 374
Na ⁺ [$g L^{-1}$]	817 ± 209	2831 ± 427	3554 ± 451	935 ± 163	11828 ± 561
Cl ⁻ [$g L^{-1}$]	1275 ± 305	1223 ± 206	1344 ± 205	359 ± 60	4607 ± 264
S-SO ₄ ²⁻ [$g S L^{-1}$]	97 ± 23	93 ± 20	104 ± 51	28 ± 8	429 ± 25
pH		10.9 ± 0.2	6.8 ± 0.1	6.9 ± 0.2	
EC [$mS cm^{-1}$]		14.6 ± 2.5	17.3 ± 1.1	5.5 ± 0.4	59.6 ± 2.8

Table S2.2: **RDP Sequence match and NCBI BLAST results for the most abundant OTUs and OTUs belonging to the *Nitrosomonas* genus.** The NCBI BLAST output (total score, coverage percentage and identity percentage) and RDP seqmatch score (S_ab) for the best hit and next best hit(s) are displayed (accession date: December 2017).

	Species	Total score	NCBI % coverage	% identity	RDP S_ab score
1	<i>Acinetobacter venetianus</i>	791	100	100	1
	<i>Acinetobacter radioresistens</i>	747	100	98	
2	<i>Comamonas</i> sp.				0.930
	<i>Comamonas badia</i>	728	100	97	0.873
	<i>Comamonas nitratorans</i>	717	100	97	
3	<i>Luteimonas aquatica</i>	745	100	98	0.906
	<i>Luteimonas cucumeris</i>	745	100	98	0.901
4	<i>Nitrosomonas aestuarii</i>	712	100	97	0.844
	<i>Nitrosomonas marina</i>	706	100	96	0.865
	<i>Nitrosomonas ureae</i>	667	100	95	0.803
	<i>Nitrosomonas europaea</i>	623	100	93	0.651
5	<i>Haliscomenobacter</i> sp.				0.703
	<i>Haliscomenobacter hydrossis</i>	508	97	89	
	<i>Lewinella nigricans</i>	508	100	88	
	<i>Portibacter lacus</i>	503	100	88	
6	<i>Defluviimonas denitrificans</i>	743	100	100	1
	<i>Thioclava pacifica</i>	693	100	98	0.902
7	<i>Acidibacter ferrireducens</i>	606	100	92	0.743
	<i>Povalibacter uvarum</i>	568	100	91	0.653
8	<i>Sphingopyxis terrae</i>	737	100	99	1
	<i>Sphingopyxis ummariensis</i>	737	100	99	
	<i>Sphingopyxis soli</i>	726	100	99	
	<i>Sphingopyxis indica</i>	726	100	99	
	<i>Sphingopyxis taejonensis</i>	726	100	99	
	<i>Sphingopyxis macrogoltabida</i>				
9	<i>Luteimonas abyssi</i>	756	100	99	0.937
	<i>Luteimonas lutimaris</i>	734	100	98	
	<i>Luteimonas aestuarii</i>	728	100	97	0.966
11	<i>Mangroviflexus xiamenensis</i>	505	99	88	
	<i>Pedobacter luteus</i>	492	100	88	
	<i>Alkaliflexus</i> sp.				0.531
	<i>Marinilabiliaceae bacterium</i>				0.519
12	<i>Pedobacter huanghensis</i>	433	99	85	
	<i>Solitalea koreensis</i>	412	99	84	
	<i>Rufibacter tibetensis</i>	412	99	85	0.5
	<i>Wandonia haliotis</i>				0.502
	<i>Bacteroidetes bacterium</i>				0.502

	<i>Flexibacter sp.</i>				0.515
13	<i>Azoarcus evansii</i>	701	100	96	
	<i>Azoarcus olearius</i>	678	100	95	0.87
	<i>Azoarcus indigens</i>	673	100	95	
	<i>Denitromonas aromaticus</i>				0.947
	<i>Denitromonas indolicum</i>				0.947
16	<i>Terrimonas sp.</i>				0.985
	<i>Terrimonas lutea</i>	630	100	94	0.776
	<i>Chitinophaga jiangningensis</i>	608	100	93	
	<i>Flavitalea gansuensis</i>	608	100	93	
	<i>Chitinophaga ginsengisegetis</i>	608	100	93	
17	<i>Vitellibacter sp.</i>				0.698
	<i>Vitellibacter echinoideorum</i>	590	99	92	
	<i>Sediminibacter furfurosus</i>	579	99	91	
	<i>Aequorivita lipolytica</i>	573	99	91	
	<i>Vitellibacter soesokkakensis</i>	568	99	91	
	<i>Cytophaga sp.</i>				0.696
19	<i>Acidobacteria bacterium</i>				0.838
	<i>Aridibacter famidurans</i>	632	100	95	0.772
	<i>Stenotrophobacter namibiensis</i>				0.772
	<i>Blastocatella fastidiosa</i>	627	100	95	
20	<i>Chryseolinea serpens</i>	612	100	93	0.725
24	<i>Nitrosomonas europaea</i>	789	100	100	1
	<i>Nitrosomonas eutropha</i>	728	100	97	0.913
	<i>Nitrosomonas halophila</i>	680	100	95	0.810
	<i>Nitrosomonas marina</i>	651	100	94	0.737
	<i>Nitrosomonas aestuarii</i>	634	100	93	0.716
64	<i>Nitrosomonas marina</i>	701	100	96	0.849
	<i>Nitrosomonas aestuarii</i>	701	100	96	0.827
	<i>Nitrosomonas ureae</i>	673	100	95	0.805
81	<i>Nitrosomonas halophila</i>	689	100	96	0.806
	<i>Nitrosomonas europeae</i>	656	100	94	0.733
91	<i>Nitrosomonas ureae</i>	750	100	98	0.928
	<i>Nitrosomonas marina</i>	684	100	96	0.805
	<i>Nitrosomonas aestuarii</i>	684	100	96	0.793
152	<i>Nitrosomonas marina</i>	684	100	96	0.824
	<i>Nitrosomonas ureae</i>	678	100	95	0.814
	<i>Nitrosomonas aestuarii</i>	667	100	95	0.790
353	<i>Nitrosomonas ureae</i>	739	100	98	0.899
	<i>Nitrosomonas marina</i>	684	100	96	0.819
	<i>Nitrosomonas aestuarii</i>	684	100	96	0.793
398	<i>Nitrosomonas nitrosa</i>	784	100	99	0.988
	<i>Nitrosomonas communis</i>	739	100	98	0.872

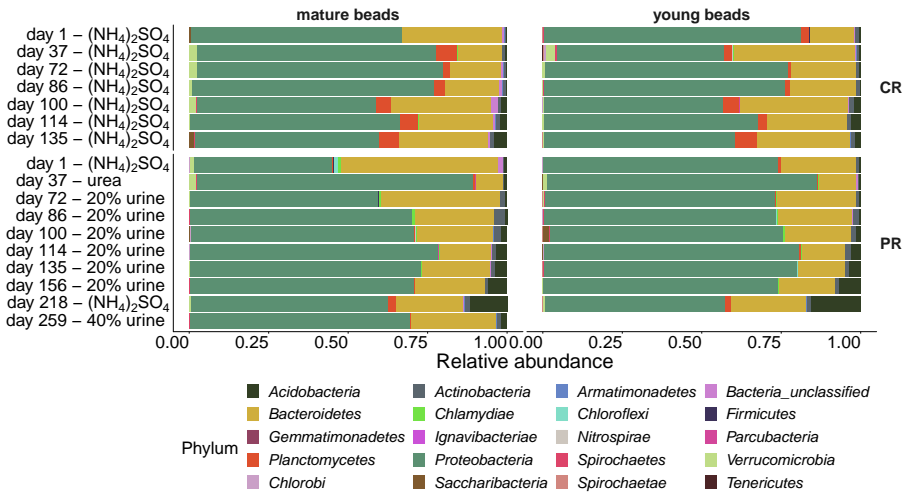


Figure S2.4: **Phylum level microbial community composition of the beads in the cultivation reactor (CR) and pilot reactor (PR) over time with varying influent composition.** A distinction was made between mature and young beads based on the difference in colour of the beads.

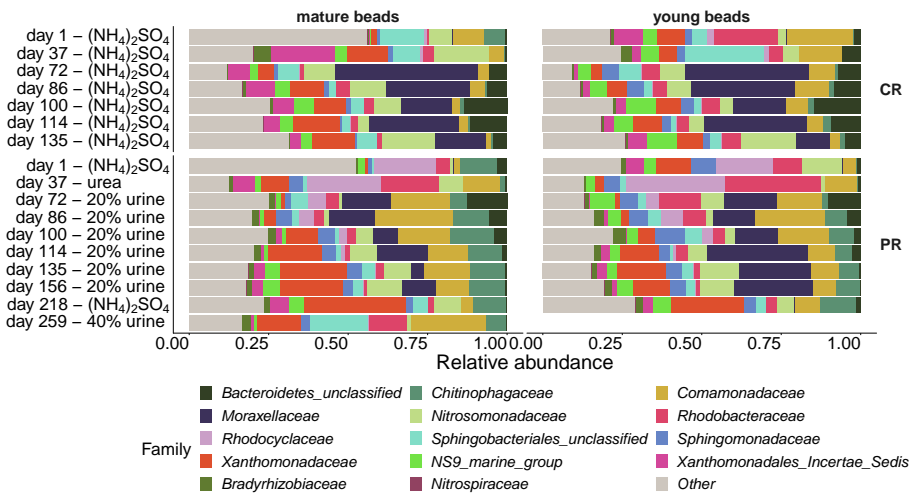


Figure S2.5: **Family level microbial community composition of the beads in the cultivation reactor (CR) and pilot reactor (PR) over time with varying influent composition.** A distinction was made between mature and young beads based on the difference in colour of the beads. The relative abundance of the 12 most abundant families, the *Bradyrhizobiaceae* and the *Nitrospiraceae* is shown.

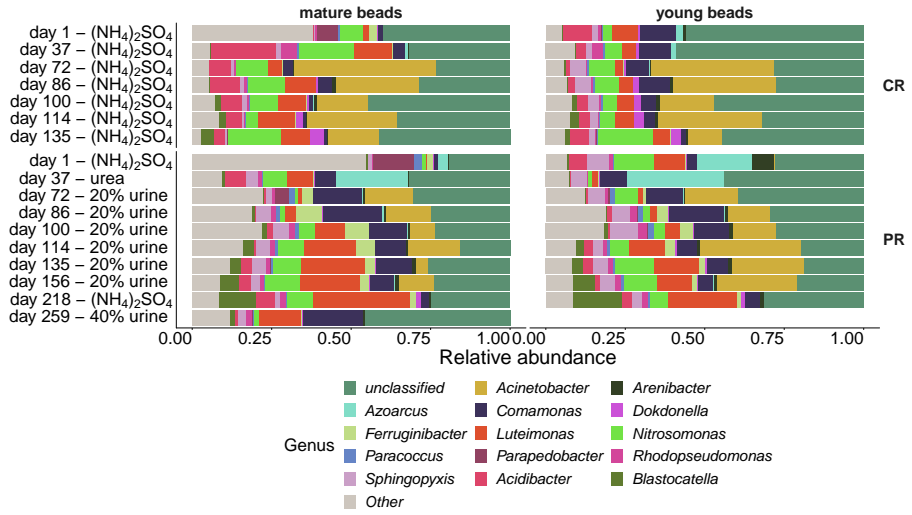


Figure S2.6: **Genus level microbial community composition of the beads in the cultivation reactor (CR) and pilot reactor (PR) over time with varying influent composition.** A distinction was made between mature and young beads based on the difference in colour of the beads. The relative abundance of the 15 most abundant genera is shown.

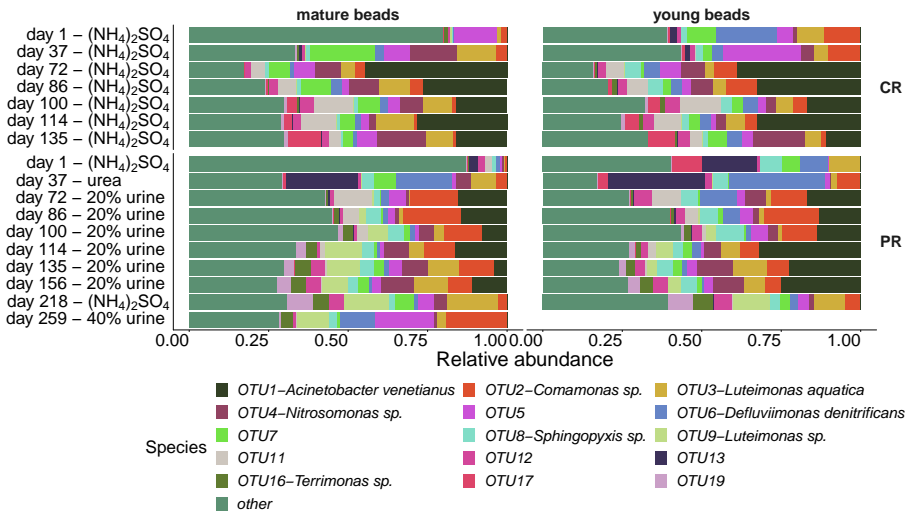


Figure S2.7: **OTU level microbial community composition of the beads in the cultivation reactor (CR) and pilot reactor (PR) over time with varying influent composition.** A distinction was made between mature and young beads based on the difference in colour of the beads. The relative abundance of the 15 most abundant OTUs is shown. OTUs were annotated using the RDP SeqMatch tool and NCBI BLAST (Table S2.2). For OTUs that could not unambiguously be identified at species level (<95%), the OTU identifier is displayed.

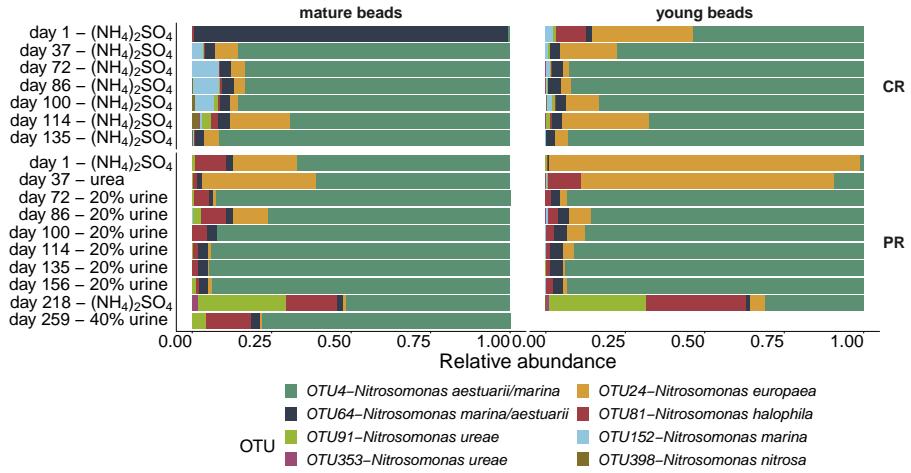


Figure S2.8: Relative abundance of the OTUs belonging to the *Nitrosomonas* genus in the microbial community colonizing the beads in the cultivation reactor (CR) and pilot reactor (PR) over time with varying influent composition, with 1.00 representing the total *Nitrosomonas* community. A distinction was made between mature and young beads based on the difference in colour of the beads. OTUs were annotated based on the RDP SeqMatch tool, NCBI BLAST and a Maximum Likelihood phylogenetic tree (Table S2.2, Figure S2.9).

Tree scale: 0.01

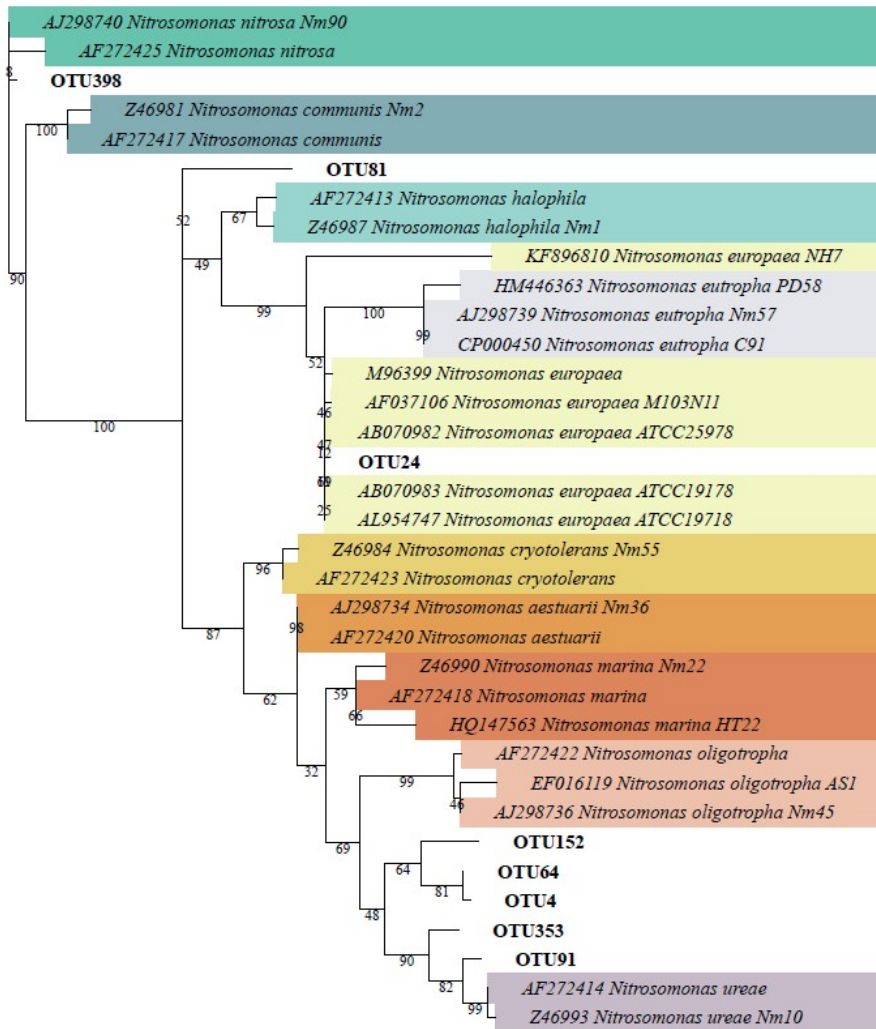


Figure S2.9: **Maximum likelihood phylogenetic tree showing the relatedness of the OTUs belonging to the *Nitrosomonas* genus identified in this study with 16S rRNA gene sequences of *Nitrosomonas* species in the RDP and NCBI database with a unique identifier.** The sequences representing previously identified *Nitrosomonas* species were downloaded from the RDP database, restricting the search results to type material with a good quality and a size ≥ 1200 nucleotides and the NCBI 16S rRNA database, selecting highly similar sequences from type material. Duplicate sequences (present in RDP and NCBI) were identified based on the identifiers and removed from the dataset. The downloaded sequences were trimmed with the 341-785 primer pair, which was used for the next generation 16S rRNA gene amplicon

sequencing and aligned in mothur version v.1.38.0, using the mothur formatted silva seed v123 reference file. RAxML was used to construct a maximum likelihood phylogenetic tree with the General Time Reversible model of nucleotide substitution under the Gamma model of rate heterogeneity (GTRGAMMA) with the parsimony random seed set to 12345 [269]. A rapid bootstrap analysis starting from N=1000 distinct randomized maximum parsimony trees and search for best scoring maximum likelihood tree was performed with rapid bootstrap random number seed 123. The best scoring maximum likelihood tree was visualized in iTOL. Branch lengths are drawn to scale and bootstrap values (%) are displayed.

Table S2.3: **Volumetric salt loading rate and coulombic efficiency of the electro dialysis (ED) unit at 20% and 40% urine.** The volumetric salt loading rate was calculated based on the electrical conductivity of the feed stream. The volumetric salt removal rate was calculated based on the difference in electrical conductivity of the feed stream and diluate. The coulombic efficiency was calculated for one HRT (volume of 2L) based on the average current, the HRT and the difference in electrical conductivity between the feed stream and diluate. The ED stack contained 10 cell pairs.

		20% urine	40% urine
Flow rate	$[L d^{-1}]$	5.8	3.5
EC feed stream	$[mS cm^{-1}]$	10.5	17.3
EC diluate stream	$[mS cm^{-1}]$	5.1	5.5
Current	$[A]$	0.053	0.059
HRT	$[d]$	8	14
Q	$[C]$ (one HRT)	1585	2913
Volumetric salt loading rate	$[mmol NaCl - eq L^{-1} d^{-1}]$	240.7	239.3
Volumetric salt removal rate	$[mmol NaCl - eq L^{-1} d^{-1}]$	123.8	163.2
Coulombic efficiency	$[mol NaCl - eq mol^{-1} e^{-}]$	0.52	0.62

Table S2.4: **Electrode power consumption of the ED stack.** Wh_{el} = electrical energy, Wh_{prim} = primary energy.

	20% urine	40% urine
Feed flow rate [L d ⁻¹]	5.8	3.5
Feed flow rate [L urine d ⁻¹]	1.2	1.3
EC feed stream [mS cm ⁻¹]	10.5	17.3
EC diluate [mS cm ⁻¹]	5.1	5.5
Potential ED stack [V]	4.1	3.9
Current ED stack [A]	0.053	0.059
Reduction in salinity		
[mS cm ⁻¹]	5.4	11.8
[g NaCl - eq L ⁻¹]	2.5	5.5
[g NaCl - eq d ⁻¹]	14.5	19.1
Electrode power consumption		
[Wh _{el}]	0.217 (4.1V*0.053A)	0.230 (3.9V*0.059A)
[Wh _{el} L ⁻¹ feed]	0.9	1.6
[Wh _{el} L ⁻¹ urine fed]	4.35	4.25
[Wh _{el} g ⁻¹ NaCl - eq]	0.36	0.29
Theoretical power consumption based on the coulombic efficiency (Table S2.3)		
[Wh _{el} L ⁻¹ urine fed]	2.3	2.68
Primary energy consumption (conversion factor of 0.31 Wh_{el}/Wh_{prim} for electricity production from Udert and Wächter (2012) [295])		
[Wh _{prim} L ⁻¹ urine fed]	14.0	13.7

Table S2.5: **Stokes radius, hydrated radius and diffusion coefficients in water of chloride, nitrate, sulfate and phosphate (adapted from Buffle et al. (2007) [33], Geise et al. (2014) [107], Tansel (2012) [278] and Paltrinieri et al. (2016)).**

Anion	Stokes radius [Å]	Hydrated radius [Å]	Diffusion coefficient [10 ⁻¹⁰ m ² s ⁻¹]
Cl ⁻	1.21	3.32	20.3
NO ₃ ⁻	1.29	3.35	19.02
SO ₄ ²⁻	2.3	3.79	10.7
H ₂ PO ₄ ⁻	2.56		9.59
HPO ₄ ²⁻	3.23		7.59

Table S2.6: **Molar ratios of phosphate species at pH 6, 7 and 8.**

		H_2PO_4^-	HPO_4^{2-}
pH 6	%	94.18	5.81
pH 7	%	61.86	38.14
pH 8	%	13.95	86.04

Table S2.7: **Molar ratios of carbonate species at pH 6, 7 and 8 [195].**

		0 S [‰], 25°C		5 S [‰], 25°C		15 S [‰], 25°C	
		H_2CO_3	HCO_3^-	H_2CO_3	HCO_3^-	H_2CO_3	HCO_3^-
pH 6	%	69.0	31.0	54.2	45.7	46.9	53.1
pH 7	%	18.2	81.8	10.6	89.1	8.1	91.3
pH 8	%	2.2	97.4	1.1	95.7	0.9	93.2

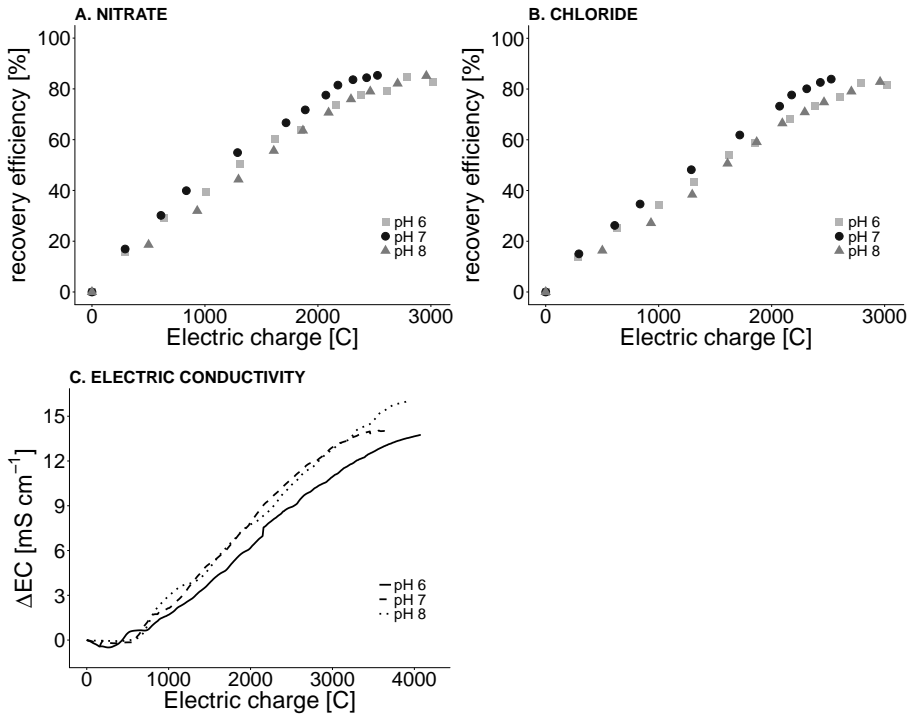


Figure S2.10: **Recovery efficiency of nitrate and chloride and electrical conductivity in function of the cumulative electric charge that passed through the stack in the ED batch experiments at pH 6, 7 and 8.** The cumulative electric charge (in Coulomb) was calculated by multiplying the applied current and time ($Q_{i+1}=Q_i + I_{i+1} \times (t_{i+1}-t_i)$). The recovery efficiencies were calculated by dividing the difference of the ion concentration in the diluate at time t and t_0 by the ion concentration at t_0 .

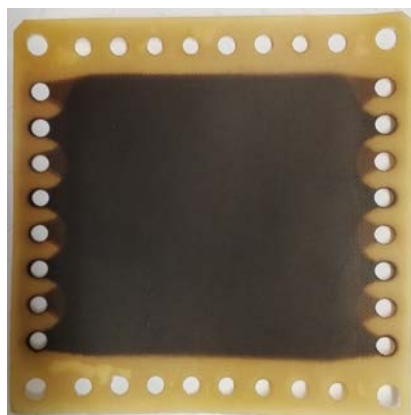


Figure S2.11: **Anion exchange membrane.** The brown colour is probably caused by adsorption of negatively charged organic molecules.

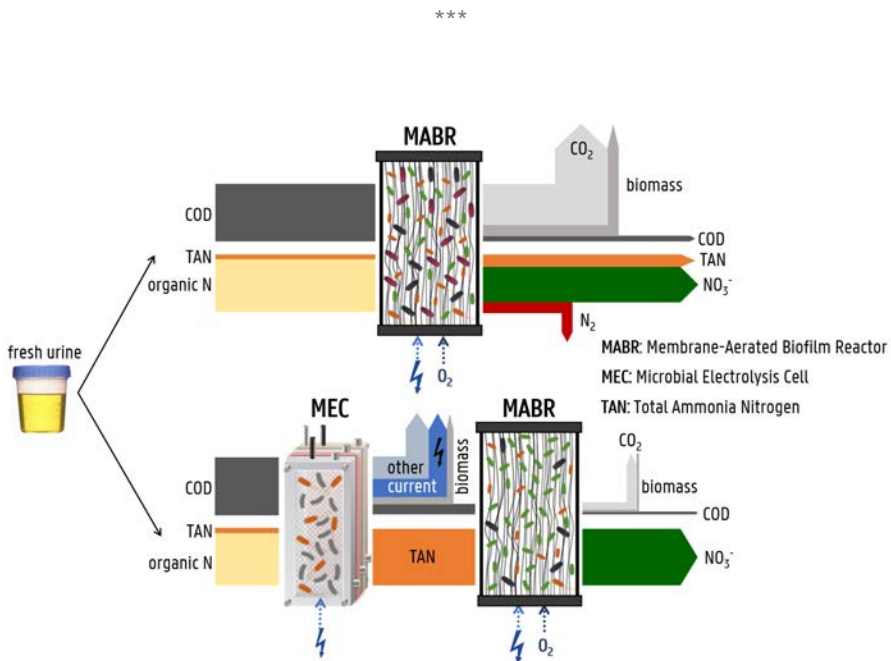
2.7 Acknowledgements

This article has been made possible through the authors' involvement in the MELiSSA project, ESA's life support system research program

The authors would like to acknowledge

- i) the financial support of the Belgian Federal Science Policy Office (BELSPO) [grant-ID 4000109518/13/NL/JC, project title: Water Treatment Unit Breadboard, managed by ESA],
- ii) the MELiSSA foundation to support JDP via the POMP1 (Pool Of MELiSSA PhD) program,
- iii) the Research Foundation Flanders (FWO, grant-ID: IWT130028, title: SBO BRANDING) and the Special Research Fund (BOF) Concerted Research Actions (GOA, BOF12/GOA/008) from the Flemish Government to support KDP,
- iv) IEC N.V. for building the installation,
- v) Avecom and dr. Kai Udert from EAWAG for providing the ABIL sludge and the urine nitrification biomass, respectively,
- vi) Tim Lacoere for designing the graphical abstract.

Bio-electrochemical COD removal for energy-efficient, maximum and robust nitrogen recovery from urine through membrane aerated nitrification



This chapter has been redrafted after:

De Paepe, J., De Paepe, K., Gòdia, F., Rabaey, K., Vlaeminck, S.E. and Clauwaert, P. Bio-electrochemical COD removal for energy-efficient, maximum and robust nitrogen recovery from urine through membrane aerated nitrification. *Water Research - under review*

3

Bio-electrochemical COD removal for energy-efficient, maximum and robust nitrogen recovery from urine through membrane aerated nitrification

Abstract

In this study, bio-electrochemical organics removal followed by membrane-aerated nitrification proved successful in transforming fresh real human urine into a stable and safe nutrient solution. Up to 85% of the COD was removed in a microbial electrolysis cell (MEC), converting part of the energy in organic compounds (27-46%) into hydrogen gas. Besides COD removal, all urea was hydrolysed in the MEC, resulting in a stream rich in ammoniacal nitrogen and alkalinity, and low in COD. This stream was fed into a membrane-aerated biofilm reactor (MABR) in order to convert the ammoniacal nitrogen to nitrate by nitrification without nitrogen loss through denitrification. Bio-electrochemical pre-treatment allowed to recover all nitrogen as nitrate in the MABR at a bulk-phase dissolved oxygen level below $0.1 \text{ mg O}_2 \text{ L}^{-1}$. In contrast, feeding the MABR directly with raw urine, at the same nitrogen loading rate, resulted in nitrogen loss (18%) due to denitrification. The MEC and MABR were characterized by very distinct and diverse microbial communities. While (strictly) anaerobic genera, such as *Geobacter* (electroactive bacteria), *Thiopseudomonas*, a *Lentimicrobiaceae* member, *Alcaligenes* and *Proteiniphilum* prevailed in the MEC, the MABR was dominated by aerobic genera, including *Nitrosomonas* (a known ammonium oxidizer), *Moheibacter* and *Gordonia*. This robust two-stage, energy-efficient, gravity-independent manner of recycling all urinary nitrogen can advance nitrogen recovery on Earth and can push the development of regenerative life support systems for long-term human spaceflights.

3.1 Introduction

In recent years, source-separated urine has gained great interest as an alternative nutrient resource, reducing the need to mine (e.g., phosphorus and potassium) or to chemically synthesize nutrients consuming fossil fuels (e.g., natural gas for ammonia), while at the same time facilitating wastewater management and reducing environmental pollution [186, 241]. Urine is also an essential resource in regenerative life support systems (RLSS) for long-duration human space missions, as it presents the major flux of nitrogen in a RLSS and contains additional macro- (i.e., phosphorus and potassium) and micro-nutrients [52].

Without stabilization of urine, urea, the main nitrogen compound in urine, quickly hydrolyses into ammonia, ammonium and (bi)carbonate, causing nutrient losses, scaling and clogging by uncontrolled precipitation, ammonia volatilization into the environment/space cabin and odor nuisance [292]. Urine also contains organics ($\sim 10 \text{ g COD L}^{-1}$ [294] of which about 90% is biodegradable), fueling bacterial growth. Nitrification has been reported as a suitable method to stabilize urine, while preserving the nutrient content, and plays a pivotal role in the Micro-Ecological Life Support System Alternative (MELiSSA), the RLSS programme from the European Space Agency (ESA) [56, 66, 105, 291, 295]. First, ammonium oxidizing bacteria (AOB) oxidize TAN (total ammonia nitrogen, i.e., sum of ammonia-N and ammonium-N) into nitrite (nitritation), which is subsequently oxidized into non-volatile and non-toxic nitrate (nitrataion) by nitrite oxidizing bacteria (NOB). Simultaneously, biodegradable organics are oxidized to CO_2 by heterotrophic bacteria, decreasing the biofouling potential of urine.

In this study, urine nitrification was performed in a membrane-aerated biofilm reactor (MABR), given its high oxygen utilization efficiency, compact design and compatibility with the reduced gravity conditions in space [63, 137, 183, 213]. In an MABR, oxygen is transferred by diffusion through gas permeable membranes to the biofilm attached to the membrane outer surface. About 30-45 $\text{g O}_2 \text{ L}^{-1}$ urine are required to oxidize all TAN and COD in urine (assuming 6-9 $\text{g of N and COD L}^{-1}$, and 4.33 $\text{g O}_2 \text{ g}^{-1} \text{ N}$ and 0.8 $\text{g O}_2 \text{ g}^{-1} \text{ COD}$). MABR systems have been validated for nitrification, and for the removal of organics (usually expressed as COD, chemical oxygen demand) and/or nitrogen from numerous types of waste streams, including waste streams relevant for space such as mixtures of urine, humidity condensate and surfactants [45, 47, 111, 137, 224]. Due to their counter-diffusional biofilm, MABR systems are often used for simultaneous nitrification-denitrification [40]. Over time, the biofilm thickness increases, and due to the oxygen consumption by nitrifiers and aerobic heterotrophs, residing deep in the biofilm close to the membrane surface, the outer layers of the biofilm (at the biofilm-liquid interface) become anoxic. In these layers, heterotrophic denitrifiers can convert the nitrate into nitrogen gas using COD as an electron donor. Nitrogen removal via nitrification-denitrification in an MABR has been investigated for water recycling from a space-based waste stream, consisting of urine (10%), grey water and humidity condensate [47, 137, 192]. Thus far, only one study reported the use of an MABR

for nitrogen recovery from urine. Udert and Wächter (2012) [295] obtained partial nitrification and COD removal in an MABR operated on stored urine. Despite additional oxygen supply via bubble aeration to prevent anoxic zones, up to 24% of the nitrogen was lost by denitrification and nitrite accumulation occurred because of oxygen limitation [295].

Hence, avoiding the presence of anoxic zones in combination with bioavailable organics is critical in preventing a loss of nitrogen through denitrification. Therefore, a microbial electrolysis cell (MEC) was used in this study in order to remove the rapidly biodegradable COD prior to membrane-aerated nitrification. In the MEC, electrochemically active bacteria oxidize COD and use the anode as an electron acceptor [176]. This way, chemical energy is converted into electrical energy, generating hydrogen gas at the cathode by applying a small potential with an external power supply [176]. In recent years, a large number of studies on bio-electrochemical treatment (MEC and MFC) of (synthetic) urine were published. Since the main focus of most of these studies is energy recovery [129, 130, 191, 256] or TAN recovery [104, 154, 158, 159, 166], low COD removal efficiencies (<50%) are generally reported (SI, Section J).

In this study, the goal was to achieve maximum nitrogen recovery at minimum energy expenditure. The aim for the MEC was therefore to achieve high COD removal efficiencies in order to prevent denitrification in the MABR. Two MEC configurations were evaluated in terms of COD removal, current production and nitrogen recovery, at a range of hydraulic residence times (HRT) and COD loadings. The MEC effluent was fed into a hollow fiber MABR for full nitrification (i.e., with base addition to convert all TAN into nitrate). The load of the MABR was gradually increased to evaluate the reactor performance at a low bulk dissolved oxygen (DO) concentration. Subsequently, raw urine was fed into the MABR to study the effect of the pre-treatment with the MEC. The microbial communities in both reactors were analysed using amplicon 16S rRNA gene Illumina sequencing.

3.2 Materials and methods

3.2.1 Experimental setup

MEC1

MEC1 (Figure 3.1A) was constructed of two Perspex® plates and frames with an internal volume of 200 mL (dimension of $20 \times 5 \times 2 \text{ cm}^3$) separated by an ion exchange membrane (100 cm^2 , Ultrex CMI-7000s or AMI-7001, Membranes International Inc., USA). The anodic compartment was filled with 200 g of graphite granules (Le Carbone, Belgium). Prior to use, the granules were washed with NaOH and HCl, rinsed with demineralized water and dried at 105°C . A graphite felt (Alfa Aesar, Germany) and a stainless steel frame were used for electrical connection to a potentiostat (VSP, Biologic, France), which controlled the anode potential at -250 or -350 mV versus an Ag/AgCl reference electrode (3M NaCl, ALS, Japan). The cathode consisted of a stainless steel wire mesh ($564 \mu\text{m}$ mesh width, $20 \times 5 \text{ cm}^2$, Solana, Belgium). A peristaltic pump was used to recirculate the anolyte and catholyte between the recirculation vessels (glass bottles) and the anodic or cathodic compartment of the MEC. Urine was fed into the anode recirculation vessel with a peristaltic pump and a timer. The catholyte consisted of a phosphate buffer solution and was operated in a closed loop (i.e., without influent and effluent). The total volume of anolyte and catholyte were 740 or 490 mL and 1 L, respectively (Table 3.1).

MEC2

MEC2 (Figure 3.1B) was similar to MEC1 but the anode consisted of a graphite felt (100 cm^2) (without granules) and a stainless steel wire mesh to collect the current. The two compartments were separated by a cation exchange membrane (CEM, Ultrex CMI-7000s, Membranes International Inc., NJ, USA). The effluent of the anode recirculation vessel was directed into the cathode recirculation vessel. The total volume of anolyte and catholyte were 615 mL and 430 mL, respectively.

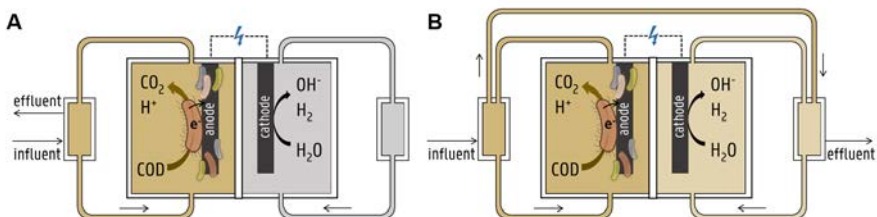


Figure 3.1: **Schematic overview of the microbial electrolysis cells MEC1 (A) and MEC2 (B).**

MABR

The MABR was composed of three hollow fiber (HF) modules (SI Figure S3.1), consisting of 180 flow-through dense (non-porous) silicone rubber hollow fibers with a length of 25 cm, an inner diameter of 0.3 mm and an outer diameter of 0.5 mm (Nagasep M100, Nagayanagi Co., Japan). Each module was made from a plastic housing and had a total membrane surface area of 0.06 m² and liquid volume of 90 mL. The liquid volume in the modules was hence 270 mL. The liquid was recirculated between the modules and two recirculation vessels (100 mL glass bottles) with a peristaltic pump at a flow rate of 11 L h⁻¹ (17 reactor volumes per hour). Including vessels, tubing and modules, the reactor had a total liquid volume of 650 mL. Humidified air was supplied through the lumen of the fibers in opposite direction of the liquid flow with aquarium pumps (air pump 400, EHEIM, Germany) at a flow rate of 0.65-0.75 L min⁻¹. The bulk liquid dissolved oxygen (DO) concentration was monitored with a luminescent DO probe (LDO10103, Hach, Belgium) and a HQ40d meter (Hach, Belgium) and logged every five minutes. The pH was controlled at 6.85 by dosing 0.25 M NaOH with a Consort R3610 controller (Consort, Belgium) to obtain full nitrification. Influent was dosed with a peristaltic pump and a timer. After 168 days, one module was removed and sacrificed for sequencing, after which the MABR was operated with two modules (total liquid volume of 500 mL).

3.2.2 Reactor operation

Urine collection

Fresh urine from healthy male donors, not taking medication, was collected using a nonwater urinal with approval from the Ethical Committee of Ghent University Hospital (registration number B670201731862). Immediately after collection, batches of 2-4 L were prepared. The urine was diluted with demineralized water (33.3vol% urine; 66.6vol% water), simulating the diluting effect of flush water in urine diverting toilets [316], and the pH was increased to above 11 with 2M NaOH to prevent urea hydrolysis during storage at 4°C prior to feeding into the MEC.

MEC operation

The anodic compartment of MEC1 was inoculated with effluent originating from an active MEC (fed with fermenter supernatans) and operated in fed-batch mode on modified M9 medium [117] to establish an electroactive biofilm on the graphite granules. Subsequently, urine was fed into the anode recirculation vessel at 111 mL d⁻¹. After 21 days, the CEM separating the electrode compartments was replaced by an AEM and the MEC was tested at different hydraulic retention times (HRT) (Table 3.1). MEC2 was inoculated with effluent from MEC1 (phase AEM2) and was operated for one month in fed-batch mode on modified M9 medium to establish an electroactive biofilm on the felt before feeding urine. MEC2 was operated at three different HRT (Table 3.1).

Table 3.1: **Overview of the different operational phases of MEC1 and MEC2.** For MEC2, the HRT in the anodic compartment and total HRT (in anodic and cathodic compartment, value between brackets) are displayed. The average influent and effluent composition is reported in SI, Section 3.6.2. IEM: Ion Exchange Membrane, CEM: Cation Exchange Membrane, AEM: Anion Exchange Membrane

Phase	MEC	IEM	Anolyte volume [mL]	Anode potential [mV] ^a	Influent flow rate [mL d ⁻¹]	HRT [d]	Duration [d]	number of HRT
MEC1-CEM	1	CEM	740	-350	111	6.6	21	3.2
MEC1-AEM1	1	AEM	740	-350	110	6.7	27	4.0
MEC1-AEM2	1	AEM	490	-250	120	4.1	53	13.0
MEC1-AEM3	1	AEM	490	-250	133	3.7	20	5.4
MEC2-CEM1	2	CEM	615	-250	144	4.3 (7.3)	52	12.2 (7.2)
MEC2-CEM2	2	CEM	615	-250	241	2.5 (4.3)	25	9.8 (5.8)
MEC2-CEM3	2	CEM	615	-250	112	5.5 (9.4)	75	13.7 (8.0)

^a versus Ag/AgCl reference electrode

Samples were taken every 2-4 days, filtered over a 0.22 μm Chromafil® Xtra filter (Macherey-Nagel, PA, USA) and stored in the fridge (4°C) prior to analysis. The coulombic efficiency (CE; in this manuscript defined as the ratio between the real current that was monitored with the potentiostat and the theoretical current calculated based on the COD removal) was calculated with the following equation [176].

CE [%] =

$$\frac{100 \times \text{current [A]}}{(COD_{in} - COD_{out}) \left[\frac{g \text{ COD}}{L} \right] \times \text{flow rate} \left[\frac{L}{d} \right] \times \frac{4 \frac{\text{mol } e^-}{\text{mol } O_2} \times 96485 \frac{C}{\text{mol } e^-}}{32 \frac{g \text{ O}_2}{\text{mol } O_2} \times (24 \times 60 \times 60) \frac{s}{d}}}
 \quad (9)$$

MABR operation

The MABR was inoculated with sludge from a urine nitrification reactor (Eawag, Switzerland) and was operated for 10 days in batch mode and for 35 days in continuous mode on a synthetic ammonium sulfate solution. Subsequently, diluted MEC effluent (16% urine) was dosed to the reactor and the loading was gradually increased by increasing the influent flow rate (phase MEC I) (Table 3.2). On day 66 and 92, the urine concentration was increased to 25% urine (MEC II) and 33% urine (MEC III), respectively, by

decreasing the dilution of the MEC effluent. At the end of phase MEC III (day 168), one HF bundle was removed for microbial community analysis and the MABR was fed with a synthetic ammonium sulfate solution until the start of phase MEC IV. To evaluate the effect of the MEC pre-treatment, the loading was increased until a bulk DO concentration below $0.1 \text{ mg O}_2 \text{ L}^{-1}$ was reached in phase MEC IV. Next, the MABR was operated at the same N loading but on raw urine (stabilized with NaOH to prevent urea hydrolysis in the influent) instead of MEC effluent for 56 days (RAW I). In phase RAW II, the air flow rate and recirculation rate were increased to 1.5 L min^{-1} and 16.3 L h^{-1} , respectively, to enhance the oxygen mass transfer. Afterwards, the MABR was operated again on MEC effluent at the same N loading and initial air flow rate and recirculation rate ($0.65\text{-}0.75 \text{ L min}^{-1}$ and 11 L h^{-1} , respectively) (phase MEC V). Between phase RAW II and MEC V, no influent was dosed for two days to allow oxidation of the TAN that accumulated during RAW II. In phase MEC VI, the N loading was further increased.

Samples were taken every 2-4 days, filtered over a $0.22 \mu\text{m}$ Chromafil® Xtra filter (Macherey-Nagel, PA, USA) and stored in the fridge (4°C) prior to analysis. Average influent and effluent compositions are reported in SI, Section 3.6.5.

3.2.3 Analytical methods

Ions were analysed on a compact ion chromatograph equipped with a conductivity detector (Metrohm 930 with Metrosep A supp 5-150/4.0 column for anions and Metrohm 761 with Metrosep A supp 5-150/4.0 column for cations, Metrohm, Switzerland). The ammonium concentration in the MABR effluent (low concentration) was determined according to the Montgomery reaction (Montgomery and Dymock 1961) with a Tecan infinite plate reader (Infinite F50 Absorbance Microplate Reader, Tecan Trading AG, Switzerland). Nanocolor tube test kits (Nanocolor TN220 and Nanocolor COD160/1500, Macherey-Nagel, PA, USA) were used to measure the total nitrogen (TN) and COD concentration. The electrical conductivity (EC) was measured with a conductivity meter (Consort C6010 with a Metrohm 6.0912.110 conductivity probe) and pH measurements were performed with a portable pH meter (C5010, Consort bvba, Belgium).

Table 3.2: Overview of different operational phases of the membrane-aerated biofilm reactor (MABR).

Phase	MEC I ^a	MEC II	MEC III ^b	MEC IV ^b	RAW I ^b	RAW II	MEC V ^b	MEC VI
Number of HF bundles	3	3	3	2	2	2	2	2
Influent	MEC1	MEC2	MEC2	MEC2	stabilized urine	stabilized urine	MEC2	MEC2
effluent	effluent	effluent	effluent	effluent	33.3%	33.3%	effluent	effluent
16.7%	25%	33.3%	33.3%	33.3%	33.3%	33.3%	33.3%	33.3%
Day	1 ^c - 65	66 - 91	92 - 168	205 - 266	267 - 322	323 - 339	340 - 381	382 - 392
Duration [d]	65	26	77	62	56	17	42	11
Duration (number of HRT)	7.2	4.5	13.4	6.5	6.3	1.8	5.5	1.8
HRT [d]	5.5 ± 0.3	5.8 ± 0.3	5.6 ± 0.2	8.8 ± 0.5	8.8 ± 0.3	9.4 ± 0.3	8.2 ± 0.6	6.2 ± 0.0
N load [<i>mg N d</i> ⁻¹]	84 ± 6	109 ± 3	151 ± 18	100 ± 8	102 ± 2	101 ± 3	93 ± 4	125 ± 5
N loading rate d [<i>mg N L</i> ⁻¹ <i>d</i> ⁻¹]	129 ± 9	168 ± 5	232 ± 28	198 ± 16	202 ± 4	199 ± 5	183 ± 9	247 ± 9
COD load [<i>mg COD d</i> ⁻¹]	18 ± 2	22 ± 2	25 ± 5	18 ± 1	101 ± 2	99 ± 2	21 ± 1	27 ± 1
COD loading rate ^d [<i>mg COD L</i> ⁻¹ <i>d</i> ⁻¹]	27 ± 3	33 ± 3	38 ± 8	35 ± 3	200 ± 3	196 ± 5	41 ± 2	54 ± 2
NOD ^e [<i>mg O</i> ₂ <i>d</i> ⁻¹]	362 ± 25	472 ± 13	653 ± 78	434 ± 35	443 ± 8	434 ± 11	401 ± 19	542 ± 21
BOD for COD oxidation ^f [<i>mg O</i> ₂ <i>d</i> ⁻¹]	0 ± 0	3 ± 2	3 ± 3	8 ± 1	72 ± 1 ^g	72 ± 2 ^g	9 ± 1	12 ± 1
Total biological oxygen demand (NOD+BOD) [<i>mg O</i> ₂ <i>d</i> ⁻¹]	362 ± 25	475 ± 16	656 ± 81	442 ± 36	514 ± 9	506 ± 13	409 ± 20	554 ± 21
Average DO [<i>mg O</i> ₂ <i>L</i> ⁻¹]	4.8 ± 0.4	4.6 ± 0.7	2.6 ± 0.4	0.1 ± 0.1	0.02 ± 0.01	0.03 ± 0.01	0.04 ± 0.14	0.03 ± 0.01
Temperature [°C]	27.1 ± 1.3	25.9 ± 1.5	30.4 ± 1.1	22.5 ± 1.0	22.1 ± 1.0	20.0 ± 0.9	22.7 ± 0.9	23.1 ± 0.8
pH influent	9.1 ± 0.1	9.2 ± 0.1	9.1 ± 0.0	9.2 ± 0.1	11.3 ± 0.1	10.8 ± 0.1	9.1 ± 0.0	9.2 ± 0.0

^a HRT, N/COD load & loading, oxygen demand and DO are calculated based on data after reaching steady state with a fixed influent flow rate (days 49-65)

^b HRT, N/COD load & loading and oxygen demand are calculated based on data after the first 3 HRT (steady state)

^c Day 1 corresponds to the first day that the reactor was operated on MEC effluent (45 days after start-up of the reactor)

^d The loading was calculated taking into account the total reactor volume (MEC I-III=650 mL, MEC IV-VI=500 mL)

^e The Nitrogenous Oxygen Demand (NOD) was estimated assuming 4.33 g O₂ g⁻¹ N for nitrification

^f The Biological Oxygen Demand (BOD) for COD oxidation is estimated assuming that all COD is removed aerobically, consuming 0.8 g O₂ g⁻¹ COD removed

^g The BOD for COD oxidation is overestimated in RAW I and RAW II since a part of the COD was removed using nitrate as an electron acceptor instead of oxygen

3.2.4 Microbial community analysis

Samples from both reactors were collected throughout the experiments for microbial community analysis. The different MEC microenvironments (MEC anolyte, graphite granules and/or felt) were sampled at the end of each experiment (Table 3.1). One of the MABR bundles ('MABR bundle 1') was sacrificed for sequencing after phase MECIII and another bundle ('MABR bundle 2') was sampled at the end of the experiment (Table 3.2). Biomass from the flocs, fibers, and firmly attached biomass (after scraping off loosely attached biomass from the fibers) were collected. The samples were stored at -20°C prior to DNA extraction and quality control, performed as described by De Paepe et al. (2017) [67]. DNA extracts were sent out to BaseClear BV (Leiden, The Netherlands) for library preparation and sequencing of the V3-V4 region of the 16S rRNA gene on an Illumina MiSeq platform (Illumina, Hayward, CA, US) with Illumina MiSeq v3 chemistry and using the 341F-785R primerpair adopted from Klindworth et al. (2013) [147]. The sequence data are available at the NCBI (National Center for Biotechnology Information) database under accession number PRJNA572564. The data was processed with the mothur software package (v.1.40.5) [259] as outlined by De Paepe et al. (2017) [67]. OTUs were defined as a collection of sequences with a length between 393 and 429 nucleotides that were found to be more than 97% similar to one another in the V3-V4 region of their 16S rRNA gene after applying OptiClust clustering [46, 258, 259, 309]. Taxonomy was assigned using the silva.nr_v132 database [55, 235, 308]. The OTU table with taxonomy assignment was loaded into R, version 3.6.1 (2019-07-05), and singletons were removed [189, 236]. A Principle Coordinate Analysis (PCoA; package stats 4.3.6.1) was used to explore differences in microbial community composition, which were visualized with ggplot2 version 3.2.1 [34, 62, 114, 239]. For this purpose, the shared file (including the duplicate samples) was filtered based on the arbitrary cut-offs described by McMurdie and Holmes (2014b), whereby OTUs observed in less than 5% of the samples and with read counts below 0.5 times the number of samples were removed. The data was rescaled to proportions and the abundance based jaccard dissimilarity matrix was calculated (package vegan 2.4-3) [6, 189, 215]. On the genus level, weighted averages of genera abundances were *a posteriori* added to the ordination plot, using the wascores function in vegan [215].

3.3 Results

3.3.1 COD removal, current production, coulombic efficiency and urea hydrolysis in the MEC

The primary goal of the MEC was to remove organics from urine in an energy-efficient way, as to prevent N loss via denitrification in the MABR. Due to the use of different batches of urine, the influent COD concentration and load were varying over time, as exemplified in Figure 3.2A and B for MEC1-AEM2 and MEC2-CEM1, respectively. Despite the fluctuating influent COD concentration, the COD concentration in the effluent remained stable. Electroactive bacteria transferred the electrons obtained by COD oxidation to the anode, generating an electric current from anode to cathode. The current density ranged between 0.5 and 2 A m⁻² (membrane projected surface) in all experiments (Table 3.3), and followed the same pattern as the influent COD concentration, i.e., a high influent COD concentration resulted in a higher current (Figure 3.2C-D). Apart from COD removal, urea hydrolysis took place in the MEC, increasing the TAN/TN ratio from <10% (influent) to ~100% (effluent) (Figure 3.2G-H, Table 3.3).

MEC1 was initially operated with a CEM separating the two electrode compartments and achieved COD removal efficiencies around 80% at an HRT of 6.6 days and an average COD loading of 22.4 ± 5.3 g COD m⁻² d⁻¹ (Table 3.3, MEC1-CEM). The average current density was 1.0 ± 0.3 A m⁻² (Table 3.3), which was about 42% of the current that was expected based on the observed COD removal (i.e., coulombic efficiency). Because of the electron flow from anode to cathode, cations migrated from the anolyte to the catholyte through the CEM to restore the charge balance. As a result, more than 65% of the N was removed from the urine (anolyte) by migration of ammonium. The average pH in the effluent of the anolyte was 8.1, and was affected by the pH of the influent, urea hydrolysis (producing TAN and bicarbonate), proton production by COD oxidation and proton migration through the CEM to the cathodic compartment.

In order to prevent the loss of ammonium by migration, the CEM was replaced by an AEM. The average COD removal efficiency equalled 86% at an HRT of 6.7 days and an average COD loading of 29.4 ± 1.5 g COD m⁻² d⁻¹ (MEC1-AEM1, Table 3.3, SI Section 3.6.3). Next, the HRT was decreased from 6.7 to 4.1 days (MEC1-AEM2) and 3.7 days (MEC1-AEM3) by decreasing the volume of the anode recirculation bottle and slightly increasing the influent flow (Table 3.1). Decreasing the HRT did not affect the COD removal efficiency (~79-86%), the current production (~1.3-1.4 A m⁻²) nor the coulombic efficiency (~38-46%), as the COD loading remained similar (Table 3.3, SI Section 3.6.3). The effluent pH was higher compared to MEC1-CEM (8.4-9 compared to 8.1) because of the OH⁻ migration from the catholyte through the AEM to the anolyte (OH⁻ ions are produced at the cathode by water reduction). Despite the replacement of the CEM by an AEM, 11-41% of the N was lost in all experiments with an AEM in MEC1. Because of the high pH (8.4-9), a substantial fraction of TAN was present as ammonia,

which can diffuse through the AEM to the cathodic compartment.

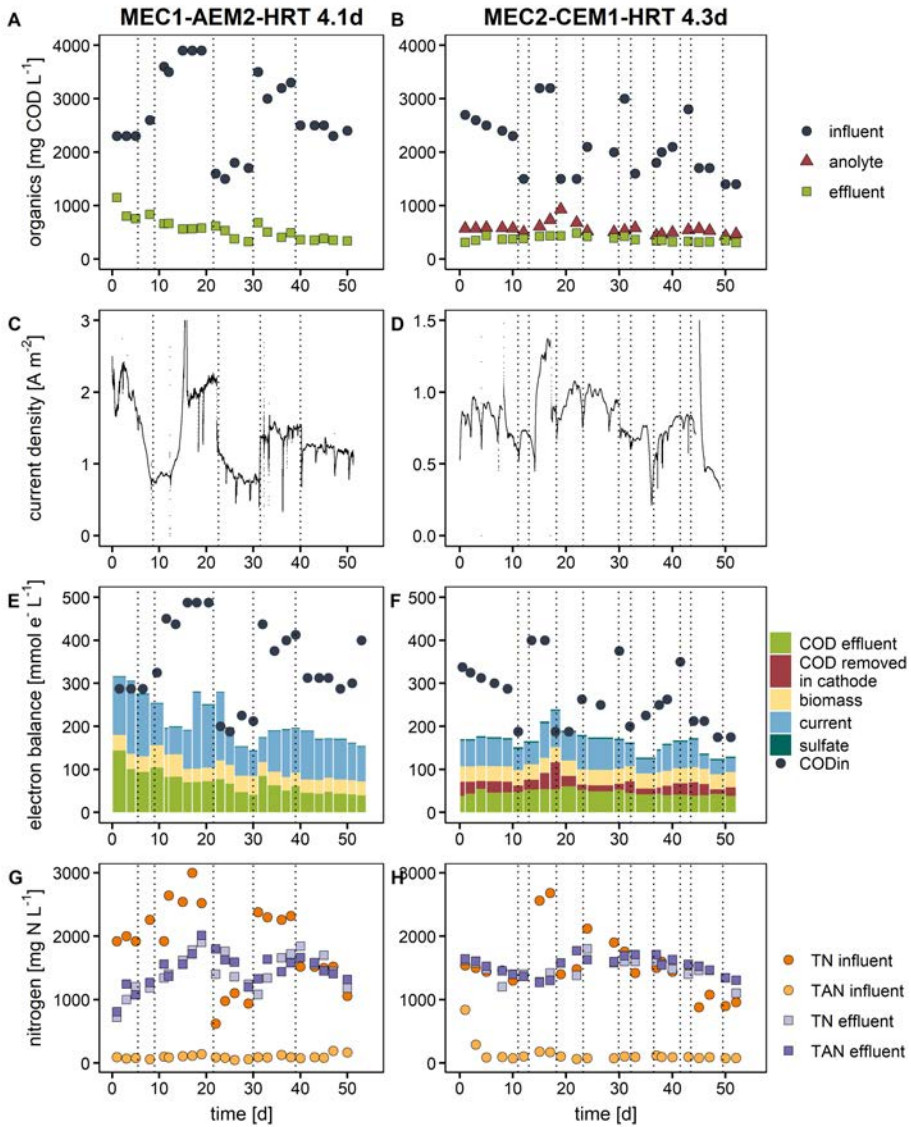


Figure 3.2: **COD removal (A-B), current density (C-D), electron balance (E-F) and nitrogen balance (G-H) of MEC1 operated with an AEM at a HRT of 4 days (MEC1-AEM2) and MEC2 operated with a CEM at a HRT of 4.5 days (MEC2-CEM1).** Different batches of urine were fed to the MECs, as indicated by the dashed lines on the graphs. The equations used to calculate the electron balance are given in SI Section 3.6.4.

Table 3.3: **MEC: average COD loading, COD removal efficiency, cell voltage, current density, coulombic efficiency, N balance ($N_{effluent}/N_{influent}$), TAN/TN (total ammonia nitrogen/total nitrogen) ratio and pH in the effluent.** The large standard deviations are caused by the use of different batches of urine (with a different composition). For MEC2, two HRT, COD removal efficiencies and pH values are reported: the value on the first row is the HRT/COD removal efficiency/pH in the anodic compartment, the value on the second row is the total HRT/COD removal efficiency/pH after passage through the cathodic compartment. Time series data are presented in SI (Figures S3.2-S3.3) and Figure 3.2 (MEC1-AEM2 and MEC2-CEM1). CEM: Cation Exchange Membrane, AEM: Anion Exchange Membrane, HRT: Hydraulic Residence Time.

	HRT	COD loading	COD removal efficiency	anode potential	cell voltage	current density	coulombic efficiency	N balance	TAN/TN	pH
	[d]	[g COD m ⁻² d ⁻¹] ^a	[%]	[mV]	[mV]	[A m ⁻²]	[%]	[%]	[%]	
MEC1-CEM	6.6	22.4 ± 5.3	80 ± 7	-350	-713 ± 57	1.0 ± 0.3	42 ± 5	34 ± 6	92 ± 8	8.1 ± 0.2
MEC1-AEM1	6.7	29.4 ± 1.5	86 ± 3	-350	-769 ± 83	1.3 ± 0.2	38 ± 5	81 ± 0	98 ± 4	8.4 ± 0.2
MEC1-AEM2	4.1	32.3 ± 8.8	79 ± 9	-250	-919 ± 93	1.4 ± 0.6	41 ± 21	59 ± 15	103 ± 13	8.7 ± 0.4
MEC1-AEM3	3.7	28.1 ± 8.9	81 ± 8	-250	-907 ± 41	1.3 ± 0.3	46 ± 13	89 ± 21	100 ± 2	9.0 ± 0.2
MEC2-CEM1	4.3	30.6 ± 7.9	73 ± 7	-250	-762 ± 25	0.8 ± 0.2	27 ± 11	98 ± 23	105 ± 9	8.7 ± 0.2
	7.3		81 ± 6							9.4 ± 0.1
MEC2-CEM2	2.5	33.7 ± 5.3	48 ± 4	-250	-781 ± 16	0.8 ± 0.1	36 ± 4	96 ± 15	115 ± 9	9.0 ± 0.1
	4.3		71 ± 5							9.3 ± 0.1
MEC2-CEM3	5.5	19.8 ± 4.9	40 ± 9	-250	-770 ± 27	0.5 ± 0.1	33 ± 18			8.9 ± 0.2
	9.4		68 ± 9							9.3 ± 0.1

^a membrane projected surface area (100 cm²)

Therefore, in MEC2, the effluent of the anodic compartment was directed to the cathodic compartment in order to capture all the N that migrated or diffused through the membrane (CEM). Also the granules were replaced by a single graphite felt to attempt to increase the coulombic efficiency, but the average coulombic efficiency (27%) did not improve (Table 3.3). Decreasing the HRT in the anodic compartment from 4.3 days to 2.5 days by increasing the influent flow (and thus COD load), resulted in a higher coulombic efficiency (36%) but decreased the COD removal efficiency in the anodic compartment from 73% to 48% (MEC2-CEM2, Table 3.3). Increasing the HRT to 5.5 days in MEC2-CEM3 did not restore the COD removal in the anodic compartment. At all HRT, the COD in the catholyte was lower than the COD in the anolyte, indicating that additional COD was removed in the cathodic compartment of MEC2 (Table 3.3, Figure 3.2B). MEC2 did not improve the COD removal and current production, but was successful in preventing N loss from the urine. On average 96-98% of the N in the influent was contained in the effluent. Moreover, by redirecting the urine to the cathodic compartment, all OH^- that was produced at the cathode was recovered, resulting in a slightly higher effluent pH compared to MEC1 (Table 3.3).

3.3.2 Nitrification and COD removal in MABR

The MEC effluent was fed into the MABR to convert TAN into nitrate by nitrification. In the first phase (MEC I, Table 3.2), the effluent of the MEC was diluted 50%, corresponding to a 16% urine solution with a TN concentration of about 760 mg N L^{-1} (Figure 3.3B and Table S3.3). The load was gradually increased from $\sim 40 \text{ mg N d}^{-1}$ (day 1) to $\sim 85 \text{ mg N d}^{-1}$ (day 49-65) by increasing the influent flow, resulting in a decreasing bulk DO concentration due to the increased bacterial activity (Figure 3.3A, SI Figure S3.4). The pH was controlled at 6.85 with NaOH to obtain full nitrification. All N in the influent was present as TAN since urea hydrolysis occurred in the MEC (Figure 3.3B). Apart from some accumulation in the first days, the TAN and nitrite concentration in the effluent were both below 10 mg N L^{-1} (Figure 3.3D). The nitrate concentration in the effluent gradually increased and equalled the TN concentration in the effluent (Figure 3.3D). Between days 49 and 65, the nitrate and TN concentration remained stable at $\sim 645 \text{ mg N L}^{-1}$, which corresponded to 92-94% of the incoming N concentration (after rescaling the influent concentration to account for the difference in influent and effluent volume caused by the NaOH addition for pH control) (Figure 3.3C). The chloride balance equalled 93%, suggesting that steady state might not have been reached yet at the end of the phase. About $150 \text{ mg COD L}^{-1}$ was present in the influent and effluent, indicating that all (readily) biodegradable COD had been removed in the MEC (HRT of 4.1 d) and the remaining COD was not removed in the MABR (HRT of 5.5 d) (Figure 3.3E).

On day 66, the urine concentration was increased to 25% urine (MEC II). As a result, the load increased to $\sim 110 \text{ mg N d}^{-1}$ (Table 3.2, SI Figure S3.4), and the nitrate and TN concentration in the effluent gradually increased (Figure 3.3D), whereas the bulk DO concentration decreased to $\sim 4.6 \text{ mg O}_2 \text{ L}^{-1}$ (Figure 3.3A). Due to an issue with

the pH controller on day 77, acid was added to the reactor resulting in a temporary decrease in nitrate and TN concentration (because of the dilution with acid) and some TAN accumulation (41 mg TAN L^{-1}).

On day 92, the urine concentration was further increased to 33% urine (MEC III). The load fluctuated between 130 and 160 mg N d^{-1} , due to the use of different batches of MEC effluent with a different N concentration ($\sim 1500 \text{ mg N L}^{-1}$ (day 92-106), $\sim 1200 \text{ mg N L}^{-1}$ (day 107-128) and $\sim 1500 \text{ mg N L}^{-1}$ (day 129-168), Figure 3.3B, SI Figure S3.4). Also the nitrate and TN concentration in the effluent and the bulk DO concentration varied between 1100 - 1500 mg N L^{-1} and 2 - $4 \text{ mg O}_2 \text{ L}^{-1}$, respectively (Figure 3.3A, D). The TN concentration in the effluent coincided with the (rescaled) influent, when steady state was reached (day 143-168), whereas the COD concentration in the effluent was $\sim 16\%$ lower than the (rescaled) influent concentration, indicating some COD removal by heterotrophic bacteria in the MABR.

From MEC I to III, the bulk DO concentration dropped because of the increasing influent flow rate (in MEC I) or increased urine concentration (MEC II & III), but was still higher than $2 \text{ mg O}_2 \text{ L}^{-1}$. Therefore, in MEC IV, the load was further increased until a DO below $0.2 \text{ mg O}_2 \text{ L}^{-1}$ was reached, at a load of $\sim 100 \text{ mg N d}^{-1}$. This load was lower compared to the load during MEC II-III, since the MABR, after sacrificing one HF bundle for microbial community analysis, only consisted of two HF bundles. Apart from some TAN accumulation at the start (day 207-224), full nitrification was obtained and no N losses were observed (rescaled TN influent coincided with TN effluent, Figure 3.3C-D) at an average bulk DO concentration of $0.1 \text{ mg O}_2 \text{ L}^{-1}$. The COD concentration in the effluent ($116 \text{ mg COD L}^{-1}$) was 63% lower than the (rescaled) concentration in the influent ($315 \text{ mg COD L}^{-1}$).

In the next phase (RAW I), the MABR was operated at the same N load ($\sim 100 \text{ mg N d}^{-1}$) but on diluted raw urine (33%), which was stabilized (i.e., NaOH was added to obtain a $\text{pH} > 11$ in order to inhibit urea hydrolysis in the influent) but not treated in a MEC. Unlike the MEC effluent in which all N was present as TAN, organic N was the predominant N species in the raw urine (Figure 3.3B). Only $\sim 7\%$ of the TN in the influent ($\sim 1850 \text{ mg N L}^{-1}$) was TAN ($\sim 135 \text{ mg N L}^{-1}$), requiring urea hydrolysis in the MABR. Furthermore, without pre-treatment in the MEC, the COD concentration in the influent was substantially higher ($1850 \text{ mg COD L}^{-1}$ compared to only $350 \text{ mg COD L}^{-1}$ in MEC IV) (Figure 3.3E). The COD concentration in the effluent did not increase (Figure 3.3E), thus the MABR was able to remove all (readily) biodegradable COD (91% of the incoming COD). However, the higher COD load and oxygen demand hampered nitrification, with oxygen becoming a limiting substrate, resulting in partial nitrification. The effluent contained 20-25% TAN and 70-75% nitrate from day 297 onwards (Figure 3.3D). The oxygen limitation furthermore gave rise to denitrification, with a TN concentration in the effluent $\sim 18\%$ lower than the (rescaled) TN concentration in the influent.

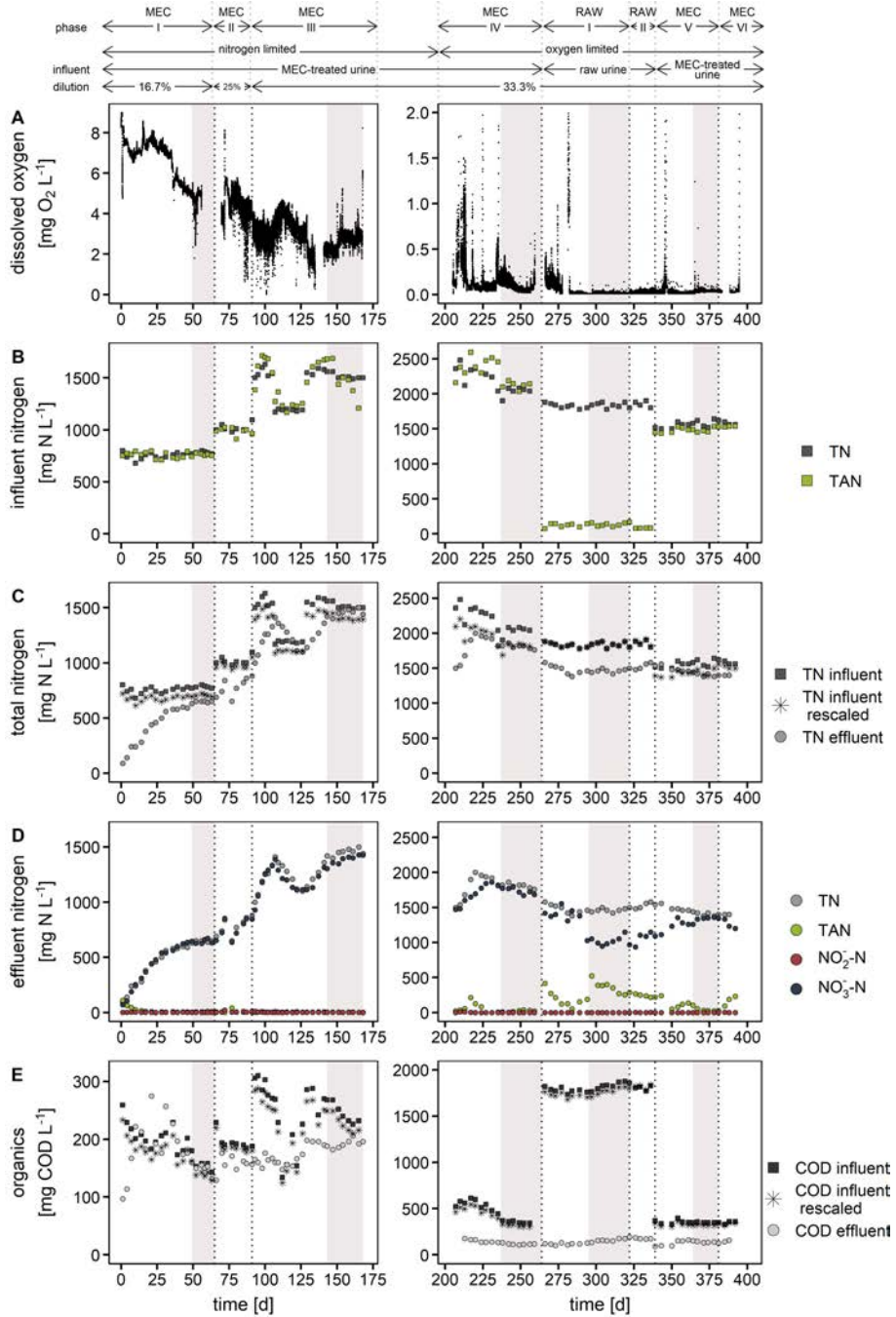


Figure 3.3: MABR: dissolved oxygen (DO) concentration in the bulk liquid (A), nitrogen speciation in the influent (B), total nitrogen (TN) concentration in influent and effluent (C), nitrogen speciation in the effluent (D) and COD concentration in influent and effluent (E). Steady state periods are indicated with a

grey background. As the influent and effluent volume were not equal due to the base addition for pH control, the influent concentration was rescaled in plots C and E. The average compositions of influent and effluent in each phase are given in SI Tables S3.3-S3.4.

On day 323, the air flow rate and recirculation rate were increased to enhance the oxygen mass transfer through the hollow fiber membranes (RAW II). As a result, the TAN concentration in the effluent decreased (14% of the TN concentration), while the TN concentration in the effluent slightly increased (83.4% of the rescaled TN concentration) (Figure 3.3C-D).

Subsequently, the MABR was operated again on MEC effluent at the same N load of 100 mg N d^{-1} (MEC V), reverting successfully to full nitrification without N loss (Figure 3.3C-D).

In a last phase (MEC VI), the MABR was operated on MEC effluent but at a load of 125 mg N d^{-1} , resulting in DO limitation and TAN accumulation, but without N loss, showing robustness against variable N loading (Figure 3.3C-D).

3.3.3 Microbial community composition of MEC and MABR

Amplicon 16S rRNA gene Illumina sequencing and principle coordinate analyses (SI Figures S3.11, S3.14 and S3.15) revealed that the MEC and MABR units were characterized by very distinct and diverse microbial communities (Figure 3.4, SI Figures S3.7-S3.15). This divergence in the first place stems from the different inocula that were introduced into the MEC and MABR. MEC1 was inoculated with effluent originating from an active MEC (fed with fermenter supernatant) and effluent from MEC1 was used to inoculate MEC2. The MABR was inoculated with sludge from a urine nitrification reactor operated at Eawag (Switzerland). The communities were further shaped by the different conditions (anoxic versus oxic, high versus low COD loading, different pH and conductivity) resulting in stable communities adapted to carry out the particular biological processes (i.e., anodic COD oxidation versus nitrification) in both MEC and MABR, even despite the influx of MEC effluent in the latter.

At phylum and family level, the MEC was rich in *Proteobacteria* (~50%, mainly *Burkholderiaceae*, *Geobacteraceae* and *Pseudomonadaceae*), *Bacteroidetes* (~25%, including *Lentimicrobiaceae* and *Dysgonomonadaceae*) and *Firmicutes* (~25%, mainly *Carnobacteriaceae* and *Clostridiaceae*) (SI Figures S3.7-S3.8), whereas the MABR was dominated by *Bacteroidetes* (~40%, amongst others *Chitinophagaceae* and *Saprospiraceae*), *Proteobacteria* (~30%, including *Burkholderiaceae* and *Nitrosomonadaceae*) and *Actinobacteria* (~15%, e.g., *Nocardiaceae*) (SI Figure S3.12).

At genus level, the MEC community was dominated by *Geobacter*, *Pseudomonas*, *Arcobacter* and *Comamonas*, genera known to comprise electroactive bacteria [26, 177, 237, 321] (SI Figures S3.9-S3.10). Furthermore, alkaliphilic genera (*Alcaligenes* and

Alkalibacter), *Thiopseudomonas*, *Lentimicrobiaceae*, *Proteiniphilum*, and *Tissierella* were abundant (pH was ~9 in MEC). Interestingly, a member of the *Tissierella* genus (*Tissierella creatinophila*) is able to grow on creatinine (one of the main COD compounds in urine) as sole carbon and energy source and degrades creatinine to acetate, mono-methylamine, ammonia and carbon dioxide [121].

Although their relative abundance varied strongly across samples, this core set of genera dominated the microbial community throughout time regardless of modifications in reactor configuration and operation, except for *Synergistaceae* which were abundant in the inoculum (~15%) and initially also in the MEC (MEC1-CEM), but almost disappeared afterwards (SI Figure S3.8). Besides the absence of a temporal effect, there were no consistent differences in microbial community between the microenvironments (i.e., anolyte, felt or granules) (Figure 3.4, SI Figures S3.7-S3.11). Even samples taken at the same moment from the graphite felt used in MEC2-CEM3 were different. This indicates that stochastic effects are responsible for the observed differences between samples and microenvironments and that there is no niche preference (no specific association of certain community members with the different microenvironments).

While (strictly) anaerobic genera prevailed in the MEC, the MABR was dominated by aerobic genera, including *Nitrosomonas*, *Moheibacter* and *Gordonia* (Figure 3.4). About 5-10% of the community in the MABR was a member of the ammonium oxidizing genus *Nitrosomonas*. *Nitrospira*, another AOB genus, was also present but at lower relative abundances (<0.5%). Members of known nitrite oxidizing genera (*Nitrobacter*, *Nitrospira*) were not retrieved, even though nitratation occurred in the MABR.

Samples originating from bundles 1 and 2 clustered separately in a principle coordinate analysis (PCoA) analysis at genus level and were clearly different from the inoculum (SI Figure S3.14). Bundle 1 was harvested after MEC III (operation without oxygen limitation), whereas bundle 2 was harvested at the end of the experiment (after MEC VI), including the period with oxygen limitation and operation on raw urine with a high COD concentration and urea as main N source. Bundle 2 was more enriched in PHOS-HE36 (member of *Ignavibacteria*) and UTCFX1 (belonging to the *Anaerolineaceae*), probably as a result of the low DO concentration and higher COD load.

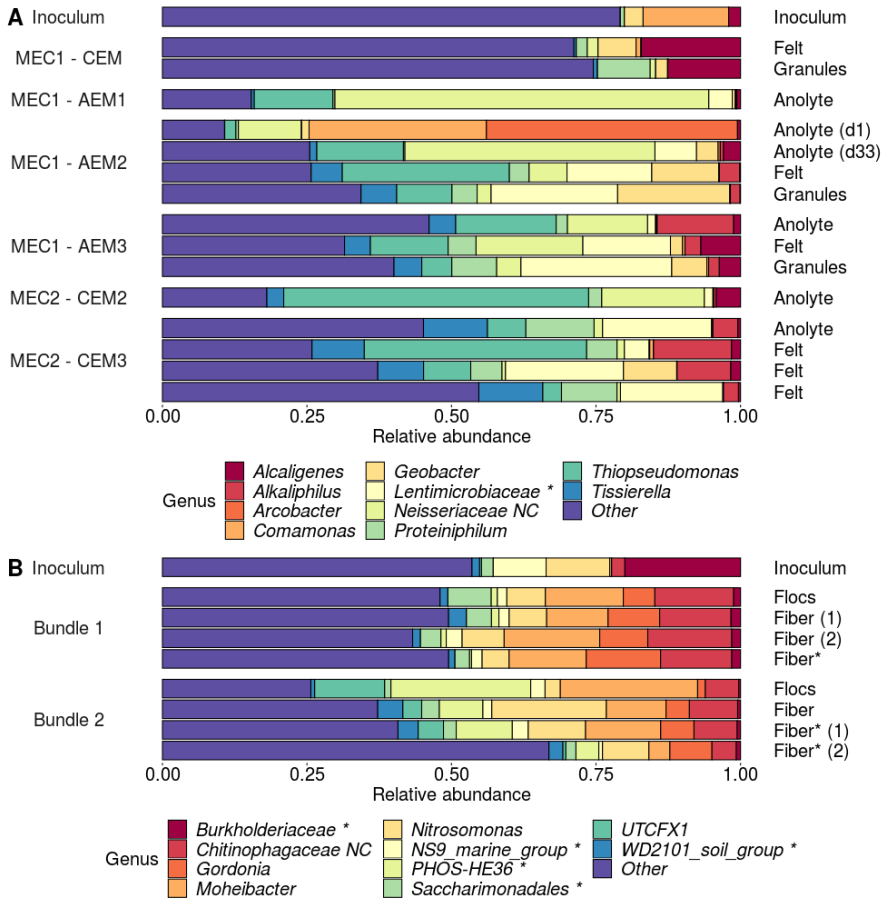


Figure 3.4: **Composition of the microbial communities at genus level (where possible) of the microbial electrolysis cell (MEC, A) and membrane-aerated biofilm reactor (MABR, B)** For the MEC, a distinction was made between biomass present in the anolyte, on the felt or on the granules. All samples were taken at the end of the experiment (except 'Inoculum' and 'Anolyte (d1)', taken on the first day) (Table 3.1). For the MABR, a distinction was made between biomass flocs in the bundle ('flocs'), biomass on the fibers ('fibers') and firmly attached biomass on the fibers after scraping off the loosely attached biomass ('fiber*'). Bundle 1 and 2 were sampled after phase MEC III and MEC VI, respectively (Table 3.2). The numbers between the brackets indicate duplicates. The relative abundance of the ten most abundant genera is shown. Taxa that could not be classified at genus level are specified at family level followed by *. Uncultured bacteria are indicated by 'NC' (not cultured).

3.4 Discussion

3.4.1 The MEC reached high COD removal efficiencies, yet converted only 25-45% of the removed COD to current

Urine was pre-treated in a MEC to remove organics in an energy-friendly manner as to enable full N recovery in the MABR. However, due to ammonium migration and ammonia diffusion through the membrane, up to 65% of the N was lost in MEC1. This issue was solved in MEC2, by directing the effluent of the anodic compartment through the cathodic compartment. Both MEC1 and MEC2 achieved up to 80-85% COD removal with HRTs between 4-7 days. Most studies on urine treatment in continuously fed bio-electrochemical systems (BES, i.e., MEC and MFC) report lower COD removal efficiencies, ranging from ~10% to 46% (SI Section 3.6.10). These studies mostly focus on energy or TAN recovery, and therefore apply a low HRT (<1d), presumably causing the lower COD removal. Only Walter et al. (2018) [306] obtained a high COD removal efficiency (88%) at a relatively low HRT of 44h, but the coulombic efficiency was only 4%, indicating that most of the COD was removed by other mechanisms than bio-anodic oxidation. In our study, fresh urine was used to feed the MEC, while most studies in literature use stored urine. Fresh urine is composed of complex organic molecules (including long-chain organic acids, creatinine, amino acids and carbohydrates), whereas in stored urine, a significant fraction of the complex organic molecules are already hydrolysed/fermented into acetate and other smaller molecules, which are easier substrates for BES because they can be directly converted into electricity by electroactive bacteria [14, 162].

The MEC operation should be further optimized in order to increase the coulombic efficiency, because, despite the high COD removal efficiencies, a low current output was obtained. Only about 27-46% of the COD removed was converted into current, indicating the presence of competing electron sinks (e.g., alternative electron acceptors such as nitrate and sulfate, biomass production, competition with non-electroactive bacteria for COD). The coulombic efficiencies in urine BES reported in literature range from 2% to 97%, but are usually lower than 30% (SI Section 3.6.10). Tice and Kim (2014) reported that the high sulfate concentration in human urine favored acetate-oxidizing and H₂-oxidizing sulfate reducing bacteria, greatly diminishing the coulombic efficiency (due to COD consumption by acetate-oxidizing sulfate reducers) and energy recovery (due to H₂ consumption by H₂-oxidizing sulfate reducers) in a MEC coupled with an IEM stack [283]. In an attempt to identify the reason for the low coulombic efficiency in our experiments, an electron balance was made in Figure 3.2E-F and SI Section 3.6.4. About 20% of the incoming COD (and electrons) was not converted and was still present in the effluent. A part of the electrons generated by COD oxidation was incorporated into biomass. This fraction was estimated at ~10% based on the volatile suspended solids (VSS) concentration in the MEC. The fraction of electrons going to alternative electron acceptors was minimal, since the nitrate and oxygen concentrations were negligible and

only a small amount of sulfate disappeared ($15\text{--}33 \text{ mg SO}_4 \text{ L}^{-1}$ in MEC1 and $57\text{--}177 \text{ mg SO}_4 \text{ L}^{-1}$ in MEC2, compared to $1\text{--}2.3 \text{ g COD L}^{-1}$). As demonstrated in Figure 3.2E-F, the electron balance could not be closed by adding up all the abovementioned electron sinks. Fermentation and methanogenesis are also known to decrease the coulombic efficiencies in BES because of substrate consumption via these metabolic pathways [176]. In general, methanogens are highly sensitive to free ammonia (FA) [157, 268, 325], which makes methanogenesis unlikely in our MEC, because of the high pH and high N concentration ($>750 \text{ mg FA L}^{-1}$). The headspace of the anolyte recirculation vessel was sampled two times and no methane was detected with gas chromatography. Fermentation is more likely because of the presence of fermentable compounds in urine (e.g., lactate and glucose) [14]. When complex organic molecules are fermented into simpler organic molecules (e.g., acetate), part of the COD is converted into hydrogen gas, which is a poor substrate for electroactive bacteria but a good electron donor for hydrogenotrophic methanogens, using bicarbonate as a terminal electron acceptor [168, 169].

3.4.2 Upstream bio-anodic COD oxidation effectively prevented denitrification in the MABR

The MEC effluent was fed into a nitrification MABR to convert all TAN into nitrate. Overall, full nitrification (effluent TAN and $\text{NO}_2^- \text{-N} < 5 \text{ mg N L}^{-1}$) without N loss was obtained when the MABR was operated on MEC effluent at N loads up to 100 mg N d^{-1} and bulk DO levels as low as $0.1 \text{ mg O}_2 \text{ L}^{-1}$. The COD concentration in the MABR effluent was slightly lower than the influent concentration, indicating some COD removal. Yet, the oxygen demand for COD oxidation was less than 2% of the total oxygen demand (Table 3.2). In MEC IV, about $\sim 160 \text{ mg O}_2 \text{ L}^{-1}$ was consumed for COD oxidation (assuming that all COD was aerobically removed consuming $0.8 \text{ g O}_2 \text{ g}^{-1} \text{ COD removed}$), while more than $7800 \text{ mg O}_2 \text{ L}^{-1}$ was required for nitrification (assuming that 4.33 g of oxygen is consumed per g of nitrate-N produced). Only in case of overloading (in MEC VI), TAN accumulated, but no N losses were observed.

In contrast, feeding the MABR directly with raw urine yielded TAN accumulation and N loss at a N load of 100 mg N d^{-1} due to the high COD influx in the MABR. The nitrification oxygen demand (NOD) was in line with MEC IV, whereas the oxygen demand for COD oxidation was significantly higher ($72 \text{ mg O}_2 \text{ d}^{-1}$ compared to $<10 \text{ mg O}_2 \text{ d}^{-1}$) (Table 3.2). Although the oxygen demand for COD oxidation was less than 15% of the total oxygen demand, the increase in oxygen demand for COD oxidation led to oxygen limitation, resulting in TAN accumulation and N loss due to denitrification. It was estimated that about 70% of the COD removed was removed via denitrification, based on the amount of N that was lost and assuming a COD/N ratio of 3.6 (i.e., cell yield of 0.2).

Interestingly, TAN (and not nitrite) accumulated in case of oxygen limitation, whereas many studies report nitrite build-up under DO limited conditions [91, 291, 295]. Generally,

NOB have a lower affinity to oxygen than AOB [291], resulting in nitrite accumulation at low DO concentrations.

3.4.3 Both MEC and MABR showed robustness against fluctuating loading rates and operational conditions

Both the MEC and MABR were challenged with various loading rates and operational scenarios. The COD loading in the MEC highly fluctuated because of the use of different urine batches (with a different COD concentration) and because different HRT were tested. Despite these fluctuations in influent composition and loading, the COD concentration in the effluent remained stable, demonstrating the robustness of the MEC. Also the MABR could handle different N and COD concentrations and loads. After start-up, the N load was gradually increased from $\sim 40 \text{ mg N d}^{-1}$ to $\sim 150 \text{ mg N d}^{-1}$ (Table 3.2, SI Figure S3.4), corresponding with volumetric loading rates of $60\text{--}230 \text{ mg N L}^{-1} \text{ d}^{-1}$ when the total MABR volume is taken into account or $150\text{--}560 \text{ mg N L}^{-1} \text{ d}^{-1}$ when only the active volume (i.e., total volume of the hollow fiber modules) is considered. A nitrification activity test (presented in SI Section 3.6.7) demonstrated that the mixed liquor in the recirculation vessels and loop was not active. In MEC IV and VI, the load was further increased to 100 mg N d^{-1} (200 or $560 \text{ mg N L}^{-1} \text{ d}^{-1}$) and 125 mg N d^{-1} (250 or $700 \text{ mg N L}^{-1} \text{ d}^{-1}$), respectively. By shifting the influent from MEC effluent to raw urine, the COD concentration and load increased from 350 to $1850 \text{ mg COD L}^{-1}$ and from 20 to $100 \text{ mg COD d}^{-1}$, respectively. More than 90% of the COD could be removed, maintaining the COD concentration in the effluent $< 200 \text{ mg COD L}^{-1}$. Also, after the period on raw urine with N loss and TAN accumulation, the MABR performance could be reverted successfully to full nitrification without N loss. All these observations illustrate the robustness of the MABR.

3.4.4 MEC-MABR integration not only prevents N losses but also reduces the overall oxygen demand, increases the alkalinity and enables energy efficient COD removal

Removing the COD prior to membrane-aerated nitrification proved to be key in preventing N losses through denitrification and allowed MABR operation at a high urine loading rate, reducing the required reactor volume. It also minimized biomass production in the MABR since less substrate (COD) was available to the heterotrophs. Bio-anodic COD removal has some clear advantages compared to other biological COD removal processes, for example aerobic COD removal in another MABR. Firstly, there is no oxygen requirement for bio-anodic COD oxidation, whereas aerobic COD removal from urine would consume $\sim 4\text{--}8 \text{ mg O}_2 \text{ L}^{-1}$ of urine. Secondly, energy can be recovered from the organics, as hydrogen gas (MEC) or electricity (MFC), although this should be further optimized as discussed in Section 3.4.1. Thirdly, OH^- production at the cathode increases the alkalinity of the urine, thereby reducing the base demand for full

nitrification in the MABR.

3.4.5 Closing the nitrogen cycle on Earth and in space

By treatment in the MEC and MABR, fresh real human urine is transformed into a stable and safe nitrate-rich, COD-low nutrient solution, which was demonstrated to be suitable for plant and microalgae cultivation by Coppens et al. (2016) [56] and Feng et al. (2007) [90]. Using processed urine as a nutrient source for protein production could reduce the need for synthetic fertilizers and the related environmental pollution, resulting in a more sustainable nitrogen cycle on Earth. Moreover, as the oxidation of COD and N is not based on bubble-dependent gas/liquid mass transfer, the concept is compatible with reduced gravity conditions and can therefore be integrated in regenerative life support systems (RLSS). On long-term deep-space missions (e.g., to Mars) and space habitation, resupply from Earth becomes practically impossible because of the long distance and duration [52]. Therefore, these missions will rely on RLSS to produce water, food and oxygen from waste streams, such as urine. In MELISSA, the RLSS programme from ESA, urine is treated by nitrification, followed by cyanobacteria and higher plant cultivation [105]. With the survival of nitrifiers demonstrated in low Earth orbit [175], the next development step would be to test a urine nitrification MABR in such conditions. As a compact, robust, highly nitrogen- and energy-efficient treatment train, the MEC-MABR system could be of interest. Application in a reduced gravity environment would, however, require the use of a gas diffusion air cathode in the BES (to prevent the production of hydrogen gas, which would be difficult to separate from the liquid in reduced gravity).

3.5 Conclusion

- Upstream bio-anodic COD oxidation effectively prevented denitrification in the MABR. Full nitrification without TAN and nitrite accumulation and without N loss was obtained when the MABR was operated on MEC effluent, whereas denitrification and partial nitrification occurred when the MABR was operated on raw urine at the same N loading rate.
- The MEC allows to operate the MABR at a high loading rate, reducing the reactor volume, and in addition, reduces the oxygen demand for COD oxidation, limits biomass production in the MABR, increases the urine alkalinity and can recover some energy from the organics.
- MEC operation should be further optimized in order to increase the coulombic efficiency, because, despite the high COD removal efficiencies, a low current output was obtained. Only about 25-45% of the COD removed was converted into current. Other electron sinks should be identified in order to identify the COD gap and improve the conversion of chemical energy into electrical energy. Further decreasing the HRT or adapting the anode potential could potentially favor electrogens compared to fermentative or methanogenic bacteria and thereby increase the coulombic efficiency. Analysing the different COD compounds in the influent and effluent could also gain new insights.
- This two-stage process yields a stable nitrate-rich nutrient solution, suitable for plant and microalgae cultivation. As gravity-independent, highly nitrogen- and energy-efficient treatment train, the concept can be useful for MELiSSA and other regenerative life support systems.

3.6 Supplementary information

3.6.1 MABR setup and operation

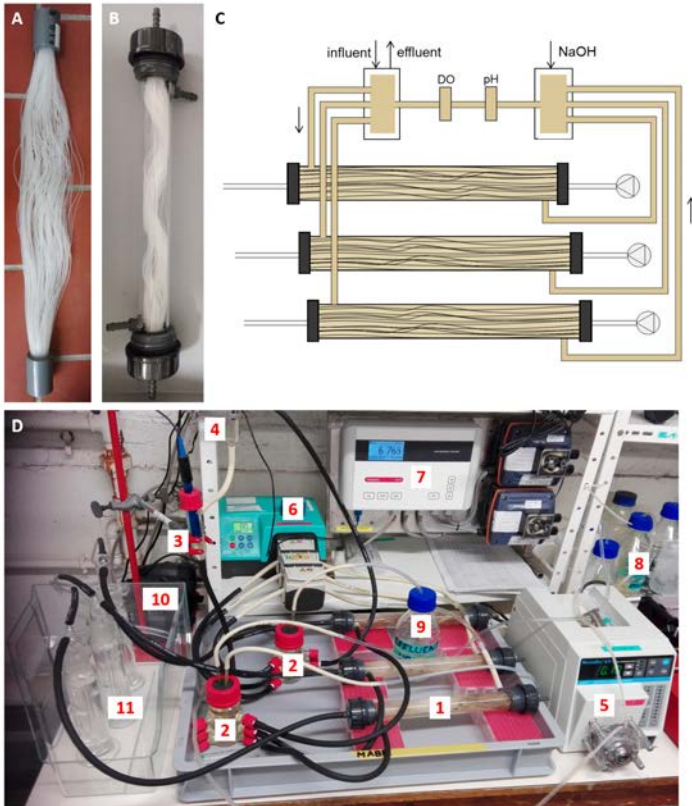


Figure S3.1: **Hollow fiber bundle (A), hollow fiber module (B) and MABR setup (C-D).**

- 1: hollow fiber module
- 2: recirculation vessel (100 mL)
- 3: flow cell with pH probe
- 4: flow cell with DO probe (LDO10103, Hach, Belgium)
- 5: influent pump (Masterflex L/S, Cole-Parmer, US), controlled with a timer
- 6: recirculation pump (Model 323E/D, Watson Marlow, MA, USA)
- 7: pH controller (Consort R3610, Consort, Belgium)
- 8: influent vessel
- 9: effluent vessel
- 10: aquarium pump (air pump 400, EHEIM, Germany)
- 11: water bottle to humidify the air

3.6.2 MEC: influent and effluent composition

Table S3.1: **Influent composition of MEC1 and MEC2.** Averages and standard deviations are given. The large standard deviations are caused by the use of different urine batches. TN: total nitrogen, TAN: total ammonia nitrogen ($\text{NH}_3 + \text{NH}_4^+$).

		MEC1-CEM	MEC1-AEM1	MEC1-AEM2	MEC1-AEM3	MEC2-CEM1	MEC2-CEM2	MEC2-CEM3
pH		11.3 ± 0.2	11.3 ± 0.4	11.5 ± 0.6	11.3 ± 0.5	11.4 ± 0.6	11.6 ± 0.3	11.1 ± 0.3
EC	$[\text{mS cm}^{-1}]$	6.0 ± 1.4	10.3 ± 1.8	7.3 ± 1.1	6.6 ± 1.8	6.3 ± 1.2	6.4 ± 0.5	6.4 ± 0.7
COD	$[\text{mg COD L}^{-1}]$	2014 ± 473	2674 ± 140	2681 ± 733	2115 ± 671	2122 ± 551	1399 ± 221	1778 ± 443
TN	$[\text{mg N L}^{-1}]$	1543 ± 448	1827 ± 78	2595 ± 759	1897 ± 474	1573 ± 433	1599 ± 389	
TAN	$[\text{mg N L}^{-1}]$	98 ± 54	156 ± 86	97 ± 34	110 ± 44	141 ± 164	87 ± 15	161 ± 23
nitrite	$[\text{mg N L}^{-1}]$		1 ± 0	1 ± 1	2 ± 1	2 ± 2	0 ± 0	3 ± 2
nitrate	$[\text{mg N L}^{-1}]$		7 ± 1	24 ± 25	23 ± 12	15 ± 11	13 ± 5	34 ± 15
phosphate	$[\text{mg L}^{-1}]$		59 ± 8	169 ± 119	174 ± 170	108 ± 113	74 ± 31	142 ± 68
sulfate	$[\text{mg L}^{-1}]$		228 ± 91	266 ± 100	264 ± 98	212 ± 81	183 ± 60	290 ± 115
chloride	$[\text{mg L}^{-1}]$		1664 ± 53	1249 ± 274	1390 ± 361	1219 ± 277	1061 ± 77	1134 ± 314
sodium	$[\text{mg L}^{-1}]$		1128 ± 45	1115 ± 226	1097 ± 271	975 ± 202	930 ± 48	1392 ± 216
potassium	$[\text{mg L}^{-1}]$		613 ± 35	783 ± 246	599 ± 253	562 ± 165	643 ± 85	927 ± 308

Table S3.2: **Effluent composition of MEC1 (anolyte) and MEC2 (after passage through cathodic compartment).** Averages and standard deviations are given. The large standard deviations are caused by the use of different urine batches. TN: total nitrogen, TAN: total ammonia nitrogen ($\text{NH}_3 + \text{NH}_4^+$).

		MEC1-CEM	MEC1-AEM1	MEC1-AEM2	MEC1-AEM3	MEC2-CEM1	MEC2-CEM2	MEC2-CEM3
pH		8.1 ± 0.2	8.4 ± 0.2	8.7 ± 0.4	9.0 ± 0.2	9.4 ± 0.1	9.3 ± 0.1	9.3 ± 0.1
EC	[<i>mS cm⁻¹</i>]	10.8 ± 1.1	20.7 ± 3.2	15.2 ± 1.8	13.9 ± 1.4	13.1 ± 1.2	13.5 ± 1.1	
COD	[<i>mg COD L⁻¹</i>]	375 ± 84	380 ± 104	513 ± 163	384 ± 105	377 ± 49	412 ± 95	613 ± 36
TN	[<i>mg N L⁻¹</i>]	495 ± 112	1426 ± 15	1456 ± 248	1633 ± 161	1459 ± 154	1490 ± 318	
TAN	[<i>mg N L⁻¹</i>]	466 ± 98	1391 ± 55	1486 ± 212	1562 ± 26	1529 ± 150	1628 ± 270	1962 ± 217
nitrite	[<i>mg N L⁻¹</i>]		4 ± 4	1 ± 7	0 ± 0	12 ± 13	0 ± 0	0 ± 0
nitrate	[<i>mg N L⁻¹</i>]		0 ± 0	2 ± 3	3 ± 1	2 ± 1	6 ± 9	2 ± 1
phosphate ^a	[<i>mg L⁻¹</i>]		1543 ± 361	1719 ± 1498	290 ± 21	123 ± 69	77 ± 26	87 ± 1
sulfate	[<i>mg L⁻¹</i>]		213 ± 132	237 ± 80	231 ± 7	155 ± 44	117 ± 50	113 ± 33
chloride	[<i>mg L⁻¹</i>]		1294 ± 150	952 ± 285	1420 ± 76	1262 ± 119	1066 ± 95	916 ± 13
sodium	[<i>mg L⁻¹</i>]		1224 ± 173	1377 ± 577	1199 ± 70	1085 ± 117	1058 ± 71	1124 ± 113
potassium	[<i>mg L⁻¹</i>]		565 ± 77	975 ± 201	706 ± 8	627 ± 74	748 ± 52	772 ± 92

^a The high phosphate concentration in the effluent of MEC1-AEM1&2 is caused by the phosphate input from the catholyte (phosphate migration through AEM)

3.6.3 MEC: COD and TAN concentration in influent and effluent

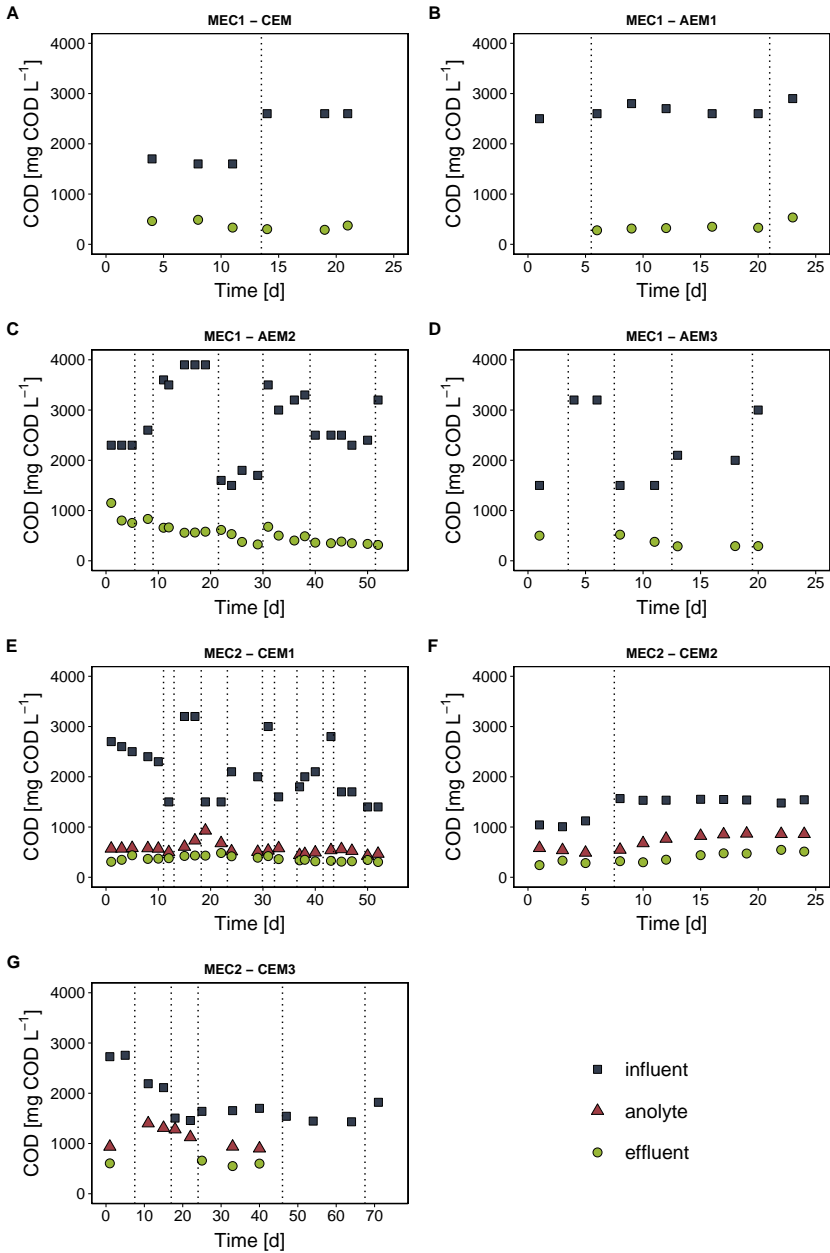


Figure S3.2: COD concentration in the influent, anolyte (MEC2) and effluent of MEC1 and MEC2. Different batches of urine were fed to the MECs, as indicated by the dashed lines on the graphs.

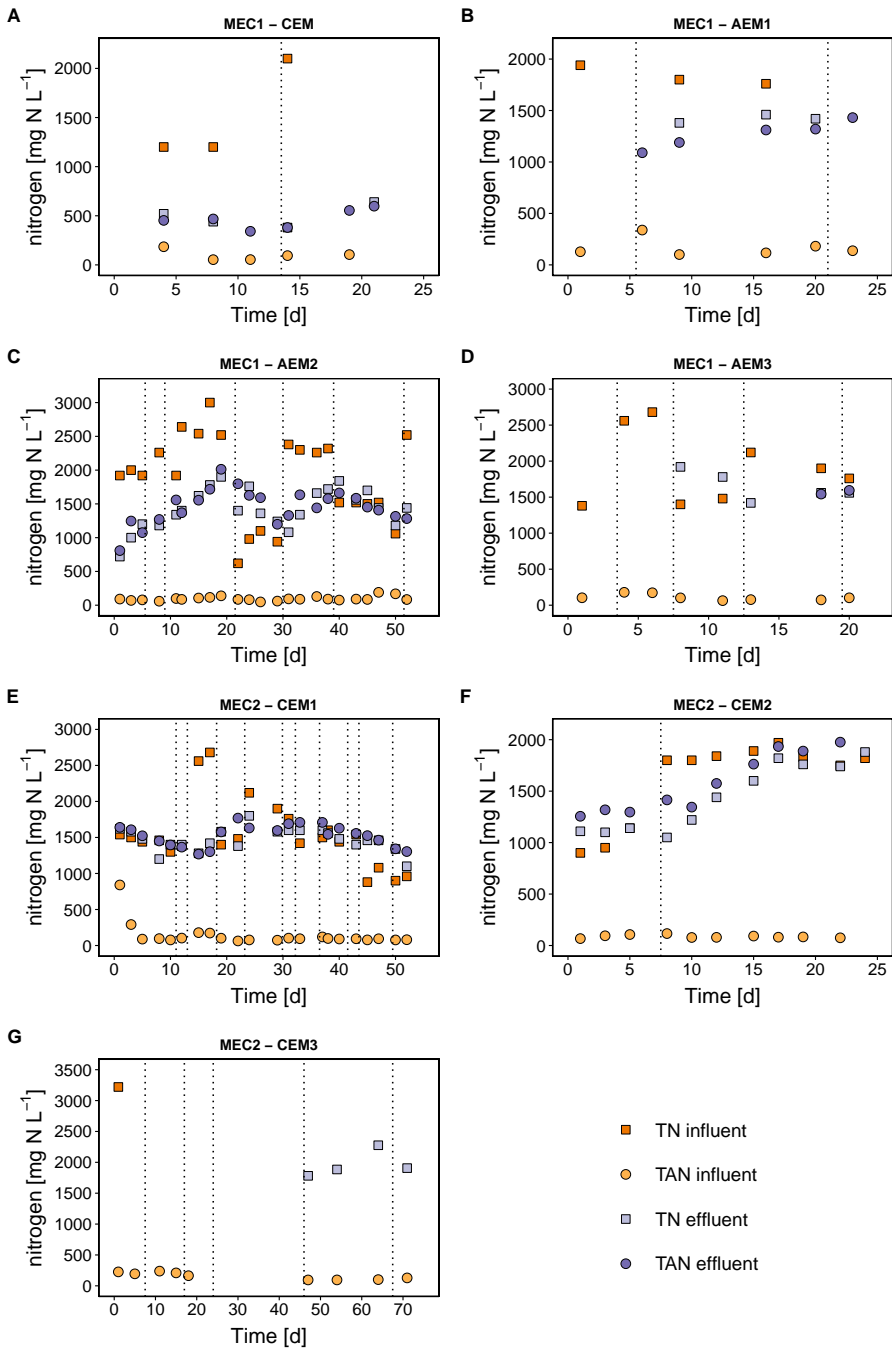


Figure S3.3: Total nitrogen (TN) and total ammonia nitrogen (TAN) concentration in the influent and effluent of MEC1 and MEC2. Different batches of urine were fed to the MECs, as indicated by the dashed lines on the graphs.

3.6.4 Electron balance

Following equations were used to make the electron balance presented in Figure 2.

Influent COD:

$$e_{in}^- \left[\frac{mmol e^-}{L} \right] = COD_{in}^- \left[\frac{mg COD}{L} \right] \times \frac{4 \frac{mol e^-}{mol COD}}{32 \frac{g COD}{mol COD}} \quad (10)$$

Effluent COD:

$$e_{eff}^- \left[\frac{mmol e^-}{L} \right] = COD_{eff}^- \left[\frac{mg COD}{L} \right] \times \frac{4 \frac{mol e^-}{mol COD}}{32 \frac{g COD}{mol COD}} \quad (11)$$

Current:

$$e_{eff \text{ current}}^- \left[\frac{mmol e^-}{L} \right] = \frac{current [mA]}{96485 \frac{s \times A}{mol e^-} \times flow \ rate \left[\frac{L}{d} \right] \times \frac{1}{(3600 \times 24) \frac{s}{d}}} \quad (12)$$

Biomass:

$$e_{eff \text{ biomass}}^- \left[\frac{mmol e^-}{L} \right] = VSS \left[\frac{mg VSS}{L} \right] \times 1.42 \left[\frac{g COD}{g VSS} \right] \times \frac{4 \frac{mol e^-}{mol COD}}{32 \frac{g COD}{mol COD}} \quad (13)$$

Sulfate reduction:

$$e_{eff \text{ sulfate}}^- \left[\frac{mmol e^-}{L} \right] = \frac{(S_{in} - S_{eff}) \left[\frac{mg SO_4}{L} \right] \times 6 \frac{mol e^-}{mol S}}{96 \frac{g SO_4}{mol SO_4}} \quad (14)$$

3.6.5 MABR: influent and effluent composition

Table S3.3: **Average influent composition of MABR.** Averages and standard deviations are given. TN: total nitrogen, TAN: total ammonia nitrogen ($\text{NH}_3 + \text{NH}_4^+$).

Phase	MEC I	MEC II	MEC III	MEC IV	RAW I	RAW II	MEC V	MEC VI
# HF bundles	3	3	3	2	2	2	2	2
Influent	MEC1 effluent 16.7%	MEC2 effluent 25%	MEC2 effluent 33.3%	MEC2 effluent 33.3%	stabilized urine 33.3%	stabilized urine 33.3%	MEC2 effluent 33.3%	MEC2 effluent 33.3%
# samples	20	8	25	15	16	5	11	4
pH	9.0 ± 0.1	9.2 ± 0.1	9.2 ± 0.1	9.3 ± 0.1	11.1 ± 0.3	10.8 ± 0.1	9.2 ± 0.0	9.2 ± 0.0
EC	[mS cm ⁻¹] 8.6 ± 0.8	9.0 ± 0.2	13.7 ± 1.2	16.5 ± 0.9	6.7 ± 0.4	6.5 ± 0.0	13.6 ± 0.3	14.1 ± 0.1
total COD	[mg COD L ⁻¹] 249 ± 47	284 ± 35	522 ± 77	662 ± 151	1796 ± 53	1829 ± 27	460 ± 23	434 ± 8
suspended COD	[mg COD L ⁻¹] 192 ± 30	195 ± 14	247 ± 47	466 ± 103	1806 ± 41	1805 ± 24	355 ± 17	346 ± 15
TN	[mg N L ⁻¹] 761 ± 30	1018 ± 37	1441 ± 164	2181 ± 166	1833 ± 34	1855 ± 44	1558 ± 48	1593 ± 31
TAN	[mg N L ⁻¹] 757 ± 26	988 ± 36	1465 ± 187	2286 ± 174	129 ± 25	82 ± 3	1479 ± 35	1532 ± 6
nitrite	[mg N L ⁻¹] 4 ± 2	3 ± 3	0 ± 0	0 ± 0	0 ± 0	0 ± 0	0 ± 0	0 ± 0
nitrate	[mg N L ⁻¹] 1 ± 1	1 ± 1	59 ± 113	2 ± 2	8 ± 2	7 ± 0	0 ± 1	0 ± 0
phosphate	[mg L ⁻¹] 842 ^a ± 349	122 ± 28	78 ± 10	140 ± 42	128 ± 16	144 ± 7	94 ± 7	98 ± 3
sulfate	[mg L ⁻¹] 154 ± 24	133 ± 17	126 ± 11	261 ± 81	240 ± 48	242 ± 10	179 ± 13	183 ± 4
chloride	[mg L ⁻¹] 511 ± 108	774 ± 24	1142 ± 114	1212 ± 160	1038 ± 88	1096 ± 40	954 ± 54	970 ± 17
sodium	[mg L ⁻¹] 577 ± 103	767 ± 51	1169 ± 157	1428 ± 161	1085 ± 70	1029 ± 9	904 ± 32	912 ± 4
potassium	[mg L ⁻¹] 483 ± 67	454 ± 67	666 ± 60	784 ± 78	592 ± 55	716 ± 4	603 ± 16	618 ± 4

^a The high phosphate concentration is caused by the use of influent from MEC1 (because of phosphate migration from the concentrated phosphate solution that was used as catholyte)

Table S3.4: **Average effluent composition of MABR.** Averages and standard deviations are given. TN: total nitrogen, TAN: total ammonia nitrogen ($\text{NH}_3 + \text{NH}_4^+$).

Phase	MEC I ^a	MEC II	MEC III ^b	MEC IV ^b	RAW I ^b	RAW II	MEC V ^b	MEC VI
# HF bundles	3	3	3	2	2	2	2	2
Influent	MEC1 effluent 16.7%	MEC2 effluent 25%	MEC2 effluent 33.3%	MEC2 effluent 33.3%	stabilized urine 33.3%	stabilized urine 33.3%	MEC2 effluent 33.3%	MEC2 effluent 33.3%
# samples	6	8	8	7	8	5	6	4
pH	7.1 ± 0.1	7.1 ± 0.1	7.3 ± 0.0	6.6 ± 0.3	6.1 ± 0.2	6.4 ± 0.4	6.2 ± 0.1	6.3 ± 0.2
EC	[mS cm ⁻¹] 8.6 ± 1.0	9.9 ± 1.7	15.3 ± 0.3	17.4 ± 0.3	13.0 ± 0.1	14.8 ± 0.1	14.0 ± 0.3	14.1 ± 0.3
COD	[mg COD L ⁻¹] 150 ± 10	157 ± 14	192 ± 7	116 ± 7	161 ± 18	146 ± 47	135 ± 7	150 ± 12
TN	[mg N L ⁻¹] 645 ± 8	781 ± 83	1451 ± 32	1809 ± 32	1465 ± 28	1560 ± 20	1400 ± 20	1400 ± 0
TAN	[mg N L ⁻¹] 6 ± 2	8 ± 13	3 ± 1	20 ± 12	356 ± 88	223 ± 8	31 ± 11	171 ± 71
nitrite	[mg N L ⁻¹] 1 ± 0	7 ± 7	1 ± 0	0 ± 0	0 ± 0	0 ± 0	0 ± 0	0 ± 0
nitrate	[mg N L ⁻¹] 645 ± 19	761 ± 90	1384 ± 44	1732 ± 46	1023 ± 59	1108 ± 33	1347 ± 10	1255 ± 71
phosphate	[mg L ⁻¹] 609 ± 251	148 ± 43	78 ± 8	165 ± 14	167 ± 18	238 ± 121	139 ± 17	126 ± 2
sulfate	[mg L ⁻¹] 132 ± 8	119 ± 10	145 ± 2	344 ± 50	332 ± 50	348 ± 48	234 ± 11	221 ± 2
chloride	[mg L ⁻¹] 532 ± 66	1135 ± 640	1110 ± 30	1177 ± 32	1082 ± 52	1106 ± 50	1091 ± 12	1111 ± 7
sodium	[mg L ⁻¹] 1317 ± 57	1630 ± 283	2798 ± 239	3549 ± 152	2042 ± 112	2211 ± 74	2388 ± 37	2028 ± 224
potassium	[mg L ⁻¹] 371 ± 35	330 ± 27	627 ± 43	967 ± 145	611 ± 70	562 ± 8	535 ± 5	536 ± 34

^a Averages and standard deviations were calculated based on data after reaching steady-state with a fixed influent flow rate (days 49-65)

^b Averages and standard deviations were calculated based on data after the first 3HRT)

3.6.6 Time profile of MABR N and COD load/loading

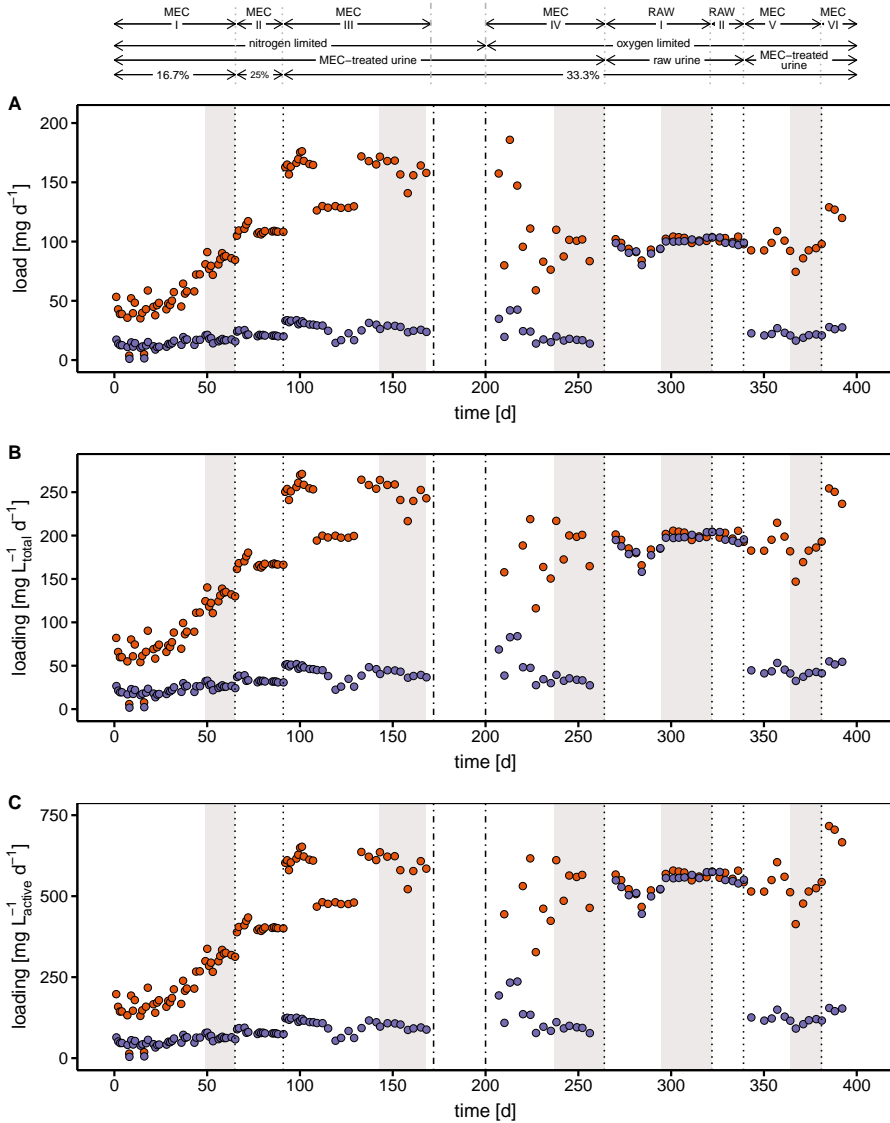


Figure S3.4: **Nitrogen (orange) and COD (purple) load (A) and volumetric loading rate (B-C) of MABR.** Plot B displays the volumetric loading rate taking into account the total MABR volume whereas plot C is the volumetric loading rate considering only the active volume (i.e., total volume of the hollow fiber modules).

3.6.7 Nitrification activity test

In order to test the nitrification activity of the mixed liquor, a new (not previously used) hollow fiber membrane bundle and recirculation bottle were filled with mixed liquor from the MABR reactor and spiked with ammonium chloride or sodium nitrite. Samples were taken frequently and the TAN or nitrite concentration was measured. As shown in Figure S3.5, neither TAN, nor nitrite, decreased over time, indicating that the mixed liquor of the MABR had no or only a very limited nitrification and nitratation activity. In contrast, spiking a hollow fiber module from the MABR with ammonium or nitrite, resulted in a decreasing TAN and nitrite concentration over time (Figure S3.6).

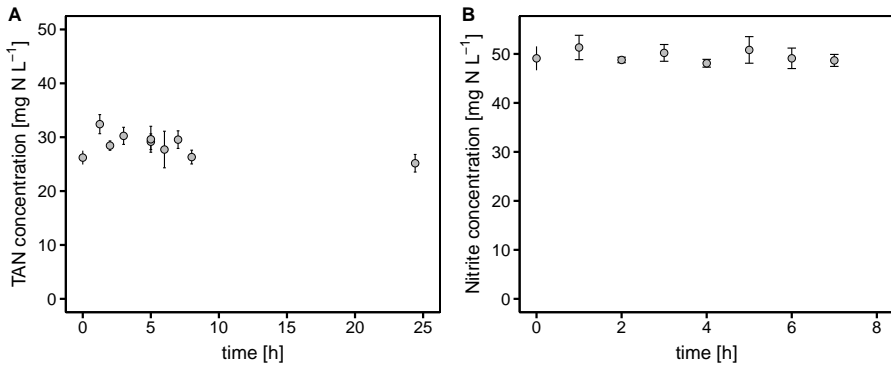


Figure S3.5: TAN (A) and nitrite (B) profile of the hollow fiber bundle filled with mixed liquor of the MABR after spiking ammonium (A) or nitrite (B).

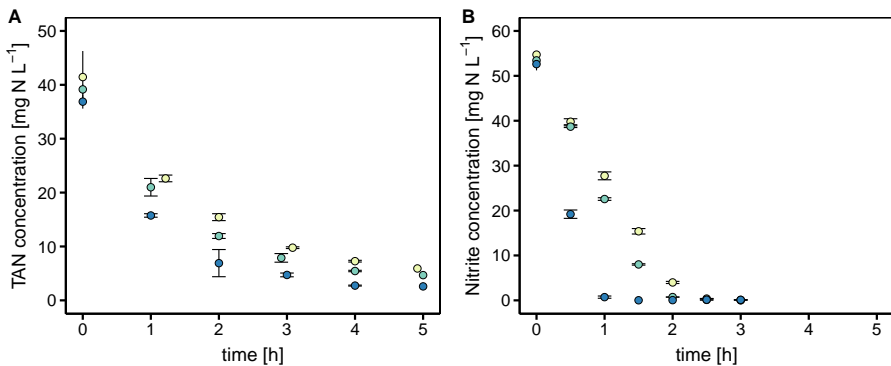


Figure S3.6: TAN (A) and nitrite (B) profile of MABR bundles after spiking ammonium (A) or nitrite (B). The three colours represent the three different hollow fiber bundles.

3.6.8 Microbial community composition of MEC

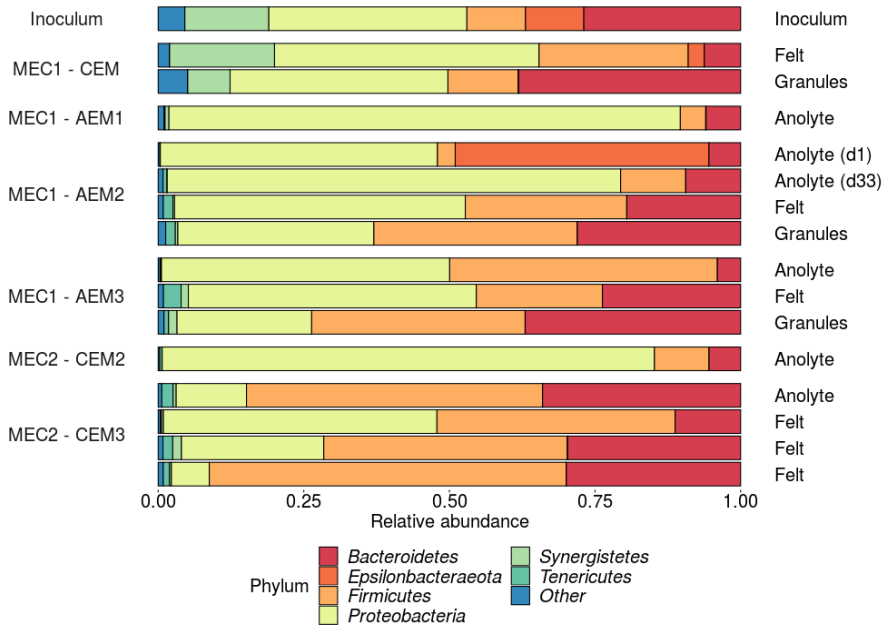


Figure S3.7: **Phylum level microbial community composition of the MEC inoculum, MEC1 and MEC2.** A distinction was made between biomass present in the anolyte, on the felt or on the granules (MEC1). All samples were taken at the end of the experiment (except 'Inoculum' and 'Anolyte (d1)', taken on the first day). The relative abundance of the seven most abundant phyla is shown.

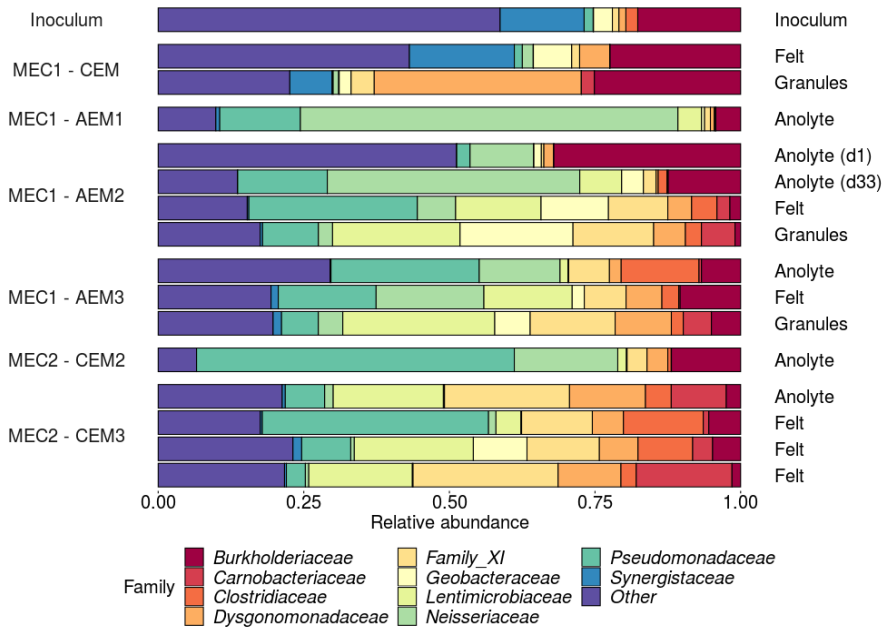


Figure S3.8: **Family level microbial community composition of the MEC inoculum, MEC1 and MEC2.** A distinction was made between biomass present in the anolyte, on the felt or on the granules (MEC1). All samples were taken at the end of the experiment (except 'Inoculum' and 'Anolyte (d1)', taken on the first day). The relative abundance of the ten most abundant families is shown. Family_XI belongs to the order of the *Clostridiales* (phylum of *Firmicutes*).

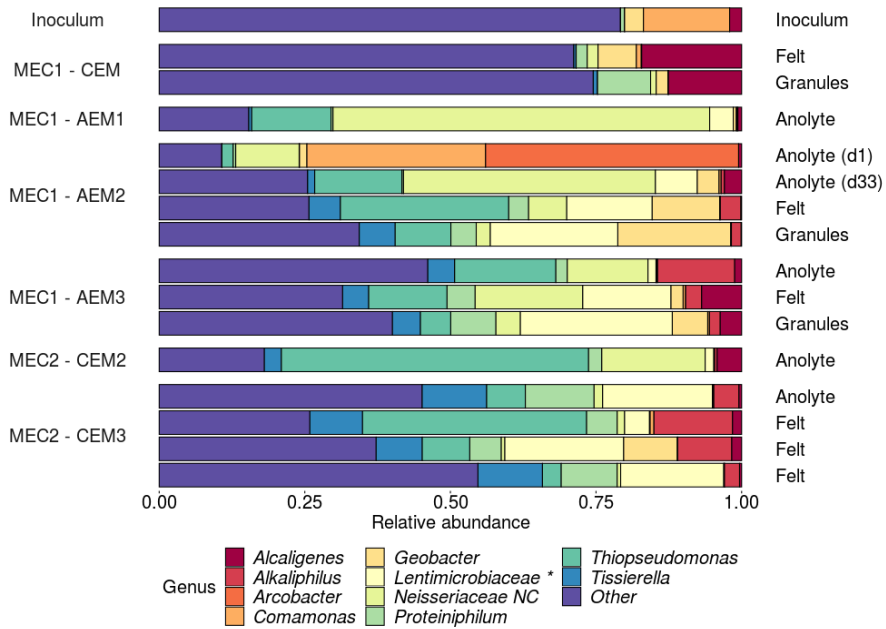


Figure S3.9: **Genus level microbial community composition of the MEC inoculum, MEC1 and MEC2.** A distinction was made between biomass present in the anolyte, on the felt or on the granules (MEC1). All samples were taken at the end of the experiment (except 'Inoculum' and 'Anolyte (d1)', taken on the first day). The relative abundance of the ten most abundant genera is shown. Taxa that could not be classified at genus level are specified at family level followed by *. Uncultured bacteria are indicated by 'NC' (not cultured).

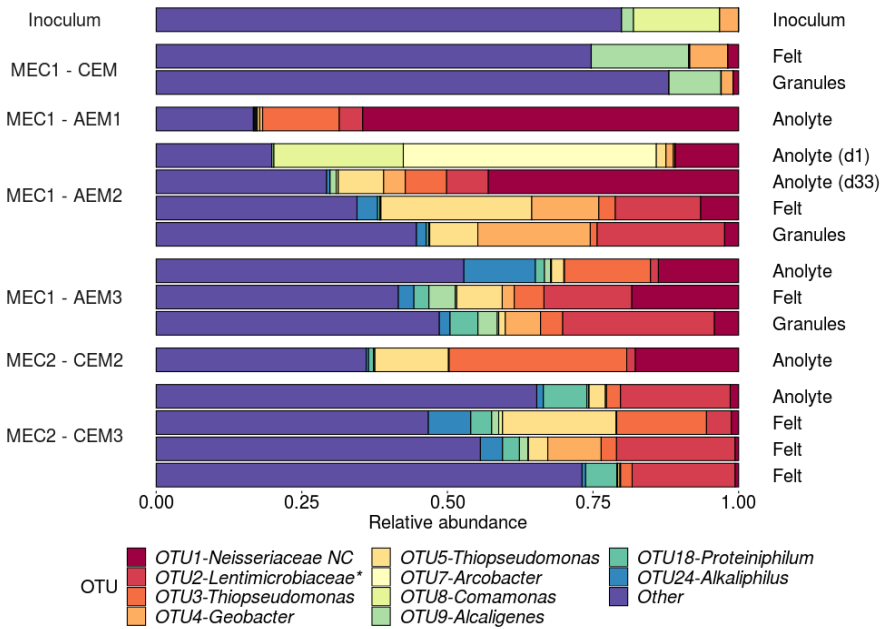


Figure S3.10: **OTU level microbial community composition of the MEC inoculum, MEC1 and MEC2.** A distinction was made between biomass present in the anolyte, on the felt or on the granules (MEC1). All samples were taken at the end of the experiment (except 'Inoculum' and 'Anolyte (d1)', taken on the first day). The relative abundance of the ten most abundant OTUs is shown. Taxa that could not be classified at genus level are specified at family level followed by *. Uncultured bacteria are indicated by 'NC' (Not cultured).

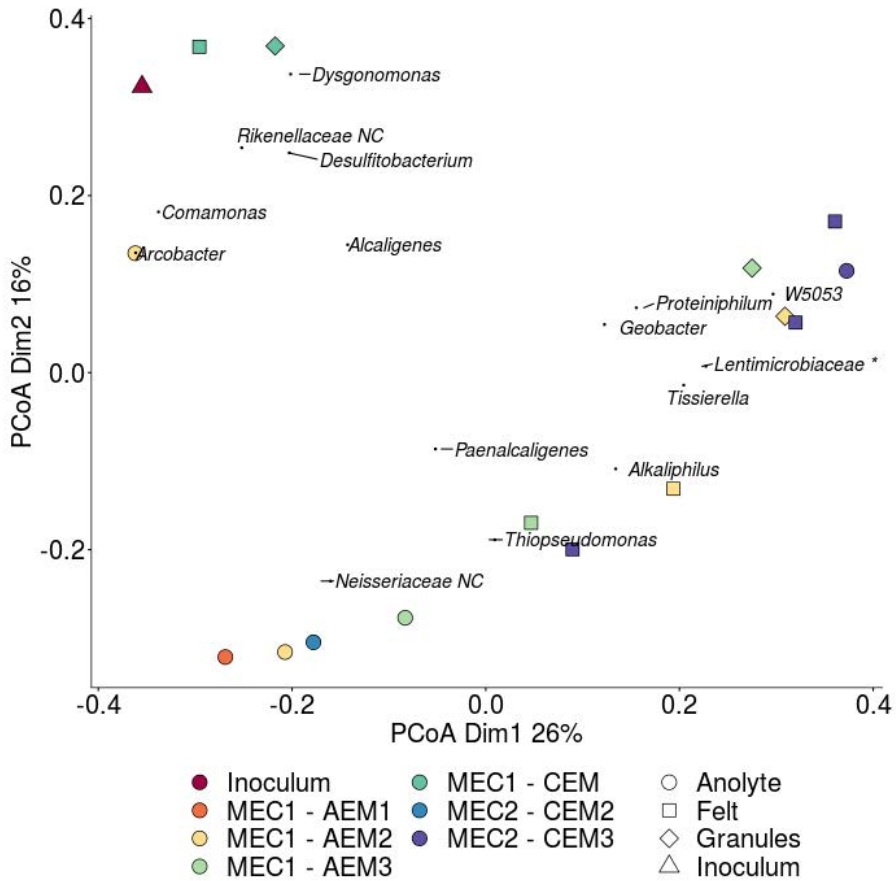


Figure S3.11: **Principle coordinate analysis (PCoA) of the microbial community composition of the MEC inoculum, MEC1 and MEC2.** The abundance based Jaccard dissimilarity metric was used and weighted average scores of the most abundant genera were *a posteriori* projected, by means of the wascores function from the package vegan. A distinction was made between biomass present in the anolyte, on the felt or on the granules (MEC1).

3.6.9 Microbial community composition of MABR

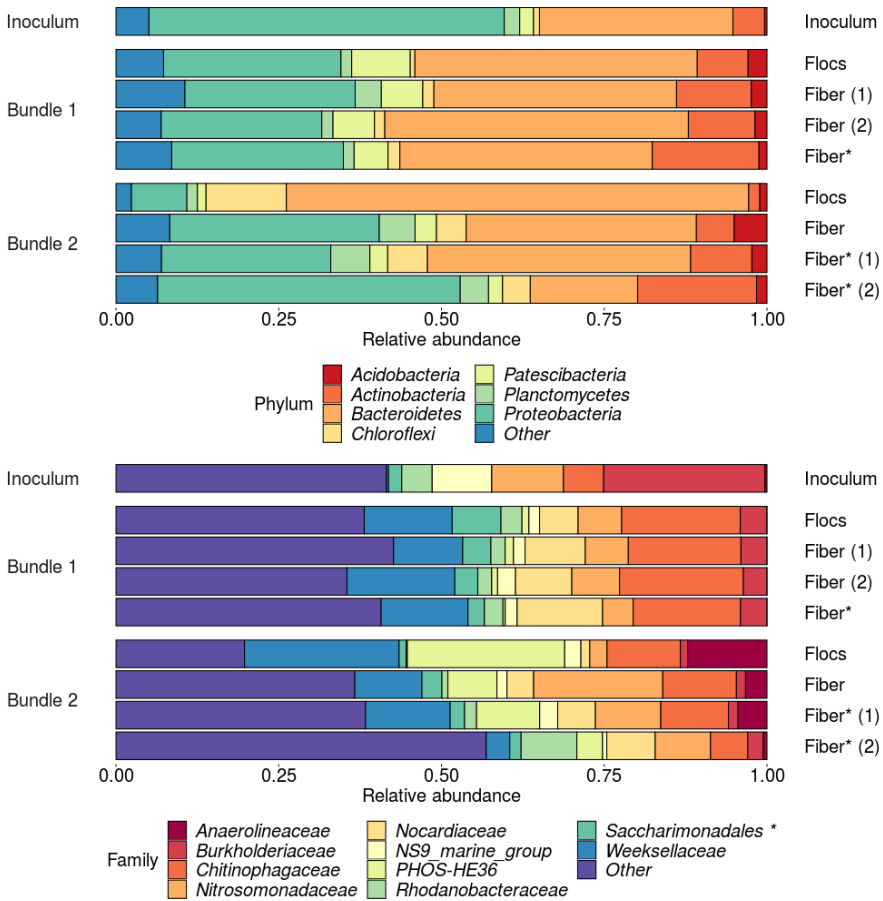


Figure S3.12: **Phylum and family level microbial community composition of the MABR inoculum, bundle 1 (harvested after MECIII) and bundle 2 (harvested after MECVIII).** A distinction was made between biomass flocs in the bundle ('flocs'), biomass on the fibers ('fibers') and firmly attached biomass on the fibers after scraping off the loosely attached biomass ('fiber*'). The numbers between the brackets indicate duplicates. The relative abundance of the seven most abundant phyla and 10 most abundant families is shown. Taxa that could not be classified at family level are specified at order level followed by *.

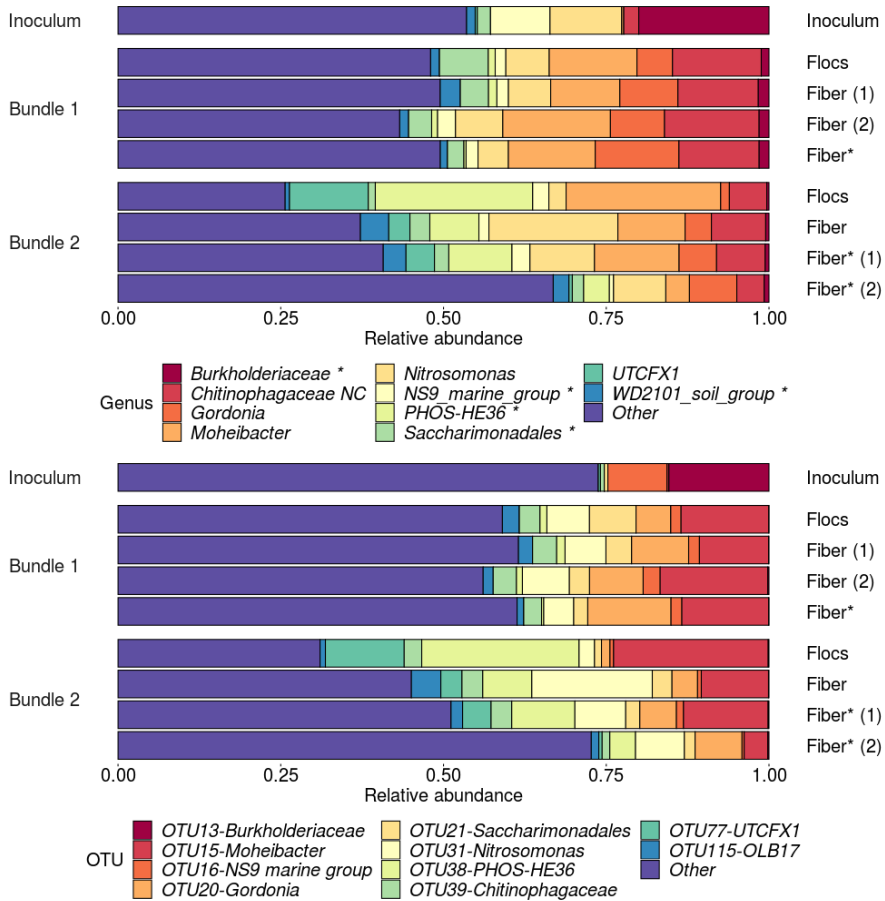


Figure S3.13: **Genus and OTU level microbial community composition of the MABR inoculum, bundle 1 (harvested after MECIII) and bundle 2 (harvested after MECVIII).** A distinction was made between biomass flocs in the bundle ('flocs'), biomass on the fibers ('fibers') and firmly attached biomass on the fibers after scraping off the loosely attached biomass ('fiber*'). The numbers between the brackets indicate duplicates. The relative abundance of the ten most abundant genera and OTU is shown. Taxa are annotated at the deepest classified level. Uncultured bacteria are indicated by 'NC' (not cultured).

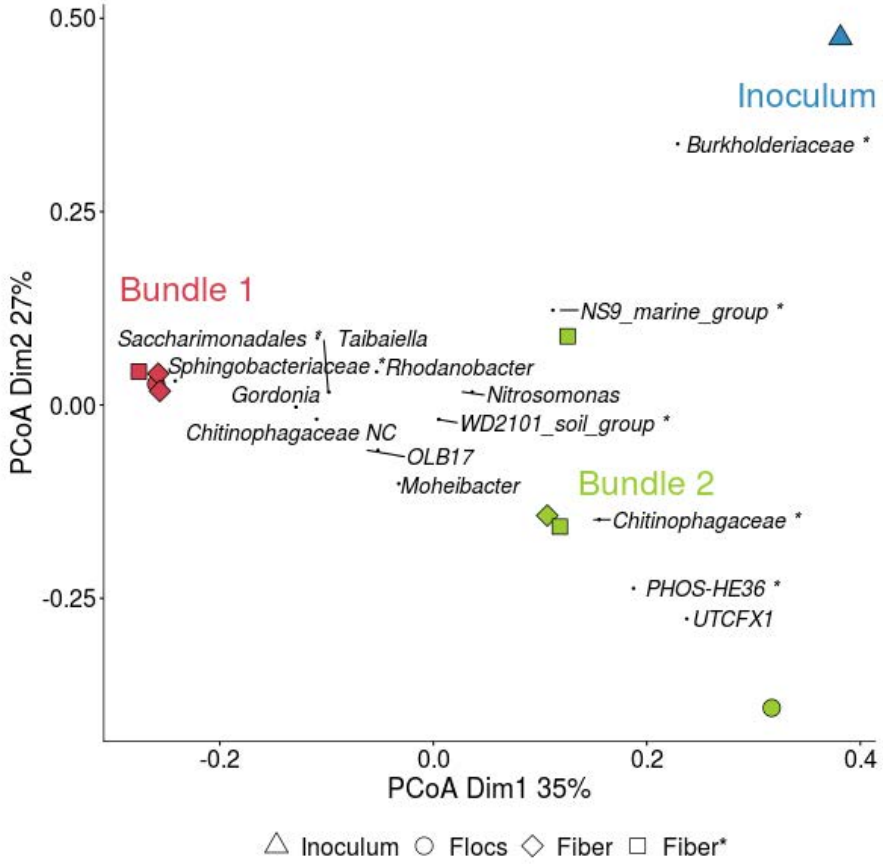


Figure S3.14: **Principle coordinate analysis (PCoA) biplot of the microbial community composition of the MABR inoculum (in blue), bundle 1 (harvested after MECIII, in red) and bundle 2 (harvested after MECVIII, in green).** The abundance based Jaccard dissimilarity metric was used and weighted average scores of the most abundant genera were *a posteriori* projected, by means of the wascores function from the package vegan. A distinction was made between biomass flocs in the bundle ('flocs'), biomass on the fibers ('fibers') and firmly attached biomass on the fibers after removing the loosely attached biomass ('fiber*').

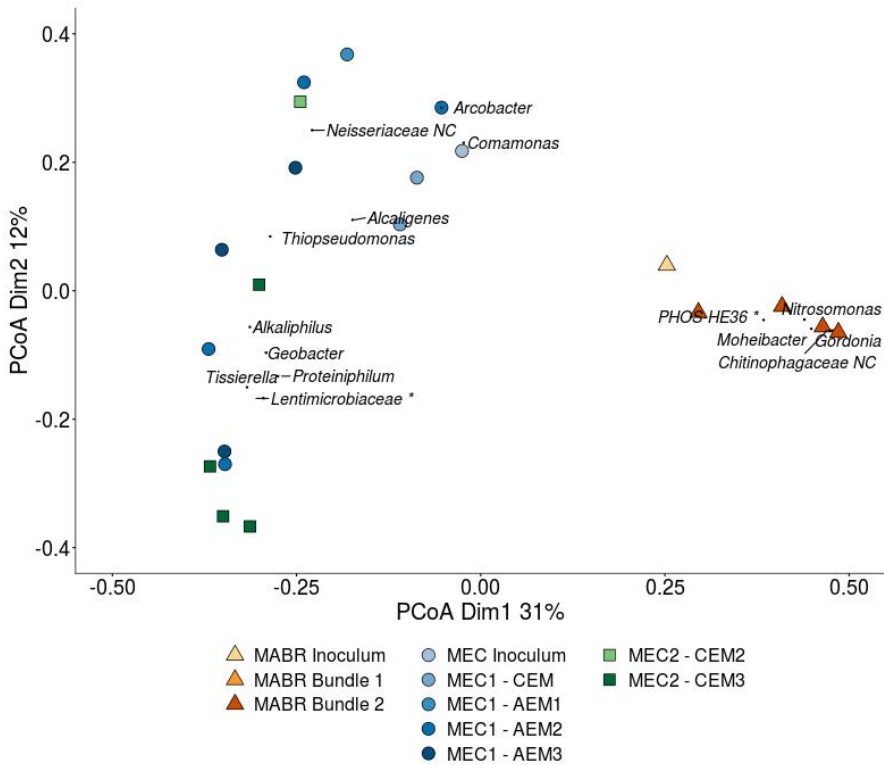


Figure S3.15: **Principle coordinate analysis (PCoA) of the microbial community composition of the MEC and MABR at genus level.** The abundance based Jaccard dissimilarity metric was used and weighted average scores of the most abundant genera were *a posteriori* projected, by means of the wascores function from the package vegan. Taxa that could not be classified at genus level are specified at family level followed by *. Uncultured bacteria are indicated by 'NC' (Not cultured).

3.6.10 Literature overview of bio-electrochemical systems on real human urine

Table S3.5: COD removal efficiencies (RE) and coulombic efficiencies (CE) reported in literature.

Reference	MFC/MEC	goal	batch/continuous	HRT	influent	COD RE (%)	CE (%)
Zang et al. (2012) [328]	MFC	energy recovery	batch		hydrolysed urine (20%) after struvite precipitation	54-65	40
Kuntke et al. (2012) [154]	MFC	TAN and energy recovery	batch	>25 d	undiluted hydrolysed urine (after centrifugation)	~60	10
Kuntke et al. (2014) [158]	MEC	TAN recovery and energy recovery	continuous	1-2 h	20% hydrolysed urine	30-46	84-97
Tice et al. (2014) [283]	MEC	nutrient concentration	batch	47 h	10% synthetic hydrolysed urine (acetate as COD)	68±21	14±8
You et al. (2016) [326]	MFC	energy recovery	continuous	54 min	fresh urine	20	
Kuntke et al. (2016) [159]	MEC	TAN recovery	continuous (duration of 20 days)	6 h	20% hydrolysed urine (after struvite precipitation and filtration)	40 ± 5	78±10
Ieropoulos et al. (2016) [130]	MFC	energy recovery	continuous (3 months)	2-3 weeks	fresh urine	>90	
Merino-Jimenez et al. (2017) [191]	MFC	energy recovery	continuous	0.9 d	hydrolysed urine (after precipitation with magnesium salts)	25 (15-70)	16-18
Salar-García et al. (2017) [256]	MFC	energy recovery	continuous	5.6 h	urine	10-26	
Barbosa et al. (2017) [13]	MFC	urine treatment	batch	40-60 d	undiluted urine, after struvite precipitation	75 ± 1	26 ± 1
Zamora et al. (2017) [327]	MEC	TAN recovery	continuous	2-6 h	hydrolysed urine (40%) after struvite precipitation	37±6	65±10
Cid et al. (2018) [50]	MFC	pre-treatment and electricity generation	fed batch	few days	urine	~40-80	~3-15
Barbosa et al. (2018) [12]	MEC	urine treatment	continuous	17-26 min	partially hydrolysed urine (after struvite precipitation with Mg source)	39-46	2-20
Gajda et al. (2019) [100]	MFC	urine treatment and energy recovery	batch	8 d	hydrolysed urine	60-78	
Walter et al. (2018) [306]	MFC	energy recovery	continuous	44 h	hydrolysed urine	88	3.8
				11.7 h		48	1.6

Barbosa et al. (2019) [14]	MEC	TAN recovery	batch	>40 d	raw (after precipitation)	urine struvite	65±10	14±2
					pre-fermented urine (after struvite precipitation and anaerobic digestion)		54 ±3	17±1
Chapter 3	MEC	COD removal	continuous	3.5-7 d	stabilized (33%)	urine	80-85	27-46

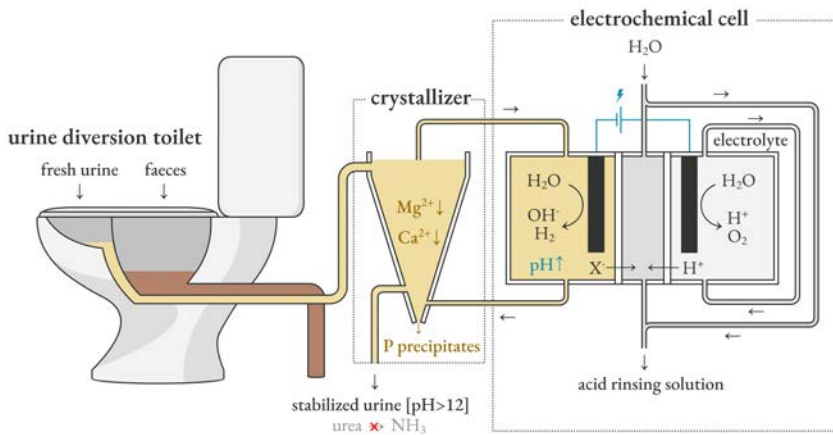
3.7 Acknowledgements

This article has been made possible through the authors' involvement in the MELiSSA project, ESA's life support system research program (<https://www.melissafoundation.org/>).

The authors would like to acknowledge

- i) the MELiSSA foundation to support J.DP. via the POMP1 (Pool Of MELiSSA PhD) program,
- ii) the Research Foundation Flanders (FWO Vlaanderen) to support K.DP. (EOS Research project nr. 30770923, project title: Quantitative profiling in applied gut microbiome research, acronym: MiQuant),
- iii) Ghent University Bijzonder Onderzoeksfonds to support K.R. (GOA grant BOF2019/GOA/026/L),
- iii) Kai Udert from Eawag (Switzerland) for providing urine nitrification culture,
- iv) Celine Bauwens and Arne Govaert for their help with reactor operation and sample analyses.

Electrochemically induced alkanization enables fresh urine stabilization and facilitates source separation



This chapter has been redrafted after:

De Paepe, J., De Pryck, L., Verliefe, A., Rabaey, K. and Clauwaert, P. Electrochemically induced precipitation enables fresh urine stabilization and facilitates source separation. *Environmental Science and Technology* 54, 6 (2020), 3618-3627.

4

Electrochemically induced alkalization enables fresh urine stabilization and facilitates source separation

Abstract

Source separation of urine can enable nutrient recycling, facilitate wastewater management, and conserve water. Without stabilization of the urine, urea is quickly hydrolysed into ammonia, ammonium and (bi)carbonate, causing nutrient loss, clogging of collection systems due to the uncontrolled pH increase and precipitation, ammonia volatilization into the environment, and odor nuisance. In this study, electrochemically induced precipitation and stabilization of fresh urine was successfully demonstrated. By recirculating the urine over the cathodic compartment of an electrochemical cell, the pH was increased due to the production of hydroxide ions at the cathode. The pH increased to 11-12, decreasing calcium and magnesium concentrations by >80%, minimizing scaling and clogging during downstream processing. At pH 11, urine could be stabilized only temporarily (~one week), while an increase to pH 12 allowed urine storage without urea hydrolysis for over 18 months. By a smart selection of membranes (anion exchange membrane in combination with a cation exchange membrane or bipolar membrane), no chemical input (except fresh water) was required in the electrochemical cell and an acidic stream was produced that can be used to periodically rinse the electrochemical cell and toilet. On-site electrochemical treatment, close to the toilet, is a promising new concept to minimize clogging in collection systems by forcing controlled precipitation and to inhibit urea hydrolysis during storage until further treatment in more centralized nutrient recovery plants. If an efficient precipitate collection system is in place, some phosphorus can be recovered by harvesting the precipitates.

4.1 Introduction

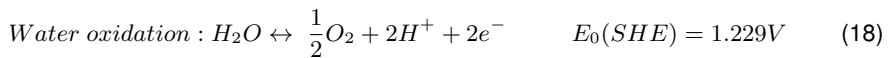
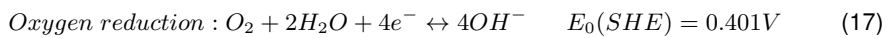
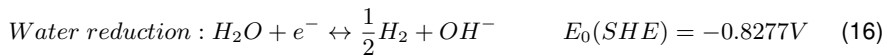
Urged by the depletion of non-renewable phosphorus reserves and the currently energy-intensive nitrogen fertilizer production using Haber-Bosch, more sustainable fertilizers are being explored to meet the rapidly increasing food demand [241, 300]. In the past decade, many technologies to recover nutrients (mainly nitrogen and phosphorus) from source-separated urine have been developed and evaluated [186, 241]. The instability of urine, caused by the enzymatic hydrolysis of urea into ammonia/ammonium and bicarbonate (Equation 25), however, presents a challenge for an efficient urine collection and recovery.



Part of the ammonia can volatilize during collection, storage, treatment, and/or application, resulting in a loss of nitrogen, odor nuisance, and environmental pollution [162, 294]. Moreover, spontaneous, uncontrolled precipitation of calcium and magnesium salts, resulting from the increase in pH to ~ 9.2 and release of ammonium and bicarbonate upon hydrolysis, leads to clogging of pipes in collection systems and a loss of phosphorus (and to a limited extent also nitrogen) [28, 288, 293]. Clogging of pipes by the precipitating salts is a common problem in nonwater urinals and urine-separating toilets, creating odor nuisance, blockages, and leakages and requiring extensive cleaning and maintenance [1, 23, 28, 162, 241, 288]. It is believed that this is currently one of the major barriers for the widespread implementation of source separation [28]. The presence of calcium and magnesium can also cause problems during further downstream urine treatment, e.g., through scaling on membranes (used in reverse osmosis, forward osmosis, electrodialysis, (bio)electrochemical systems, etc.), which reduces the efficiency and requires thorough cleaning [154, 162, 178, 327, 332].

Urea hydrolysis is initiated by urease-positive bacteria growing in the pipes of urine collection systems and is usually completed within a few days [292]. Urea hydrolysis can be prevented by inhibiting the microbial activity and hence the production of urea-degrading enzymes [160]. This can be achieved by (i) the addition of acids to decrease the pH [125, 243, 254], (ii) the addition of caustics, wood ash or biochar to increase the pH [240, 262], (iii) the addition of hydrogen peroxide [333] or urease inhibitors [243], (iv) filtration, (v) evaporation [222], (vi) electrochemical chlorine production [132] and (vii) thermal treatment [336]. Interestingly, increasing the pH not only prevents urea hydrolysis, but also can reduce the scaling potential of urine by inducing controlled precipitation of calcium and magnesium salts in a designated precipitation tank. Randall et al. (2016) [240] proposed dosing $\text{Ca}(\text{OH})_2$ powder to increase the pH in order to stabilize urine. The authors recommended a dosage of 10 g of $\text{Ca}(\text{OH})_2 \text{ L}^{-1}$ of fresh urine to ensure sufficiently high pH values and oversaturation, obviating the need for pH control. The same approach is used in the Autarky toilet, the on-site resource recovery toilet currently under development in the Blue Diversion Autarky project, to

stabilize the urine before evaporation. Senecal and Vinneras [262] used a bed of wood ash to alkalinize urine (20 L of urine kg^{-1} ash) before drying. The high pH (13-14) inhibited enzymatic urea hydrolysis, but promoted nonenzymatic urea hydrolysis, resulting in some nitrogen loss (5-35%) during drying. Due to the addition of calcium or ash, these stabilization methods do not address the scaling issue besides requiring the addition of external chemicals to the urine. In this study, the pH of fresh urine is increased by means of an electrochemical cell, which can be integrated into the source separation toilet to stabilize the urine immediately after collection. The setup is inspired by a concept developed for water softening by Clauwaert et al. (2019) [51] and consists of a crystallizer coupled to an electrochemical cell, in which the electrode compartments are separated by an ion-exchange membrane in order to create a pH gradient between the anode and cathode. In this research, urine is fed to the system and continuously recirculated between the crystallizer and the cathodic compartment of the electrochemical cell. By applying electrical energy, water (Equation 16) or oxygen (Equation 17) is reduced at the cathode, releasing hydroxide ions that increase the pH of the urine, while water is oxidized at the anode (Equation 18), creating an acidic stream. The pH of fresh urine was increased above 11, which was reported as the upper limit for enzymatic urea hydrolysis [240]. The high pH also results in supersaturation and thus triggers precipitation. As a result, most of the calcium and magnesium ions are removed from the urine, reducing the scaling potential in downstream processing.



Electrochemically induced precipitation has already been applied for water softening, i.e., to remove hardness ions in tap water, brackish water and/or seawater [99, 123, 330]. This study aims to increase the pH of fresh urine with an electrochemical cell in order to stabilize the urine and to precipitate divalent ions to reduce the scaling potential downstream of the unit. Four different configurations of the electrochemical cell (two- or three-chamber cell with an anion exchange membrane (AEM), cation exchange membrane (CEM) and/or bipolar membrane (BPM)) were compared in terms of pH increase, energy requirement, divalent cation and phosphate removal and ion migration in order to identify the best performing configuration. Stabilization was assessed by storing the effluent (at pH 11 and 12) and measuring the pH, electrical conductivity (EC) and total ammonia nitrogen (TAN, i.e., sum of ammonium-N and ammonia-N) concentration over time.

4.2 Materials and methods

4.2.1 Urine collection

Fresh urine from healthy male donors, not taking any medication, was collected using a nonwater urinal and stored for a maximum of one day at 4°C to prevent urea hydrolysis prior to the tests. Urine collection was approved by the Ethical Committee of Ghent University Hospital (registration number B670201731862). The urine was diluted 1:1 (50%) with demineralized water at the start of each experiment to simulate flushing with water (urine composition is given in Table S4.1).

4.2.2 Electrochemical cell and crystallizer

The setup was tested with a two-chamber and three-chamber electrochemical cell, separated by an AEM, a CEM and/or a BPM (Figure 4.1, SI Figure S4.2). A crystallizer with an active volume of 4 L was used as a precipitation vessel. The content of the crystallizer was continuously recirculated over the cathodic compartment of the electrochemical cell by means of a peristaltic pump. A recirculation rate of 15 L h⁻¹ was applied to efficiently distribute the alkalinity generated in the vicinity of the electrode over the content of the whole cathodic compartment and crystallizer in order to minimize scaling on the electrode. The inlet of the recirculation loop was located at the top of the crystallizer. The outlet was located at the bottom of the crystallizer to obtain a good mixing in the crystallizer and to promote precipitation by contact with the crystal seeds at the bottom of the crystallizer. The anolyte was recirculated over a glass bottle and the anodic compartment of the electrochemical cell with a peristaltic pump at a flow rate of 1.2 L h⁻¹. For the tests with the three-chamber cell, a sodium sulfate solution was recirculated over a glass bottle and the middle compartment with a peristaltic pump at a flow rate of 1.7 L h⁻¹.

The electrochemical cell consisted of two Perspex® plates and frames with an internal volume of 200 mL (dimension of 20 x 5 x 2 cm³), a stainless steel wire mesh (564 μm mesh width, 20 x 5 cm², Solana, Belgium) as a cathode and a dimensionally stable titanium anode coated with iridium oxide (Magneto Special Anodes, The Netherlands). The compartments were separated by an ion-exchange membrane with a surface area of 100 cm² to create a pH gradient between the electrode compartments. The middle compartment in the three-chamber electrochemical cell was made from a rubber frame (~5 mm thick). The cell was galvanostatically controlled at a current density of 60 A m⁻² (membrane projected surface) using a digital-control DC power supply (LABPS3005, Velleman, Belgium).

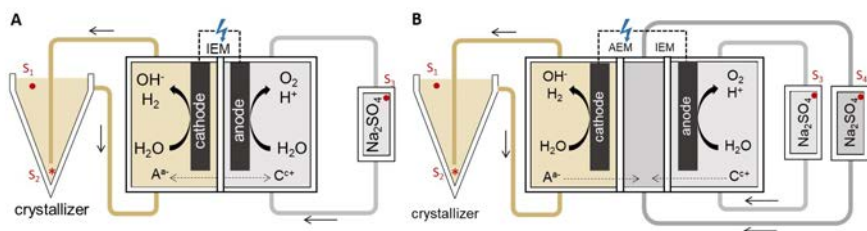


Figure 4.1: **Schematic overview of the experimental setup. A) two-chamber electrochemical cell with AEM or CEM, B) three-chamber electrochemical cell with AEM-CEM or AEM-BPM.** A picture of the setup is shown in SI (Figure S4.1). $S_{1,2,3,4}$ = sampling point for catholyte (1), precipitate (2), anolyte (3) and middle compartment (4). A^{a-} = any a-valent anion. C^{c+} = any c-valent cation.

4.2.3 Experimental protocol

Four different membrane configurations were tested (SI Figure S4.2). In configuration A1 (CEM), the anodic and cathodic compartment were separated by a CEM (Ultrex CMI-7000s, Membranes International Inc., NJ, USA). In configuration A2 (AEM), the CEM was replaced by an AEM (Ultrex AMI-7001, Membranes International Inc., NJ, USA). In the CEM configuration, a higher anolyte concentration (1.5 L of 0.2 M Na_2SO_4) was used to compensate for ion migration out of the anodic compartment, in contrast to the AEM configuration (1.5 L of 0.05 M Na_2SO_4) where ions migrate towards the anolyte. Configuration B1 (AEM+CEM) and B2 (AEM+BPM) consisted of a three-chamber electrochemical cell with an AEM separating the cathodic from the middle compartment. The middle compartment was separated from the anodic compartment by a CEM or a BPM (Fumasep FBM, Fumatech, Germany), respectively. All experiments with the three-chamber cell were conducted with initially 1 L of 0.05M Na_2SO_4 as an anolyte and 1 L of 0.05M Na_2SO_4 as a middle compartment solution.

The setup was operated as a batch reactor. The crystallizer was filled with 4 L of fresh, diluted urine (2 L of urine and 2 L of demineralized water) at the start of each test. Subsequently, the recirculation pumps and power supply were switched on. Samples were taken every hour, filtered (0.20 μm Chromafil® Xtra filter, Macherey-Nagel, PA, USA) and stored in a fridge prior to analysis. Once the pH set point was reached, the power supply was switched off and the crystallizer and anode vessel were emptied. A pH of 11 was targeted in the tests with the two-chamber setup, whereas the tests with a three-chamber cell were ceased at a pH of 12 to investigate the urine stabilization at pH 11 and pH 12 (Section 4.2.4). All tests were performed in triplicate with different batches of urine to account for the variability in urine composition. Samples were analysed for pH, EC, anions and cations.

4.2.4 Assessment of urine stabilization

A pH higher than 11 was targeted in the crystallizer to stabilize the urine. Fresh (non-treated, 1:1 (50%) diluted) urine and stabilized urine (effluent at pH 11 from the tests with a CEM ($n=3$) and at pH 12 from the tests with the AEM-CEM ($n=3$) setup) was stored in falcon tubes at room temperature to follow the urea hydrolysis over time. Samples were taken regularly to measure the pH, EC and TAN concentration. The stabilization experiment with fresh urine and the effluent from the tests with the CEM setup (pH 11) was conducted for 25 days, whereas the effluent of the tests with the AEM-CEM setup (pH 12) was stored for 568 days. After 561 days, Jack bean urease (Sigma Aldrich, USA, 0.53 g L^{-1} after Ray et al. (2018) [243]) was added to the falcon tubes to initiate urea hydrolysis and samples were taken after two and seven days. Urea hydrolysis was evaluated by measuring the TAN (total ammonia nitrogen)/TN (total nitrogen) ratio over time.

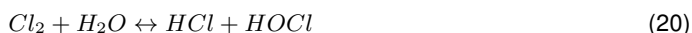
4.2.5 Analytical methods

Anions (chloride, nitrite, nitrate, sulfate and phosphate) were analysed on a Metrohm 930 compact ion chromatograph, equipped with a conductivity detector and a Metrosep A supp 5-150/4.0 column (Metrohm, Switzerland). Sodium, TAN and potassium were quantified using a Methrom 761 compact ion chromatograph, equipped with a conductivity detector and a Metrosep C6-250/4.0 column (Metrohm, Switzerland). Calcium and magnesium concentrations were measured by flame atomic absorption spectro-metry (Shimadzu AA-6300, Shimadzu, Japan). Prior to analysis, samples were diluted with milli-Q water and acidified with 1% nitric acid and 2% of lanthanum solution. Nanocolor tube test kits (Nanocolor® TN220, Macherey-Nagel, PA, USA) were used to determine the total nitrogen concentration. The EC was measured with a conductivity meter (Consort C6010 with a Metrohm 6.0912.110 conductivity probe), calibrated with 0.01, 0.1 and 1 M KCl solutions before use. pH measurements were performed with a portable pH meter (744 pH meter, Metrohm with a 6.0228.000 electrode).

4.3 Results and discussion

4.3.1 Configuration specific electromigration

The electrode compartments were separated by an ion-exchange membrane to create a pH gradient between the anode and cathode. At the cathode, hydroxide ions were generated, increasing the pH of the urine, while at the anode, protons were generated, acidifying the anolyte. To restore the electroneutrality in the electrode compartments, ions migrated between the anodic and cathodic compartments. In the CEM configuration, only cations are expected to migrate (when assuming perfect permselectivity of the membrane) due to the negatively charged functional groups (i.e., sulfonic acid) on the CEM. Mainly sodium, originating from the sodium sulfate solution that was used as anolyte, migrated from the anodic to the cathodic compartment (Figure 4.2). As a result, the sodium concentration in the urine increased by 30%. Because of the high anolyte Na_2SO_4 concentration (0.2M), protons accounted for only ~8% of the migration, although evidently over a longer time duration the impact of protons would be more substantial due to sodium depletion. The disadvantage of this configuration is thus that the anolyte solution needs to be replaced during long-term operation since the sodium sulfate solution is gradually replaced by sulfuric acid (due to the migration of sodium to the cathodic compartment and the proton production at the anode). Once the sodium gets depleted in the anodic compartment, the migration of protons to the cathodic compartment will increase and compensate the hydroxide produced at the cathode. In configurations where an AEM is used, the anolyte does not need to be replaced as ions move from the catholyte (urine) to the anolyte to maintain the charge balance. Chloride, sulfate and phosphate accounted for 55, 8 and 3%, respectively, of the migration of charges through the AEM. Due to the migration and some precipitation of phosphate and sulfate, the concentrations of chloride, sulfate and phosphate in urine decreased by 30, 26 and 44%, respectively. Due to the chloride migration to the anodic compartment and the limited selectivity of the anode, some chlorine can be formed at the anode (Equation 19) besides the intended water oxidation. The chlorine can diffuse to the atmosphere or react with water to form hydrochloric and hypochlorous acid (Equation 20), which can oxidize materials such as the membrane [330]. When chlorine gas diffuses to the cathode compartment, it could react with the organics or ammonia present in urine.



Chlorine production can be prevented by a more selective electrode designed to suppress chlorine generation [330] or by using a three-chamber cell. In the AEM+CEM and AEM+BPM configuration, migration of chloride from the urine to the anodic compartment is prevented by the CEM or BPM membrane between the middle compartment

and the anodic compartment. Similar to the AEM configuration, chloride was the predominant migrating ion through the AEM (accounting for 55-57%), followed by sulfate (18-22%). Also, the reduction in chloride, sulfate and phosphate concentrations and EC in the crystallizer was comparable in all configurations with an AEM. In the AEM+CEM configuration, sodium and protons migrated from the anodic compartment to the middle compartment. Relatively more protons migrated through the CEM in the AEM+CEM configuration compared to those in the CEM configuration, due to the lower sodium concentration in the anolyte (0.05 M Na_2SO_4 instead of 0.2M). Similar to the CEM configuration, the proton migration will increase over time as the sodium in the anolyte becomes depleted. In conjunction with the AEM, however, the protons cannot reach the catholyte, by which the pH gradient can be maintained. Hence, unlike the CEM configuration, the anolyte does not need to be replaced during long-term operation with the AEM+CEM configuration. In the AEM+BPM configuration, sodium migration from the anodic compartment to the middle compartment is mostly prevented by the BPM. A BPM consists of an AEM and a CEM layer joined together [330]. Due to the electric field across the membrane, water molecules split in the transition region between the layers. The protons migrate through the CEM layer to the middle compartment, whereas hydroxide ions migrate through the AEM layer to the anodic compartment. Hence, the anolyte composition does, at least theoretically, not change.

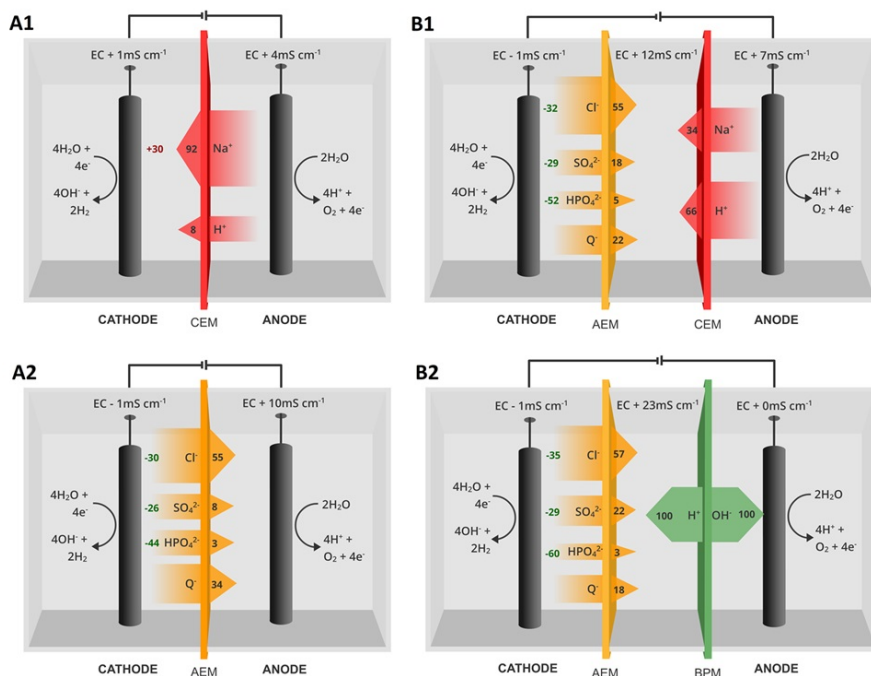


Figure 4.2: **Schematic overview of the ion migration in the four configurations: CEM (A1), AEM (A2), AEM+CEM (B1) and AEM+BPM (B2).** The difference in electrical conductivity (EC) between the start and the end (at pH 11) of the experiment is mentioned at the top of each compartment. The arrows illustrate the direction of the migration through the membranes. The numbers displayed on the arrows represent the relative contribution (%) of each ion to the total migration (calculation in SI Section 4.4.2). Q^- represents the residual anions that were not quantified (including hydroxide ions, (bi)carbonate ions and negatively charged organics). The percentages mentioned in the cathodic compartment (in green or red) indicate the increase (+, red) or decrease (-, green) in concentration in the urine, caused by the migration and/or precipitation (in case of phosphate and sulfate). All values are averages ($n=3$). Standard deviations can be found in SI Table S4.2.

4.3.2 pH profile in the crystallizer

A high pH was induced in the crystallizer by recirculating the urine over the cathodic compartment of the electrochemical cell, in which hydroxide ions were produced through the reduction of water and/or oxygen. The pH increased as a function of the amount of hydroxide ions produced by the electrochemical cell (Figure 4.3), calculated by dividing the cumulative electric charge by the Faraday constant and crystallizer volume, assuming a Faradaic (current) efficiency of 100%. All curves display a characteristic pH increase in three stages: the slope decreases at a pH above 8.5 due to the buffering

activity of the $\text{NH}_4^+/\text{NH}_3$ equilibrium, followed by the $\text{HCO}_3^-/\text{CO}_3^{2-}$ equilibrium and the curve flattens out as the pH approaches to pH 12 due to the buffering activity of the $\text{HPO}_4^{2-}/\text{PO}_4^{3-}$ equilibrium. The differences between the tests can be explained by the use of different batches of urine (with different TAN, bicarbonate and/or phosphate concentrations and initial pH). There were no profound differences between the four configurations. The pH increase in the crystallizer coincides with a titration curve of fresh urine with NaOH (black line in Figure 4.3), indicating a high Faradaic efficiency and a limited migration and diffusion of hydroxide ions or protons from and to the cathodic compartment. About 20 mmol $\text{OH}^- \text{ L}^{-1}$ was needed to raise the pH to 11. An additional 10-15 mmol $\text{OH}^- \text{ L}^{-1}$ was required to reach a pH of 12 in the tests with the three-chamber cell. This corresponds to applied total electric charges of about 2000 C L^{-1} and 3500 C L^{-1} to obtain pH values of 11 and 12, respectively (SI Section 4.4.3). In theory (without overpotentials and Ohmic drop), an applied cell voltage between 1.3 and 1.7 V is necessary to drive the water reduction and water oxidation reactions at the cathode and anode (SI Section 4.4.3), which would require $1.5 \pm 0.3 \text{ Wh L}^{-1}$ urine or $2.9 \pm 0.3 \text{ Wh L}^{-1}$ urine to increase the pH of fresh urine to 11 and 12, respectively. The real electrochemical energy consumption in the tests was between 4.9 and 8.8 Wh L^{-1} urine (pH 11) and 14.3 Wh L^{-1} urine (pH 12) (SI Section 4.4.3). The lower voltage and, hence, the lower energy consumption in the tests with a CEM (SI Table S4.3) can be attributed to the lower electrical resistance of the CEM ($<30 \Omega \cdot \text{cm}^2$, according to the supplier) compared to that of the AEM ($<40 \Omega \cdot \text{m}^2$) and to the higher electrical conductivity of the anolyte ($\sim 35 \text{ ms cm}^{-1}$ compared to only $\sim 10\text{-}20 \text{ mS cm}^{-1}$ in all other configurations). The voltage and electrode energy consumptions of the three-chamber cells (AEM+CEM and AEM+BPM) were not substantially higher than those of the two-chamber cell with the AEM, despite the additional membrane and increased distance between the electrodes ($\sim 0.5 \text{ cm}$, corresponding to a theoretical Ohmic drop of $\sim 0.1\text{-}0.3\text{V}$, which is low compared to the total voltage of $\sim 7.5\text{V}$).

4.3.3 Precipitation of divalent cations at high pH

The pH increase shifts the speciation of phosphate and carbonate ions, creating supersaturation of calcium and magnesium phosphate and carbonate salts (e.g., hydroxyapatite and calcite), and thus precipitation in the crystallizer. As a result, calcium and magnesium are removed from the urine, reducing the scaling potential in downstream processing. The higher the pH, the higher the supersaturation and thus the lower the final remaining calcium and magnesium concentrations (Figure 4.4). At a pH of ~ 9.25 , which is the pH of urine after urea hydrolysis, only about $53 \pm 16\%$ of the calcium and $52 \pm 29\%$ of the magnesium were removed, whereas at a pH of 11, $93 \pm 3\%$ of the calcium and $79 \pm 16\%$ of the magnesium were precipitated. The removal efficiencies increased to $96 \sim 3\%$ (calcium) and $85 \pm 9\%$ (magnesium) at a pH of 12. The final calcium and magnesium concentrations were $0.065 \pm 0.039 \text{ mmol Ca}^{2+} \text{ L}^{-1}$ and $0.15 \pm 0.11 \text{ mmol Mg}^{2+} \text{ L}^{-1}$ (pH 11), and $0.042 \pm 0.035 \text{ mmol Ca}^{2+} \text{ L}^{-1}$ and

$0.14 \pm 0.07 \text{ mmol Mg}^{2+} \text{ L}^{-1}$ (pH 12). Overall, there was a similar pH increase and calcium and magnesium removal in all configurations.

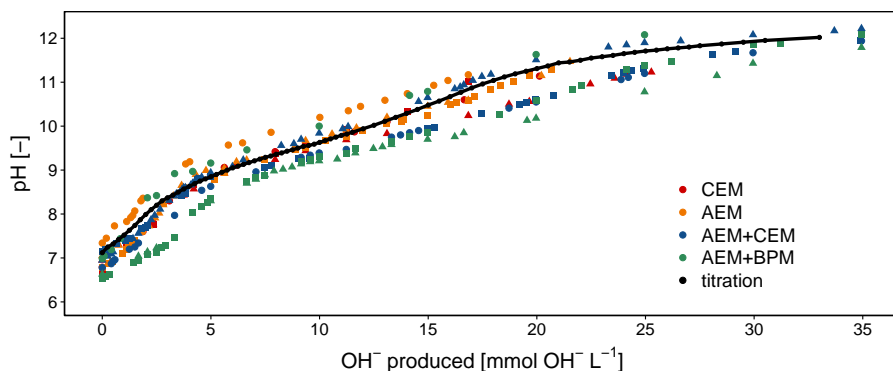


Figure 4.3: **pH increase in the crystallizer as a function of the OH^- produced by the electrochemical cell.** The amount of hydroxide [$\text{mmol OH}^- \text{ L}^{-1}$] produced by the electrochemical cell was calculated by dividing the cumulative electric charge by the Faraday constant and crystallizer volume, assuming a Faradaic (current) efficiency of 100% (i.e., one mole of electrons corresponds to one mole of hydroxide ions). Each configuration was tested in triplicate (shown with different shapes) with 1:1 diluted urine. The black line represents a titration curve of fresh urine with 1M NaOH (90 data points).

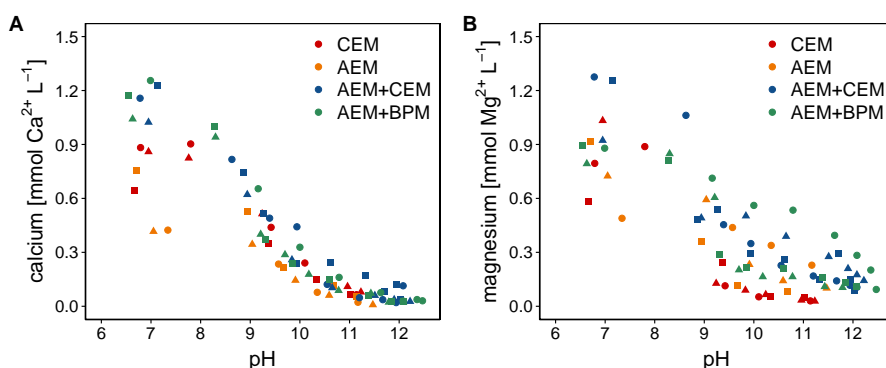


Figure 4.4: **Calcium (A) and magnesium (B) concentration as a function of the pH in the crystallizer.** Each configuration was tested in triplicate (shown with different shapes). The concentration for each individual test is displayed in SI Figures S4.5 and S4.6.

4.3.4 Urine long-term stabilization

The aim of this study was to stabilize fresh urine by increasing the pH. Ideally, it should be possible to preserve the treated urine for a long time without urea hydrolysis to avoid malodor and ammonia volatilization during storage. pH 11 was identified as the upper limit for enzymatic urea hydrolysis by Randall et al. (2016) [240]. Urine could be stored for one month without urea hydrolysis by increasing the pH to 11 with NaOH [240]. To follow up the urea hydrolysis in the electrochemically stabilized urine produced in this study over time, the effluent from the three tests with the CEM configuration with a pH around 11 was stored at room temperature and the pH, EC and TAN concentration were measured regularly (Figure 4.5). Urea hydrolysis is characterized by a sharp increase in pH to ~ 9.25 due to the release of TAN and bicarbonate, whereas the EC gradually increases during urea hydrolysis because of the conversion of uncharged urea into charged molecules (ammonium and bicarbonate). Hence, the pH is a good indicator of the onset of urea hydrolysis, while the EC can be used as a measure of the urea hydrolysis progression [243, 331]. Fresh, non-treated urine (in red) was included as a control and started to hydrolyse immediately, resulting in a sharp increase in pH, EC and TAN concentration. After two days, the pH reached a plateau at ~ 9.25 , while it took 10-15 days to reach the maximum EC and TAN concentration. No significant increase in EC or TAN concentration occurred in the stabilized urine at pH 11 (in blue) during the first ~ 7 days, indicating that urea hydrolysis was inhibited. However, the pH gradually decreased and reached a pH of ~ 9.25 after 7-10 days. Due to the lower pH, urea hydrolysis was no longer inhibited, resulting in an increase in EC and TAN concentration. It is not known what caused the pH decrease, possibly alkaline hydrolysis of urine constituents (e.g., organics) or some CO_2 absorption from the headspace or during sampling. In the study by Randall et al. (2016), the pH was daily adjusted with NaOH to keep the pH at 11, which might explain the different outcomes of the study. Overall, the increase in EC corresponds well to the increase in TAN concentration, confirming the results obtained by Zhang et al. (2013) [331] and Ray et al. (2018) [243]. Since increasing the pH to 11 did not suppress the enzymatic urea hydrolysis for longer than one week, a pH of 12 was targeted in the tests with the AEM+CEM configuration. To reach this set point, almost double the amount of hydroxide ions was added compared to a pH of 11, due to the buffering effect of the $\text{HPO}_4^{2-}/\text{PO}_4^{3-}$ equilibrium. As a result, the pH decreased much slower during storage and was still sufficiently high (>11) to inhibit urea hydrolysis for up to 18 months (Figure 4.5, green). Over a period of 18 months, the TAN/TN ratio only increased from ~ 5 to $\sim 8\%$ (SI Table S4.4). The urine also did not have the typical dark colour and smell of hydrolysed urine (SI Figure S4.7). The presence of organics in urine ($\sim 10 \text{ g COD L}^{-1}$) fuels biological growth, resulting in the production of volatile fatty acids, which contribute to the strong smell of urine [294, 331]. The high pH probably inhibits the biological growth and, hence, prevents malodor.

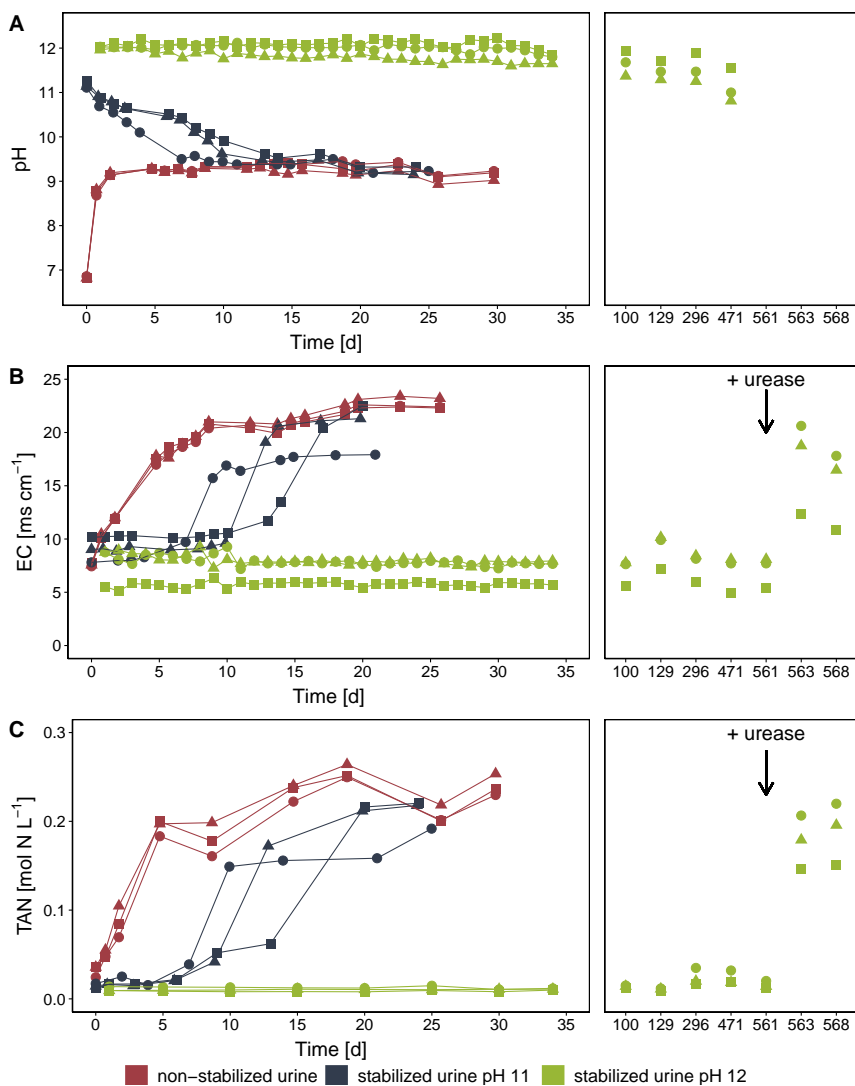


Figure 4.5: **pH, electrical conductivity (EC) and total ammonia nitrogen (TAN) concentration in non-stabilized urine and stabilized urine at a pH of 11 and 12 over time.** The triplicates are represented with different symbols. After 561 days, Jack bean urease (0.53 g L^{-1}) was added to the stabilized urine (pH 12) to initiate urea hydrolysis (indicated with the arrow).

Some nitrogen recovery technologies (e.g., NH_3 stripping and NH_3 extraction with (bio-)electrochemical systems) require ammonium or ammonia as nitrogen input instead of urea [48]. After 561 days, Jack bean urease was added to initiate urea hydrolysis in the stabilized urine. Two days after addition, 80-100% of the total nitrogen was converted into TAN (Figure 4.5, SI Table S4.4). Mixing with stale (hydrolysed) urine

[331] or treatment in an anaerobic ureolysis reactor [48] can probably also induce urea hydrolysis in stabilized urine after long-term storage.

4.3.5 Phosphorus recovery from precipitates

The phosphate concentration in the crystallizer decreased by $48 \pm 14\%$. This is mainly due to the precipitation of phosphates with calcium and magnesium, accounting for a $38 \pm 11\%$ ($1.12 \pm 0.31 \text{ mmol PO}_4 \text{ L}^{-1}$) removal. In addition, migration through the membrane accounted for $13 \pm 3\%$ in the three configurations with an AEM (SI Figure S4.8). Measurements [288] and simulations [293] with undiluted urine by Udert et al. (2003) showed that about 30% of the phosphate was precipitated by urea hydrolysis. The amount of phosphate that can be precipitated in urine is limited by the calcium and magnesium concentrations in urine and by competition with other anions such as (bi)carbonate [288, 293].

Precipitation reduces the phosphate content of the urine and thus limits the P recovery potential in later treatment [293]. On the other hand, if the precipitates can be harvested, they can be valorized as inorganic fertilizers in agriculture or resources for the phosphate industry [241, 294]. Randall and Naidoo (2018) [241] proposed to install a replaceable conical cartridge at the bottom of the toilet to allow user-friendly precipitate harvesting.

Udert et al. (2003) [288] identified struvite, calcite and calcium phosphate minerals (e.g., hydroxyapatite) as the main precipitates in urine after urea hydrolysis. Hydroxyapatite and struvite are believed to be good slow-release fertilizers on acid soils [288]. The precipitates formed by electrochemical precipitation are probably more enriched in calcium phosphate minerals, since fresh urine contains less ammonium and (bi)carbonate, which are necessary for struvite and calcite precipitation, respectively. Moreover, computer simulations by Randall et al. (2016) pointed out that magnesium mainly precipitates as $\text{Mg}(\text{OH})_2$ at high pH values. The precipitate produced in this study could not be identified with X-ray diffraction (XRD) (no clear diffraction peaks). X-ray fluorescence (XRF) identified calcium and phosphate as the predominant ions in the precipitate. More research is necessary to characterize the composition of the precipitates to assess their fertilizer potential.

4.3.6 Implementation & application of electrochemical urine precipitation and stabilization

In this study, the pH of fresh urine was increased using an electrochemical cell in order to prevent urea hydrolysis during storage and to facilitate downstream processing by the controlled precipitation of calcium and magnesium. Urea hydrolysis already starts in urine collection systems since urease-positive bacteria are widespread [197, 288, 292]. This can lead to odor nuisance, ammonia volatilization, and clogging of pipes. As it is more difficult to increase the pH of partially hydrolysed urine due to the stronger $\text{NH}_4^+/\text{NH}_3$ and $\text{HCO}_3^-/\text{CO}_3^{2-}$ buffer, it is important that an electrochemical cell for urine

stabilization is installed as close to the toilet as possible (or is integrated into the toilet) in order to minimize the time before stabilization. The setup can be operated as a batch reactor, in which the pH of consecutive batches (donations) of urine is gradually increased from ~ 7 to 11-12. When the pH set point is reached, the crystallizer is emptied and the urine is sent to a storage tank until further treatment. If an efficient precipitate collection system is in place, phosphorus can be recovered by harvesting the precipitates. In this study, the urine was diluted 1:1 (50%) to simulate flushing with water. Treating undiluted urine instead would likely result in more precipitation (due to the higher divalent cation concentration) and a lower energy consumption per volume of urine treated (due to the higher conductivity and thus lower Ohmic resistance of the catholyte).

The higher the pH in the crystallizer, the more calcium and magnesium are removed, and thus the lower the risk for scaling during further treatment. While precipitation is limited by the low calcium and magnesium concentrations, it can still occur since the ion product approximates the solubility product. To completely eliminate the risk for scaling, the pH should be lowered during or just before treatment. For stabilization, pH 11 was not sufficient to inhibit urea hydrolysis for longer than one week, whereas the urine at pH 12 could be preserved for ~ 18 months without hydrolysis. A pH $\gg 12$ is unfavorable because a lot of energy needs to be invested to increase the pH of fresh urine due to the strong $\text{HPO}_4^{2-}/\text{PO}_4^{3-}$ buffer. Moreover, chemical urea hydrolysis can start to occur above pH 13 [240], which should be prevented. Hence, the optimal pH for electrochemical stabilization and precipitation is around 12. Interestingly, according to literature, most of the bacteria and viruses are inactivated or killed at this high pH [240].

From the four electrochemical cell configurations that were tested, the three-chamber cells (AEM+CEM and AEM+BPM) are the most promising. Unlike the CEM configuration, no chemical input is required when an AEM is used, as ions migrate from the cathode (urine) to the anode. Due to this ion migration, the concentration of chloride is reduced with 30-35% in urine, which is beneficial as a high salinity (and in particular chloride) challenges biological processing (e.g., nitrification [48, 200]) and plant production [204, 223]. By incorporating a CEM or BPM in the cell, chlorine production at the anode can be prevented, protecting the membrane and electrode from highly oxidizing hypochlorous acid that can be formed.

During the experiments, the AEM in all configurations turned brown (SI Figure S4.3), probably due to the adsorption of organics to the positively charged functional groups of the AEM [10, 66]. It is not known whether this can affect the performance of the electrochemical cell during long-term operation. Using a monovalent AEM, through which only monovalent ions can pass, or an AEM with a modified surface might decrease the adsorption of organics to the AEM, but this has not been tested yet with urine [109, 203]. Moreover, a monovalent AEM could prevent the migration and hence loss of phosphate to the middle compartment.

Due to the migration of anions from the cathode and protons from the anode,

an acidic stream (mix of HCl, H₂SO₄, H₃PO₄, HNO₃, H₂CO₃ and organic acids) is produced in the middle compartment of the three-chamber cells. Likely, the best strategy to minimize salt accumulation (and the associated back diffusion to the catholyte or diffusion to the anolyte) is to regularly replenish a part of the middle compartment fluid with water. The acidic middle compartment fluid can be used to periodically rinse the cathodic compartment of the electrochemical cell in order to remove the precipitates accumulated on the electrode surface and/or membrane. It can also be used to periodically flush the toilet to remove scaling and to hygienize/suppress microbial activity in the toilet. Flushing urine diversion toilets with acids to remove precipitates is already a common practice [23]. After a flushing event, some acidified urine could enter the electrochemical cell, resulting in a temporary increase in hydroxide requirement to reach a pH of 12. The anolyte solution of a three-compartment setup will also need to be replenished with water after some time because of osmotic and electro-osmotic water transport to the middle compartment, resulting from the high concentration gradient between the anolyte and middle compartment solution and the migration of cations (including hydration shell) to the middle compartment. The hydrogen gas produced at the cathode would spontaneously degas; however, a small aeration could be installed to avoid any accumulation. On a large scale, it could be recovered and valorized as an energy source.

By a smart selection of membranes, no chemical input is required to increase the pH, which is not only interesting for terrestrial applications, where chemical storage and dosing are a nuisance, but could also prove useful in regenerative life support systems (RLSS) for human deep-space exploration. Currently, on board of the International Space Station (ISS), water is recovered from urine using vapor compression distillation and filtration. Since ammonia volatilization can pose a hazard to the crew, the urine is pre-treated with hazardous and toxic chemicals (sulfuric/phosphoric acid and chromium trioxide) to inhibit urea hydrolysis [38, 201]. Furthermore, the distillation unit faces severe scaling problems due to uncontrolled calcium sulfate precipitation. The electrochemical pre-treatment studied here allows the reduction of the scaling potential and the stabilization of urine, without consumables and the logistics related to the storage of chemicals. In MELISSA (Micro-Ecological Life Support System Alternative), urine is converted into a liquid fertilizer for plants and microalgae (cyanobacteria) by nitrification [105, 163]. Apart from reducing the scaling potential and stabilizing the urine before nitrification, the electrochemical pre-treatment would reduce the salinity of the urine due to the migration of anions (mainly chloride) to the middle compartment and the acid that is produced can be used to decrease the pH in the plant compartment. Moreover, nitrification lowers the pH, decreasing the ion product and thus eliminating the risk for scaling.

Further research should focus on the long-term (semi)continuous functioning of the electrochemical cell, the design of a precipitate collection system, and the implementation/integration into a source separation toilet.

4.4 Supplementary information

4.4.1 Experimental setup

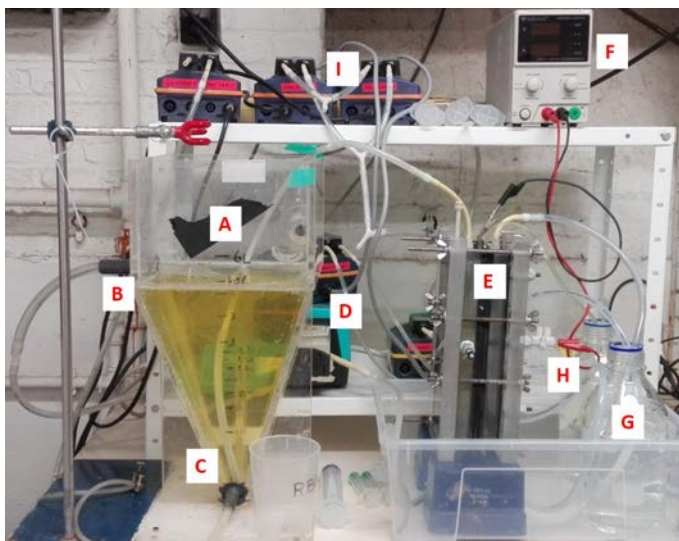


Figure S4.1: **Experimental setup (with three-chamber cell).**

A: crystallizer (decanter with active volume of 4 L)

B: inlet recirculation loop crystallizer (at the top of the crystallizer)

C: outlet recirculation loop crystallizer (at the bottom of the crystallizer)

D: recirculation pump (Watson Marlow 323E/D, MA, USA)

E: electrochemical cell

F: digital-control DC power supply (LABPS3005, Velleman, Gavere, Belgium)

G: recirculation vessel anolyte

H: recirculation vessel middle compartment solution

I: recirculation pumps anodic and middle compartment (DULCOflex ® DF2a, ProMinent GmbH, Heidelberg, Germany)

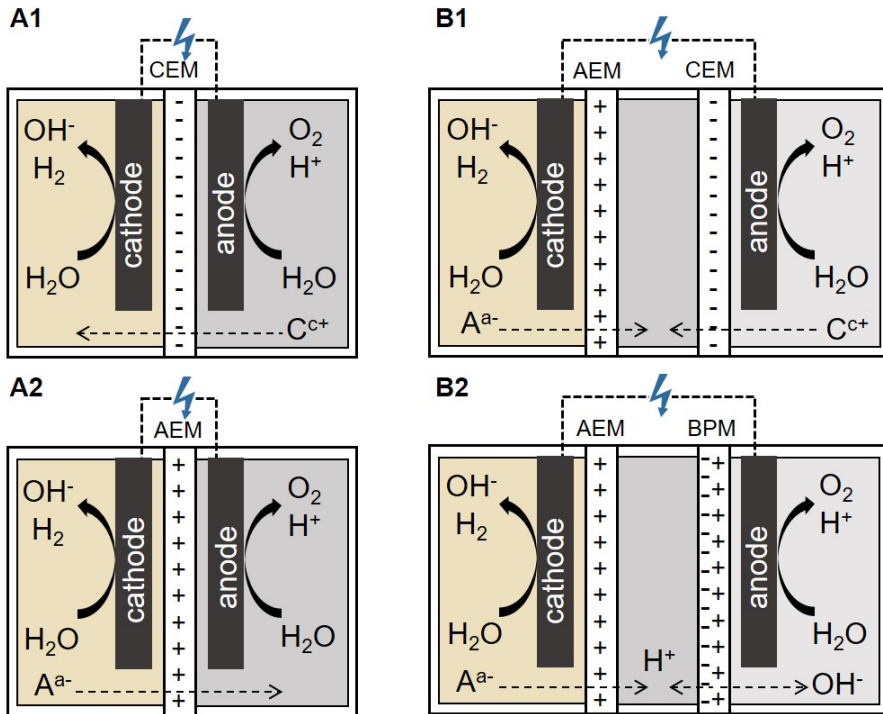


Figure S4.2: **Schematic overview of the four configurations: CEM (A1), AEM (A2), AEM+CEM (B1) and AEM+BPM (B2).** The arrows show the direction of the electromigration. A^{a-} = any a-valent anion. C^{c+} = any c-valent cation.

Table S4.1: **Urine composition after dilution with demineralized water.** AV= average, SD= standard deviation.

	AEM					CEM				
[mmol L ⁻¹]	1	2	3	AV	SD	1	2	3	AV	SD
Cl ⁻	44.0	34.1	33.6	37.3	5.9	37.0	43.8	42.7	41.2	3.6
PO ₄ ³⁻	2.7	3.1	2.6	2.8	0.3	2.4	4.0	3.0	3.1	0.8
SO ₄ ²⁻	3.1	2.7	2.9	2.9	0.2	3.2	3.8	3.8	3.6	0.3
Na ⁺	34.3	29.6	23.1	29.0	5.6	33.2	37.8	32.1	34.4	3.0
NH ₄ ⁺	22.6	11.0	17.4	17.0	5.8	10.7	10.8	6.6	9.4	2.4
K ⁺	20.6	14.8	15.3	16.9	3.2	15.6	20.3	16.2	17.4	2.6
Ca ²⁺	0.8	0.4	0.4	0.5	0.2	0.6	0.9	0.9	0.8	0.1
Mg ²⁺	0.9	0.7	0.5	0.7	0.2	0.6	1.0	0.8	0.8	0.2

	AEM+CEM					AEM+BPM				
[mmol L ⁻¹]	1	2	3	AV	SD	1	2	3	AV	SD
Cl ⁻	38.5	32.1	49.0	39.9	8.5	58.3	60.7	38.9	52.6	12.0
PO ₄ ³⁻	3.9	2.7	3.9	3.5	0.7	3.5	3.8	1.6	3.0	1.2
SO ₄ ²⁻	4.2	2.7	3.5	3.5	0.7	3.4	3.9	2.8	3.4	0.5
Na ⁺	26.3	27.1	36.8	30.1	5.8	40.7	46.3	56.9	48.0	8.2
NH ₄ ⁺	7.9	7.7	6.7	7.5	0.6	5.7	13.8	14.5	11.3	4.9
K ⁺	23.7	19.3	22.6	21.9	2.3	19.8	26.8	17.6	21.4	4.8
Ca ²⁺	1.2	1.0	1.2	1.1	0.1	1.2	1.0	1.3	1.2	0.1
Mg ²⁺	1.3	0.9	1.3	1.2	0.2	0.9	0.8	0.9	0.9	0.1

Figure S4.3: **Anion exchange membrane after two days of operation.**

4.4.2 Electromigration

Calculations

Based on the electric charge that was applied during the test, the amount of electrons that went from the anode to the cathode was determined as follows:

$$[mmol e^-] = \frac{time [s] \times current [A]}{96485.3 \frac{C}{mol e^-}} \times 10^3 \quad (21)$$

An equal amount of charge should migrate between the compartments to restore the electroneutrality of the system. For the AEM, the relative contribution of chloride, sulfate, nitrate and phosphate to the total migration was calculated as follows:

relative contribution [%]

$$= \frac{\left(Q_{pH11}^- \left[\frac{mg}{L} \right] - Q_{t_0}^- \left[\frac{mg}{L} \right] \right) \times V_{middle\ compartment} [L] \times valence\ of\ ion}{MM \left[\frac{mg}{mmol} \right] \times amount\ of\ electrons [mmol e^-]} \times 100 \quad (22)$$

with

- $Q_{pH11}^- \left[\frac{mg}{L} \right]$ = concentration of anion in the middle compartment at the end of the test (when the pH in the crystallizer equaled 11)
- $Q_{t_0}^- \left[\frac{mg}{L} \right]$ = concentration of anion in the middle compartment at the start of the test
- $V_{middle\ compartment} [L]$ = volume of the middle compartment
- valence of ion = -1 for chloride and nitrate, -2 for sulfate and phosphate (HPO_4^{2-} is the dominating speciation between pH 7-12)
- $MM \left[\frac{mg}{mmol} \right]$ = molar mass of ion
- amount of electrons $[mmol e^-]$ = amount of electrons that were transferred from anode to cathode

For the CEM, the relative contribution of sodium and protons to the total migration was calculated as follows:

relative contribution of sodium [%]

$$= \frac{\left(Na_{pH11}^+ \left[\frac{mg}{L} \right] - Na_{t_0}^+ \left[\frac{mg}{L} \right] \right) \times V_{anodic\ compartment} [L] \times \text{valence of ion}}{MM \left[\frac{mg}{mmol} \right] \times \text{amount of electrons} [mmol\ e^-]} \times 100 \quad (23)$$

with

- $Na_{pH11}^+ \left[\frac{mg}{L} \right]$ = sodium concentration in the anodic compartment at the end of the test (when the pH in the crystallizer equaled 11)
- $Na_{t_0}^+ \left[\frac{mg}{L} \right]$ = sodium concentration in the anodic compartment at the start of the test
- $V_{anodic\ compartment} [L]$ = volume of the anodic compartment
- valence of ion = +1
- $MM \left[\frac{mg}{mmol} \right]$ = molar mass of sodium
- amount of electrons $[mmol\ e^-]$ = amount of electrons that were transferred from anode to cathode

relative contribution of protons [%]

$$= 100 - \text{relative contribution of sodium} [\%] \quad (24)$$

Since no sodium migrated from the anodic compartment to the middle compartment in the AEM+BPM configuration, it was assumed that protons accounted for 100% of the migration.

Table S4.2: **Electrical conductivity, pH, removal percentages in the crystallizer and contribution of each ion to the total electromigration.** The removal percentages in the crystallizer are calculated by dividing the difference in concentration between the start and the end (pH 11) of the experiment by the initial concentration in the crystallizer. Positive values indicate that the ion is removed from the urine (due to migration and/or precipitation). Negative values indicate an increase in concentration. Other anions include anions that were not quantified (including hydroxide ions, (bi)carbonate ions and negatively charged organics). About 7% of the COD migrated through the AEM. Averages and standard deviations are given.

		CEM	AEM	AEM+CEM	AEM+BPM
electrical conductivity (EC, [$mS\ cm^{-1}$])					
crystallizer	start	8.0 ± 1.1	8.0 ± 1.1	6.9 ± 1.8	9.2 ± 2.7
	end	9.0 ± 1.2	7.5 ± 0.6	6.1 ± 1.4	8.0 ± 2.9
anolyte	start	34.3 ± 0.8	12.5 ± 0.3	8.8 ± 0.1	9.9 ± 0.8
	end	38.7 ± 0.3	22.7 ± 1.7	15.9 ± 0.5	10.1 ± 1.8
middle compartment	start			8.6 ± 0.3	9.7 ± 1.0
	end			20.1 ± 2.1	32.9 ± 12.2
pH					
anolyte	start	3.9 ± 0.3	5.8 ± 2.5	5.1 ± 2.2	5.2 ± 0.6
	end	2.1 ± 0.0	1.8 ± 0.1	1.3 ± 0.2	3.2 ± 0.2
middle compartment	start			5.0 ± 2.4	4.8 ± 1.0
	end			1.2 ± 0.2	1.1 ± 0.2
removal percentages in the crystallizer [%]					
chloride		0.8 ± 8.1	30.0 ± 3.5	31.6 ± 2.3	34.6 ± 7.3
sulfate		13.4 ± 3.4	25.5 ± 7.9	29.1 ± 1.0	29.4 ± 10.3
nitrate				26.8 ± 3.9	30.4 ± 4.9
phosphate		34.7 ± 5.7	43.9 ± 15.6	52.0 ± 1.4	59.7 ± 16.7
precipitation		34.7 ± 5.7	34.2 ± 15.8	36.8 ± 1.9	48.2 ± 14.9
sodium		-29.5 ± 31.2	-6.6 ± 1.7	-16.0 ± 8.6	-5.7 ± 12.4
potassium		1.2 ± 14.2	-2.1 ± 15.0	-7.3 ± 3.9	-2.7 ± 34.3
migration [%]					
AEM					
chloride			54.9 ± 5.2	54.6 ± 3.4	56.6 ± 3.5
nitrate				0.5 ± 0.1	0.4 ± 0.1
phosphate			2.8 ± 0.3	4.6 ± 0.6	2.7 ± 0.6
sulfate			7.8 ± 3.3	17.7 ± 5.6	22.3 ± 14.0
other anions			34.4 ± 5.0	23.2 ± 8.7	18.1 ± 17.3
CEM/BPM					
sodium		92.4		33.7 ± 5.7	0.0 ± 0.0
protons		7.6		66.3 ± 5.7	100.0 ± 0.0

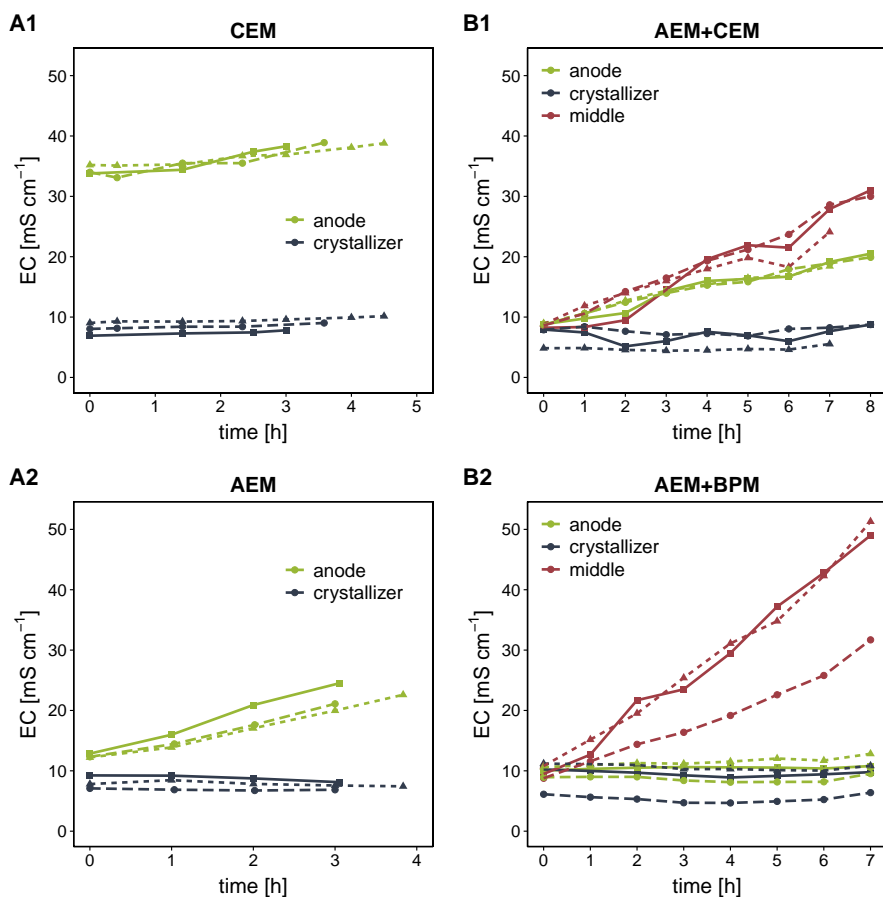


Figure S4.4: **Electrical conductivity in the four configurations: CEM (A1), AEM (A2), AEM+CEM (B1) and AEM+BPM (B2).** Each configuration was tested in triplicate (indicated with different symbols and linetypes).

4.4.3 Electric charge and electrode energy consumption

Cell potential

The cell potential depends on the pH in the compartments and can be calculated with the Nernst equation. The pH of the catholyte (urine) increased from ~ 7 to ~ 11 , while the pH of the anolyte decreased from ~ 5 to ~ 2 (Table S4.2).

cathode reaction: $2 \text{H}_2\text{O} + 2 \text{e}^- \leftrightarrow \text{H}_2 + 2 \text{OH}^-$

- pH 7 ($[\text{OH}^-] = 10^{-7} \frac{\text{mol}}{\text{L}}$, $p_{\text{O}_2} = 1 \text{ bar}$):

$$E_c = -0.8277 \text{ V} - \frac{0.059}{2} \times \log \frac{1 * (10^{-7})^2}{1} = -0.4147 \text{ V}$$

- pH 11 ($[\text{OH}^-] = 10^{-3} \frac{\text{mol}}{\text{L}}$, $p_{\text{O}_2} = 1 \text{ bar}$):

$$E_c = -0.8277 \text{ V} - \frac{0.059}{2} \times \log \frac{1 * (10^{-3})^2}{1} = -0.6507 \text{ V}$$

anode reaction: $2 \text{H}_2\text{O} \leftrightarrow \text{O}_2 + 4 \text{H}^+ + 4 \text{e}^-$

- pH 5 ($[\text{H}^+] = 10^{-5} \frac{\text{mol}}{\text{L}}$, $p_{\text{O}_2} = 1 \text{ bar}$):

$$E_a = 1.229 \text{ V} - \frac{0.059}{4} \times \log \frac{1}{1 * (10^{-5})^4} = 0.934 \text{ V}$$

- pH 2 ($[\text{H}^+] = 10^{-2} \frac{\text{mol}}{\text{L}}$, $p_{\text{O}_2} = 1 \text{ bar}$):

$$E_a = 1.229 \text{ V} - \frac{0.059}{4} \times \log \frac{1}{1 * (10^{-2})^4} = 1.052 \text{ V}$$

cell potential:

- start (pH 7-5): $E_{\text{cell}} = E_a - E_c = 0.934 - (-0.4147) = 1.3487 \text{ V}$
- start (pH 11-2): $E_{\text{cell}} = E_a - E_c = 1.052 - (-0.6507) = 1.7027 \text{ V}$

Table S4.3: **Electric charge and electrode energy consumption.** The electric charge [C] was calculated by multiplying the applied current (0.6 A) with the time needed to reach the pH setpoint (in seconds). The theoretical electrochemical energy consumption (electrical input to the electrochemical cell) was calculated by multiplying the cell potential to drive the water reduction/oxidation reactions (1.5 V, Section 4.4.3) with the current density to reach pH 11 or 12 [$C L^{-1}urine$], divided by 3600 (to convert seconds into hour). The electrochemical energy consumption was calculated in the same way, but with the average (measured) cell voltage instead of the theoretical cell potential. Averages and standard deviations are given. Wh_{el} = electrical energy

	CEM	AEM	AEM+CEM	AEM+BPM
current applied [A]	0.6 ± 0.0	0.6 ± 0.0	0.6 ± 0.0	0.6 ± 0.0
average cell voltage [V]	4.5 ± 0.1	7.5 ± 1.1	7.6 ± 1.4	7.4 ± 0.8
initial pH	6.8 ± 0.1	7.0 ± 0.3	7.0 ± 0.2	6.7 ± 0.2
pH end (11)	11.1 ± 0.1	11.2 ± 0.3	11.1 ± 0.1	11.1 ± 0.3
pH end (12)			12.1 ± 0.0	12.0 ± 0.2
time to pH 11 [h]	3.6 ± 0.6	3.3 ± 0.5	3.8 ± 0.7	4.0 ± 1.2
time to pH 12 [h]			6.4 ± 0.9	6.4 ± 0.6
Electric charge to reach pH 11 or 12				
pH 11				
[kC]	7.79 ± 1.30	7.25 ± 1.08	8.26 ± 1.46	8.67 ± 2.63
[$kC L^{-1}$]	1.95 ± 0.33	1.81 ± 0.27	2.07 ± 0.36	2.17 ± 0.66
[$kC L^{-1}urine$]	3.90 ± 0.65	3.62 ± 0.54	4.13 ± 0.73	4.33 ± 1.31
pH 12				
[kC]			13.86 ± 2.03	13.86 ± 1.40
[$kC L^{-1}$] ^a			3.47 ± 0.51	3.47 ± 0.35
[$kC L^{-1}urine$] ^b			6.93 ± 1.02	6.93 ± 0.70
Theoretical electrochemical energy consumption				
cell potential [V]	1.5	1.5	1.5	1.5
pH 11				
[$Wh_{el} L^{-1}urine$]	1.6 ± 0.3	1.5 ± 0.2	1.7 ± 0.3	1.8 ± 0.5
pH 12				
[$Wh_{el} L^{-1}urine$]			2.9 ± 0.0	2.9 ± 0.0
Real electrochemical energy consumption				
pH 11				
[$Wh_{el} L^{-1}urine$]	4.9 ± 0.7	7.6 ± 1.7	8.6 ± 1.9	8.8 ± 2.4
pH 12				
[$Wh_{el} L^{-1}urine$]			14.4 ± 2.5	14.3 ± 2.4

^a volume of crystallizer = 4 L

^b volume of urine = 2 L (urine dilution = 1:1 (50%))

4.4.4 Divalent cation removal

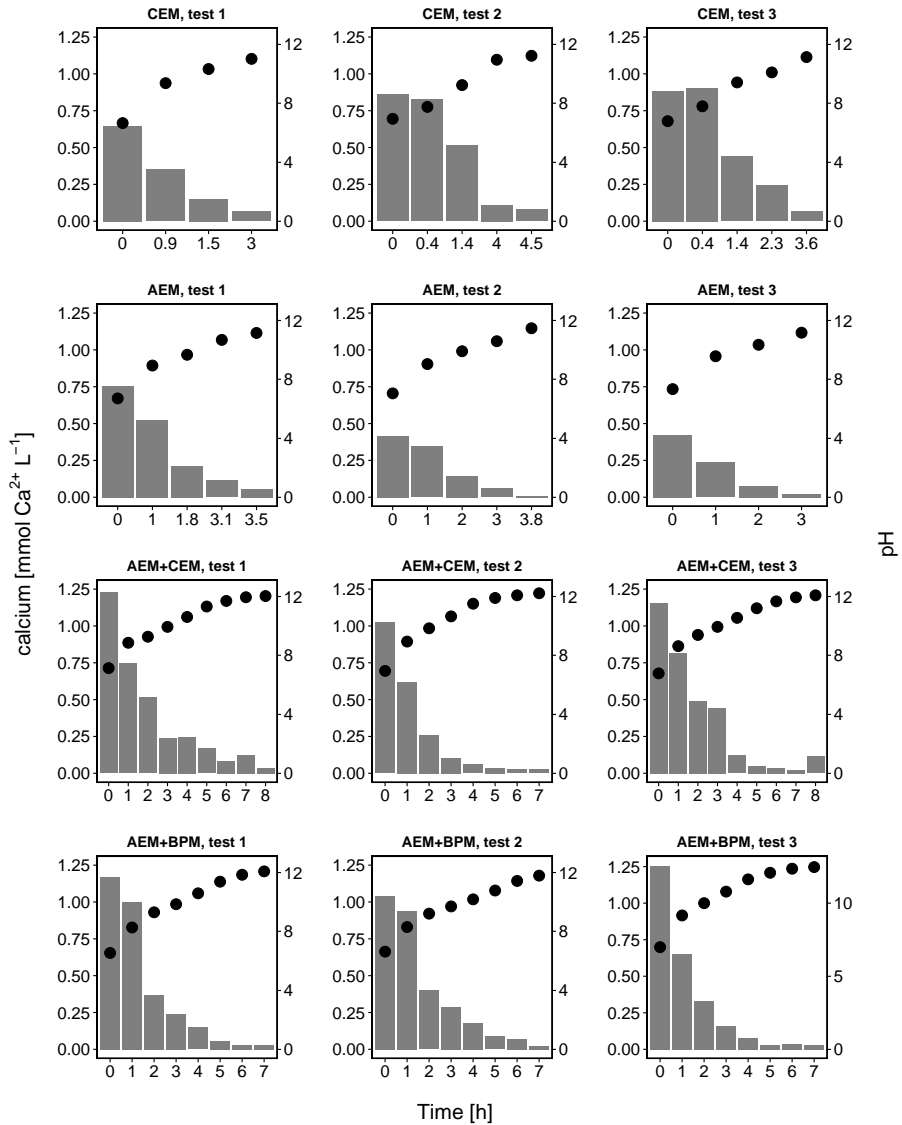


Figure S4.5: **Calcium concentration in the crystallizer.** The black dots display the corresponding pH in the crystallizer (secondary y-axis).

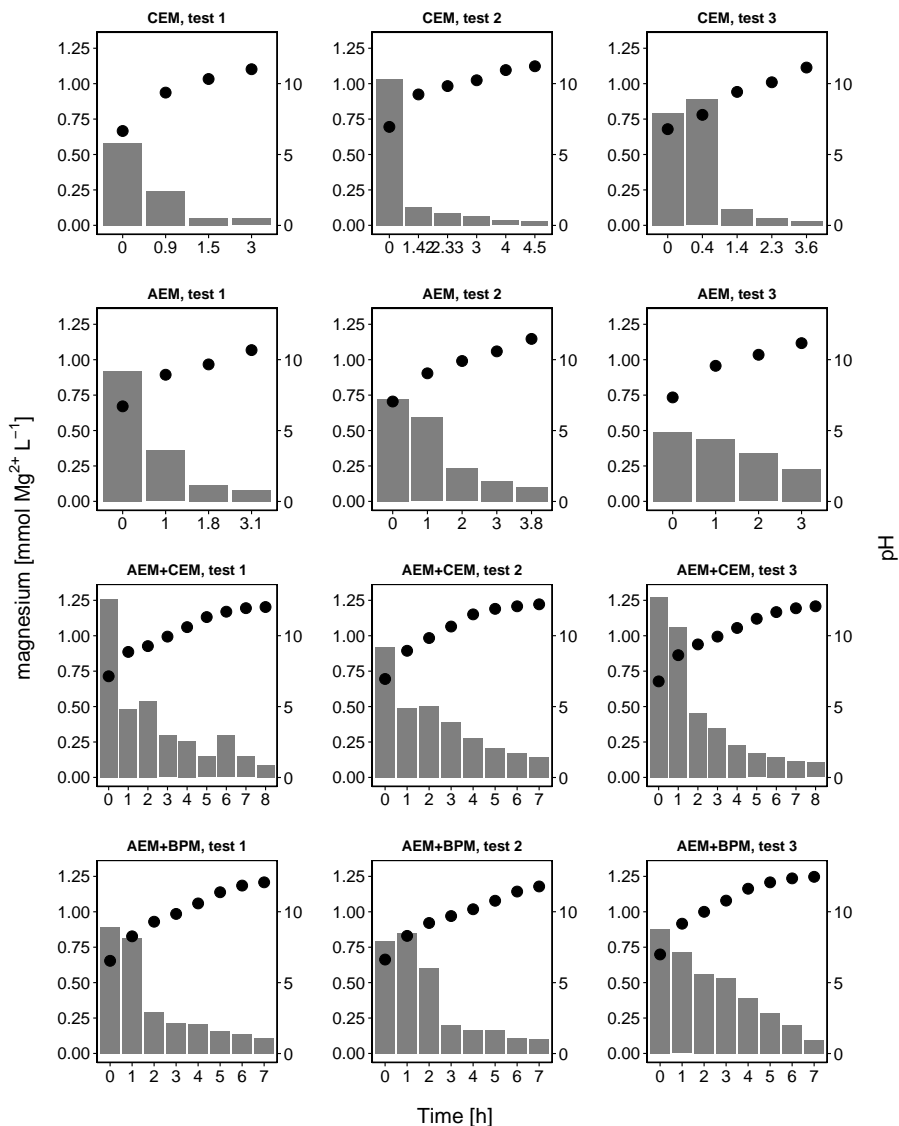


Figure S4.6: **Magnesium concentration in the crystallizer.** The black dots display the corresponding pH in the crystallizer (secondary y-axis).

4.4.5 Long-term stabilization

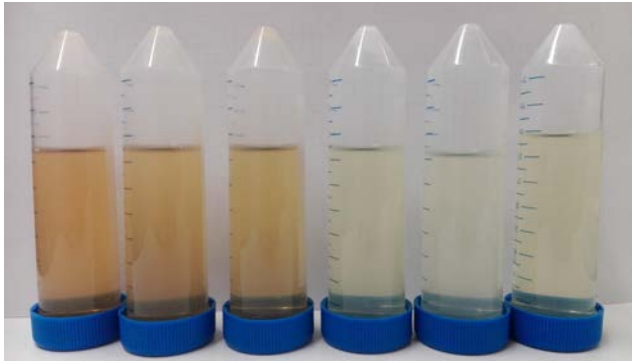


Figure S4.7: Falcon tubes with non-stabilized urine (left) and stabilized urine (right).

Table S4.4: Total nitrogen (TN) concentration and total ammonia nitrogen (TAN)/TN ratio in the effluent of the AEM+CEM tests (pH 12) after 0, 561 (before urease addition), 563 (after urease addition) and 568 days. The test was performed in triplicate ('1', '2' and '3').

	1	2	3
TN [$mmol\ N\ L^{-1}$]	260	147	194
TAN/TN [%] (day 0)	5.3	6.4	4.8
TAN/TN [%] (day 561)	7.8	8.4	7.3
TAN/TN [%] (day 563)	79.5	99.7	92.2
TAN/TN [%] (day 568)	84.6	102.2	100.8

4.4.6 Phosphate removal

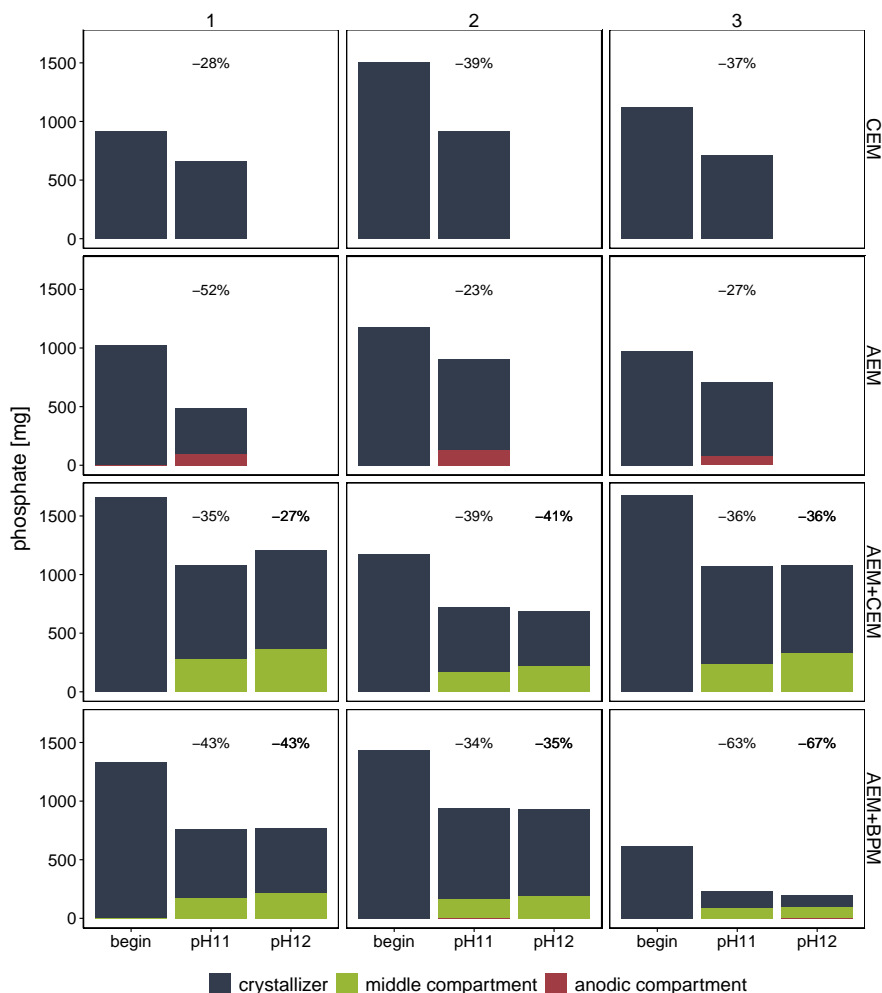


Figure S4.8: **Mass of phosphate in the crystallizer, middle compartment and anodic compartment at the start and end (pH 11 and/or pH 12) of each experiment.** At the start of the experiments, all phosphate was present in the crystallizer. Over the course of the experiment, some phosphate migrated through the AEM to the anodic compartment (AEM configuration) or to the middle compartment (AEM+CEM and AEM+BPM configuration) and some phosphate precipitated in the crystallizer. The percentages represent the decrease in total mass due to precipitation. Each configuration was tested in triplicate ('1', '2' and '3').

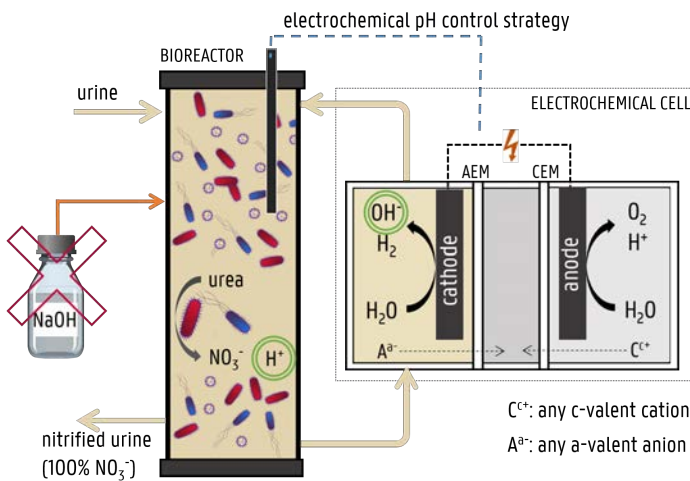
4.5 Acknowledgements

This article has been made possible through the authors' involvement in the MELiSSA project, ESA's life support system research program.

The authors would like to acknowledge:

- i) the MELiSSA foundation to support JDP via the POMP1 (Pool Of MELiSSA PhD) program,
- ii) Tim Lacoere for the help with the graphics,
- iii) Kim De Paepe and Inka Vanwonderghem for critically commenting on the manuscript.

Electrochemical in-situ pH control enables chemical-free full urine nitrification with concomitant nitrate extraction



This chapter has been redrafted after:

De Paepe, J., Clauwaert, P., Gritti, M.C., Ganigué, R., Vlaeminck, S.E., and Rabaey, K. Electrochemical in-situ pH control enables chemical-free full urine nitrification with concomitant nitrate extraction. In preparation

5

Electrochemical in-situ pH control enables chemical-free full urine nitrification with concomitant nitrate extraction

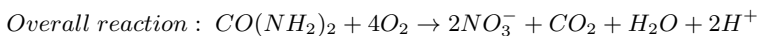
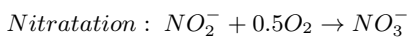
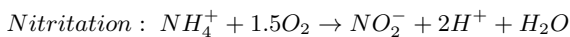
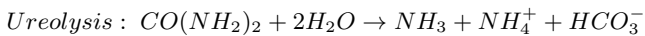
Abstract

Urine presents a valuable nutrient source to reduce the need for unsustainable synthetic fertilizers. Stabilization is, however, required to prevent ammonia volatilization, uncontrolled precipitation and malodor. This was achieved by alkalization and subsequent biological conversion of urea and total ammonia nitrogen (TAN) into nitrate (nitrification) and organics into CO_2 . Yet, without pH control, the extent of nitrification was limited to 60% as a result of insufficient alkalinity. Simply increasing the alkalinity of the influent with NaOH increased the nitrate/TAN ratio in the effluent, but proved difficult to control due to the N variability in urine. Therefore, this study explored the feasibility of an integrated electrochemical cell to obtain on-demand hydroxide production through water reduction at the cathode, compensating for the acidification caused by nitrification, thereby enabling full nitrification. To deal with the inherent variability of the urine influent and bioprocess, the electrochemical cell was steered via a controller, modulating the current based on the pH in the bioreactor. This provided a reliable and innovative alternative to base addition, enabling full nitrification while avoiding the use of chemicals, the logistics associated with base storage and dosing, and the associated increase in salinity. Moreover, the electrochemical cell could be used as in-situ extraction and concentration technology, yielding an acidic concentrated nitrate-rich stream. The make-up of the end product could be tailored by tweaking the process configuration, offering versatility for applications on Earth and in space.

5.1 Introduction

Human urine is a widely available, relatively concentrated source of nitrogen and phosphorus, two essential nutrients in agriculture. Urine source separation at the toilet/urinal allows urine to be collected separately and used as a nutrient resource [186]. The use of urine as a fertilizer or as a raw material for fertilizer production is, however, impeded by the difficulty of collecting the urine and keeping it stable. Urea, the main nitrogen compound in urine, easily and rapidly hydrolyses due to microbial activity, thereby releasing volatile ammonia, which can be harmful for humans (negative impact on respiratory tract [212]) and the environment (e.g., toxic, and causing eutrophication and acidification) [292, 294]. This leads to nitrogen and phosphorus loss (consequently lowering the recovery potential), malodor and uncontrolled precipitation of calcium and magnesium salts [65, 294]. The biofouling potential, caused by the presence of organics in urine which fuel microbial growth, further challenges urine treatment and reuse.

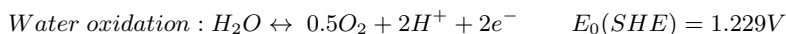
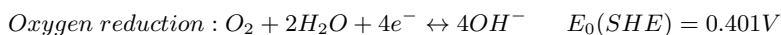
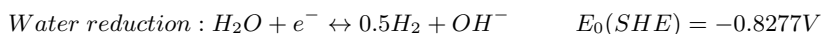
Urea hydrolysis can be inhibited by increasing the pH, as demonstrated by Randall et al. (2016) [240] Senecal et al. (2017) [262] and De Paepe et al. (2020) [65] (Chapter 4). The pH increase furthermore triggers precipitation of calcium and magnesium salts, thereby minimizing the risk for downstream scaling and capturing part of the phosphate in precipitates [65]. Yet, urine is only temporarily stabilized by increasing the pH and still contains urea (which can hydrolyse when the pH is lowered or urease is added [65]) and organics. Treatment in a nitrification-based bioreactor has been reported as a suitable method to biologically stabilize urine [48, 56, 66, 91, 291], yielding a stable nitrate-rich urine solution low in organics. Urine nitrification requires a well-tuned interplay between heterotrophic and autotrophic bacteria. First, urea is hydrolysed to total ammonia nitrogen (TAN, i.e. sum of ammonia-N and ammonium-N) by urease, an enzyme excreted by urease positive (mainly heterotrophic) bacteria (a process commonly referred to as 'ureolysis'). Subsequently, TAN is oxidized by ammonium oxidizing bacteria (AOB) with oxygen into nitrite ('nitritation'), which is further oxidized with oxygen into nitrate by nitrite oxidizing bacteria (NOB) ('nitratation'). Concomitantly, heterotrophic bacteria convert the biologically degradable organics into CO₂.



Due to the release of protons by nitritation (2 mol H⁺ mol⁻¹ N nitrified) and the limited alkalinity in urine, only about half of the TAN in urine can be converted into nitrate, while the remaining TAN is protonated as non-volatile ammonium due to the acidification, yielding a slightly acidic ammonium nitrate solution [97, 291, 295]. Full conversion of

TAN into nitrate can be achieved by hydroxide addition, typically using a base (e.g., NaOH), and is usually preferred because of the higher process stability (optimal pH and no TAN accumulation) and safety (ammonium nitrate is thermally instable and can be misused as an explosive) [56, 66, 295]. On the other hand, it requires supply, storage of and dealing with hazardous chemicals. Moreover, the increase in salinity resulting from the cation addition (e.g., sodium originating from the use of NaOH) can negatively affect the fertilizer potential of the nitrified urine, because many plants are sensitive to high salinities (i.e., the ratio of Na^+ per N should be limited) [204, 223].

In order to obtain full nitrification while avoiding base addition and the undesirable associated increase in salinity, the bioreactor content is recirculated over the cathodic compartment of an electrochemical cell in this study. Water and/or oxygen reduction at the cathode produces hydroxide ions, which can compensate for the acidification caused by nitrification. At the anode, water is oxidized, producing an acidic stream.



To deal with the inherent variability of the urine influent and bioprocess, on-demand and automated OH^- production is essential. This can be implemented by controlling the current flow through the electrochemical cell based on the pH in the bioreactor. In-situ electrochemical pH control has already been applied in hydroponic systems [260, 266], in a bioreactor for continuous culture of yeast cells [307], and in fermentation reactors [5], but has, to the best of our knowledge, not yet been used in combination with nitrification.

Nitrified urine can be used as a fertilizer in agriculture (e.g., Aurin, commercial fertilizer produced by VUNA) [27, 97] or as a culture medium for microalgae (e.g., cyanobacteria) [56, 91, 207], but the nutrient concentrations are relatively low compared to synthetic fertilizers. Hence, for terrestrial applications, a concentration step is preferred in order to reduce the storage and transportation volumes [186]. Interestingly, the electrochemical cell can be used as an in-situ extraction and concentration technology, as demonstrated by Andersen et al. (2015) for a fermentation reactor [5]. Besides countering acidogenic fermentation, the electric field in the electrolysis cell drove carboxylate ions over the anion exchange membrane into a clean, concentrated VFA (volatile fatty acids) stream in the latter study [5]. Similarly, in a nitrification reactor, nitrate migration through an anion exchange membrane can yield a clean and concentrated nitrate rich stream.

This study aimed to explore the feasibility of an integrated electrochemical cell to dose hydroxide on-demand in a urine nitrification reactor, and to concentrate/refine the produced nitrate. Alkalinized urine (pH 12, to prevent urea hydrolysis during storage) was fed into a moving bed biofilm reactor (MBBR) which was coupled to an electrochemical cell. Three different configurations were tested at different pH set points and/or concentration factors. Results were compared with an MBBR with a

conventional pH control strategy (i.e., NaOH addition). A third MBBR was operated without pH control, resulting in partial nitrification. This set-up was used to study the effect of an increased influent alkalinity on the effluent TAN/NO₃⁻-N ratio.

5.2 Materials and methods

5.2.1 Experimental setup

Three identical MBBRs (SI Figure S5.1) were used for (i) partial nitrification without pH control (PN), (ii) full nitrification with NaOH addition (FN-NaOH), or (iii) full nitrification with electrochemical hydroxide addition (FN-EC). An MBBR with biofilm carriers was chosen in order to minimize the amount of suspended biomass which could clog the cathodic compartment in the FN-EC setup. Each MBBR consisted of a plastic cylinder with an active volume of 3.2 L, of which 24% was filled with polyvinyl alcohol (PVA) beads (Kuraray Aqua Co, Ltd., Tokyo, Japan), confined in bags made from fine fishnet material and kept in suspension by the aeration and liquid recirculation. The reactor liquid was recirculated from the top to the bottom of the reactor via an external recirculation loop using a peristaltic pump at a flow rate of 18.7 L h⁻¹ (5.8 reactor volumes per hour). The reactors were aerated with humidified air using an aquarium pump (~2-3L d⁻¹, Air pump 400, Eheim, Germany) connected to diffuser stones that were installed at the bottom of the reactor. Influent (~500 mL d⁻¹) was dosed using a peristaltic pump and timer, and effluent (and suspended biomass) left the reactor via an overflow at the top of the reactor. The temperature was not controlled and ranged between 20-24°C.

The partial nitrification reactor without pH control (PN) consisted of the basic MBBR design.

In the full nitrification reactor with NaOH addition (FN-NaOH), a pH probe (Consort, Belgium) was installed in the reactor and was connected to a pH controller (VP-PRO-PH/RX, Verder, Belgium) in order to control the pH at 6.7 or 7.5 by adding 1 or 1.5 M NaOH at the top of the MBBR. This reactor only served as a 'control' to compare the OH⁻ consumption and reactor salinity with the full nitrification reactor with electrochemical hydroxide addition. Therefore, all information regarding the operation and the results of this MBBR are given in SI Section 5.5.3.

An electrochemical cell was installed in the recirculation loop of the MBBR used for full nitrification with electrochemical hydroxide addition (FN-EC). The bioreactor liquid was recirculated over the cathodic compartment of the electrochemical cell and the pH was measured at the outlet. The cell was galvanostatically controlled at a current density of 0-20 A m⁻² (membrane projected surface) depending on the pH using a programmable power supply (Z+ series, TDK lambda, Japan), pH probe (Consort SP10B, Belgium) and control loop programmed in LabVIEW (National Instruments) (SI Section 5.5.1). The pH, current and voltage were recorded every 15 seconds.

The electrochemical cell consisted of three compartments, made from Perspex plates

and frames with an internal volume of 200 mL ($20 \times 5 \times 2 \text{ cm}^3$, anodic and cathodic compartment) or 100 mL ($20 \times 5 \times 1 \text{ cm}^3$, middle compartment). A stainless steel wire mesh ($564 \mu\text{m}$ mesh width, $20 \times 5 \text{ cm}^2$, Solana, Belgium) functioned as a cathode and a dimensionally stable titanium electrode coated with iridium oxide (Magneto Special Anodes, The Netherlands) was used as anode. The cathodic and middle compartment were separated by a monovalent anion exchange membrane (AEM, 100 cm^2 , PC MVA PCA GmbH, Germany), whereas a cation exchange membrane (CEM, 100 cm^2 , Ultrex CMI-7000s, Membranes International Inc., NJ, USA) was installed between the middle compartment and the anodic compartment. Peristaltic pumps were used to recirculate the anolyte and middle compartment solution between the recirculation vessels and electrochemical cell.

In configuration 1 (Figure 5.1A), the effluent of the bioreactor was pumped from the effluent vessel into the recirculation vessel of the middle compartment using a peristaltic pump ($\sim 500 \text{ mL d}^{-1}$). Effluent left the middle compartment recirculation vessel via overpressure. The anodic compartment (initially filled with $0.2 \text{ M KH}_2\text{PO}_4$) was operated in a closed loop (i.e., without influent or effluent).

In configuration 2 (Figure 5.1B), demineralized water ($\sim 100\text{-}225 \text{ mL d}^{-1}$) was fed into the middle compartment recirculation vessel using a peristaltic pump and effluent left the recirculation vessel by overpressure. The anodic compartment (initially filled with $0.1 \text{ M Na}_2\text{SO}_4$) was again operated in a closed loop.

In configuration 3 (Figure 5.1C), the effluent of the bioreactor was pumped from the effluent vessel into the recirculation vessel of the anodic compartment using a peristaltic pump ($\sim 500 \text{ mL d}^{-1}$). The middle compartment was fed with demineralized water (~ 90 or 180 mL d^{-1}). Effluent left the recirculation vessels via overpressure.

5.2.2 Urine collection and alkalization

Fresh male urine was collected using a nonwater urinal with approval from the Ethical committee of Ghent University hospital (registration number B670201731862). Immediately after collection, the urine was diluted with water (33.3% urine-66.6% water) simulating the diluting effect of flush water in urine diverting toilets [316] and the urine was stabilized by increasing the pH to 12 in order to prevent urea hydrolysis during storage. The influent of FN-NaOH was stabilized using 2M NaOH whereas the influent of FN-EC and PN was stabilized with an electrochemical cell according to De Paepe et al. (2020) [65] (SI Section 5.5.1). The influent was stored in large vessels (10-25 L) at room temperature prior to feeding into the MBBRs. The average influent composition is displayed in SI Tables S5.1 (PN), S5.4 (FN-NaOH) and S5.6 (FN-EC).

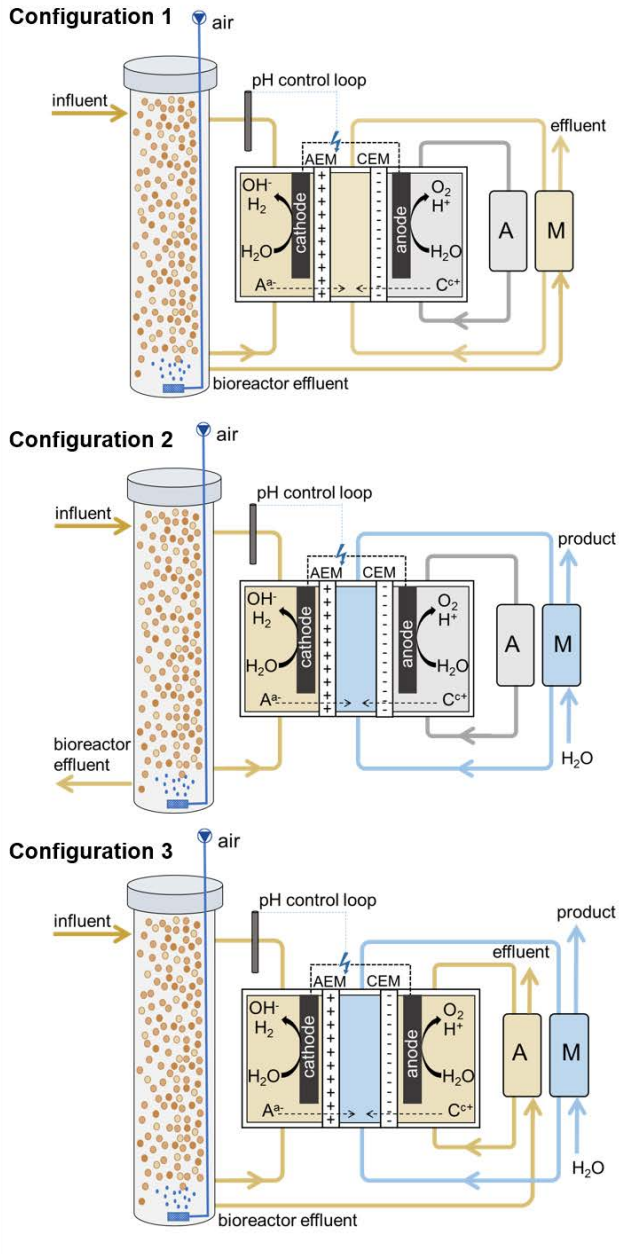


Figure 5.1: Schematic overview of the three configurations of the full nitrification reactor with electrochemical hydroxide addition (FN-EC). Configuration 1: bioreactor effluent is fed into the middle compartment. Configuration 2: demineralized water is fed into the middle compartment. Configuration 3: bioreactor effluent is fed into the anodic compartment and demineralized water is fed into the middle compartment. A: anodic compartment recirculation vessel, M: middle compartment recirculation vessel.

5.2.3 Reactor operation

Reactor inoculation and start-up

PVA beads, previously used for urine nitrification [66], were reactivated in aerated vessels receiving spikes of a buffered ammonium sulfate solution after storage for more than one year at 4°C. Subsequently, the beads were transferred into the MBBRs and an additional 250 mL of nitrifying inoculum (ABIL, Avecom, Belgium) was added (0.19 g VSS L⁻¹ with an activity of 0.4 g TAN g⁻¹ VSS d⁻¹, as indicated by the provider). After inoculation, the MBBRs were operated for 7 days in fed-batch mode (to allow for additional biofilm formation on the beads) and for 33 days in continuous mode on a buffered synthetic ammonium sulfate solution with a stepwise increasing N concentration (50-360 mg N L⁻¹). After 40 days, alkalized urine (1.75 g N L⁻¹) was dosed to the MBBRs and the loading was gradually increased over a period of 30 days by increasing the influent flow rate from 0.2 L d⁻¹ to 0.5 L d⁻¹.

Operation of the partial nitrification reactor without pH control (PN)

After a start-up of 70 days, the target loading rate was reached (corresponds to 'day 1') and MBBR PN was operated for 52 days on electrochemically alkalized urine (at a pH of 11.9 ± 0.2 , containing ~ 29 mmol OH⁻ L⁻¹) (PN-I) (Table 5.1). In order to investigate if the NO₃⁻-N/TAN ratio in the effluent could be increased by feeding more alkaline influent, the MBBR was fed with NaOH-alkalized urine containing 66 mmol NaOH L⁻¹ between day 73 and 126 (PN-III). Prior to PN-III, the bioreactor was conditioned with NaOH-alkalized influent (22 mmol NaOH L⁻¹ to obtain the same influent pH as in PN-I) between day 52 and 73 (PN-II).

Operation of the full nitrification reactor with electrochemical hydroxide addition (FN-EC)

After reaching the target loading rate, the MBBR with electrochemical hydroxide addition was first operated on electrochemically alkalized urine with regular pH control (i.e., NaOH addition) at a pH set point of 7.5 (Table 5.2). On day 13, the electrochemical cell was installed in the recirculation loop of the bioreactor and the reactor was operated in configuration 1 with a pH set point of 7.5 for 43 days and with a pH set point of 6.7 for 27 days. Subsequently, configuration 2 was tested with a pH set point of 7.5 at two different concentration factors: factor 2 ($\sim Q_{in}$ bioreactor/ Q_{in} middle compartment, i.e., influent flow rate to the middle compartment of ~ 225 mL d⁻¹) for 35 days and factor 5 (~ 95 mL d⁻¹) for 23 days. Afterwards, the concentration factor was again decreased to 2 for 26 days before changing to configuration 3. Configuration 3 was also tested with a concentration factor of 2 (between day 168 and day 182) and 5 (between day 182 and day 195).

Table 5.1: **Overview of the different operational phases of the partial nitrification reactor without pH control (PN).** Average influent and effluent compositions are reported in SI Section 5.5.2. HRT: hydraulic residence time

		PN-I	PN-II	PN-III	
				PN-IIIa	PN-IIIb
Influent alkalization method		electrochemical OH ⁻ addition	NaOH addition	NaOH addition	NaOH addition
Hydroxide dosage		~29 mmol OH ⁻ L ⁻¹	22 mmol OH ⁻ L ⁻¹	66 mmol OH ⁻ L ⁻¹ (batch 1+2)	66 mmol OH ⁻ L ⁻¹ (batch 3) ^a
Day		1 - 52	52 - 73	73 - 115	115 - 126
HRT	[d]	7.0 ± 0.3	7.0 ± 0.1	7.0 ± 0.2	6.9 ± 0.3
Duration	[number of HRT]	6.4	3.1	6.1	1.6
Influent flow rate Q_{in}	[L d ⁻¹]	460 ± 17	458 ± 4	457 ± 15	479 ± 8
N load	[mg N d ⁻¹]	807 ± 59	884 ± 54	790 ± 48	331 ± 43
N loading rate ^b	[mg N L ⁻¹ d ⁻¹]	251 ± 18	274 ± 17	245 ± 15	103 ± 13
COD load	[mg COD d ⁻¹]	677 ± 29	1057 ± 28	912 ± 71	426 ± 7
COD loading rate ^b	[mg COD L ⁻¹ d ⁻¹]	210 ± 9	328 ± 9	283 ± 22	132 ± 2

^a Batch 3 is represented separately since this batch was less concentrated which resulted in a substantially lower N and COD load

^b Reactor volume = 3.2 L

Table 5.2: **Overview of the different operational phases of the full nitrification reactor with electrochemical pH control (FN-EC).** Q_{in} =influent flow rate, Q_{out} =effluent flow rate. Average influent and effluent compositions are reported in SI Section 5.5.4.

	NaOH	Configuration 1		Configuration 2			Configuration 3	
			pH 7.5	pH 6.5	Factor 2	Factor 5	Factor 2	Factor 2
Configuration	NaOH control	1	1	2	2	2	3	3
pH set point	7.5	7.5	6.5	7.5	7.5	7.5	7.5	7.5
Concentration factor	1	1	1	2	5	2	2	5
Day	1 - 13	13 - 56	56 - 84	84 - 118	118 - 141	141 - 168	168 - 182	182 - 195
HRT in reactor [d]	6.8 ± 0.2	7.1 ± 0.3	7.1 ± 0.2	6.9 ± 0.3	6.5 ± 0.3	6.8 ± 0.7	7.8 ± 0.7	7.3 ± 0.4
Number of reactor HRT	1.9	6.2	4.1	5.1	3.7	2.6	1.8	1.9
HRT in middle compartment				2.0 ± 0.1	2.6 ± 0.1	2.0 ± 0.3	1.6 ± 0.1	2.5 ± 0.3
Number of HRT in middle compartment				17.2	9.2	17.5	9	5.6
HRT in anodic compartment							1.3 ± 0.1	1.2 ± 0.1
Number of HRT in anodic compartment							11.2	11.8
Q_{in} bioreactor [$L d^{-1}$]	488 ± 21	488 ± 22	495 ± 9	501 ± 22	531 ± 24	493 ± 21	447 ± 741	472 ± 24
Q_{out} bioreactor [$L d^{-1}$]	502 ± 4 ^b	484 ± 21	483 ± 11	489 ± 16	511 ± 20	507 ± 4	401 ± 43	423 ± 9
Q_{in} middle compartment [$L d^{-1}$]				223 ± 16	94 ± 4		180 ± 11	90 ± 5
Q_{out} middle compartment [$L d^{-1}$]				223 ± 9	119 ± 6		200 ± 10	125 ± 16
N load [$mg N d^{-1}$]	791 ± 42	783 ± 87	716 ± 35	773 ± 23	802 ± 28	796 ± 42	748 ± 74	760 ± 47
N loading rate ^a [$mg N L^{-1} d^{-1}$]	247 ± 13	277 ± 25	208 ± 10	224 ± 6.5	233 ± 8	252 ± 13	217 ± 21	220 ± 14
COD [$mg COD d^{-1}$]	697 ± 30	676 ± 44	650 ± 36	679 ± 27	538 ± 188	702 ± 30	810 ± 100	753 ± 42
COD loading rate ^a [$mg COD L^{-1} d^{-1}$]	218 ± 9	196 ± 13	188 ± 10	197 ± 8	156 ± 54	223 ± 9	235 ± 29	218 ± 12

^a Volume of 3.2 L in NaOH control or 3.45 L (volume of MBBR and cathodic compartment) in all other phases

^b Effluent flow rate is higher than influent flow rate due to NaOH addition

Sampling

Samples were taken every 2-3 days, filtered over a 0.22 μm Chromafil® Xtra filter (Macherey-Nagel, PA, USA) and stored in a fridge (4°C) prior to analysis. The bulk liquid dissolved oxygen (DO) concentration and pH were measured during sampling using a luminescent DO probe (LDO10103, Hach, Belgium) connected to a HQ40d meter (Hach, Belgium) and a portable pH meter (C5010, Consort, Belgium).

5.2.4 Analytical methods

Ion chromatography was used to determine the concentration of anions (Metrohm 930 equipped with a Metrosep A supp 5-150/4.0 column and conductivity detector) and cations (Metrohm 761 equipped with a Metrosep C6-250/4.0 column and conductivity detector). The total nitrogen (TN) and COD concentrations were measured with Nanocolor® tube test kits (Nanocolor TN220 and Nanocolor COD160/1500, Macherey-Nagel, PA, USA). The electrical conductivity (EC) was measured using a conductivity meter (Consort C6010 with a Metrohm 6.0912.110 conductivity electrode).

5.3 Results and discussion

5.3.1 Two-step urine stabilization: alkalization and subsequent nitrification

This study aimed to stabilize urine by biological conversion of urea and organics into nitrate, CO₂ and biomass. In order to prevent urea hydrolysis during storage, which could reduce the nutrient content and create odor nuisance and scaling, the pH of the urine was increased to ~12 immediately after collection using a chemical-free electrochemical method developed by De Paepe et al. (2020) (Chapter 4) [65]. Batches of 2-4 L of urine were alkalized with an electrochemical cell, pooled together into large batches of alkalized urine (10-25 L) to average out fluctuations in urine composition in order to provide a stable influent (with a constant composition) to the nitrification bioreactor. The influent batches were stored for up to three months at room temperature. The TAN/TN ratio remained below 5% in the influent of the bioreactor (SI Figures S5.5 and S5.9, Table S5.6), confirming that urea hydrolysis was inhibited by the high pH. Also the COD concentration in the influent did not decrease. Only one batch (used in configuration 2, between day 132 and 136) got contaminated, resulting in a lower influent pH (~9.2) and COD concentration and an increased TAN concentration in the influent (SI Figure S5.9). This batch was replaced after 5 days.

The electrochemical pre-treatment also reduced the scaling potential by precipitation of divalent cations with phosphate and sulfate. Additionally, the salinity of the urine decreased through the migration of anions (mainly chloride) to the middle compartment. Combined, these two processes resulted in a removal of 88 ± 7% of calcium, 91 ± 6% of magnesium, 78 ± 16% of phosphate, 64 ± 14% of chloride and 58 ± 18% of sulfate (SI Figure S5.4).

Yet, urine is only temporarily stabilized by increasing the pH and still contains urea (which can easily hydrolyse when the pH is lowered or urease is added [65]) and organics (which can cause biofouling). Therefore, the urine was further processed in an aerated nitrification bioreactor.

5.3.2 The extent of nitrification (NO₃⁻-N/TAN ratio in the effluent) increases as a function of the influent alkalinity

The extent of nitrification on alkalized urine (pH influent ≥ 11.9) was studied in an MBBR without pH control. In a first phase (PN-I), with an influent pH of 11.9 ± 0.2, about 40% of the nitrogen in the effluent consisted of TAN, whereas ~60% was nitrified to nitrate (Figure 5.2). This NO₃⁻-N/TAN ratio (60:40) is higher than reported in literature (typically ~50:50 [22, 90, 291]), because of the hydroxide addition in the electrochemical pre-treatment (~29 mmol OH⁻ L⁻¹, assuming a coulombic efficiency of 100%). Notably, the observed 60% of nitrification corresponds well with the interpolated value of 62%, calculated by comparing the added OH⁻ equivalents to the OH⁻ demand for full

nitrification, which was estimated based on the TN concentration in the influent (SI Section 5.5.1). At the end of PN-I, after interrupting the influent flow for two days, the nitrate and TAN concentration remained unaffected (SI Figure S5.6), confirming that the extent of nitrification was solely limited by the lack of alkalinity and not by a too slow nitrification rate (i.e., TAN accumulates when the nitrification rate is lower than the N loading rate).

In an attempt to increase the NO_3^- -N/TAN ratio, influent with a higher alkalinity was fed to the reactor in phase PN-III. The influent was alkalized with NaOH instead of an electrochemical cell, in order to define the exact amount of OH^- added to the urine. The latter is difficult to determine in electrochemically alkalized urine, since the coulombic efficiency might drop at high pH (>12) due to hydroxide migration from the cathode to the middle compartment. Prior to PN-III, the bioreactor was conditioned with NaOH-alkalized influent ($22 \text{ mmol OH}^- \text{ L}^{-1}$ to obtain the same influent pH of 11.8 ± 0.3 as in PN-I), resulting in a similar NO_3^- -N/TAN ratio (60:40) as in phase PN-I on electrochemically alkalized urine (Figure 5.2). After increasing the OH^- content of the influent to $66 \text{ mmol OH}^- \text{ L}^{-1}$ (pH of 12.8 ± 0.2), the NO_3^- -N/TAN ratio increased to 73:27 in phase PN-IIIa. In phase PN-IIIb, the NO_3^- -N/TAN ratio further increased to 93:7, because of the lower N concentration in the influent (other batch of urine with only $668 \pm 90 \text{ mg N L}^{-1}$ compared to $1706 \pm 126 \text{ mg N L}^{-1}$ in PN-IIIa) and, hence, a lower OH^- demand. Similar to PN-I, the increased extent of nitrification in response to the increased influent alkalinity throughout operation on NaOH-alkalized urine was in line with the interpolated values (SI Section 5.5.1).

Over the course of 130 days, the partial nitrification reactor was stably operated at a N and COD loading rate of 103 mg N L^{-1} (PN-IIIb) - 250 mg N L^{-1} (PN-I, PN-II, PN-IIIa) and $132 \text{ mg COD L}^{-1}$ (PN-IIIb) - $328 \text{ mg COD L}^{-1}$ (Table 5.1). The pH was low enough to prevent free ammonia inhibition, even with a large fraction of TAN in the reactor liquid (up to 621 mg N L^{-1}). The nitrite concentration stayed below 15 mg N L^{-1} . The TN concentration in the effluent equalled the sum of the TAN and NO_3^- -N concentration in the effluent and corresponded to the TN concentration in the influent, indicating that all urea was hydrolysed and no nitrogen was lost through denitrification or ammonia stripping (Figure 5.2). After switching to NaOH-alkalized urine, the sodium concentration increased threefold, increasing the salinity from $\sim 10 \text{ mS cm}^{-1}$ (PN-I) to $\sim 15 \text{ mS cm}^{-1}$ (PN-III a) (Table S5.2).

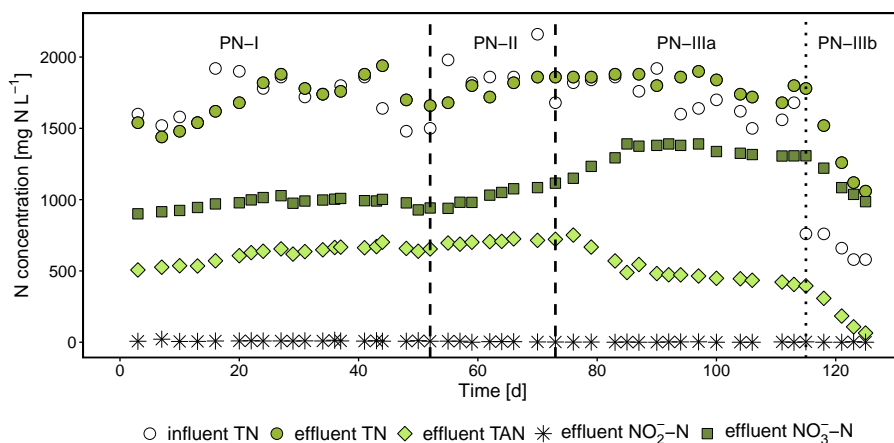


Figure 5.2: **Partial nitrification reactor without pH control (PN): TN (total nitrogen) concentration in the influent and TN, TAN (total ammonia nitrogen), nitrite and nitrate concentration in the effluent.** The influent and effluent composition is given in SI Figure S5.5 and Tables S5.1-S5.2

5.3.3 Electrochemical hydroxide production enables full nitrification by dynamically compensating for the associated acidification

The OH⁻ addition to increase the pH to 12 in the electrochemical pre-treatment (~29 mmol L⁻¹) was not sufficient to obtain fully nitrified urine in the MBBR without pH control (Section 5.3.2, PN-I). Although the NO₃⁻-N/TAN could be steered via the influent alkalinity, it was difficult to control since the OH⁻ demand depends on the N concentration in the urine, which highly fluctuates (Section 5.3.2, PN-IIIb). In order to control the pH in the reactor at a given set point, an electrochemical cell producing hydroxide through water reduction at the cathode was coupled to the MBBR. The current applied by the power supply was controlled based on the pH of the reactor. At a low pH, a relatively high current was applied in order to increase the OH⁻ production and, hence, the pH, whereas a high pH in the bioreactor resulted in a lower applied current. After optimizing the settings (i.e., pH set points and corresponding current, SI Section 5.5.1) during the first 2 weeks (day 13-26), the pH could be controlled in a narrow range (7.6 ± 0.1) between day 26 and 56 (Figure 5.3A), resulting in full nitrification in the MBBR. The TAN and nitrite concentration in the bioreactor remained below 2 mg N L⁻¹ (Figure 5.4A). The nitrate concentration in the effluent equalled the TN concentration in the effluent, indicating that all urea was hydrolysed and nitrified, but was lower than the TN concentration in the influent, due to nitrate migration over the AEM (Section 5.3.4). On average 0.055 ± 0.023 A was applied, supplying 101 mmol OH⁻ L⁻¹ to the reactor (assuming a coulombic efficiency of 100%). Together with the hydroxide added during the electrochemical pre-treatment (~29 mmol OH⁻ L⁻¹), a total of 130 mmol

$\text{OH}^- \text{ L}^{-1}$ was added which was slightly higher than the theoretical OH^- demand for full nitrification (SI Table S5.10).

To investigate whether a lower pH set point would result in a lower current and thus reduce the energy consumption, the MBBR was controlled at a pH of 6.5 ± 0.1 between day 56 and 84. All urea and TAN were converted into nitrate (Figure 5.4A), but the average current (0.056 ± 0.015) was indifferent from the current at a pH set point of 7.5 (Figure 5.3B). Titration curves of the middle compartment effluent (SI Figure S5.11) revealed that only a small increment of 3-5 mmol $\text{OH}^- \text{ L}^{-1}$ was required to increase the pH from 6.5 to 7.5, which is low compared to the total of ~ 130 mmol $\text{OH}^- \text{ L}^{-1}$ added. Hence, lowering the pH set point did not have a significant impact on the energy consumption, but it might affect the nitrification rate. This was observed in the control MBBR with NaOH addition, where the nitrification rate decreased with 35% by changing the set point from 7.5 to 6.7, causing TAN accumulation (since the loading rate was higher than the nitrification rate) (SI Section 5.5.3).

To obtain a concentrated nitrate rich stream in the middle compartment, the configuration was adapted as further outlined in Section 5.3.5 and 5.3.6. Apart from some peaks (e.g., on day 97, 106, 152) caused by malfunctioning of the software control system, the pH was stably controlled at a pH of 7.4, resulting in full nitrification in configuration 2 and 3 (effluent TAN and $\text{NO}_2^- \text{-N} < 10 \text{ mg N L}^{-1}$, except on day 141 after a shift to a more concentrated influent batch) (Figure 5.4A). The OH^- demand for full nitrification was similar to configuration 1 (SI Table S5.10), since the nitrogen loading rate was stable over time (Table 5.2). Because of the higher proton concentration in the middle compartment (due to the concentration obtained by the lower influent flow rate to the middle compartment), more protons diffused through the AEM from the middle compartment to the cathodic compartment in configuration 2 and 3. To compensate for this acidification, more OH^- had to be produced by the electrochemical cell. As a result, a higher current was required to keep the pH at 7.4 compared to configuration 1 (Figure 5.3B). A higher concentration factor (5 instead of 2) in the middle compartment required a higher OH^- production and current (235 mmol $\text{OH}^- \text{ L}^{-1} \sim 0.139 \text{ A}$ in configuration 2, factor 5 instead of 111 mmol $\text{OH}^- \text{ L}^{-1} \sim 0.062 \text{ A}$ in configuration 2, factor 2). Similar findings were obtained in configuration 3, aiming at both anion and cation extraction and concentration.

Throughout the course of 182 days, the voltage fluctuated between 2.8 and 3.5 V, depending on the current (i.e., a higher current resulted in a higher voltage) (SI Figure S5.10). The voltage did not display an increasing trend over time, indicating that no or very limited membrane scaling and fouling occurred. The average energy consumption ranged between 7.9 Wh L^{-1} (without concentration in the middle compartment, configuration 1) and 21.3 Wh L^{-1} (with a concentration factor of 5, configuration 2).

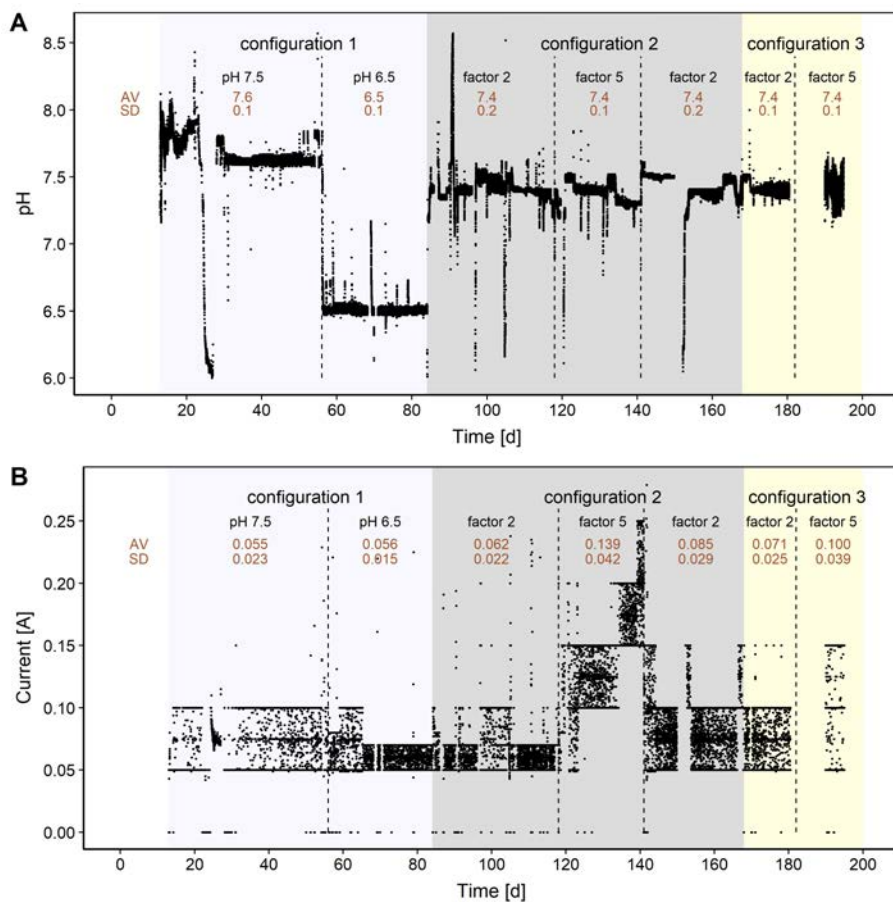


Figure 5.3: Full nitrification reactor with electrochemical hydroxide addition (FN-EC): **A**) pH profile, **B**) current applied by the electrochemical cell. Averages (AV) and standard deviations (SD) for each operational phase are displayed at the top.

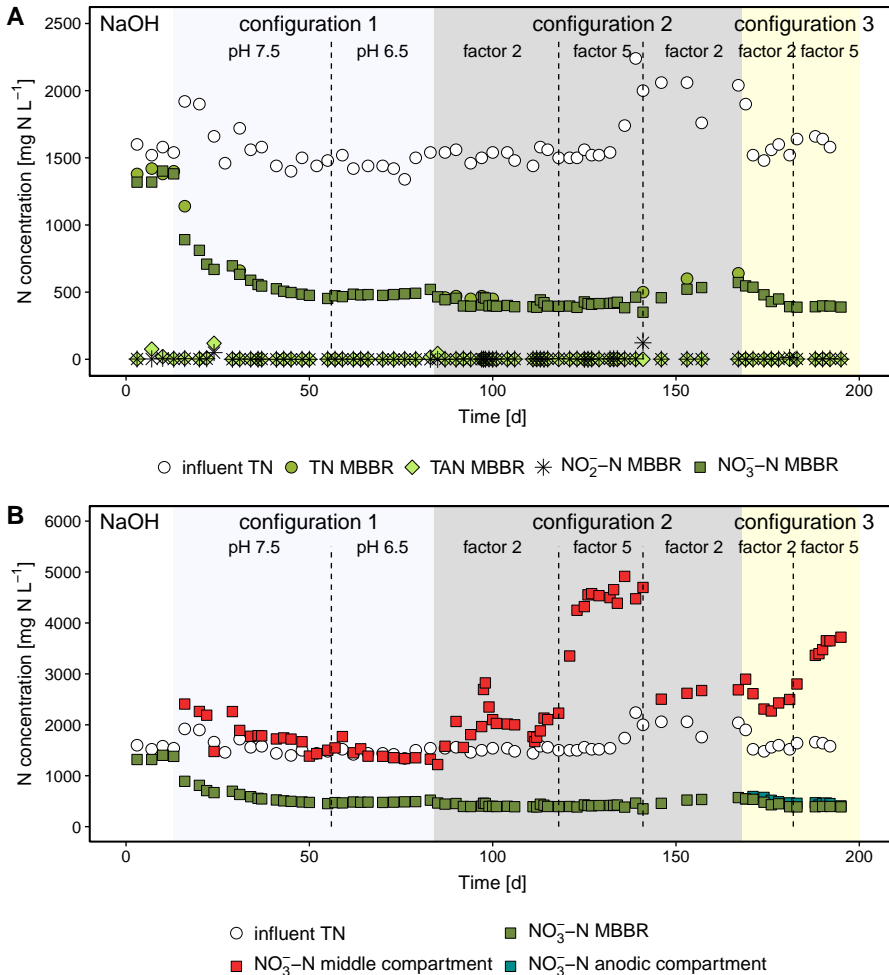


Figure 5.4: **Full nitrification reactor with electrochemical hydroxide addition (FN-EC): A) TN (total nitrogen) concentration in the influent and TN, TAN (total ammonia nitrogen), nitrite and nitrate concentration in the effluent, B) TN concentration in the influent and nitrate concentration in the effluent of the bioreactor, middle compartment and anodic compartment.** The average composition of the influent and effluent of the bioreactor, middle compartment and cathodic compartment are given in SI Tables S5.6-S5.9.

5.3.4 Configuration 1 enables full nitrate recovery

Due to the electron flow driven by the power supply, anions need to migrate from the cathodic compartment through the AEM to the middle compartment to restore the charge balance. Nitrate was the predominant anion in the nitrified urine and accounted for an estimated 68-78% of the migration through the AEM in configuration 1 (SI Section 5.5.3). Chloride accounted for ~9% of the migration, whereas the contribution of sulfate and phosphate was negligible (<1.5%). The remaining 12-22% can likely be attributed to bicarbonate (was not measured) or hydroxide migration, or to some leakage proton diffusion from the middle compartment ($\text{pH} < 2$) to the cathodic compartment. Due to migration, the nitrogen and chloride concentration in the bioreactor were respectively 67-70% and 54-55% lower than the influent concentration, while the concentration of sodium, potassium, phosphate and sulfate did not decrease (Figures 5.4A, 5.5). In order to recover all nitrogen, the effluent from the bioreactor was sent through the middle compartment in configuration 1. The nitrate and chloride concentration in the effluent of the middle compartment corresponded to the TN and chloride concentration in the influent (Figure 5.4B, SI Tables S5.6 and S5.8). Hence, all nitrate and chloride that migrated through the membrane could be captured again in the urine. Evidently, this does not enable creating a concentrate of nitrate.

Likewise, proton production at the anode resulted in cation migration from the anodic compartment to the middle compartment (Figure 5.5). The anolyte initially consisted of 0.2 M KH_2PO_4 , resulting in proton and potassium migration through the CEM. However, after a few days, potassium was depleted in the anolyte, yielding only proton migration. Due to proton migration, the urine was acidified in the middle compartment (effluent $\text{pH} < 1.5$). Assuming that all protons migrated from the anode to the middle compartment, about $100 \text{ mmol H}^+ \text{ L}^{-1}$ was supplied to the middle compartment (based on the current). This was confirmed by means of titrations of the middle compartment effluent, where about 90-115 $\text{mmol OH}^- \text{ L}^{-1}$ was required to increase the pH to 6.5-7.5 (SI Figure S5.11).

The salinity of the effluent of the middle compartment was markedly lower compared to the salinity of the control reactor with NaOH addition (FN-NaOH) (SI Section 5.5.3). This is on the one hand due to the upstream electrochemical stabilization (to pH 12), which reduced the chloride concentration in the influent of FN-EC with more than 60% compared to the NaOH-alkalinized influent used to feed FN-NaOH (Section 5.3.1). On the other hand, sodium addition (originating from the use of NaOH for alkalization and full nitrification) increased the sodium concentration fivefold in FN-NaOH compared to the original concentration in urine (before pH increase), whereas no sodium was dosed to FN-EC.

An additional advantage of the electrochemical pH control is that the nitrifiers in the bioreactor are exposed to an even lower salinity (EC of $\sim 5 \text{ mS cm}^{-1}$), because of anion migration to the middle compartment. This is particularly relevant when working with salt-sensitive synthetic communities in high strength urine [48].

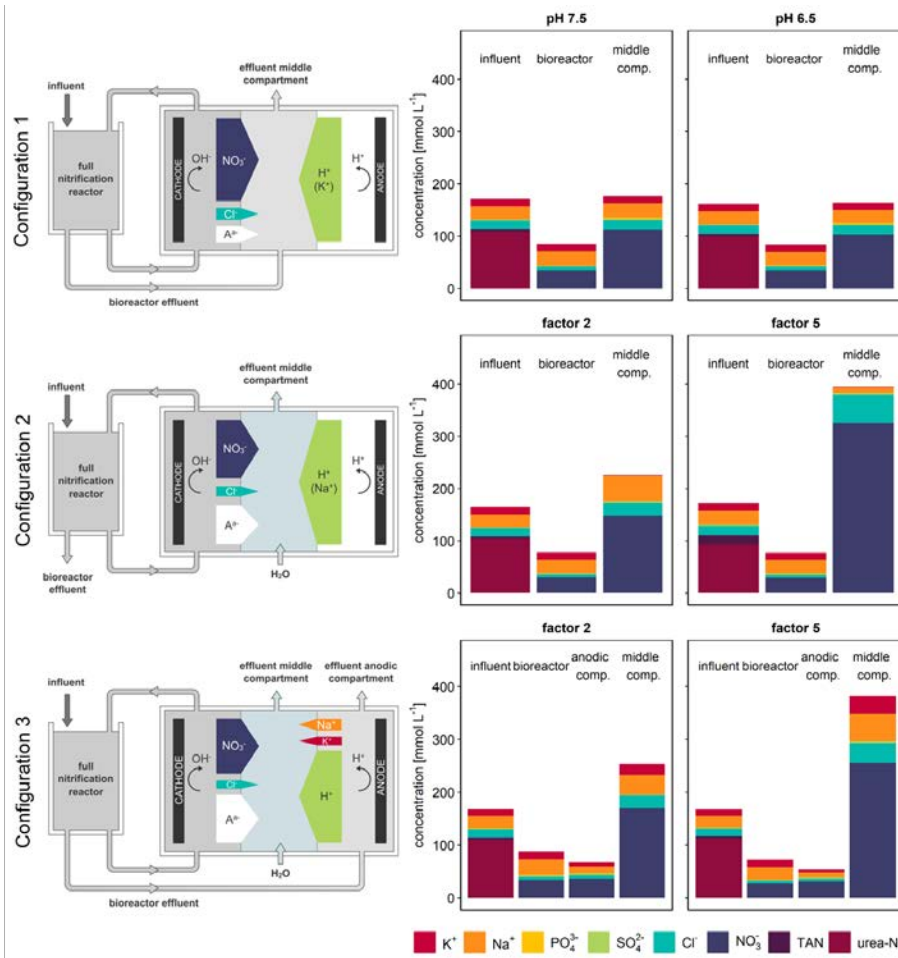


Figure 5.5: Full nitrification reactor with electrochemical hydroxide addition (FN-EC): ion migration through the AEM and CEM and composition of the influent, bioreactor liquid, middle compartment and anodic compartment in configuration 1-3. The size of the arrows represent the relative contribution of each ion to the total migration (estimated based on the electric charge) (calculation in SI Section 5.5.3). (Comp: compartment.)

5.3.5 Configuration 2 enables anion extraction and concentration in the middle compartment

In configuration 2, nitrate was extracted from the urine and concentrated in the middle compartment, which was fed not with nitrified urine but with demineralized water, yielding a purified acidic nitrate-rich side stream (effluent of the middle compartment) and a nitrate-depleted urine stream (effluent of the bioreactor). Similar to configuration 1, nitrate and protons were the predominant migrating ions through the AEM and CEM,

respectively (Figure 5.5). Besides protons, sodium migrated from the anolyte (initially 0.2 M Na_2SO_4) through the CEM at an initially high rate. After all sodium was depleted, the sodium concentration in the middle compartment rapidly decreased, as apparent from the difference between the two tested concentration factors (since the anolyte was not replaced when shifting from factor 2 to 5). Cation migration from the urine to the middle compartment was mostly prevented by the AEM, and also sulfate and phosphate migration was negligible due to their low concentration. Hence, the effluent from the middle compartment mainly consisted of nitrate ($2083 \pm 320 \text{ mg NO}_3^- \cdot \text{N L}^{-1}$ at factor 2 and $4561 \pm 167 \text{ mg NO}_3^- \cdot \text{N L}^{-1}$ at factor 5), chloride ($861 \pm 163 \text{ mg Cl}^- \cdot \text{L}^{-1}$ at factor 2 and $1909 \pm 186 \text{ mg Cl}^- \cdot \text{L}^{-1}$ at factor 5), and sodium (originating from the anolyte) in an aqueous matrix with a pH below 1.2 (Figure 5.5, SI Table S5.8). This is in contrast to configuration 1, where only one effluent stream, derived from the middle compartment, with a composition and matrix similar to the influent was obtained (only urea was converted into nitrate and COD was removed). While most pathogens and micropollutants are retained by the ion exchange membrane [82, 229, 230, 231], these urine originating contaminants can be reintroduced in the effluent of configuration 1 by redirecting the bioreactor content to the middle compartment. This as opposed to configuration 2, where a contaminant-free aqueous end product is obtained, although in depth analysis would be necessary to fully confirm this.

About 30% of the nitrate remained in the urine and was not recovered in the middle compartment. As anion migration restores the charge balance by compensating for the production of negatively charged OH^- ions, the extent of nitrate migration is limited by the OH^- demand, which in turn depends on the N load. Hence, the nitrate recovery could be increased by increasing the OH^- demand in the bioreactor. The latter could be achieved by eliminating the electrochemical pre-treatment (which provided 11-22% of the OH^- , SI Table S5.10). However, given the discontinuous nature of urine supplies, the high variability in composition and the fact that nitrifiers are very susceptible to peak loadings, storage in an equalization tank is important in order to provide a constant influent flow and loading to the bioreactor. Eliminating or minimizing the OH^- addition in the electrochemical pre-treatment would result in a $\text{pH} < 12$, thereby increasing the risk for urea hydrolysis during storage. In Chapter 4 [65], increasing the pH to 11 was insufficient to prevent urea hydrolysis for longer than one week. Moreover, no or less chloride would be removed by the electrochemical pre-treatment, increasing the competition between nitrate and chloride for migration in the electrochemical cell in the recirculation loop of the bioreactor. Alternatively, the OH^- demand could be increased by redirecting a part of the anolyte to the bioreactor. This would result in an acidification of the bioreactor, and, a concurrent increase of the OH^- demand, at the expense of a higher energy consumption. A third option to improve the nitrate recovery, is the use of an AEM with a high nitrate to chloride selectivity in order to favor nitrate migration. The chloride/nitrogen ratio in the middle compartment corresponded to the ratio of the influent, indicating that the monovalent AEM used in this study had the same selectivity

for nitrate and chloride. Membranes with a nitrate to chloride selectivity of 2 [86] to 4.68 [144] have been developed.

In addition to extraction, concentration was achieved in the middle compartment by minimizing the influent (water) flow, thereby capturing the nutrients in a smaller volume. In a first phase, with an influent water flow rate of 223 mL d^{-1} (Q_{in} bioreactor/ Q_{in} middle compartment ~ 2), the nitrate concentration was about 1.3 times higher compared to the TN concentration in the influent of the MBBR. By further decreasing the influent water flow rate to $94 \pm 4 \text{ mL d}^{-1}$ (Q_{in} bioreactor/ Q_{in} middle compartment ~ 5), this value increased to 3. As for nitrate, protons were more concentrated at factor 5 (pH of 0.7 ± 0.1 compared to 1.1 ± 0.1 at factor 2) (SI Figure S5.12). The discrepancy between the theoretical concentration factor (~ 2 and ~ 5) and the actual nitrate concentration factor (1.3 and 3) is due to incomplete nitrate recovery (i.e., 30% remained in urine). Osmotic and electro-osmotic water transport became more substantial with an increasing concentration factor because of the increased concentration gradient and ion migration. In case of factor 5, with an influent water flow rate of 94 mL d^{-1} , the effluent flow rate of the middle compartment amounted to 120 mL d^{-1} , corresponding to an influent ratio (Q_{in} bioreactor/ Q_{in} middle compartment) of 6.7 and an effluent ratio (Q_{in} bioreactor/ Q_{out} middle compartment) of only 4.5. This presents limits to the maximum achievable concentration in the middle compartment. Furthermore, the energy consumption increases with the concentration factor. Three times more energy was required for a factor 5 concentration compared to configuration 1 without concentration.

Table 5.3: **Overview of concentration factors and nitrogen recovery in configuration 2 and 3.**

	Configuration 2		Configuration 3	
	Factor 2	Factor 5	Factor 2	Factor 5
Concentration factor				
$\frac{Q_{in} \text{ bioreactor}}{Q_{in} \text{ middle compartment}}$	2.24	5.67	2.48	5.26
$\frac{Q_{in} \text{ bioreactor}}{Q_{out} \text{ middle compartment}}$	2.24	4.47	2.24	3.78
$\frac{[NO_3^- - N] \text{ middle compartment}}{[TN] \text{ influent}}$	1.3	3.0	1.5	2.3
Nitrogen recovery				
$1 - \frac{[NO_3^- - N] \text{ bioreactor}}{[TN] \text{ influent}}$	73	74	70-73	76

5.3.6 Configuration 3 enables anion and cation extraction and concentration in the middle compartment

In configuration 2, all cations, including potassium, were retained in the urine. In order to recover part of the potassium (important plant nutrient), the effluent of the bioreactor was sent through the anodic compartment in configuration 3. As a result, besides protons produced at the anode, also sodium and potassium from the urine migrated through the CEM to the middle compartment, accounting for an estimated 8-11% and 4-6% of the migration, respectively (Figure 5.5, SI Section 5.5.3). This resulted in a recovery of on average 40% of the potassium and 44% of the sodium from urine. Due to the increased competition for migration through the CEM, less protons migrated, resulting in a slightly higher pH in configuration 3 (pH of 1.5 ± 0.1) compared to configuration 2 (pH of 0.7 ± 0.1) (SI Figure S5.13). A lower proton concentration in the middle compartment limited the proton diffusion to the cathode, giving way to a lower current and energy consumption by the electrochemical cell.

Anion migration through the AEM was identical to configuration 2, meaning that $\sim 30\%$ of the nitrate and $\sim 40\%$ of the chloride remained in the urine. As a consequence, by diverting the effluent of the bioreactor to the anodic compartment, chloride entered the anodic compartment, where it could be oxidized to chlorine, and further react to HOCl, a known disinfectant. If this were to diffuse to the bioreactor, it could inactivate or kill the microbial community, hampering nitrification and COD oxidation. The latter was not observed, indicating that configuration 3 is a promising alternative to configuration 2, offering the advantage of both anion and cation recovery. As HOCl decreases the life span of most membranes, a HOCl resistant CEM might be required for long-term operation.

No major differences were observed with respect to the concentration effects. In line with configuration 2, a 5 times concentration factor showed a higher concentration of nitrate, a lower pH in the middle compartment, more osmotic and electro-osmotic water transport, and a higher energy consumption compared to a concentration factor of 2.

5.3.7 COD removal eliminates the risk for downstream biofouling

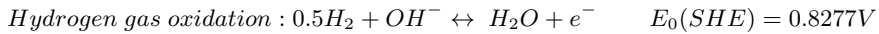
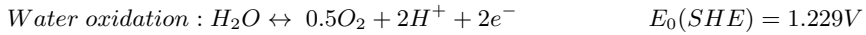
Besides nitrification, COD was converted into CO_2 and biomass by heterotrophic bacteria in the bioreactor. In all reactors, throughout all operational phases, 82-95% of the COD was removed, which is in line with typical COD removal percentages reported in literature by open communities (SI Tables S5.1, S5.2, S5.4, S5.6 and S5.7) [22, 44, 56, 66, 139, 291, 295]. The COD removal percentage was not affected by the pH set point in configuration 1 or by the concentration factor in configuration 2 and 3. Since all rapidly biodegradable COD was removed, the risk for downstream biofouling was likely eliminated.

5.3.8 Application of electrochemical in-situ pH control and extraction

In this study, we showed that coupling of an urine nitrification bioreactor with an electrochemical system can provide a convenient and innovative alternative to base addition, enabling full nitrification while avoiding the use of chemicals (bases), the logistics associated with base storage and dosing, and the associated increase in salinity. Furthermore, the electrochemical cell can flexibly be integrated with the nitrification reactor, and each resulting configuration has its own benefits and application potential. When full nitrogen recovery is sought and further nitrogen concentration/refinery is not important, configuration 1 proved to be the better option. All urine compounds, including macronutrients and trace elements (except organics and the phosphorus, calcium and magnesium precipitated in the alkalization step) are then recovered in the nitrified urine. The urine precipitates could be redissolved in the acidic nitrified urine. In contrast, configurations 2 and 3 each yielded two streams, i.e., a purified concentrated acidic nitrate-rich product stream and a nitrate-depleted treated urine effluent. These configurations result in a lower nitrate recovery but are particularly valuable when interested in a refined and concentrated end product, which facilitates storage and transport. Only a limited number of compounds is recovered in the concentrated stream, which can be an advantage (if only nitrate recovery is targeted) or a disadvantage (since other macronutrients and trace elements are lost). Important in this respect is that configuration 3 allows to recover more compounds, including potassium (an important fertilizer constituent). The concentration factors fall within the same range as those obtained by electrodialysis [66, 229, 233], while the electrode power consumption is higher (25-60 kWh electrical energy or 80-194 kWh primary energy m^{-3} urine compared to 4.4 kWh electrical energy m^{-3} urine [66]). Distillation reaches higher concentration factors but at the expense of a higher energy investment (~ 700 kWh primary energy m^{-3} urine) [295].

Besides hydroxide ions or protons, hydrogen gas (25-62 mmol H_2 d^{-1}) and oxygen gas (12-31 mmol O_2 d^{-1}) were produced by water reduction and water oxidation at the cathode and anode, respectively. Redirecting the oxygen gas to the bioreactor could cover 10-25% of the theoretical oxygen demand for nitrification and COD oxidation (assuming an oxygen demand of 4.33 g O_2 g^{-1} N nitrified and 0.8 g O_2 g^{-1} COD removed). Alternatively, recycling of the cathodically generated hydrogen gas to the anode could shift the anode reaction from water oxidation to hydrogen gas oxidation, thereby decreasing the anode potential and thus the energy consumption by the electrochemical cell, as demonstrated by Kuntke et al. in a TAN recovery electrochemical system [155, 156]. This implies that a gas stream (containing hydrogen gas) is recirculated over the anodic compartment (containing a gas diffusion electrode) instead of a liquid stream (anolyte solution). This is not compatible with configuration 3, since the bioreactor effluent is redirected over the anodic compartment. In configuration 1 and 2 on the contrary, it can be implemented, but requires additional stripping of the

hydrogen gas from the bioreactor liquid at the exit of the cathodic compartment.



Urine treatment and recycling is not only relevant on Earth, but is of major importance in regenerative life support systems (RLSS) as urine is the main resource of water and nutrients. Even when recovery is not envisaged, urine stabilization is essential since ammonia, originating from urea hydrolysis, can pose a hazard to the crew upon volatilization. Currently, on board of the International Space Station, sulfuric/phosphoric acid and toxic chromium trioxide are added to urine in order to inhibit urea hydrolysis [201]. Subsequently, water is recovered from the urine using vapor compression distillation and filtration, while the nutrients are concentrated in a toxic brine [37]. Alternatively, urine could be stabilized by our two-step approach. Immediately after collection, the pH should be increased to 12 in order to prevent urea hydrolysis during storage, which is essential to provide a constant flow and composition (i.e., no peak loading) to the bioreactor, where all urea is nitrified to nitrate. The nitrified urine can be valorized as substrate for plants and microalgae. Nitrification combined with the production of microalgae and plants is being explored in the framework of the Micro-Ecological Life Support System Alternative (MELiSSA), the RLSS programme from the European Space Agency [48, 105]. To take this one step further, this study addressed the issue of payload limitations to space by implementation of electrochemical cells enabling in-situ production of acids and bases, obviating the need for transportation and storage of these hazardous consumables. Configuration 1 is most appropriate for space application as maximum recovery is pivotal while concentration does not present an added value in space. Furthermore, the low salinity and acidity ($\sim 1 \text{ mol H}^+ \text{ mol}^{-1} \text{ NO}_3^- \text{-N}$) of the end product of configuration 1 is compatible with hydroponic plant production, as $0\text{-}1 \text{ mol H}^+ \text{ mol}^{-1} \text{ NO}_3^- \text{-N}$ is required to compensate for the release of OH^- ions ($0\text{-}1 \text{ mol OH}^- \text{ mol}^{-1} \text{ NO}_3^- \text{-N}$) that accompanies nitrate uptake by most plants [24, 88, 266].

5.4 Conclusions

- Urine was stabilized through alkalization and subsequent nitrification. Alkalization (by electrochemical OH^- addition) prevented urea hydrolysis during storage and yielded controlled precipitation of P (70%) with calcium and magnesium ($\sim 90\%$), minimizing the scaling potential during downstream processing and enabling P recovery, if the precipitates can be harvested. Storage in an equalization tank is important to provide a constant influent flow and loading to the bioreactor, in which urea and organics were converted into nitrate, CO_2 and biomass through nitrification and COD oxidation.
- The extent of nitrification (NO_3^- -N/TAN ratio in the effluent) was limited by the alkalinity, but could be increased by dosing alkalinity to the influent. The NO_3^- -N/TAN ratio was, however, difficult to control due to the high variability in N.
- Coupling of an urine nitrification bioreactor with a dynamically controlled electrochemical system can provide a convenient and innovative alternative to base addition, enabling full nitrification while avoiding the use of chemicals (bases), the logistics associated with base storage and dosing, and the associated increase in salinity. Moreover, oxygen production at the anode can provide a part of the oxygen demand for nitrification and COD oxidation.
- The make-up of the end product can be tailored by tweaking the process configuration, offering versatility for application on Earth and in space. Configuration 1 enabled full nitrate recovery by redirecting the bioreactor effluent through the middle compartment. In configuration 2, anions (predominantly nitrate) were extracted and concentrated by migration over the AEM separating the cathodic and middle compartment of the electrochemical cell. Besides anions, cations could be extracted and concentrated in configuration 3 by redirecting the bioreactor effluent over the anodic compartment of the electrochemical cell.

5.5 Supplementary information

5.5.1 Experimental setup and operation

Experimental setup



Figure S5.1: **Experimental setup.**

A: full nitrification reactor with electrochemical hydroxide addition (FN-EC)

B: partial nitrification reactor without pH control (PN)

C: full nitrification reactor with NaOH addition (FN-NaOH)

D: sampling port

E: influent pump (Masterflex L/S, Cole-Parmer, USA)

F: influent bottles

G: pH electrode

H: effluent bottle

I: gas washing bottle (to humidify the air)

J: air pump (Air pump 400, Eheim, Germany)

K: recirculation pump (Watson Marlow 520, USA)

L: electrochemical cell

M: pH electrode

N: control unit

O: digital-control power supply (Z+ series, TDK lambda, Japan)

P: recirculation bottle of the middle compartment

Q: effluent bottle of the middle compartment

R: recirculation bottle of the anodic compartment

S: influent pump of the middle compartment

T: recirculation pump of the anodic compartment



Figure S5.2: **Bags with PVA beads.** Each MBBR was filled with polyvinyl alcohol (PVA) beads (Kuraray Aqua Co, Ltd., Tokyo, Japan), contained in bags made from fine fishnet material and kept in suspension by the aeration and liquid recirculation. The bags prevented the beads from entering the recirculation loop and from clogging/covering the aeration stones.

Control system to adapt the current of the power supply based on the pH in the bioreactor

The electrochemical cell was galvanostatically controlled at a current density between 0 and 20 A m^{-2} depending on the pH at the outlet of the cathodic compartment using a control system programmed in LabVIEW. When the pH was low, a relatively high current was applied in order to increase the pH, whereas a high pH resulted in a lower applied current. As an example (Figure S5.3), in configuration 1, a pH below 7.4 resulted in a current of 0.15 A. When the pH was between 7.4 and 7.6, a current of 0.1 A was applied. A pH between 7.6 and 7.8 resulted in a current of 0.05 A. When the pH was above 7.8, the voltage was fixed at 2 V (no current). This allowed to control the pH relatively stably at ~ 7.5 .

The pH values and corresponding current values were altered for the different configurations and/or operational phases. For instance, configuration 1 was tested at two different pH set points: 7.5 and 6.5. Due to the concentration in the middle compartment in configuration 2 and 3 (and thus a higher proton concentration), a higher current was needed in order to compensate for the increased diffusion of protons towards the cathodic compartment.

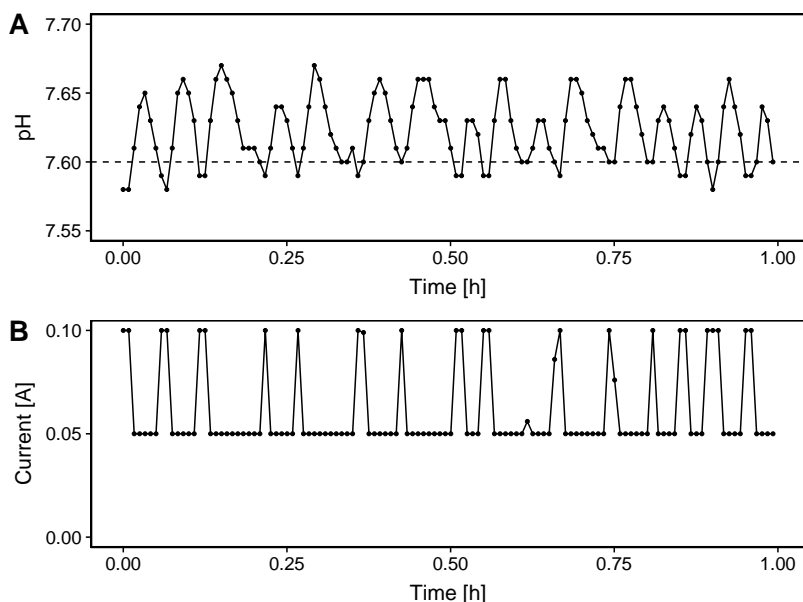


Figure S5.3: **Full nitrification reactor with electrochemical hydroxide addition: pH and current profile over 1 hour (in configuration 1, pH set point of 7.5).** When the pH was between 7.4 and 7.6, a current of 0.1 A was applied. A pH between 7.6 and 7.8 resulted in a current of 0.05 A.

Electrochemical urine stabilization

MBBR PN and MBBR FN-EC were fed with electrochemically alkalized urine (PN: only in phase PN-I). The urine was alkalized with a three chamber electrochemical cell (with AEM+CEM) according to De Paepe et al. (2020) [65]. Briefly, a crystallizer was filled with 2-4L of diluted fresh urine (33%) and the content was continuously recirculated over the cathodic compartment of the electrochemical cell. The electrochemical cell consisted of three compartments, made from Perspex plates and frames, a stainless steel wire mesh ($564\ \mu\text{m}$ mesh width, $20 \times 5\ \text{cm}^2$, Solana, Belgium) as cathode and a dimensionally stable titanium anode coated with iridium oxide (Magneto Special Anodes, The Netherlands). The cathodic compartment was separated from the middle compartment by an anion exchange membrane (AEM, Ultrex AMI-7001, Membranes International Inc., NJ, USA), whereas the middle compartment and the anodic compartment were separated with a cation exchange membrane (CEM, Ultrex CMI-7000s, Membranes International Inc., NJ, USA). The anolyte and middle compartment solution initially consisted of 1L 0.05M or 0.02M Na_2SO_4 , respectively. The cell was galvanostatically controlled at a current density of 100 or $150\ \text{A m}^{-2}$ (membrane projected surface) using a digital-control DC power supply (LABPS3005, Velleman, Belgium). On average, an electric charge of $\sim 2.8\ \text{kC L}^{-1}$ was required to increase the pH to 12. Once

a pH of 12 was reached, the power supply was switched off and the alkaline urine was collected from the crystallizer, filtered over a porous fibre cloth to retain the precipitates, and stored at room temperature in closed vessels. Every ~ 5 batches, the cathodic compartment was rinsed with the acidic middle compartment solution in order to remove scaling on the electrode, spacer and membrane.

Besides temporarily stabilizing the urine prior to nitrification, the electrochemical pre-treatment reduced the scaling potential (by precipitation of divalent cations with phosphate and sulfate) and the salinity of the urine (by migration of anions (mainly chloride) to the middle compartment). On average, $88 \pm 7\%$ of calcium, $91 \pm 6\%$ of magnesium, $78 \pm 16\%$ of phosphate, $64 \pm 14\%$ of chloride and $58 \pm 18\%$ of sulfate were removed from the urine by the electrochemical pre-treatment (Figure S5.4).

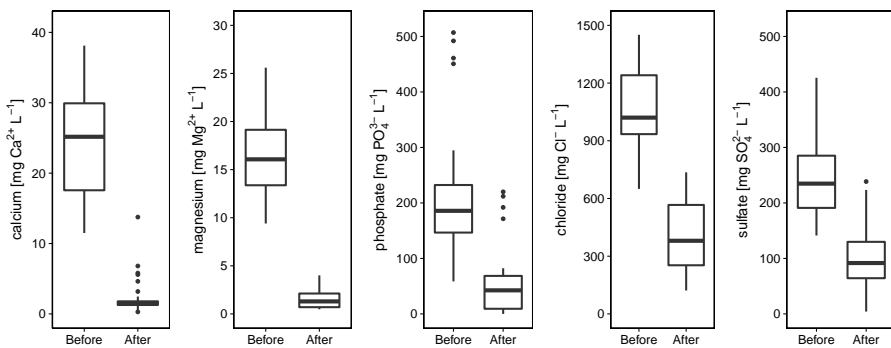


Figure S5.4: **Calcium, magnesium, phosphate, chloride and sulfate concentration in diluted urine (33%) before and after electrochemical pre-treatment ($n = 32$).**

5.5.2 Partial nitrification without pH control (PN)

Influent and effluent composition

Table S5.1: **Influent composition of the partial nitrification reactor without pH control (PN).** TAN: total ammonia nitrogen

	PN-I	PN-II	PN-IIIa	PN-IIIb
Influent alkalization method	electrochemical OH ⁻ addition	NaOH addition	NaOH addition	NaOH addition
Hydroxide dosage	~29 mmol OH ⁻ L ⁻¹	22 mmol OH ⁻ L ⁻¹	66 mmol OH ⁻ L ⁻¹ (batch 1+2)	66 mmol OH ⁻ L ⁻¹ (batch 3) ^a
Number of samples	18	8	15	5
pH	11.9 ± 0.2	11.8 ± 0.3	12.8 ± 0.2	12.6 ± 0.1
EC	[mS cm ⁻¹] 3.9 ± 0.4	7.0 ^b ± 1.1	15.2 ^b ± 0.8	16.1 ^b ± 0.1
Suspended COD	[mg COD L ⁻¹] 1468 ± 43	2151 ± 389	1975 ± 184	882 ± 20
Total nitrogen (TN)	[mg N L ⁻¹] 1710 ± 150	1863 ± 217	1706 ± 126	668 ± 90
TAN	[mg N L ⁻¹] 72 ± 8	69 ± 7	66 ± 5	35 ± 1
Nitrite	[mg N L ⁻¹] 1 ± 1	0 ± 0	1 ± 0	1 ± 0
Nitrate	[mg N L ⁻¹] 3 ± 1	6 ± 1	7 ± 2	8 ± 3
Phosphate	[mg L ⁻¹] 76 ^c ± 31	137 ± 44	188 ± 31	61 ± 23
Sulfate	[mg L ⁻¹] 127 ^c ± 8	255 ± 58	274 ± 25	163 ± 14
Chloride	[mg L ⁻¹] 510 ^c ± 59	1157 ± 264	1125 ± 152	525 ± 47
Sodium	[mg L ⁻¹] 588 ± 42	1125 ^b ± 233	1855 ^b ± 131	1793 ^b ± 25
Potassium	[mg L ⁻¹] 553 ± 18	662 ± 53	665 ± 100	306 ± 54

^a Batch 3 is represented separately since this batch was less concentrated resulting in a substantially lower N and COD loading

^b The EC and Na⁺ concentration in NaOH-stabilized urine is higher compared to the EC and Na⁺ concentration in electrochemically stabilized urine because of the NaOH addition

^c A part of the phosphate, sulfate and chloride in urine was removed by migration in the electrochemical pre-treatment

Table S5.2: Effluent composition of the partial nitrification reactor without pH control (PN). TAN: total ammonia nitrogen

	PN-I	PN-II	PN-IIIa	PN-IIIb
Influent alkalization method	electrochemical OH ⁻ addition	NaOH addition	NaOH addition	NaOH addition
Hydroxide dosage	~29 mmol OH ⁻ L ⁻¹	22 mmol OH ⁻ L ⁻¹	66 mmol OH ⁻ L ⁻¹ (batch 1+2)	66 mmol OH ⁻ L ⁻¹ (batch 3) ^a
Number of samples	18	8	15	5
pH	6.7 ± 0.4	5.8 ± 0.3	5.7 ± 0.1	5.4 ± 0.2
EC	[mS cm ⁻¹]	10.4 ± 1.1	13.1 ± 1.1	15.1 ± 0.5
Suspended COD	[mg COD L ⁻¹]	212 ± 29	246 ± 64	141 ± 7
Total nitrogen (TN)	[mg N L ⁻¹]	1697 ± 152	1790 ± 75	1815 ± 69
TAN	[mg N L ⁻¹]	621 ± 56	707 ± 13	498 ± 99
Nitrite	[mg N L ⁻¹]	9 ± 3	4 ± 3	1 ± 1
Nitrate	[mg N L ⁻¹]	974 ± 36	1032 ± 61	1326 ± 67
Phosphate	[mg L ⁻¹]	106 ± 39	161 ± 21	224 ± 74
Sulfate	[mg L ⁻¹]	203 ± 14	335 ± 66	385 ± 42
Chloride	[mg L ⁻¹]	540 ± 75	1007 ± 178	1173 ± 71
Sodium	[mg L ⁻¹]	598 ± 50	975 ± 158	1867 ± 157
Potassium	[mg L ⁻¹]	542 ± 22	636 ± 20	643 ± 56

^a Batch 3 is represented separately since this batch was less concentrated resulting in a substantially lower N and COD loading

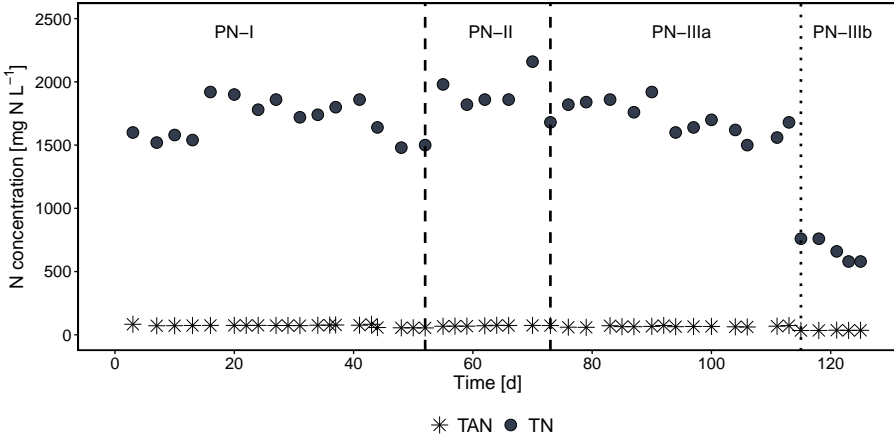


Figure S5.5: **Total nitrogen (TN) and total ammonia nitrogen (TAN) concentration in the influent of the partial nitrification reactor without pH control (PN).** The influent used in PN-I was alkalized with an electrochemical cell, whereas NaOH was used to alkalize the influent in phase PN-II to PN-III.

Nitrification activity test

On day 50-51, the influent flow was stopped to examine if the NO_3^- -N/TAN ratio was limited by a too slow nitrification rate. The TAN and NO_3^- -N concentrations were followed over time (Figure S5.6).

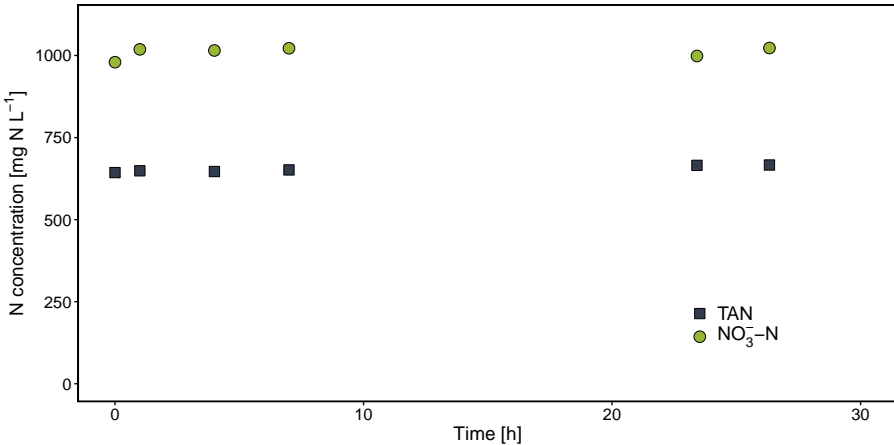


Figure S5.6: **Total ammonia nitrogen (TAN) and nitrate concentration over time during the nitrification activity test.** The influent flow was stopped at time 0.

Extent of nitrification as a function of the influent alkalinity

The combination of urea hydrolysis and nitrification results in a net acidification in a urine nitrification bioreactor ($1 \text{ mol H}^+ \text{ mol}^{-1} \text{ N}$). If all urea is hydrolysed, about 50% of the nitrogen can be nitrified to nitrate (producing $2 \text{ mol H}^+ \text{ mol}^{-1} \text{ N}$ nitrified).

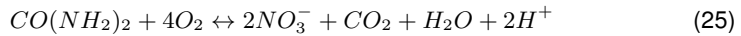


Table S5.3: Estimated hydroxide demand for full nitrification and theoretical extent of nitrification (effluent NO_3^- -N/TN). The hydroxide demand for full nitrification was estimated based on the average total nitrogen (TN) concentration in the influent, assuming that $1 \text{ mol OH}^- \text{ mol}^{-1} \text{ N}$ is required to obtain full nitrification. The theoretical nitrification percentage was estimated by interpolation. For example, in PN-I, an estimated 122 mmol OH^- is required to obtain full nitrification (effluent NO_3^- -N/TN=100). Without any hydroxide addition, an effluent NO_3^- -N/TN of 50% would be obtained. Hence, with 29 mmol $OH^- \text{ L}^{-1}$, the effluent NO_3^- -N/TN is estimated at 62%.

	PN-I	PN-II	PN-III	
			PN-IIIa	PN-IIIb
Average influent TN concentration				
$[mg \text{ N } L^{-1}]$	1710	1863	1706	668
OH^- demand for full nitrification (NO_3^- -N:TAN of 100:0)				
$[mmol \text{ OH}^- \text{ L}^{-1}]$	122	133	122	48
OH^- addition for stabilization				
$[mmol \text{ OH}^- \text{ L}^{-1}]$	29	22	66	66
Theoretical nitrification percentage (effluent NO_3^- -N/TN)				
[%]	62	58	75	>100
Nitrification percentage (effluent NO_3^- -N/TN) obtained in reactor				
[%]	60:40	60:40	73:27	93:7 ^a

^a NO_3^- -N/TN ratio in the sample at the last time point (reactor was not yet in steady-state)

5.5.3 Full nitrification with NaOH addition

Influent and effluent composition

Table S5.4: Nitrogen and COD load, and composition of the influent and effluent of the full nitrification reactor with NaOH addition.

Day		1 - 51
HRT in reactor	[d]	6.1 ± 0.2
Duration	[number of HRT]	8.4
Q_{in}	[L d ⁻¹]	489 ± 15
Q_{out}	[L d ⁻¹]	539 ± 19
N load	[mg N d ⁻¹]	939 ± 162
N loading rate	[mg N L ⁻¹ d ⁻¹]	289 ± 33
COD load	[mg COD d ⁻¹]	948 ± 92
COD loading rate	[mg COD L ⁻¹ d ⁻¹]	292 ± 28
Influent composition		
pH		11.3 ± 0.4
EC	[mS cm ⁻¹]	6.6 ± 0.7
Suspended COD	[mg COD L ⁻¹]	1929 ± 152
Total nitrogen (TN)	[mg N L ⁻¹]	1966 ± 184
Total ammonia nitrogen (TAN)	[mg N L ⁻¹]	73 ± 7
Nitrite	[mg N L ⁻¹]	0 ± 0
Nitrate	[mg N L ⁻¹]	6 ± 1
Phosphate	[mg L ⁻¹]	119 ± 19
Sulfate	[mg L ⁻¹]	302 ± 33
Chloride	[mg L ⁻¹]	1164 ± 130
Sodium	[mg L ⁻¹]	1159 ± 93
Potassium	[mg L ⁻¹]	659 ± 33
Effluent composition		
pH		8 ± 0.5
EC	[mS cm ⁻¹]	15.7 ± 1.6
Suspended COD	[mg COD L ⁻¹]	345 ± 71
Total nitrogen (TN)	[mg N L ⁻¹]	1659 ± 197
Total ammonia nitrogen (TAN)	[mg N L ⁻¹]	56 ± 82
Nitrite	[mg N L ⁻¹]	16 ± 35
Nitrate	[mg N L ⁻¹]	1484 ± 279
Phosphate	[mg L ⁻¹]	134 ± 47
Sulfate	[mg L ⁻¹]	378 ± 88
Chloride	[mg L ⁻¹]	1076 ± 241
Sodium	[mg L ⁻¹]	2960 ± 532
Potassium	[mg L ⁻¹]	6130 ± 113

Nitrification performance

Full nitrification was obtained in the first 51 days at a pH set point of 7.5 and an average N loading rate of $289 \text{ mg N L}^{-1} \text{ d}^{-1}$, apart from some TAN and NO_2^- -N accumulation on day 23 (due to DO limitation caused by clogging of the aeration stones). The nitrate concentration in the effluent equalled the TN concentration in the effluent (indicating that all urea was converted into nitrate) and equalled the TN concentration in the influent (indicating that no nitrogen was lost through denitrification or ammonia stripping) (Figure S5.7). About $20\text{--}25 \text{ mmol OH}^- \text{ L}^{-1}$ was added to increase the pH to 12 before storage and $106 \text{ mmol OH}^- \text{ L}^{-1}$ was added by the pH controller in the bioreactor. The total amount of hydroxide added ($\sim 130 \text{ mmol OH}^- \text{ L}^{-1}$) corresponded well to the estimated hydroxide demand for full nitrification ($138 \text{ mmol OH}^- \text{ L}^{-1}$). After lowering the pH set point to 6.7, TAN and NO_2^- -N started to accumulate. Due to the decreased nitrification activity, the loading was reduced from day 59 onwards. Since the nitrification activity could not be restored (increasing TAN and NO_2^- -N concentrations), the pH set point was again increased to 7.5 on day 100 and the bioreactor was emptied and filled with diluted effluent from the electrochemically controlled full nitrification reactor (decreasing the TAN, NO_2^- -N and NO_3^- -N concentrations). Next, the loading was gradually increased. The TAN and NO_2^- -N concentrations remained below 10 mg N L^{-1} , and the NO_3^- -N concentration coincided with the TN concentration in the effluent. On day 112, the pH set point was again lowered to 6.7 and the loading was gradually increased to $\sim 300 \text{ mg N L}^{-1} \text{ d}^{-1}$. The NO_3^- -N and TN concentration gradually increased and equalled the influent TN concentration at the end.

Nitrification activity test

On day 48-50, before shifting to a lower pH set point, the maximum nitrification rate was determined in a batch experiment. The influent was disconnected and the bioreactor was spiked with 150 mL of urine. The TAN and nitrite concentrations were followed up over time. The nitrification rate was derived from the slope of the TAN concentration as a function of time (between peak and 0 mg N L^{-1}). The same experiment was repeated on day 52, 55 and 57 at a pH set point of 6.5. The nitrification rate at pH 6.5 was significantly lower ($p=0.0121$) compared to pH 7.5. This caused TAN and NO_2^- -N accumulation in the bioreactor after shifting the pH set point, since the nitrogen loading rate was higher than the nitrification rate.

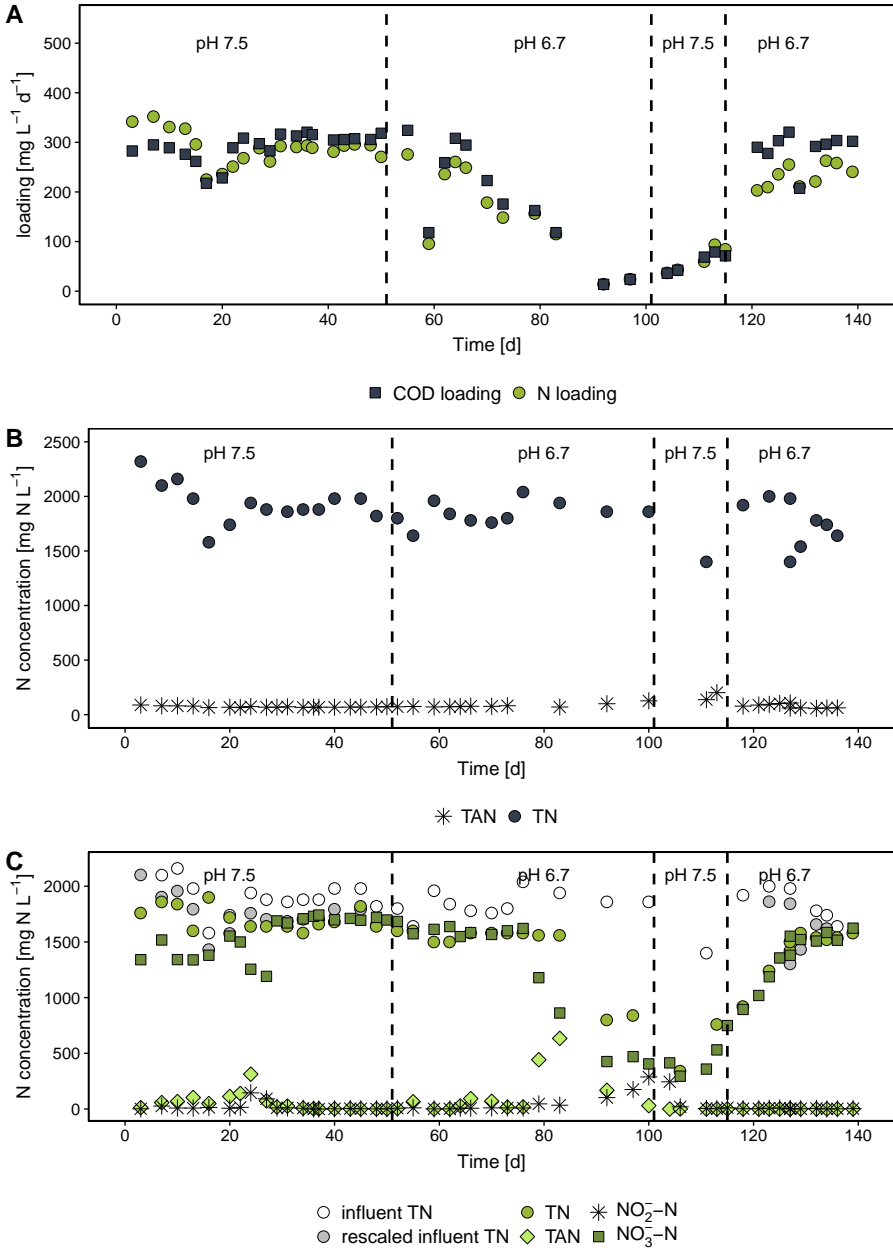


Figure S5.7: **Full nitrification reactor with NaOH addition.** A: Nitrogen and COD loading; B: TN (total nitrogen) and TAN (total ammonia nitrogen) concentration in the influent; C: TN concentration in the influent, rescaled TN concentration in the influent (to account for the difference in influent and effluent flow due to the NaOH addition), TN, TAN, nitrite and nitrate concentration in the effluent.

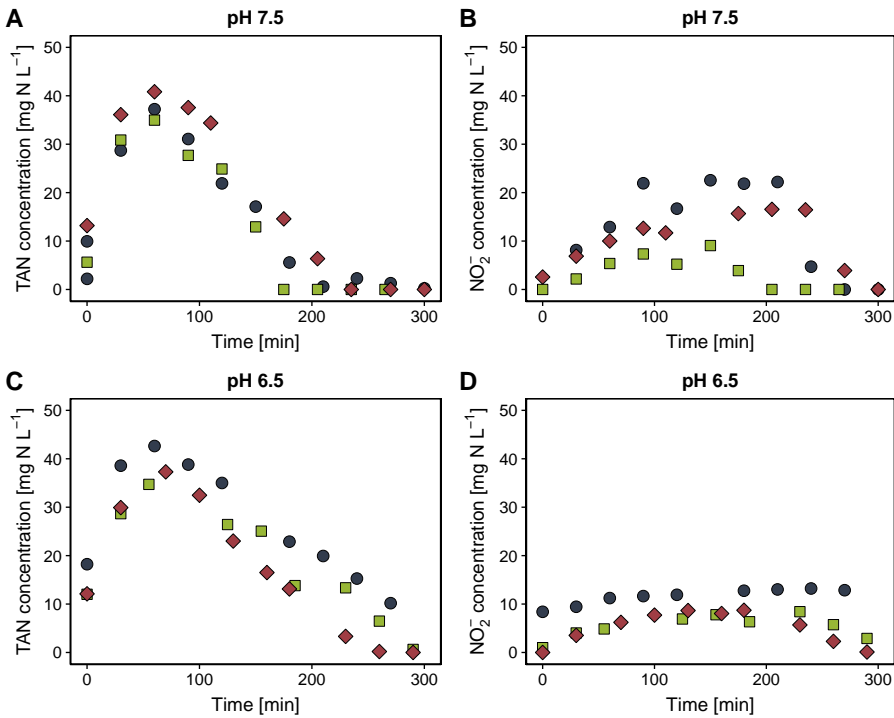


Figure S5.8: **Total ammonia nitrogen (TAN) and nitrite concentration over time.** A spike of urine was given at time 0. During the first 50 minutes, TAN increased because of ureolysis. Subsequently, TAN decreased due to nitrification.

Table S5.5: **Nitrification rate at pH 7.5 and 6.7.** The nitrification rate was derived from the slope of the TAN concentration as a function of time (between peak and 0 mg N L⁻¹).

	pH 7.5		pH 6.7	
	Rate	R ²	Rate	R ²
1	-0.25	0.99	-0.15	1.00
2	-0.29	0.93	-0.14	0.96
3	-0.25	0.99	-0.20	0.99
Average ($n=3$) [mg N L ⁻¹ min ⁻¹]	-0.26		-0.167	
Standard deviation	0.0223		0.0313	

5.5.4 Full nitrification with electrochemical hydroxide addition

Composition of influent, bioreactor effluent, middle compartment effluent and anodic compartment effluent

Table S5.6: Influent composition of the full nitrification reactor with electrochemical hydroxide addition. TN: total nitrogen, TAN: total ammonia nitrogen.

	Configuration 1		Configuration 2			Configuration 3	
	pH 7.5	pH 6.5	Factor 2	Factor 5	Factor 2	Factor 2	Factor 5
Number of samples	17	10	12	10	4	6	4
pH	11.8 ± 0.3	11.1 ± 0.5	11.2 ± 0.5	10.7 ± 1.0	11.9 ± 0.2	11.4 ± 0.1	11.3 ± 0.1
EC	[mS cm ⁻¹] 3.9 ± 0.4	4.3 ± 0.2	4.3 ± 0.1	5.7 ± 2.2	6.6 ± 0.2	4.4 ± 0.6	4.3 ± 0.1
Suspended COD	[mg COD L ⁻¹] 1376 ± 63	1304 ± 78	1345 ± 21	1351 ± 514	1993 ± 284	1697 ± 170	1592 ± 20
TN	[mg N L ⁻¹] 1588 ± 177	1453 ± 65	1520 ± 47	1548 ± 81	1980 ± 147	1597 ± 154	1630 ± 35
TAN	[mg N L ⁻¹] 60 ± 7	60 ± 6	58 ± 3	242 ± 484	64 ± 8	59 ± 6	57 ± 2
Nitrite	[mg N L ⁻¹] 1 ± 1	1 ± 1	0 ± 0	1 ± 1	1 ± 0	1 ± 0	1 ± 0
Nitrate	[mg N L ⁻¹] 4 ± 2	2 ± 1	3 ± 1	2 ± 3	3 ± 0	3 ± 0	2 ± 0
Phosphate	[mg L ⁻¹] 58 ± 25	40 ± 4	47 ± 10	90 ± 44	159 ± 15	69 ± 25	62 ± 3
Sulfate	[mg L ⁻¹] 144 ± 18	132 ± 5	137 ± 16	160 ± 13	210 ± 56	152 ± 13	150 ± 5
Chloride	[mg L ⁻¹] 581 ± 66	586 ± 13	563 ± 49	638 ± 131	828 ± 23	546 ± 59	518 ± 11
Sodium	[mg L ⁻¹] 574 ± 27	573 ± 49	553 ± 9	602 ± 53	799 ± 12	532 ± 94	496 ± 20
Potassium	[mg L ⁻¹] 550 ± 27	563 ± 54	545 ± 7	576 ± 18	672 ± 16	497 ± 79	477 ± 19

Table S5.7: **Composition of the liquid in the full nitrification reactor with electrochemical hydroxide addition.** TN: total nitrogen, TAN: total ammonia nitrogen.

	Configuration 1		Configuration 2		Configuration 3			
	pH 7.5	pH 6.5	Factor 2	Factor 5	Factor 2	Factor 2	Factor 5	
Number of samples	15	10	19	12	4	6	5	
pH	7.6 ± 0.1	6.5 ± 0.3	7.3 ± 0.3	7.6 ± 0.2	7.4 ± 0.1	7.4 ± 0.1	7.1 ± 0.3	
EC	[<i>mS cm⁻¹</i>]	5.3 ± 1.3	4.7 ± 0.2	4.6 ± 0.2	4.9 ± 0.3	6.4 ± 0.5	6.0 ± 0.6	4.9 ± 0.1
Suspended COD	[<i>mg COD L⁻¹</i>]	180 ± 39	122 ± 8	114 ± 13	113 ± 49	110 ± 16	132 ± 18	108 ± 4
TAN	[<i>mg N L⁻¹</i>]	9 ± 30	2 ± 5	3 ± 10	0 ± 1	0 ± 0	0 ± 0	0 ± 0
Nitrite	[<i>mg N L⁻¹</i>]	5 ± 13	0 ± 0	2 ± 1	12 ± 35	1 ± 0	3 ± 5	2 ± 1
Nitrate	[<i>mg N L⁻¹</i>]	603 ± 130	484 ± 15	416 ± 28	409 ± 28	521 ± 47	472 ± 61	392 ± 4
Phosphate	[<i>mg L⁻¹</i>]	51 ± 24	52 ± 3	61 ± 48	57 ± 20	120 ± 15	120 ± 30	50 ± 5
Sulfate	[<i>mg L⁻¹</i>]	118 ± 54	85 ± 14	164 ± 40	199 ± 31	220 ± 17	212 ± 31	160 ± 12
Chloride	[<i>mg L⁻¹</i>]	301 ± 33	263 ± 41	224 ± 33	207 ± 16	265 ± 15	222 ± 27	166 ± 3
Sodium	[<i>mg L⁻¹</i>]	872 ± 293	591 ± 58	579 ± 12	591 ± 23	737 ± 52	678 ± 82	538 ± 17
Potassium	[<i>mg L⁻¹</i>]	562 ± 41	570 ± 60	539 ± 131	550 ± 37	618 ± 45	612 ± 48	548 ± 38

Table S5.8: **Composition of the middle compartment effluent of the full nitrification reactor with electrochemical hydroxide addition.**

TN: total nitrogen, TAN: total ammonia nitrogen.

	Configuration 1		Configuration 2			Configuration 3		
	pH 7.5	pH 6.5	Factor 2	Factor 5	Factor 2	Factor 2	Factor 5	
Number of samples	15	10	19	12	4	6	5	
pH	1.2 ± 0.1	1.3 ± 0.1	1.1 ± 0.1	0.7 ± 0.1	0.9 ± 0.1	0.9 ± 0.1	0.7 ± 0.1	
EC ^b	[<i>mS cm⁻¹</i>]	44.0 ± 3.9	43.4 ± 7.2	59.6 ± 17.6	174.0 ± 8.0	107.0 ± 3.0	80.0 ± 15.0	111.0 ± 10.0
Suspended COD	[<i>mg COD L⁻¹</i>]	142 ± 7	132 ± 15					
TN	[<i>mg N L⁻¹</i>]	1590 ± 77	1530 ± 151					
TAN	[<i>mg N L⁻¹</i>]	0 ± 0	1 ± 1	0 ± 0	0 ± 0	0 ± 0	2 ± 4	0 ± 0
Nitrite	[<i>mg N L⁻¹</i>]	0 ± 0	0 ± 0	0 ± 1	0 ± 1	0 ± 0	0 ± 0	0 ± 0
Nitrate	[<i>mg N L⁻¹</i>]	1575 ± 154	1443 ± 139	2083 ± 320	4561 ± 167	2621 ± 83	2377 ± 105	3579 ± 136
Phosphate	[<i>mg L⁻¹</i>]	287a ± 47	262 ^a ± 60	39 ± 67	2 ± 7	0 ± 0	3 ± 7	0 ± 0
Sulfate	[<i>mg L⁻¹</i>]	175 ± 18	163 ± 18	295 ± 166	348 ± 162	223 ± 29	85 ± 13	259 ± 29
Chloride	[<i>mg L⁻¹</i>]	661 ± 53	621 ± 58	861 ± 163	1909 ± 186	1141 ± 68	868 ± 53	1334 ± 53
Sodium	[<i>mg L⁻¹</i>]	612 ± 31	576 ± 71	1130 ± 435	241 ± 138	323 ± 202	863 ± 22	1201 ± 62
Potassium	[<i>mg L⁻¹</i>]	547 ± 7	555 ± 73	20 ± 27	23 ± 31	5 ± 1	802 ± 18	1340 ± 150

^a High phosphate concentration in the middle compartment effluent is caused by diffusion of phosphate from the anolyte (KH₂PO₄) through the CEM

^b The high EC is caused by the very high specific conductivity of protons

Table S5.9: **Composition of the anodic compartment effluent of the full nitrification reactor with electrochemical hydroxide addition.** TN: total nitrogen, TAN: total ammonia nitrogen.

		Configuration 3	
		Factor 2	Factor 5
Number of samples		4	5
pH		1.6 ± 0.1	1.5 ± 0.1
EC	[<i>mS cm⁻¹</i>]	16.3 ± 1.3	15.4 ± 0.3
TAN	[<i>mg N L⁻¹</i>]	0 ± 0	0 ± 0
Nitrite	[<i>mg N L⁻¹</i>]	0 ± 0	0 ± 0
Nitrate	[<i>mg N L⁻¹</i>]	512 ± 47	441 ± 24
Phosphate	[<i>mg L⁻¹</i>]	96 ± 19	47 ± 2
Sulfate	[<i>mg L⁻¹</i>]	235 ± 21	182 ± 4
Chloride	[<i>mg L⁻¹</i>]	223 ± 15	176 ± 3
Sodium	[<i>mg L⁻¹</i>]	298 ± 29	212 ± 5
Potassium	[<i>mg L⁻¹</i>]	299 ± 14	244 ± 24

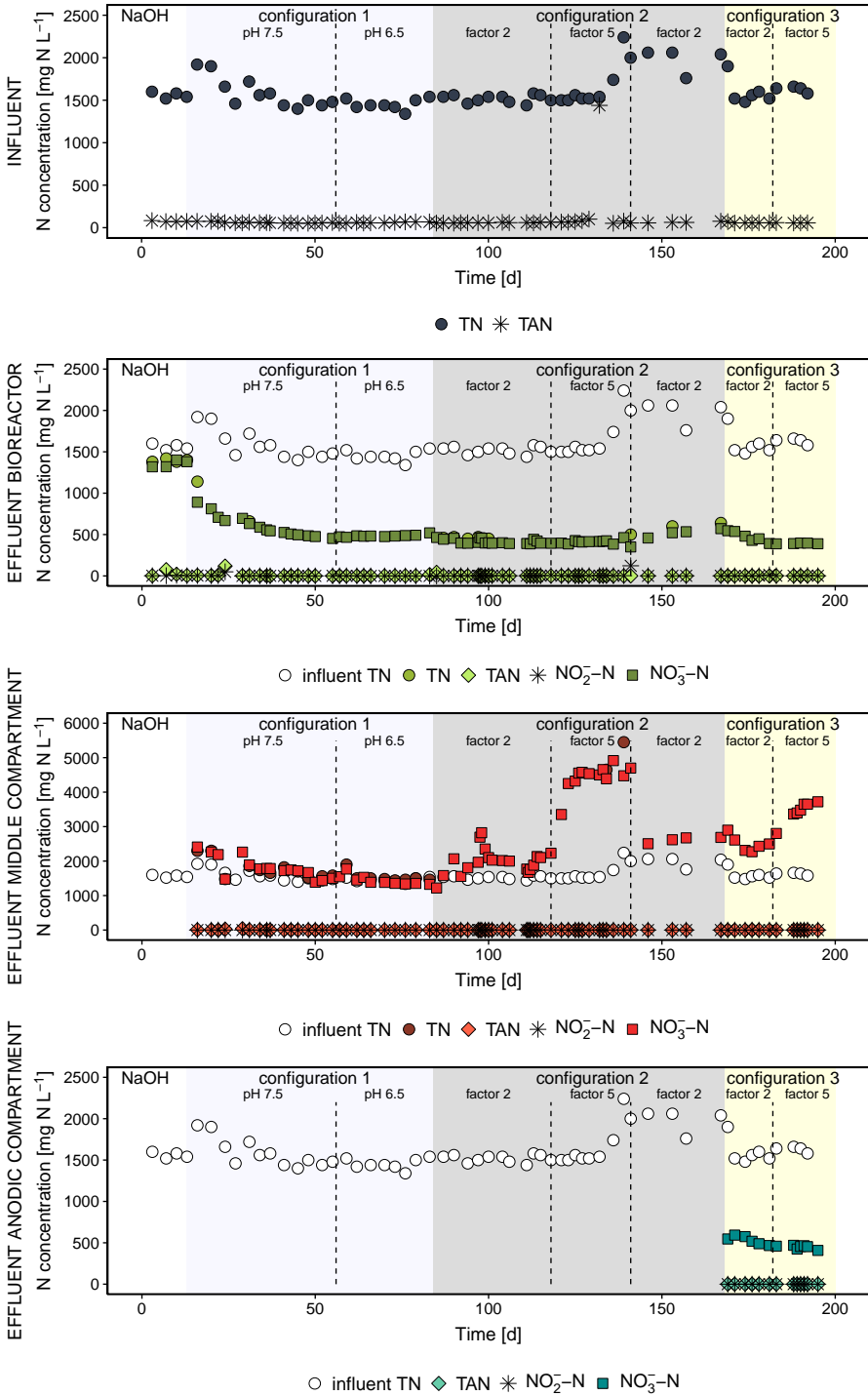


Figure S5.9: Nitrogen species in the influent and effluent of the bioreactor, middle compartment and anodic compartment.

Electrochemical hydroxide production

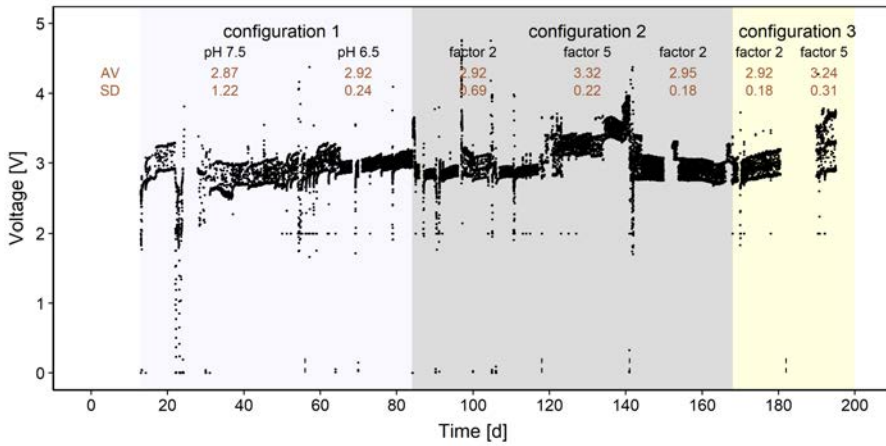


Figure S5.10: **Voltage applied by the electrochemical cell.** Averages (AV) and standard deviations (SD) for each operational phase are displayed.

Table S5.10: **Estimated hydroxide demand for full nitrification and total hydroxide addition.** The hydroxide demand for full nitrification was estimated based on the average total nitrogen (TN) concentration in the influent, assuming that $1 \text{ mol OH}^- \text{ mol}^{-1} \text{ N}$ is required to obtain full nitrification. The hydroxide addition in the pre-treatment and hydroxide addition by the electrochemical cell in the recirculation loop of the bioreactor are estimated based on the current and influent flow (Equation 26).

		Configuration 1		Configuration 2		Configuration 3	
		pH 7.5	pH 6.5	Factor 2	Factor 5	Factor 2	Factor 5
Average influent TN concentration	$[\text{mg N L}^{-1}]$	1588	1453	1520	1548	1597	1630
OH^- demand for full nitrification	$[\text{mmol OH}^- \text{ L}^{-1}]$	113	104	109	111	114	116
OH^- addition in pre-treatment	$[\text{mmol OH}^- \text{ L}^{-1}]$	29	29	29	29	29	29
OH^- addition in bioreactor	$[\text{mmol OH}^- \text{ L}^{-1}]$	101	101	111	234	142	190
Total OH^- addition	$[\text{mmol OH}^- \text{ L}^{-1}]$	130	130	140	263	161	219

$$\text{OH}^- \text{ addition } [\text{mol OH}^- \text{ L}^{-1}] = \frac{I [\text{A}] \times (24 \times 60 \times 60) \left[\frac{\text{s}}{\text{d}} \right]}{96485.3329 \left[\frac{\text{C}}{\text{mol e}^-} \right] \times 1 \frac{\text{mol e}^-}{\text{mol OH}^-} \times Q_{in \text{ bioreactor}} \left[\frac{\text{L}}{\text{d}} \right]} \quad (26)$$

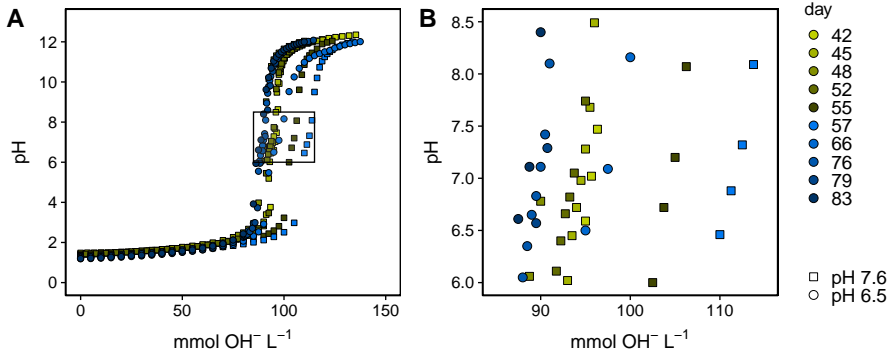


Figure S5.11: Titration curves of the effluent of the middle compartment in configuration 1. About 90-115 $\text{mmol OH}^- \text{L}^{-1}$ was required to bring the pH to 6.5-7.5.

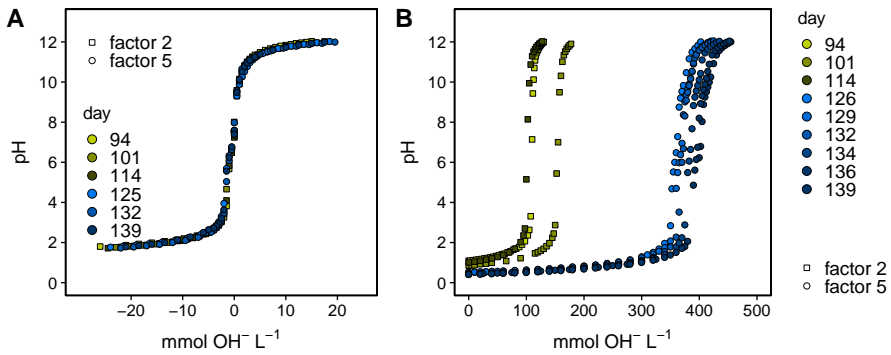


Figure S5.12: Titration curves of the effluent of the bioreactor (A) and middle compartment (B) in configuration 2.

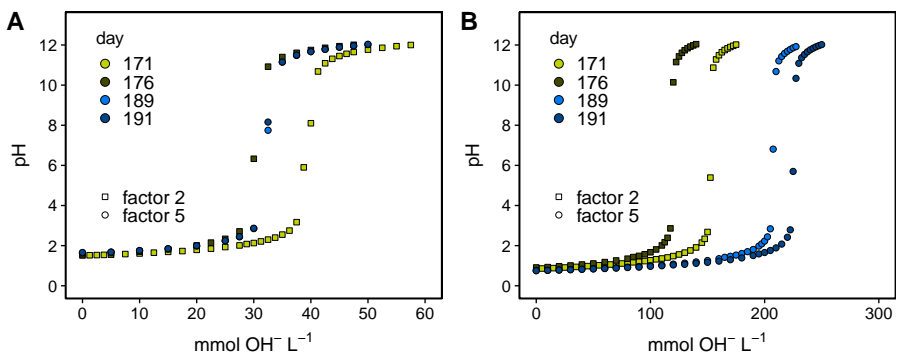


Figure S5.13: Titration curves of the effluent of the anodic compartment (A) and middle compartment (B) in configuration 3.

Electromigration

Calculations

Based on the electric charge that was applied by the electrochemical cell, the amount of electrons that went from the anode to the cathode in one HRT (in the bioreactor) was determined as follows:

$$[mmol e^- \text{ per HRT}] = \frac{HRT [d] \times current [A] \times (24 \times 60 \times 60) \left[\frac{s}{d} \right]}{96485.3 \frac{C}{mol e^-}} \times 10^3 \quad (27)$$

An equal amount of charge should migrate between the compartments to restore the charge balance. For the AEM, the relative contributions of nitrate, chloride, sulfate and phosphate to the total migration were calculated as follows:

$$relative \ contribution \ [%] = 100 \times$$

$$\frac{\left(Q_{influent}^- \left[\frac{mmol}{L} \right] - Q_{bioreactor}^- \left[\frac{mmol}{L} \right] \right) \times V_{MBBR} [L] \times valence \ of \ ion}{amount \ of \ electrons \ [mmol \ e^-]} \quad (28)$$

with

- $Q_{influent}^- \left[\frac{mmol}{L} \right]$ = concentration of anion in influent (for nitrate, the total nitrogen concentration in the influent was used)
- $Q_{bioreactor}^- \left[\frac{mmol}{L} \right]$ = concentration of anion in bioreactor
- $V_{MBBR} [L]$ = volume of the MBBR (+ cathodic compartment)
- valence of ion = -1 for chloride and nitrate, -2 for sulfate and phosphate (HPO_4^{2-} is the dominating speciation at pH 7)
- amount of electrons $[mmol e^-]$ = amount of electrons that were transferred from anode to cathode in one HRT

For the CEM in configuration 3, the relative contributions of sodium, potassium and protons to the total migration were calculated as follows:

$$relative \ contribution \ [%] = 100 \times$$

$$\frac{\left(Q_{bioreactor}^+ \left[\frac{mmol}{L} \right] - Q_{effluent \ anodic \ comp}^+ \left[\frac{mmol}{L} \right] \right) \times V_{MBBR} [L] \times valence \ of \ ion}{amount \ of \ electrons \ [mmol \ e^-]} \quad (29)$$

with

- $Q_{bioreactor}^+ \left[\frac{mmol}{L} \right]$ = concentration of cation in the bioreactor
- $Q_{effluent\ anodic\ comp}^+ \left[\frac{mmol}{L} \right]$ = concentration of cation in the effluent of the anodic compartment
- $V_{MBBR} [L]$ = volume of the MBBR (+ cathodic compartment)
- valence of ion = +1
- amount of electrons $[mmol\ e^-]$ = amount of electrons that were transferred from anode to cathode in one HRT

Table S5.11: **Contribution of nitrate, chloride, phosphate and sulfate to the total electromigration through the AEM.** Q^- includes hydroxide ions, carbonate ions, and protons (diffusing through the AEM).

	Nitrate [%]	Chloride [%]	Sulfate [%]	Phosphate [%]	Q^- [%]
Configuration 1					
pH 7.5	77.8	8.8	1.4	0.1	11.9
pH 6.5	68.3	9.0	1.0	0	22.1
Configuration 2					
Factor 2	71.0	8.6	0	0	20.8
Factor 5	34.7	5.2	0	0.1	60.2
Configuration 3					
Factor 2	55.9	6.4	0	0	37.8
Factor 5	46.6	5.3	0	0	48.1

Table S5.12: **Relative contribution of sodium, potassium and protons to the total electromigration through the CEM.**

	Sodium [%]	Potassium [%]	H^+ (100-Na ⁺ -K ⁺) [%]
Configuration 3			
Factor 2	11.5	5.6	82.9
Factor 5	7.5	4.1	88.4

Salinity

Table S5.13: Nitrogen over sodium ratio and nitrogen over chloride ratio in the influent and effluent.

	N/Na ratio (mol/mol)		N/Cl (mol/mol)			
	Influent	Bioreactor	Influent	Bioreactor		
Partial nitrification reactor without pH control (PN)						
PN-I	4.8	4.7	8.5	8.0		
PN-II	2.7	3.0	4.1	4.5		
PN-IIIa	1.5	1.6	3.8	3.9		
PN-IIIb	0.6	1.0	3.2	4.0		
Full nitrification reactor with NaOH control (FN-NaOH)						
pH 7.6	2.8	0.9	4.3	3.9		
pH 6.7	2.8	0.9	3.9	3.8		
Full nitrification reactor with electrochemical pH control (FN-EC)						
	Influent	Bioreactor	Middle	Influent	Bioreactor	Middle
Configuration 1			comp.			comp.
pH 7.5	4.5	1.1	4.3	6.9	4.6	6.1
pH 6.5	4.2	1.3	4.4	6.3	4.7	6.2
	Influent	Bioreactor	Middle	Influent	Bioreactor	Middle
Configuration 2			comp.			comp.
Factor 2	4.5	1.2	3.0	6.8	4.7	6.2
Factor 5	4.2	1.1	31.1	6.1	5.0	6.0
	Influent	Anodic	Middle	Influent	Anodic	Middle
Configuration 3		comp.	comp.		comp.	comp.
Factor 2	4.9	2.8	4.5	7.4	5.8	6.9
Factor 5	5.4	3.4	4.9	8.0	6.4	6.8

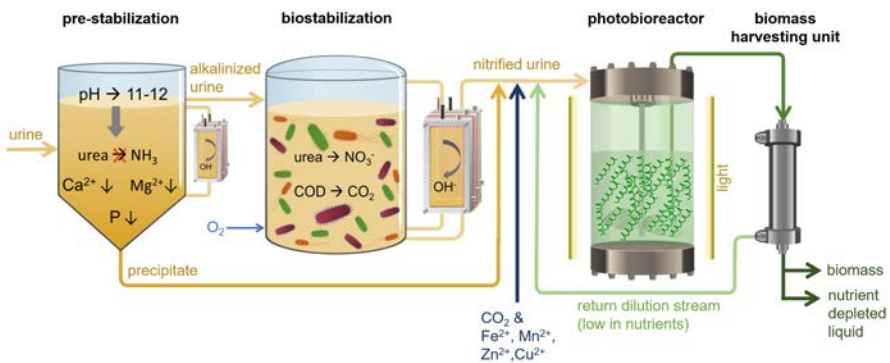
5.6 Acknowledgements

This article has been made possible through the authors' involvement in the MELiSSA project, the life support system research program from the European Space Agency (ESA) (<https://www.melissafoundation.org/>).

The authors would like to acknowledge

- i) the MELiSSA foundation to support JDP via the POMP1 (Pool Of MELiSSA PhD) program,
- ii) the Belgian Science Policy (BELSPO) to support RG via the URINIS-A phase 2 project,
- iii) Mike Taghon and Annick Beyaert for making the Labview control system,
- iv) Avecom for providing the ABIL sludge,
- v) Kim De Paepe for critically reviewing the manuscript.

Limited supplementation maximizes nitrogen recovery from nitrified urine through continuous cultivation of microalgae



This chapter has been redrafted after:

De Paepe, J., Garcia Gragera, D., Arnau Jiminez, C., Rabaey, K., Vlaeminck, S.E., and Gòdia Casablanças, F. Limited supplementation maximizes nitrogen recovery from nitrified urine through continuous cultivation of microalgae. *In preparation*.

NOTE: Some analyses could not yet be performed due to the Covid-19 crisis. Data about the elemental biomass composition (CHNPS) and medium composition (concentrations of Ca^{2+} , Mg^{2+} , Fe^{2+} and trace elements) will be added when available.

6

Limited supplementation maximizes nitrogen recovery from nitrified urine through continuous cultivation of microalgae

Abstract

In recent years, microbial protein has gained great interest as a sustainable alternative to plant and animal protein, especially in combination with treatment and valorization of waste streams. Urine is a widely available source of nutrients, but needs to be stabilized to prevent ammonia volatilization, uncontrolled precipitation and malodor. In this study, nitrified urine (stabilized through alkalization and subsequent nitrification in a bioreactor) served as a culture medium for the edible microalga *Limnospira indica*. Nitrified urine without additional supplements yielded a lower biomass concentration, nitrogen and phosphorus uptake and protein content compared to modified Zarrouk medium, as standard medium, in batch culture. To enhance the nutrient removal efficiency and biomass production, nitrified urine was supplemented with potentially limiting elements. Different mixtures were composed and evaluated in batch culture experiments. Nitrified urine supplemented with limited amounts of phosphorus, calcium, magnesium, iron and EDTA was as effective as modified Zarrouk medium in terms of biomass production, nutrient uptake and protein yield. Urine precipitates formed by alkalization could in principle supply enough phosphorus, calcium and magnesium, requiring only external addition of iron, trace minerals and inorganic carbon. Subsequently, the suitability of supplemented nitrified urine as a culture medium was confirmed in continuous *Limnospira* cultivation in a photobioreactor. This qualifies nitrified urine as a valuable and sustainable microalgae growth medium, thereby opening up novel nutrient loops on Earth and in space, i.e., in regenerative life support systems for human deep-space missions.

6.1 Introduction

Besides optimizing the use of nutrients in agriculture, recovery and recycling of nitrogen and phosphorus from waste streams will be key in the future to catch up with the growing food demand as current synthetic fertilizer production and use is pushing the Earth's life support system to its planetary boundaries or even beyond [79, 80, 249, 270]. Nutrient recovery from waste streams such as wastewater could close and/or shorten the nutrient cycles, thereby reducing the need for energy intensive ammonia production using the Haber-Bosch process and mining of non-renewable phosphorus and potassium [300]. Urine is one of the targeted waste streams, as it presents the major nutrient source in domestic wastewater and has good fertilizing properties (i.e., contains all macro/micronutrients and trace elements required for plant growth) [27, 124, 167, 289, 314]. Urine recycling is also of key interest for the purpose of nutrient and water recovery in regenerative life support systems (RLSS) for deep-space exploration [52, 300].

Besides the use as an alternative fertilizer in agriculture, urine can be valorized as a nutrient source for microbial protein (MP) production [41, 49, 56, 89, 323]. In recent years, MP, i.e., the protein-rich biomass of cultivated microorganisms including fungi (yeasts and others), bacteria and microalgae, has gained a revived interest as a more sustainable alternative to plant and animal protein [226, 300]. In contrast to plants and animals, microorganisms can be highly efficient in their nutrient conversions and can be cultured in fully controlled bioreactors at high volumetric biomass production rates, enabling near full nutrient recycling from a recovered stream with a minimal land or space usage [52, 87, 300]. Depending on the production process and the final quality, in the food production chain, MP may be used as a food ingredient for humans, as a feed ingredient for livestock production, or as an organic fertilizer for plant nutrition [41, 225, 265]. Microalgae are an interesting source of MP and have been cultivated and used as food or feed supplements/ingredients for many years [119, 206, 247, 273]. As photoautotrophic organisms, they use light as an energy source and inorganic carbon (CO_2) as carbon source to produce organic compounds via photosynthesis [119]. Microalgae cultivation is particularly relevant in RLSS, such as MELiSSA, the Micro-Ecological Life Support System Alternative under development by the European Space Agency (ESA) [105, 163]. Besides being a proteinaceous food source for the astronauts, microalgae can be used for cabin atmosphere revitalization as they produce O_2 and consume CO_2 [185, 324]. One of the commercially most widely-produced microalgae is known as '*Spirulina*' [267], which refers to cyanobacteria belonging to the genera *Arthrospira* or *Limnospira* as recently proposed by Nowicka-Krawczyk et al. (2019). These filamentous microalgae are rich in protein (46-71% protein on a dry weight basis), vitamins, minerals (e.g., iron), essential amino acids and fatty acids, photosynthetic pigments (chlorophyll and carotenoids) and antioxidants [17, 69, 119, 143, 206, 210, 216].

Urea is the main nitrogen compound in fresh urine, but rapidly decomposes into TAN (total ammonia nitrogen, i.e., $\text{NH}_3\text{-N}$ and $\text{NH}_4^+\text{-N}$) and (bi)carbonate by enzymatic urea

hydrolysis, causing nutrient losses (through ammonia volatilization and uncontrolled precipitation of phosphorus with divalent cations) and malodor. The high fraction of biodegradable organic compounds furthermore fuels microbial growth in urine [172, 294]. Urine can be stabilized by biological conversion of instable urea and/or volatile ammonia into nitrate and organics into CO₂ in a nitrification bioreactor [56, 66, 291]. To prevent urea hydrolysis during storage prior to biostabilization, alkalization (OH⁻ addition to increase the pH to 12) can be applied immediately after collection [65].

Several studies reported successful batch cultivation of microalgae, including *Arthrospira/Limnospira*, on urine (Supplementary Information (SI), Table S6.1) [41, 56, 89, 90, 91, 284, 285, 335], but reports on continuous reactors producing microalgae on urine are scarce. Most of the studies using fresh or stored urine (with urea/TAN as nitrogen source) as culture medium for *Arthrospira/Limnospira* reported that the biomass was yellow-green, easy to precipitate and had a lower protein content compared to the dark green biomass obtained on standard medium such as (modified) Zarrouk medium containing nitrate as N source [41, 89, 90]. Feng et al. [90, 91] and Coppens et al. (2016) [56] pre-treated urine in a nitrification bioreactor, and obtained a reduced lag phase and higher cell concentration on nitrified urine compared to fresh or stored urine. Although nitrified urine yielded biomass with a similar ash, protein, lipid and chlorophyll content as on (modified) Zarrouk medium [56, 90], a 33% lower dry weight was obtained in batch culture experiments by Coppens et al. (2016), which could possibly be linked to specific (micro)nutrient limitations. Tuantet et al. (2014) [285], for instance, identified phosphorus and magnesium as the limiting elements for continuous *Chlorella sorokiniana* cultivation in urine (with urea/TAN as N source and supplemented with Fe-EDTA and trace elements). Supplementing urine with phosphorus and magnesium increased the biomass productivity and nutrient removal efficiency [285].

As a high resource utilization efficiency is of utmost importance to circularize nutrient management sustainably on Earth, or to reduce the need for resupply in RLSS, the goal of this study was to optimize the growth of *Limnospira indica*, the selected microalga for MELiSSA, on real human urine stabilized by alkalization and nitrification. The growth of *Limnospira* on nitrified urine was compared to the growth on modified Zarrouk medium, a synthetic alkaline saline culture medium commonly used for *Limnospira* cultivation, first described by Zarrouk (1966) [329] and modified by Cogne et al. (2003) [54]. In order to improve the biomass production and nitrogen utilization efficiency, the nitrified urine was supplemented with, amongst others, phosphate, calcium, magnesium, iron and trace elements. Different mixtures were composed and evaluated in batch culture experiments by monitoring the optical density, dry weight, nitrate and phosphate uptake, and protein content of the biomass in order to identify the limiting element(s) in the nitrified urine. Subsequently, continuous cultivation of *Limnospira* on the optimized nitrified urine solution was performed in a photobioreactor for more than 6 hydraulic retention times (HRT).

6.2 Materials and methods

6.2.1 Urine pre-treatment through alkalization and biostabilization

Nitrified urine (Table 6.1) was obtained from the setup described in Chapter 5 (MBBR with electrochemical pH control, configuration 1, pH 7.5). Briefly, immediately after collection, the urine was diluted with water (33% urine - 67% H₂O) to simulate dilutions that would be obtained with flush water and the pH was increased to 12 by means of an electrochemical cell in order to prevent urea hydrolysis during storage. Alkalinization removed ~90% of the calcium and magnesium, and ~78% of phosphate, 58% of sulfate and 64% of chloride by precipitation and/or electromigration. The alkaline urine was fed into a moving bed biofilm reactor (MBBR) for nitrification and COD removal. Hydroxide production at the cathode of a dynamically controlled electrochemical cell compensated for the acidification caused by nitrification, enabling full nitrification. The effluent from the reactor was sent through the middle compartment of the electrochemical cell to capture all nitrate that migrated over the anion exchange membrane separating the cathodic and middle compartment. By redirecting the nitrified urine through the middle compartment, the urine was acidified (pH 1.3) due to proton migration from the anode to the middle compartment. KOH was added to neutralize the nitrified urine prior to medium preparation. Phosphate diffusion from the anolyte to the middle compartment increased the phosphate concentration with a factor ~4.5.

Table 6.1: **Composition of the nitrified urine used in this study (before addition of KOH and supplements).** The urine was diluted (33% urine - 67% water) prior to alkalization and biostabilization.

Nitrified urine		
pH		1.3
EC	[<i>mS cm⁻¹</i>]	42
COD	[<i>mg COD L⁻¹</i>]	188
TN	[<i>mg N L⁻¹</i>]	1840
NO ₃ ⁻ -N	[<i>mg N L⁻¹</i>]	1788
NH ₄ ⁺ -N	[<i>mg N L⁻¹</i>]	10
Cl ⁻	[<i>mg L⁻¹</i>]	767
PO ₄ ³⁻	[<i>mg P L⁻¹</i>]	93
SO ₄ ²⁻	[<i>mg L⁻¹</i>]	271
Na ⁺	[<i>mg L⁻¹</i>]	1066
K ⁺	[<i>mg L⁻¹</i>]	1210
Ca ²⁺	[<i>mg L⁻¹</i>]	13
Mg ²⁺	[<i>mg L⁻¹</i>]	2

6.2.2 Batch culture experiments

Optimization of a nitrified urine-based culture medium

Batch culture experiments (Table 6.2) were performed to optimize the medium composition for the growth of *Limnospira indica*, with the aim to maximize the nitrogen conversion efficiency on nitrified urine. As the nitrogen uptake is limited by the biomass concentration, which is in turn limited by the light availability in the culture flask, the maximum nitrate uptake in the given setup was determined in a preliminary batch experiment with modified Zarrouk medium [54]. Based on the nitrate uptake in this experiment, the initial nitrate concentration was set at $\sim 165 \text{ mg N L}^{-1}$ for the following experiments (except NU 4x). NaHCO_3 (10.5 g L^{-1}) and Na_2CO_3 (7.6 g L^{-1}) were used in all experiments as a carbon source (2.4 g C L^{-1}).

Batch culture set-up

The batch culture experiments were conducted in 1L Erlenmeyer flasks with a vented cap ($0.22 \mu\text{m}$) under axenic conditions. The culture medium was composed of three or four solutions (i.e., i) a urine solution, ii) a phosphate and inorganic carbon solution, iii) a (micro)nutrient solution, iv) a trace elements solution) (Table 6.2), which were autoclaved separately to avoid precipitation, and aseptically added to the Erlenmeyer flasks (total volume of 490 mL) in a laminar flow cabinet. The flasks were inoculated with 5-10 mL of *Limnospira indica* culture originating from an axenic 83 L pilot photobioreactor operated on modified Zarrouk medium (OD_{750} of 2-3) or from the previous batch culture experiment (OD_{750} of ~ 1.2) (resulting initial OD_{750} of ~ 0.05), and incubated for two weeks at 35°C . The incubator (F-4 refrigerated incubator, Ibercex, Spain) was equipped with fluorescent lamps (average light intensity of $40 \mu\text{mol m}^{-2} \text{ s}^{-1}$ in incubator) and magnetic stirrers. Sampling was performed every 2-3 days in a laminar flow cabinet with sterile pipettes. After sampling, the flasks were randomized in the incubator to minimize positional effects on growth. The OD_{750} , pH and electrical conductivity (EC) were measured immediately after sampling. Samples were filtered (Millipore Millex-LG, Philic PTFE $0.2 \mu\text{m}$) prior to nitrate and total inorganic carbon (TIC) analyses. The axenicity was verified by plating immediately after inoculation and at the end of the experiment. The biomass was harvested at the end of the experiment to determine total suspended solids (TSS) and the protein content (after lyophilization).

Table 6.2: **Overview of culture media in the batch culture experiments based on modified Zarrouk medium (ZM) and pre-alkalinized nitrified urine (NU).** ZM: modified Zarrouk medium from Cogne et al. (2003) [54], ZM N_{low} : modified Zarrouk Medium with a lower $NaNO_3$ concentration, NU 1x: nitrified urine with the same N concentration as ZM N_{low} , NU 4x: nitrified urine, four times more concentrated than NU 1x, NU all: nitrified urine (1x) with all supplements, NU+Ca/Mg/P $_{low}$: nitrified urine (1x) supplemented with Ca^{2+} , Mg^{2+} and P (low concentration), NU+Ca/Mg/P: nitrified urine (1x) supplemented with Ca^{2+} , Mg^{2+} and P, NU all – x: nitrified urine (1x) with all supplements except x. (TE: trace elements.) Each culture medium was tested in three or more replicates.

		ZM	ZM N_{low}	NU 1x	NU 4x	NU all	NU + Ca/Mg/P $_{low}$	NU + Ca/Mg/P	NU all – Ca	NU all – Mg	NU all – Fe	NU all – TE
Dilution and neutralization												
Urine %	[%]	0	0	3.1	12.3	3.1	3.1	3.1	3.1	3.1	3.1	3.1
H ₂ O	[mL L ⁻¹]	1000	1000	908	632	908	908	908	908	908	908	908
Nitrified urine	[mL L ⁻¹]			92	368	92	92	92	92	92	92	92
KOH	[g L ⁻¹]			1	3.7	1	1	1	1	1	1	1
Phosphate and inorganic carbon												
P (K ₂ HPO ₄)	[mg P L ⁻¹]	89	89			36	8	36	36	36	36	36
HCO ₃ ⁻ (NaHCO ₃)	[g C L ⁻¹]	1.5	1.5	1.5	1.5	1.5	1.5	1.5	1.5	1.5	1.5	1.5
CO ₃ ²⁻ (Na ₂ CO ₃)	[g C L ⁻¹]	0.9	0.9	0.9	0.9	0.9	0.9	0.9	0.9	0.9	0.9	0.9
Other (micro)nutrients												
N (NaNO ₃)	[mg N L ⁻¹]	412	165									
K ⁺ (K ₂ SO ₄)	[mg K ⁺ L ⁻¹]	224	224									
Na ⁺ (NaCl)	[mg Na ⁺ L ⁻¹]	393	393									
Mg ²⁺ (MgSO ₄ ·7H ₂ O)	[mg Mg ²⁺ L ⁻¹]	7.89	7.89			7.89	7.89	7.89	7.89		7.89	7.89
Ca ²⁺ (CaCl ₂ ·2H ₂ O)	[mg Ca ²⁺ L ⁻¹]	12.19	12.19			12.19	12.19	12.19		12.19	12.19	12.19
Fe ²⁺ (FeSO ₄ ·7H ₂ O)	[mg Fe ²⁺ L ⁻¹]	2.01	2.01			2.01			2.01	2.01		2.01
Na ₂ -EDTA·2H ₂ O	[mg L ⁻¹]	88.5	88.5			88.5			88.5	88.5	88.5	88.5
Trace elements												
Mn ²⁺ (MnCl ₂ ·4H ₂ O)	[mg Mn ²⁺ L ⁻¹]	0.064	0.064			0.064	0.064	0.064	0.064	0.064	0.064	0.064
Zn ²⁺ (ZnSO ₄ ·7H ₂ O)	[mg Zn ²⁺ L ⁻¹]	0.025	0.025			0.025	0.025	0.025	0.025	0.025	0.025	0.025
Cu ²⁺ (CuSO ₄ ·5H ₂ O)	[mg Cu ²⁺ L ⁻¹]	0.0076	0.0076			0.0076	0.0076	0.0076	0.0076	0.0076	0.0076	0.0076

6.2.3 Cultivation in a continuous photobioreactor

Continuous cultivation of *Limnospira indica* on supplemented nitrified urine was evaluated in a bench scale photobioreactor (F1 Laboratory bioreactor, Bionet, Spain). The reactor had a total volume of 5 L, inner diameter of 13 cm and was equipped with a pH probe (EasyFerm Plus, Hamilton, Switzerland), dissolved oxygen (DO) probe (VisiFerm, Hamilton, Switzerland), temperature sensor and Rushton impeller. The temperature was controlled at 36°C with a double-wall water jacket and the pH was controlled at 9.5 by means of base (2M NaOH) and acid (2M H₂SO₄) addition. Antifoam (Y-30) was added manually during sampling. An air flow of 1.01 L min⁻¹, enriched in CO₂ (1%, i.e., 0.01 L min⁻¹) was supplied to the reactor, providing inorganic carbon for the microalgae. The reactor content was gently stirred at 80 rpm. Continuous illumination was provided by a light module consisting of 6 racks, each with 30 LEDs (LUXEON SunPlus 20 Line Cool White, Lumileds, USA), surrounding the bioreactor. The light intensity was increased in a stepwise manner during the batch cultivation from 31 μmol m⁻² s⁻¹ (6.7 W m⁻²) to 923 μmol m⁻² s⁻¹ (198 W m⁻²). After autoclaving, the reactor was inoculated with 200 mL of *Limnospira* culture with an OD₇₅₀ of ~2, resulting in an initial OD₇₅₀ of ~0.2 (active volume of 2 L). After 6/7 days of operation in batch mode (no influent and effluent flow), the active volume was decreased to 1.5 L and autoclaved fresh medium was fed at a flow rate of 0.5 L d⁻¹ (dilution rate of 0.33 d⁻¹). Effluent left the reactor via overpressure and was collected in a sterile bottle with venting filter (Sartorius). The first reactor run was performed with modified Zarrouk Medium (2.5 g NaNO₃ L⁻¹, without NaHCO₃ and Na₂CO₃). Subsequently, the reactor was emptied, cleaned and autoclaved prior to the reactor run on nitrified urine (23% corresponding to ~420 mg N L⁻¹) supplemented with K₂HPO₄ (53 mg P L⁻¹), MgSO₄·7H₂O (7.89 mg Mg²⁺ L⁻¹), CaCl₂·2H₂O (12.19 mg Ca²⁺ L⁻¹), FeSO₄·7H₂O (2.01 mg Fe²⁺ L⁻¹), Na₂-EDTA·2H₂O (88.5 mg L⁻¹) and trace elements (0.064 mg Mn²⁺ L⁻¹, 0.025 mg Zn²⁺ L⁻¹ and 0.0076 mg Cu²⁺ L⁻¹). Both experiments lasted for 3 weeks (i.e., 6 HRT). Samples were taken five times a week and analysed for OD₇₅₀, NO₃⁻, TIC, pH and EC. Axenicity was verified once a week by means of plating. TSS/VSS and the phosphate concentration were determined once a week. At the end of the experiment, the biomass was harvested and lyophilized prior to protein analyses.

6.2.4 Analytical methods

The optical density (OD) was measured at 750 nm with a spectrophotometer (DR6000, Hach, Germany). Anion chromatography (Dionex ICS2000, equipped with AS18 anion-exchange column and ASRS-ULTRA II suppressor, Thermo Fisher Scientific, US) was used to determine the nitrate concentration. The phosphate concentration was determined with phosphate Hach tube test kits (LCK 350, Hach, Germany) and TIC was measured on a TIC/TOC/TN analyzer (Multi N/C, model 2100S/1, analytikjena, Germany). EC was measured by means of a conductivity meter (Cond 8 Basic, XS

Instruments, Italy) and pH measurements were performed with a pH meter (pH 50+ DHS, XS Instruments, Italy). Total suspended solids (TSS) and volatile suspended solids (VSS) were determined by filtering the culture medium over borosilicate glass microfiber filters (GMFC-52047 (1.2 μm), Scharlab, Spain) and subsequent drying at 105°C (Memmert UF75, Germany) and 550°C for at least 2 hours. The biomass was centrifuged (Avanti™ J-20 centrifuge, Beckman), washed, frozen at -80°C for at least 24 hours and lyophilized (VirTis sentry) prior to protein and carbohydrate analyses. Proteins were measured using the Lowry method (with BSA standard). Axenicity was checked by plating (in duplicates) on PDA plates (potato dextrose agar, 30°C, 13 days) for fungi, PCA plates (plates count agar, 37°C, 5 days) for aerobic bacteria and plates with modified Zarrouk medium supplemented with Tryptone Soy Agar (35°C, 13 days) for aerobic bacteria able to grow on modified Zarrouk medium. Prior to operation, photon flux densities were measured on 24 spots distributed homogeneously over the inner wall of the photobioreactor using a Li-Cor 190R Quantum sensor. The reported light intensity was averaged over the reactor surface.

6.3 Results and discussion

6.3.1 Urine dilution is essential to obtain high N conversion efficiencies

As an efficient use of recovered resources is important to circularize nutrient management sustainably on Earth or to reduce the need for resupply in space life support systems, the goal was to achieve high N conversion efficiencies. N is after C the second most important macronutrient and is required for the synthesis of macromolecules including proteins, peptides, enzymes, chlorophyll and nucleic acids (DNA/RNA) [255]. N uptake levels in *Limnospira* cultivation depend on the biomass concentration, which is limited by the light availability. Dense microalgae cultures are known to 'self-limit' their growth because of self-shading.

The maximum N uptake in the given batch culture set-up (Erlenmeyer flasks in incubator) was determined in a preliminary experiment with modified Zarrouk medium. The maximum OD₇₅₀ (1.2) was reached after two weeks (SI Figure S6.2). Afterwards, the OD₇₅₀ decreased and the colour of the culture changed from dark green to yellowish green, indicating decay. The nitrate concentration in the culture medium slowly decreased and stabilized when the maximum OD₇₅₀ was reached (SI Figure S6.2). Only 110-120 mg N L⁻¹ (corresponding to 22-27% of the initial N concentration) was removed from the culture medium. Based on these results, it was decided to lower the initial nitrate concentration to ~165 mg N L⁻¹ for the following experiments to enable higher N conversion efficiencies, while still avoiding N limitation by providing ~50 mg N L⁻¹ in excess. N deficiencies can result in an increased lipid and a reduced protein content [89]. To obtain this concentration of 165 mg N L⁻¹, the nitrified urine (containing ~1800 mg N L⁻¹) was diluted more than 10 times (or more than 30 times taking into account the dilution prior to alkalinization and biostabilization).

A higher biomass concentration (OD₇₅₀ up to 4) and consequently, a higher N uptake could be obtained in the photobioreactor because of a higher light availability (Section 6.3.5). Nonetheless, even with a highly optimized light system and short light-path reactor systems, biomass concentrations are limited to several grams per liter, which correspond to a N uptake below 1 g N L⁻¹ [285, 286]. Since undiluted urine can contain up to 9 g N L⁻¹ [294], urine dilution is essential to achieve high N conversion efficiencies. This was also concluded by Tuantet et al. (2019) [286] who found that extremely low dilution rates would be required to accomplish complete N removal by *Chlorella sorokiniana* grown on undiluted urine in a short light-path photobioreactor. In practice, the nitrified urine could be diluted by redirecting a part of the N-depleted effluent back to the reactor after biomass separation (e.g., by filtration or settling), as was also suggested by Tuantet et al. (2019) [286].

6.3.2 Nitrified urine sustains *Limnospira* biomass production, but growth stagnates earlier than on modified Zarrouk medium

This study aimed to compare *Limnospira* cultivation on nitrified urine versus modified Zarrouk medium based on several growth parameters such as OD₇₅₀, N and P uptake and biomass protein content. Similar as in the preliminary experiment with modified Zarrouk medium (Section 6.3.1), a maximum OD₇₅₀ of 1.23 ± 0.05 and N uptake of $130 \pm 4 \text{ mg N L}^{-1}$ was reached after two weeks on N-reduced modified Zarrouk medium (ZM N_{low}, i.e., modified ZM with a lower sodium nitrate concentration) (Figure 6.1, Table 6.4). A higher N conversion efficiency could be obtained (~70% instead of ~25%) because of the lower initial N concentration. Due to CO₂ uptake by *Limnospira*, TIC decreased by 25% (but was still $>1.5 \text{ g L}^{-1}$) and the pH increased from ~9.8 to ~11.5 (SI Figures S6.5-S6.6).

The increase in OD₇₅₀ and decrease in nitrate concentration in the flasks with nitrified urine (NU 1x) followed the same trend as ZM N_{low} during the first 7-10 days, but then stagnated (Figure 6.1). The maximum OD₇₅₀ amounted to 0.95 ± 0.01 and only 65 mg N L^{-1} or 35% (instead of 70%) of the nitrate was removed from the medium. This was also reflected in the lower TSS concentration and protein content of the biomass (Table 6.4). Furthermore, the P uptake on NU 1x was remarkably lower compared to ZM N_{low}. The nitrified urine only contained 12 mg P L^{-1} , compared to $\sim 100 \text{ mg P L}^{-1}$ in ZM N_{low}, but, in principle, this should be sufficient since the P uptake on ZM N_{low} was $\sim 10 \text{ mg P L}^{-1}$. Yet, only 2 mg P L^{-1} was removed from the NU 1x medium. The growth profile on NU 1x was very similar to the one obtained by Coppens et al. (2016) [56] using nitrified urine (20%, containing 1.3 g N L^{-1}) supplemented with trace elements. Also in the latter study with *Arthrospira platensis*, nitrified urine yielded a similar growth rate but a 33% lower biomass concentration compared to modified Zarrouk medium.

These results clearly demonstrate that some compounds limited growth on NU 1x. Next to P, NU 1x also contains less Ca²⁺, Mg²⁺ and other micronutrients compared to ZM N_{low} (Table 6.3). It was hypothesized that a lack of one or more of these elements is limiting the growth of *Limnospira* on nitrified urine. To confirm this hypothesis, the dilution of the nitrified urine was lowered to increase the concentrations of P and microelements in the culture medium. The OD₇₅₀ on four times more concentrated nitrified urine (NU 4x) was higher compared to NU 1x, at least in two of the three replicates (Figure 6.1, SI Figure S6.3). Although the N uptake ($132 \pm 40 \text{ mg N L}^{-1}$), P uptake and protein content were higher compared to NU 1x and approaching ZM N_{low}, the OD₇₅₀ and TSS were lower, indicating that there was still a limitation. P was probably no longer the limiting nutrient, since the N:P uptake ratio decreased from 32:1 (NU 1x) to 16:1 (NU 4x), which is close to the ratio on ZM N_{low} (14:1). Furthermore, lowering the dilution reduces the N conversion efficiency. Only 17% of the nitrate was consumed. Further reducing the dilution would further decrease the N conversion efficiency and could even result in nitrate inhibition. Coppens et al. (2016) reported inhibition of *Arthrospira platensis* at nitrate concentrations above 1 g N L^{-1} .

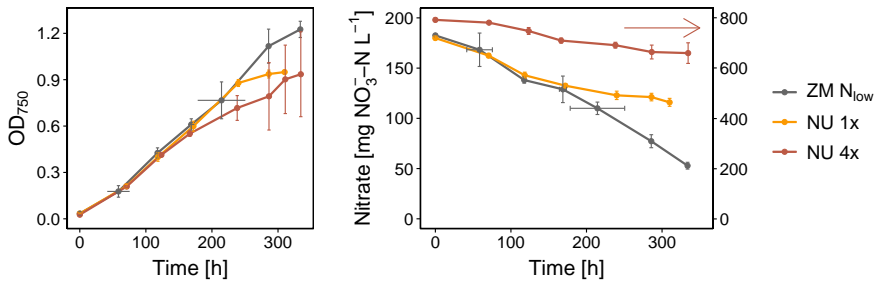


Figure 6.1: **Optical density (OD₇₅₀, measured at 750 nm) and nitrate profile in the flasks with N-reduced modified Zarrouk medium (ZM N_{low}), diluted nitrified urine (NU 1x) and four times more concentrated nitrified urine (NU 4x).** The nitrate concentration in NU 4x is displayed on the right y-axis. The vertical error bars represent the standard deviation. Horizontal error bars indicate slight variations in sampling time across replicates.

Table 6.3: **Relevant element concentrations of N-reduced modified Zarrouk medium (ZM N_{low}), diluted nitrified urine (NU 1x) and four times more concentrated nitrified urine (NU 4x).** N.D.: not yet determined (will be added when the data become available over the coming weeks).

	ZM N _{low} [mg L ⁻¹]	NU [mg L ⁻¹]	NU 4x [mg L ⁻¹]
NO ₃ ⁻ -N	165	165	660
PO ₄ ³⁻ -P	89	8.7	34.8
K ⁺	673	111	444
Na ⁺	1070 ^a / 7240 ^b	98	392
Cl ⁻	628	71	284
SO ₄ ²⁻	586	25	100
Ca ²⁺	12.2	1.2	4.8
Mg ²⁺	7.9	0.2	0.8
Fe ²⁺	2.01	N.D.	N.D.
Mn ²⁺	0.06	N.D.	N.D.
Zn ²⁺	0.03	N.D.	N.D.
Cu ²⁺	0.01	N.D.	N.D.

^a without addition of NaHCO₃/Na₂CO₃

^b with addition of NaHCO₃/Na₂CO₃ as C source

Table 6.4: **Biomass production and N, P and TIC consumption.** Averages and standard deviations are given. The linear growth rate equals the slope of the linear range of the OD curve. The maximum linear growth rate is determined by the light availability in the given setup.

	ZM N _{low}	NU 1x	NU 4x	NU all	NU + Ca/Mg/P _{low}	NU + Ca/Mg/P	NU all – Ca	NU all – Mg	NU all – Fe	NU all – TE
Biomass production										
TSS [$g L^{-1}$]	1.73±0.13	1.52±0.16	1.36±0.18	1.49±0.12	1.50±0.21	1.45±0.15	0.74±0.39	1.34±0.03	1.48±0.12	1.52±0.19
max OD ₇₅₀	1.23±0.05	0.95±0.01	0.94±0.27	1.21±0.09	0.86±0.09	0.95±0.03	0.43±0.55	1.18±0.10	1.21±0.09	1.21±0.16
linear growth rate [d^{-1}]	0.097±0.012	0.094±0.004	0.065±0.024	0.088±0.008	0.086±0.004	0.080±0.012	0.024±0.047	0.101±0.002	0.090±0.005	0.096±0.022
N consumption [$mg NO_3^- - N L^{-1}$]										
initial N concentration	183±1	180±2	792±7	176±13	188±4	161±2	2040±16	216±3	208±13	192±1
total N uptake	130±4	64±2	132±40	131±1	93±24	89±5	30±43	91±14	113±15	146±2
conversion efficiency [%]	71±2	36±2	17±5	74±6	49±12	55±3	19±6	42±7	55±11	76±1
biomass protein content [%] ^a	51.9±9.4	21.3±3.9	46.5±6.8	46.8±8.6	30.0±4.7	41.1±9.3	57.9±3.8	24.8±3.0	43.5±3.7	
P consumption [$mg PO_4^{3-} - P L^{-1}$]										
initial P concentration	97.25±1.53	11.70±0.10	39.92±0.14	49.40±0.22	18.38±0.89	49.60±0.00	51.20±1.62	51.87±0.61	52.13±0.46	32.57±0.73
total P uptake	9.2±2.3	2.0±0.1	7.8±0.7	10.3±1.0	7.3±0.8	12.0±0.4	4.2±4.9	2.1±0.6	9.9±0.8	10.7±0.9
conversion efficiency [%]	9.4±2.3	17.1±1.0	19.6±1.8	20.8±2.0	39.5±2.5	24.2±0.8	16.7±5.8	4.1±1.2	18.9±1.5	33.0±2.4
N:P uptake ratio (g/g)	14.1	32.0	16.9	12.7	12.7	7.4	7.1	43.3	11.4	13.6
TIC consumption [$mg C L^{-1}$]										
initial TIC concentration	2271±54	2199±35	2264±66	2272±87	2259±11	2337±15	2198±72	2143±27	2193±52	2156±20
total TIC uptake	549±46	349±59	543±50	552±64	391±34	518±16	356±122	392±44	387±50	483±33
conversion efficiency [%]	25±2	16±2	24±2	25±2	17±2	22±1	16±6	18±2	18±2	22±2

^a protein concentration divided by biomass concentration (5 mg lyophilized biomass dissolved in 10 mL of MilliQ water)

6.3.3 Supplementing nitrified urine can yield the same biomass production and N uptake as modified Zarrouk medium

Alternatively, nitrified urine can be supplemented with chemicals to increase the concentration of P, Ca^{2+} , Mg^{2+} and/or other microelements. In a first stage, all compounds in ZM, except for NaNO_3 , NaCl and K_2SO_4 , were added to the nitrified urine in the same concentration as in ZM N_{low} , except for K_2HPO_4 (concentration was reduced since only $\sim 10\%$ of the P was consumed in ZM N_{low}). The increase in OD_{750} and decrease in nitrate concentration in the flasks with the supplemented nitrified urine (NU all) coincided with the curves of ZM N_{low} (Figure 6.2). Also the protein content, P uptake and TIC removal were very similar to ZM N_{low} (Table 6.4). These results demonstrate that *Limnospira* growth on nitrified urine without supplements was limited by a deficiency of one of the supplied elements (i.e., P, Ca^{2+} , Mg^{2+} , Fe^{2+} , EDTA and trace elements).

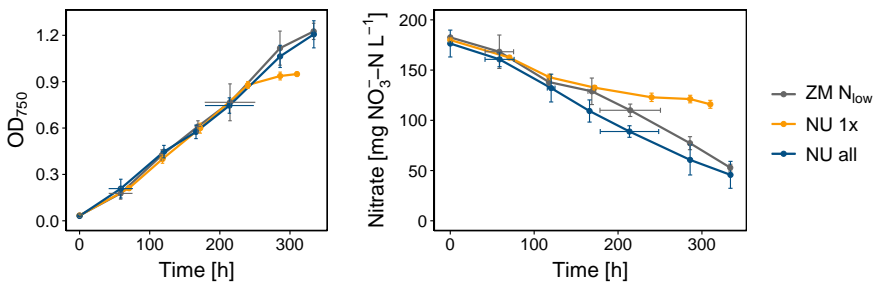


Figure 6.2: **Optical density (OD_{750} , measured at 750 nm) and nitrate profile in the flasks with N-reduced modified Zarrouk medium (ZM N_{low}), nitrified urine (NU 1x) and nitrified urine supplemented with P, Ca^{2+} , Mg^{2+} , Fe^{2+} , EDTA and trace elements (NU all).** The vertical error bars represent the standard deviation. Horizontal error bars indicate slight variations in sampling time across replicates.

6.3.4 Identifying the limiting element(s) for *Limnospira* growth in nitrified urine

Supplementing nitrified urine with P and micronutrients yielded the same biomass production as N-reduced modified Zarrouk medium. In a next phase, one or more elements were removed from the medium in order to determine which element(s) is/are essential to ensure optimal growth on nitrified urine.

The low P uptake on nitrified urine without supplements (NU) already pointed out that the P concentration in the nitrified urine was insufficient to sustain high biomass concentrations and N conversion efficiencies. P is an essential macronutrient in microalgal metabolism, given its presence in nucleotides, energy molecules, lipids and polysaccharides [209]. Most of the P (78%) was removed from the urine in the alkalization pre-treatment by precipitation with Ca^{2+} and Mg^{2+} . Since Ca^{2+} and Mg^{2+}

also play an important role in several metabolic pathways and their concentration in the nitrified urine was more than 10 times lower than ZM (Table 6.3), it was decided to supply them to the medium. As the central element of the chlorophyll molecule, Mg^{2+} is pivotal for photosynthesis [77]. Mg^{2+} is furthermore involved in the aggregation of ribosomes in functional units, in the formation of catalase and as an important enzyme cofactor, it for instance catalyzes reactions of RuBisCo (CO_2 fixing enzyme complex) [77, 145]. Ca^{2+} is important to form rigid gels in microalgae cell walls by crosslinking pectin polymers [120]. Two different P concentrations (0.0453 and 0.2 mg L^{-1}) were tested, whereas Ca^{2+} and Mg^{2+} were added in the same concentration as ZM N_{low} . In the flasks with the lowest P concentration ($+0.0453 \text{ mg P L}^{-1}$, $NU+Ca^{2+}/Mg^{2+}/P_{low}$), the maximum OD_{750} (0.86 ± 0.09), nitrate uptake ($93 \pm 24 \text{ mg N L}^{-1}$) and TIC removal efficiency ($17.3 \pm 1.5 \%$) were lower compared to the nitrified urine with all supplements (NU all) (Figure 6.3, Table 6.4). Higher OD_{750} values and TIC removal efficiencies were reached in the flasks with the same P concentration as NU all ($NU+Ca^{2+}/Mg^{2+}/P$), but the growth was still not as optimal as for NU all, indicating that a deficiency in at least one of the other elements (EDTA, Fe^{2+} or trace elements) was still limiting *Limnospira* growth.

In a next set of experiments, one element at a time was removed from the culture medium NU all. Removing Ca^{2+} from the culture medium ($NU \text{ all}-Ca^{2+}$) resulted in very poor growth in five out of six replicates. The OD_{750} did not exceed 0.25 and less than 50 mg N L^{-1} was removed from the medium (Figure 6.3, Table 6.4), which is even lower compared to the unsupplemented nitrified urine. This can possibly be attributed to the addition of EDTA in $NU \text{ all}-Ca^{2+}$. While EDTA was added with the aim to increase Ca^{2+} bioavailability by avoiding precipitation, an adverse affect on *Limnospira* growth was observed, likely due to the formation of a strong EDTA- Ca^{2+} complex which made the Ca^{2+} in nitrified urine unavailable (EDTA first binds with Ca^{2+} and then with Mg^{2+} [205]). Surprisingly, one of the six flasks performed rather well (OD_{750} of 1.06 and N uptake of 110 mg N L^{-1}) (SI Figures S6.3-S6.4).

Removing Mg^{2+} from the nitrified urine with all supplements ($NU \text{ all}-Mg^{2+}$) yielded a similar growth rate and final OD_{750} (Figure 6.3), but a much lower N and P uptake and protein content compared to NU all. Also the colour of the culture changed to yellowish green instead of dark green (SI Figure S6.7). This could be related to the fact that Mg^{2+} is a key compound of the chlorophyll pigment.

Likewise, Fe^{2+} amendment proved to be important to obtain a high N uptake. The N uptake on $NU \text{ all}-Fe^{2+}$ was about 15% lower compared to NU all. The increase in OD_{750} and P uptake, on the other hand, were similar to NU all. Iron is an important micronutrient given its ability to function as electron donor/acceptor and plays a role in many metabolic functions, including electron transport in the Calvin cycle, respiratory electron transport, synthesis of DNA and chlorophyll, detoxification/degradation of reactive oxygen species and nitrite reduction [77, 81]. The latter could possibly explain the lower N uptake on $NU \text{ all}-Fe^{2+}$ as nitrite reduction is essential for nitrate assimilation

in microalgae. In contrast to ammonium which can be directly incorporated into amino acids, nitrate has to be converted to ammonium via nitrite [280]. The conversion of nitrite into ammonium is catalysed by ferredoxins, i.e., clusters of iron and sulfur [280]. Iron deficiency could thus affect the nitrate uptake. Moreover, iron is one of the main contributors to the nutritional value of *Spirulina/Arthrospira* [69].

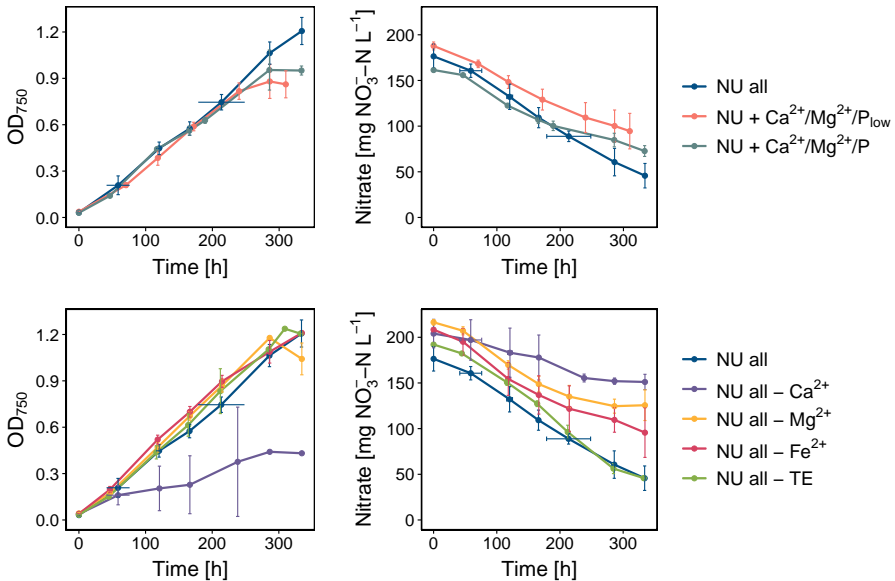


Figure 6.3: Optical density (OD_{750} , measured at 750 nm) and nitrate profile in the flasks with nitrified urine supplemented with P, Ca^{2+} , Mg^{2+} , Fe^{2+} , EDTA and trace elements (NU all), nitrified urine supplemented with P (0.0453 g L^{-1}), Ca^{2+} and Mg^{2+} (NU+ $Ca^{2+}/Mg^{2+}/P_{low}$), nitrified urine supplemented with P (0.2 g L^{-1}), Ca^{2+} and Mg^{2+} (NU+ $Ca^{2+}/Mg^{2+}/P$) and nitrified urine supplemented with all elements, except Ca^{2+} (NU all- Ca^{2+}), Mg^{2+} (NU all- Mg^{2+}), Fe^{2+} (NU all- Fe^{2+}) or TE (NU all-TE). The vertical error bars represent the standard deviation. Horizontal error bars indicate slight variations in sampling time across replicates.

The medium without trace elements (i.e., Zn^{2+} , Cu^{2+} and Mn^{2+}) performed equally good as NU all (Figure 6.3, Table 6.4). Trace elements are only required in small amounts. Hence, the concentrations present in urine (data not yet available) might have been sufficient to ensure optimal growth or the inoculum (<2% of culture medium) may have contained enough trace elements to support microalgae growth. A deficiency in trace elements, however, might still appear during long-term continuous culture or after subculturing. Cogne et al. (2003) [54] could not detect copper uptake in batch culture, whereas in continuous cultures, about $2 \mu\text{g Cu}^{2+} \text{ g}^{-1}$ dry weight was removed from the medium. Manganese and zinc were assimilated by *Arthrospira platensis* both in batch

and continuous cultures.

EDTA could not be left out of the medium as this resulted in precipitation and the formation of a pink coloured salt solution during autoclaving (presumably due to iron oxidation). EDTA is used as a chelate/complexing agent in the culture medium, enhancing the solubility of metal ions (Fe^{2+} , Mg^{2+} and Ca^{2+}), thereby increasing their availability by microalgae [245]. Too high levels of EDTA, on the other hand, are known to decrease the bio-availability since the metal ions are strongly chelated to EDTA and therefore no longer available [108, 245].

6.3.5 Long-term continuous *Limnospira* cultivation in a photobioreactor confirmed the application potential of supplemented nitrified urine as a culture medium

Given the promising results in batch culture, supplemented nitrified urine was evaluated for long-term continuous *Limnospira* cultivation in a photobioreactor. Due to the higher light availability, a higher biomass concentration and N uptake could be achieved in the photobioreactor. Hence, modified Zarrouk medium and more concentrated nitrified urine (23% corresponding to $\sim 450 \text{ mg N L}^{-1}$ instead of 9.2%) were used as culture media. This resulted in a higher N uptake, requiring a proportional increase in supplemented P compared to the batch culture experiments ($0.3 \text{ g L}^{-1} \text{ K}_2\text{HPO}_4$ instead of 0.2 g L^{-1}). $\text{MgSO}_4 \cdot 7\text{H}_2\text{O}$, $\text{CaCl}_2 \cdot 2\text{H}_2\text{O}$, $\text{FeSO}_4 \cdot 7\text{H}_2\text{O}$, $\text{EDTA} \cdot 2\text{H}_2\text{O}$ and trace elements ($\text{MnCl}_2 \cdot 4\text{H}_2\text{O}$, $\text{ZnSO}_4 \cdot 7\text{H}_2\text{O}$ and $\text{CuSO}_4 \cdot 5\text{H}_2\text{O}$) were supplemented in the same concentration as in ZM.

After inoculation, the photobioreactor was started in batch mode on modified Zarrouk medium at an initial OD_{750} of 0.2. The light intensity was stepwise increased from 31 to $923 \mu\text{mol m}^{-2} \text{ s}^{-1}$ to prevent photoinhibition in the early stages of the batch culture. After 6 days, an OD_{750} of 2.7 was reached and $\sim 68\%$ (320 mg N L^{-1}) of the N had been removed from the culture medium. Subsequently, the reactor was operated in continuous mode with an HRT and SRT of 3 days. The OD_{750} and N concentration remained stable at 2.7 ± 0.2 and $178 \pm 19 \text{ mg N L}^{-1}$, respectively (Figure 6.4). The volumetric biomass production amounted to $1 \text{ g VSS L}^{-1} \text{ d}^{-1}$. On average 335 mg N L^{-1} and 25 mg P L^{-1} were assimilated, corresponding to volumetric uptake rates of $112 \text{ mg N L}^{-1} \text{ d}^{-1}$ and $8.3 \text{ mg P L}^{-1} \text{ d}^{-1}$ and specific uptake rates of $0.11 \text{ g N g}^{-1} \text{ VSS}$ and $0.009 \text{ g P g}^{-1} \text{ VSS}$.

Subsequently, the photobioreactor was autoclaved and started in batch mode on supplemented nitrified urine at an initial OD_{750} of 0.2. After 7 days, an OD_{750} of 2.8 was reached and $\sim 62\%$ (314 mg N L^{-1}) of the N had been removed from the culture medium. After shifting to continuous mode, the OD_{750} further increased to 3.9 and then dropped and stabilized at 2.9, whereas the dry weight (DW) remained stable at 3.9 g TSS L^{-1} throughout the experiment. Some changes in cell morphology probably affected the scattering properties of the cell, resulting in fluctuations in OD_{750} and $\text{OD}_{750}/\text{DW}$ ratio. The N concentration remained stable at $166 \pm 28 \text{ mg N L}^{-1}$ (Figure

6.4). The volumetric biomass production amounted to $1.1 \text{ g VSS L}^{-1} \text{ d}^{-1}$. On average 331 mg N L^{-1} was assimilated, corresponding to a volumetric uptake rate of $110 \text{ mg N L}^{-1} \text{ d}^{-1}$ and a specific uptake rates of $0.11 \text{ g N g}^{-1} \text{ VSS}$.

With an HRT of 3 days, about 30% of the N was not consumed by the microalgae. Light was the limiting growth factor since the microalgae were grown at their optimal conditions (temperature of 36°C and pH of 9.5) and the effluent was still rich in nutrients ($\sim 180 \text{ mg N L}^{-1}$ and $>50 \text{ mg P L}^{-1}$) and inorganic carbon ($0.8\text{-}2 \text{ g C L}^{-1}$). Increasing the HRT would probably have resulted in a higher biomass concentration and nutrient removal. At long HRT, dense microalgae cultures develop, favoring nutrient removal (as nutrients are assimilated in the biomass). This, however, at the expense of the biomass productivity and photosynthetic efficiency (due to the increased self-shading, thereby creating dark volumes within the reactor where biomass is lost through cellular maintenance or endogenous respiration) [286]. Alternatively, increasing the urine dilution factor could improve the N removal while still maintaining a low HRT and high productivity rate [286].

When the data become available over the coming weeks, a table with the biomass composition, protein content and influent and effluent concentrations of (micro)nutrients will be added.

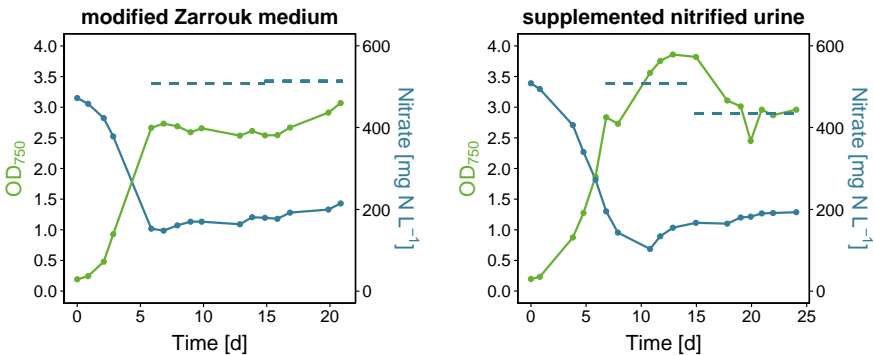


Figure 6.4: **Optical density (OD_{750}) and nitrate concentration during the continuous cultivation of *Limnospira indica* on modified Zarrouk medium (left) and supplemented nitrified urine (right).** The blue dashed lines represent the nitrate concentration in the influent.

6.3.6 Overall concept

This study aimed to evaluate and optimize nitrified urine as a culture medium for *Limnospira indica*. Urine is a very rich medium, containing all macro- and micronutrients required for microalgae growth, but not necessarily in the right proportions and also the pre-treatment (alkalinization and nitrification) reduced the concentration of some essential elements. As a result, nitrified urine yielded a lower biomass concentration

compared to modified Zarrouk medium.

P was clearly limiting the growth on nitrified urine. The N:P ratio in fresh urine (~12 g N:g P [294]) corresponds rather well to the N:P uptake ratio on modified Zarrouk medium (i.e., ~14). However, precipitation caused by alkalization reduced the P concentration in urine with 78%, resulting in a suboptimal N:P ratio [284]. In the subsequent nitrification step, the phosphate concentration was increased due to some phosphate diffusion from the anolyte to the middle compartment (Chapter 5). This only occurs, however, during start-up and when a phosphate solution is used as initial anolyte solution. The low P concentration in the nitrified urine resulted in a poor P uptake and a high N:P uptake ratio (32 compared to 14 on ZM N_{low}). In contrast, P addition resulted in a N:P uptake ratio close to 14 in the batch culture experiments (Table 6.4), except for NU all– Mg^{2+} (N:P of 43), NU+ $Ca^{2+}/Mg^{2+}/P$ (N:P of 7.4) and NU all– Ca^{2+} (N:P of 7.1). The low N:P uptake ratio in the latter two cases can be caused by luxury P uptake (i.e., P accumulation as polyphosphate granules) or by P precipitation [285]. The former is unlikely since luxury P uptake is induced by high phosphate levels and all culture media contained less P compared to ZM N_{low} (with an N:P uptake ratio of 14.1). Precipitation might occur during batch cultivation, triggered by the increase in culture pH (up to 11.5) [41]. In NU 1x and NU 4x, precipitation was limited by the low Ca^{2+} and Mg^{2+} concentration (most of the Ca^{2+} and Mg^{2+} had been removed in the alkalization step by the pH increase to 12), whereas EDTA addition limited precipitation of P with Ca^{2+} , Mg^{2+} and Fe^{2+} in the other experiments, except in NU+ $Ca^{2+}/Mg^{2+}/P_{low}$ and NU+ $Ca^{2+}/Mg^{2+}/P$ where no EDTA was added. Hence, a part of the P in NU+ $Ca^{2+}/Mg^{2+}/P$ might have been precipitated instead of assimilated, explaining the low N:P uptake ratio.

If the precipitates formed during alkalization could be captured, they could be used as a source of P to restore the optimal N:P ratio in urine. Alternatively, struvite could be a cheap and effective source of P (and Mg^{2+}) for microalgae, as demonstrated by Muys et al. (2019) [208]. The low pH of the nitrified urine after passage through the middle compartment of the electrochemical cell used to control the pH in the nitrification reactor is moreover well suited for dissolving precipitates. Adding the urine precipitates to the nitrified urine would furthermore increase the concentration of Ca^{2+} and Mg^{2+} , which proved to be essential in our experiments. Alkalization removed ~90% of the Ca^{2+} and Mg^{2+} , resulting in a lack of Ca^{2+} and Mg^{2+} in the nitrified urine, containing ~140 g N:g Ca^{2+} and ~920 g N:g Mg^{2+} . Several studies reported a Mg^{2+} uptake of around 2 mg $Mg^{2+} g^{-1}$ *Arthrospira* biomass (dry weight) [36, 54, 141]. Considering that about 12% of the dry matter consists of N, a N: Mg^{2+} ratio of 60 is required in the medium. Interestingly, the N: Mg^{2+} ratio in fresh urine, without Mg^{2+} precipitation or when all precipitated Mg^{2+} can be recovered and redissolved in nitrified urine amounts ~90 g N g^{-1} Mg^{2+} [294].

Besides addition of P, Ca^{2+} and Mg^{2+} , supplementing nitrified urine with Fe^{2+} and EDTA proved to be key in obtaining a high biomass concentration and maximizing the N conversion efficiency. Further research in continuous culture or with multiple subcultures

(to deplete trace elements in the original culture medium) is necessary to investigate whether addition of trace elements (i.e., Zn^{2+} , Mn^{2+} and Cu^{2+}) to nitrified urine is required. Urine contains a broader range of trace elements than modified Zarrouk medium including molybdenum, cobalt and vitamins which may benefit *Limnospira* growth [91].

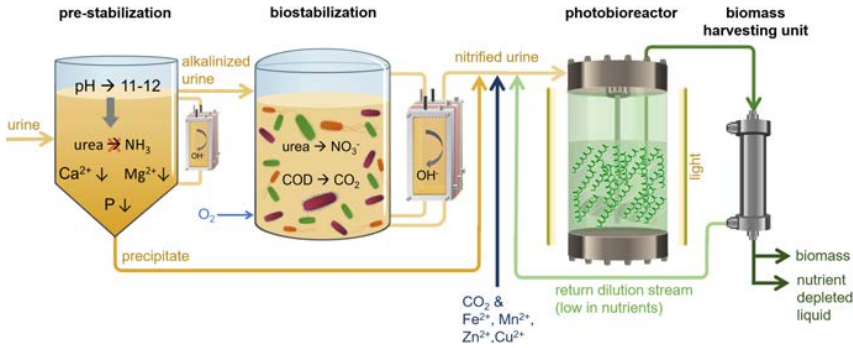


Figure 6.5: **Optimized process design to maximize the nutrient potential of urine and minimize the external input.**

The above findings are in line with several studies reporting a microalgae growth stimulation by the addition of P, Mg^{2+} , Fe^{2+} , EDTA and/or trace elements to synthetic or real urine. However, unlike the current work, none of these studies systematically evaluated the growth enhancing impact of each of these individual elements. Adamsson (2000) [3] found that addition of Mg^{2+} , Fe^{2+} and EDTA improved the growth of *Scenedesmus acuminatus* in hydrolysed urine. Tuantet et al. (2014) [284] showed that Fe^{2+} , Mg^{2+} and trace elements are present in low concentrations in urine, mainly due to precipitation by urea hydrolysis. Supplementing urine with these elements improved the growth of *Chlorella sorokiniana* in batch culture. Continuous culture of *Chlorella sorokiniana* on synthetic and hydrolysed urine by Tuantet et al. (2014) [285] revealed that growth was restricted by P (medium N:P ratio of 15-22 g N:g P) and Mg^{2+} . Supplementing P (to lower the N:P ratio) and Mg^{2+} enhanced the biomass production and nutrient removal [284]. Coppens et al. (2016) [56] added trace elements to nitrified urine, but obtained a 33% lower biomass yield compared to ZM, indicating that other micronutrients were limiting growth. On the other hand, Chang et al. (2013) [41] obtained >95% of N and P removal on real, fresh urine without additions, but used a high dilution factor (1.25% of urine, N:P ratio of 11), which probably prevented precipitation, and only evaluated the growth of *Arthrospira platensis* over 10 days.

Finally, the three major compounds in modified Zarrouk medium (i.e., $NaNO_3$, $NaCl$ and K_2SO_4) did not need to be amended to the nitrified urine, since the observed growth on nitrified urine supplemented with P, Ca^{2+} , Mg^{2+} , Fe^{2+} , EDTA and trace elements was equivalent to the growth on modified Zarrouk medium. This qualifies nitrified urine as a valuable and sustainable alternative microalgae growth medium, particularly with

recycling of the urine precipitates formed by alkalization, likely requiring only external addition of Fe^{2+} and EDTA. Carbon dioxide (in the atmosphere or in flue gases) can be used as inorganic carbon source, rendering CO_2 sequestration [43].

6.4 Conclusions

- This study demonstrated that nitrified human urine can be used as a culture medium for *Limnospira indica* and that the biomass production and N uptake were promoted by addition of P and micronutrients.
- Nitrified urine supplemented with phosphate, magnesium, calcium, iron, EDTA and trace elements (manganese, zinc and copper) was as effective as modified Zarrouk medium in terms of biomass production, nutrient uptake and protein yield.
- Nitrified urine can replace the three major salt compounds in modified Zarrouk medium (i.e., NaNO_3 , NaCl and K_2SO_4). Urine precipitates harvested in the alkalization step could potentially supply enough P and magnesium, as the N:P and N: Mg^{2+} ratio in fresh urine correspond to the typical uptake ratios.
- Continuous *Limnospira* cultivation on supplemented nitrified urine was, for the first time, evaluated and yielded similar results as modified Zarrouk medium. The N conversion efficiency should be further increased by lowering the N concentration in the influent (thus by increasing the urine dilution) or by increasing the HRT.
- Further research is required to investigate whether addition of trace elements is required and to evaluate the nutritional quality of the biomass. Since urine can contain micropollutants and pathogens, an additional treatment step (e.g., activated carbon adsorption, UV or ozone treatment) is recommended before microalgae cultivation.

6.5 Supplementary information

6.5.1 Literature overview

Table S6.1: Literature overview of microalgae cultivation on urine. PBR: photobioreactor

Reference	Microalga	Culture medium	Batch/continuous culture	Recipient	Purpose of the study
Adamsson (2000) [3]	<i>Scenedesmus acuminatus</i>	<ul style="list-style-type: none"> – diluted urine (2%) – diluted urine (2%) + Fe²⁺, Mg²⁺ and EDTA – diluted urine (0.5%) + Fe²⁺ and EDTA 	<ul style="list-style-type: none"> – batch culture (10 d) – semi-continuous culture (SRT=4 or 8 d) 	<ul style="list-style-type: none"> – beakers – algal tank cylinder (open system) 	Construction of a food chain: microalgae were cultivated on urine, and the resulting urine-algae solution was used as feed for zooplankton. The zooplankton solution was subsequently added to a hydroponic system for tomato cultivation
Feng and Wu (2006) [89]	<i>Arthrospira platensis</i>	<ul style="list-style-type: none"> – synthetic urine (urea, <1%) – real urine (TAN, <1%) 	batch culture (14 d)	bubble column PBR	Microalgae cultivation for biomass and oxygen production in space life support systems
Feng et al. (2007) [90]	<i>Arthrospira platensis</i>	<ul style="list-style-type: none"> – synthetic urine (urea or TAN, <1%) – synthetic urine (NO₂ or NO₃, 10%) – real nitrified urine (10%) 	batch culture (14 d)	bubble column PBR	Microalgae cultivation for biomass and oxygen production in space life support systems
Feng et al. (2008) [91]	<i>Arthrospira platensis</i>	<ul style="list-style-type: none"> – nitrified urine (10%) – partially nitrified urine (NH₄NO₃, 10%) – partially short-nitrified urine (NH₄NO₂, 10%) 	batch culture (14 d)	bubble column PBR	Microalgae cultivation for biomass and oxygen production in space life support systems
Yang et al. (2008) [323]	<i>Arthrospira platensis</i>	synthetic urine (urea, 1.25%) + Fe ²⁺ , EDTA and trace elements	<ul style="list-style-type: none"> – batch culture (12 d) – continuous culture (28 d at an HRT/SRT of 43 d) 	PBR	Microalgae cultivation for biomass and oxygen production in space life support systems

Chang et al. (2013) [41]	<i>Arthrospira platensis</i>	<ul style="list-style-type: none"> – synthetic urine (TAN, <1%) – synthetic urine (<1%) + glucose or NaAc – real urine (urea, <1%) 	batch culture (10 d)	bubble column PBR	Microalgae cultivation for biomass production (to serve as biofuel feedstock) and nutrient removal
Tuantet et al. (2014b) [285]	<i>Chlorella sorokiniana</i>	<ul style="list-style-type: none"> – synthetic urine (TAN, 2-50%^a) + Fe-EDTA and trace elements – real urine (urea, 5-50%^a) + Fe-EDTA and trace elements – real urine (urea/TAN, 2-10%) + Fe-EDTA and trace elements 	continuous culture (80 days)	short light-path flat panel PBR	Cultivation of <i>C. sorokiniana</i> on high-concentration nitrified urine for nutrient removal and concomitant microalgae production
Jaatinen et al. (2016) [136]	<i>Chlorella vulgaris</i>	<ul style="list-style-type: none"> – real urine (urea, 0.3-4%) – real urine (urea, 1%) + trace elements 	batch culture (21 d)	Erlenmeyer flasks	Microalgae cultivation for nutrient removal with concomitant biomass production
Coppens et al. (2016) [56]	<i>Arthrospira platensis</i>	<ul style="list-style-type: none"> – synthetic urine (with urea, TAN, NO₂⁻ or NO₃⁻) – fresh/hydrolysed/nitrified urine – real nitrified urine (20%) + trace elements 	batch culture (5-10 d)	<ul style="list-style-type: none"> – 96-well plate, axenic conditions – Erlenmeyer flasks, axenic conditions 	Cultivation of <i>A. platensis</i> on high-concentration nitrified urine
Muys et al. (2018) [207]	mixed culture dominated by <i>Scenedesmus</i>	synthetic urine (12%) + NaCl and trace elements	semi-continuous culture (HRT/SRT=6.7 d)	nitrifying bubble column PBR	Synthetic urine was nitrified in a PBR through photosynthetic oxygenation (obviating the need for conventional aeration)
Chatterjee et al. (2019) [42]	<i>Scenedesmus acuminatus</i>	<ul style="list-style-type: none"> – real urine (TAN, 4-100%) – real urine (TAN, 5-6.7%) 	<ul style="list-style-type: none"> – batch culture (7 d) – batch or semi-continuous culture (HRT=15 d) 	Erlenmeyer flasks	Outdoor cultivation of microalgae on urine, with subsequent methane production from the harvested biomass using anaerobic digestion

Tuantet et al. (2019) [286]	<i>Chlorella sorokiniana</i>	<ul style="list-style-type: none"> – synthetic urine (urea, 10-55%^a) supplemented with Fe-EDTA and micronutrients – real urine supplemented with Fe-EDTA, Mg²⁺ and micronutrients 	PBR with short optical paths	Studied the impact of the reactor dilution rate (HRT) on the productivity and photosynthetic efficiency
-----------------------------	------------------------------	---	------------------------------	---

^a The optimal pH of *Chlorella sorokiniana* (6.8-7.2 [286]) is lower than the optimal pH of *Spirulina* (9-11). As a result, *C. sorokiniana* can be cultivated in less diluted urine since the fraction of TAN present as NH₃ is lower at low pH, minimizing the risk for NH₃ inhibition.

6.5.2 Supplementary materials and methods



Figure S6.1: **Bionet F1 photobioreactor.**

A: reactor vessel (total volume of 5L, active volume of 1.5-2L)

B: control software

C-F: peristaltic pump head for influent (C), base (D), acid (E) and antifoam (F) addition

G: glass bottles with acid, base and antifoam

H: gas supply (air and CO₂)

I: influent bottle

J: effluent bottle

K: sampling bottle

L: Glass bottle for inoculation

6.5.3 Preliminary batch culture experiment with modified Zarrouk medium

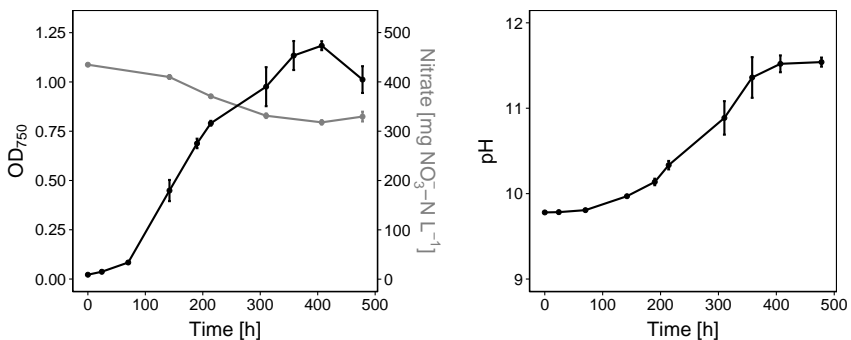


Figure S6.2: **Time profile of the optical density (OD₇₅₀), nitrate concentration and pH in the preliminary batch culture experiment on modified Zarrouk medium.**

6.5.4 Optimization of the nitrified urine-based culture medium

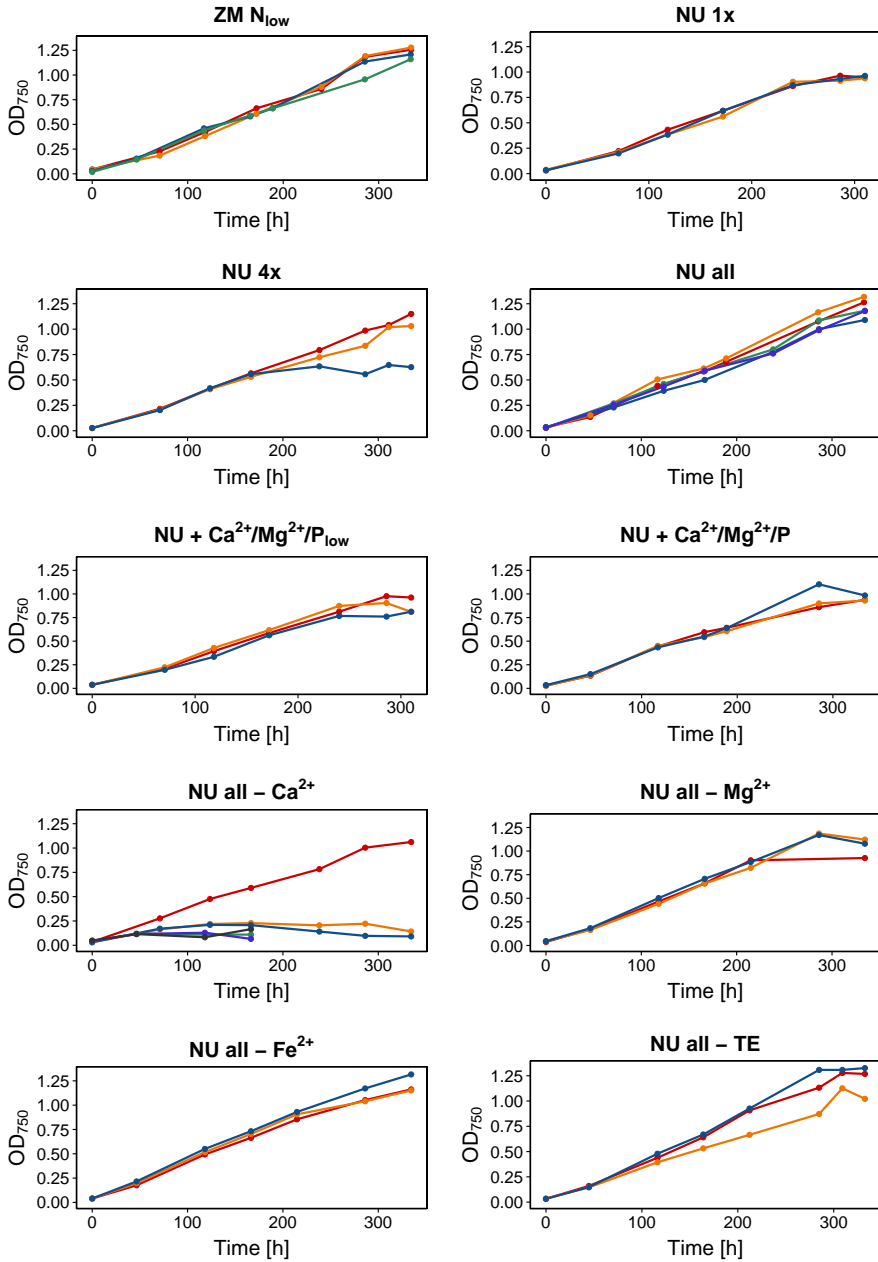


Figure S6.3: Optical density (OD) over time in all batch culture experiments.

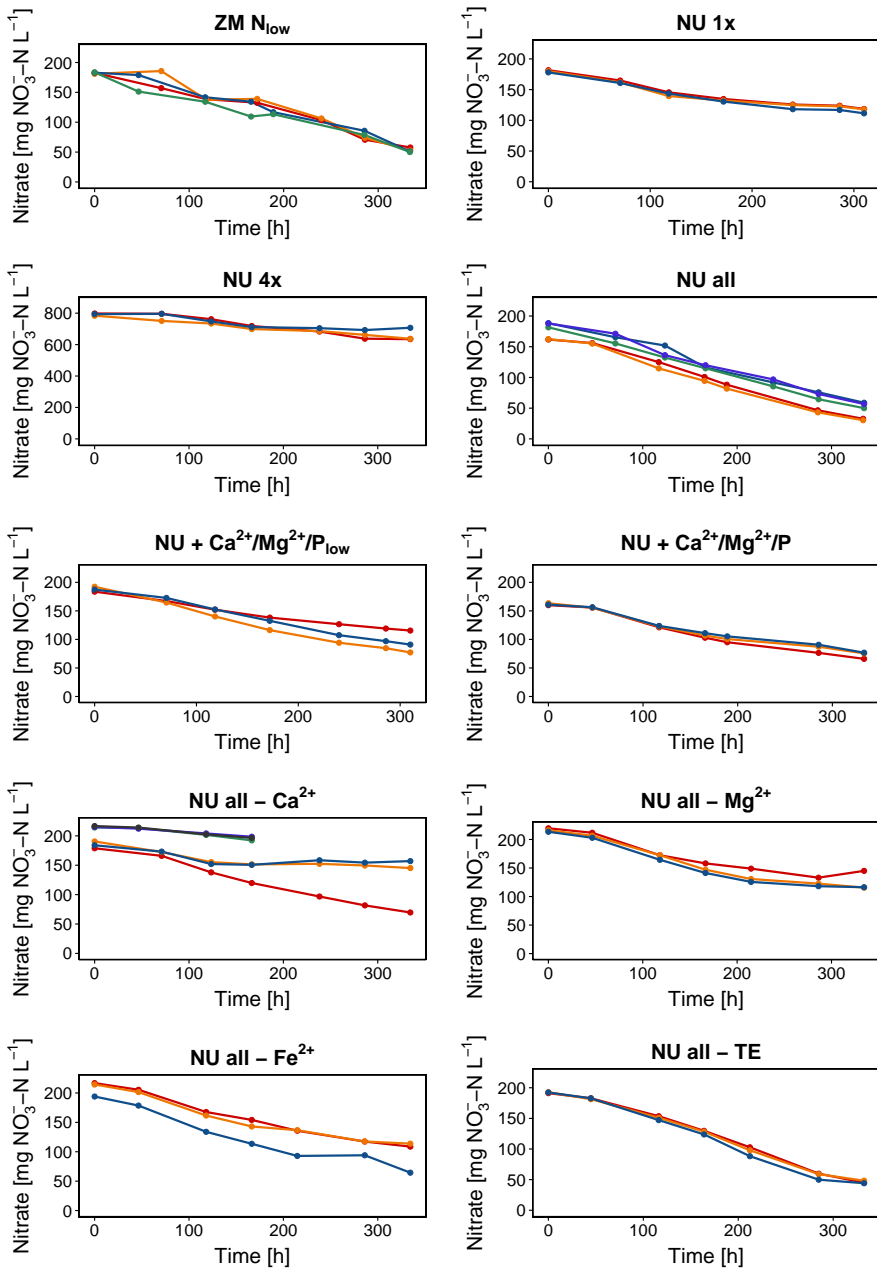


Figure S6.4: Nitrate concentration over time in all batch culture experiments.

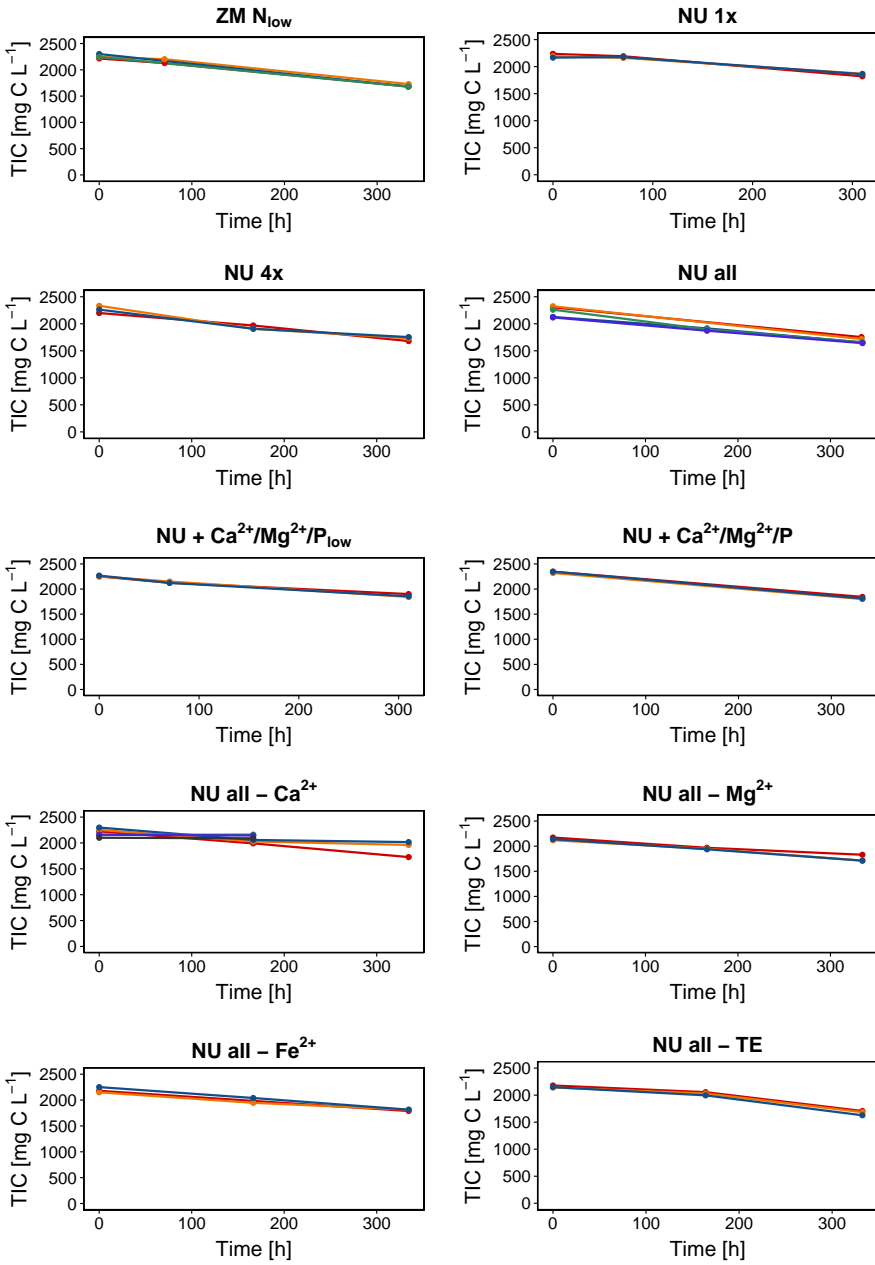


Figure S6.5: Total inorganic carbon (TIC) concentration over time in all batch culture experiments.

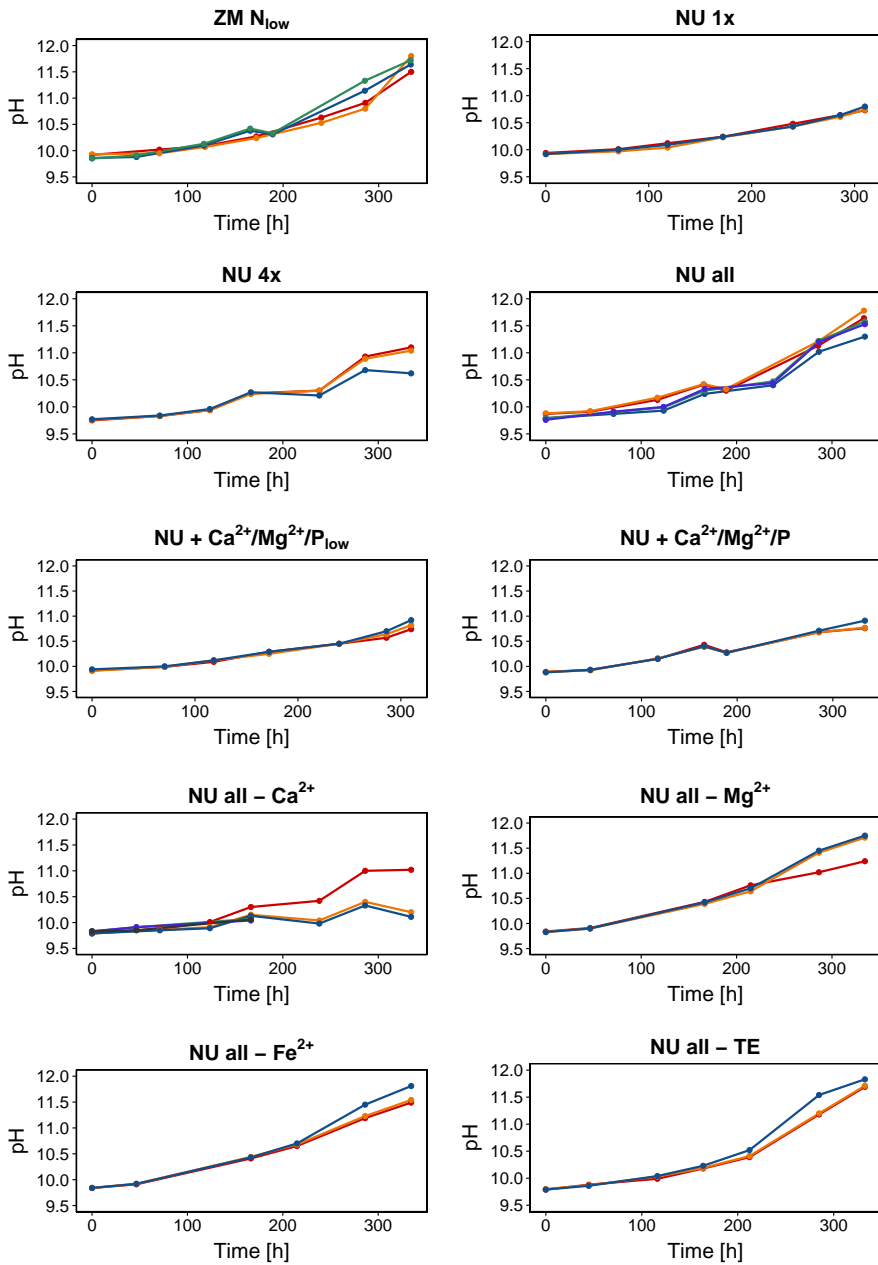


Figure S6.6: pH increase in all batch culture experiments.

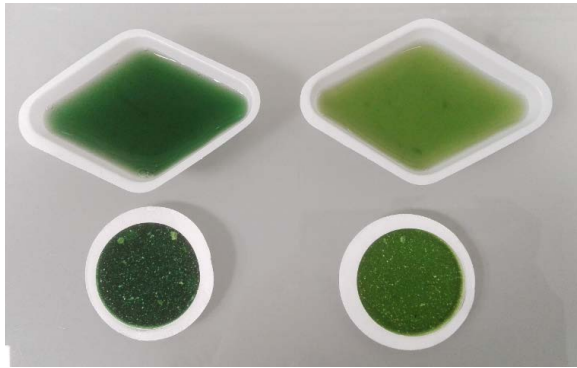


Figure S6.7: **Colour of the culture medium. Left: NU all. Right: NU all - Mg²⁺**

6.6 Acknowledgements

This article has been made possible through the authors' involvement in the MELiSSA project, the life support system research program from the European Space Agency (ESA) (<https://www.melissafoundation.org/>). J.D.P. was supported by the MELiSSA foundation via the POMP1 (Pool Of MELiSSA PhD) program and Fonds Wetenschappelijk Onderzoek Vlaanderen (FWO grant for a long stay abroad). The authors would like to acknowledge Kim De Paepe for critically reviewing the manuscript.

General discussion & perspectives

A journey of a thousand miles begins with a single step.

7

General discussion & perspectives

7.1 Main research outcomes

Human presence in outer space is currently supported by a regular resupply of life support consumables. However, to enable deep-space exploration or space habitation, in-situ oxygen, water and food production and waste management will be necessary in regenerative life support systems (RLSS) as resupply from Earth becomes practically impossible due to the long distance and duration. Urine recycling is of key interest in RLSS, given its high content of nitrogen and other macro-/micronutrients, which can be recovered to serve as a fertilizer for plants and microalgae [52].

Urine source separation and recycling also gains attention on Earth to close and/or shorten the terrestrial nutrient cycles, which play a pivotal role in our food supply. This would amongst others reduce the pressure on resource availability (e.g., phosphorus and fossil fuels) and the environmental burden (waste pollution). Other benefits stemming from terrestrial urine recycling include the reduced water consumption for flushing and the decreased nutrient load to wastewater treatment plants.

Urine contains many valuable compounds, but the compositional complexity of urine also presents a challenge for urine treatment and recycling. A first challenge is the hydrolysis of urea, the main nitrogen compound in urine. Without stabilization, urea quickly hydrolyses into ammonium, ammonia and bicarbonate. Ammonia is volatile and toxic and can pose a hazard to the crew upon volatilization. Secondly, calcium and magnesium can cause scaling and clogging due to uncontrolled precipitation with phosphate, sulfate or bicarbonate, which is triggered by the pH increase caused by urea hydrolysis. Precipitation of calcium sulfate (gypsum) in the distillation unit of the urine processor at the ISS led to malfunctioning of the equipment, limiting the obtained water recovery from 85% to 75% [201]. Thirdly, biodegradable organics, which are a carbon and energy source for many bacteria, fuel microbial growth, causing biofouling in the system. Finally, salts, naturally present in urine and potentially added during urine processing (e.g., sodium by NaOH addition), can complicate biological treatment and plant production since many bacteria and plants are sensitive to high salinities (especially sodium and chloride) [200, 204, 223]. Space further adds to the complexity, requiring highly compact and efficient recovery technologies (to minimize losses) which use a minimal amount of consumables (as resupply is limited) and are able to work at

the reduced gravity conditions, affecting amongst others gas-liquid interactions (e.g., oxygen transfer from the gas phase into the liquid phase).

The goal of this PhD thesis was to develop resource-efficient urine recycling technologies that can be implemented in MELiSSA or used for on-site/decentralized urine treatment on Earth. Nitrification was the preferred treatment technology, as it produces a stable nitrate-rich urine solution low in biodegradable organics, that can be used as a fertilizer for plants or as a culture medium for microalgae and is a key technology in MELiSSA. Different urine treatment trains combining nitrification with (electro)chemical processes were investigated.

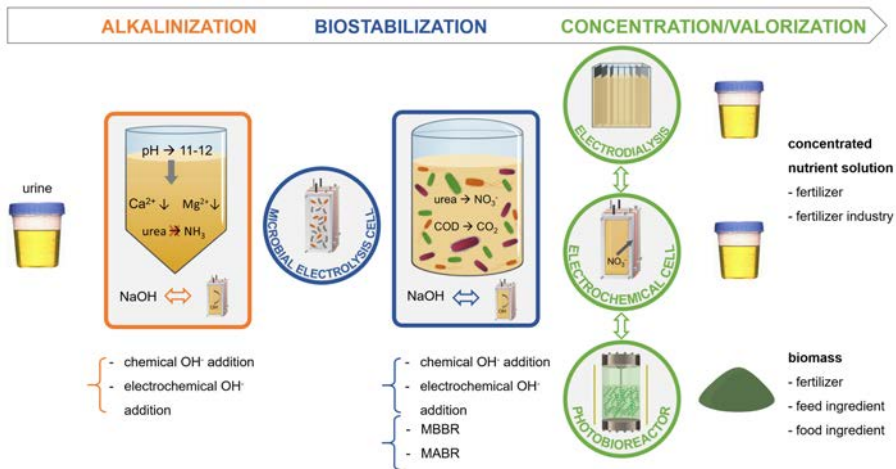


Figure 7.1: **Overview of the different building blocks of the urine treatment trains studied in this PhD research.** Rectangles represent essential processes, whereas the processes in circles are optional.

An alkalization step was included to prevent urea hydrolysis during storage and to remove calcium and magnesium by controlled precipitation, thereby minimizing the risk for scaling in the following treatment steps. In **Chapter 2** and **3**, NaOH was used to increase the pH of fresh urine, whereas **Chapter 4** investigated the use of an electrochemical cell to increase the pH. Urine was fed to a crystallizer and continuously recirculated over the cathodic compartment of the electrochemical cell, which was separated from the anodic compartment by ion exchange membranes to create a pH gradient. By applying electrical energy, water was reduced at the cathode, releasing hydroxide ions that increased the pH of the urine. By using an AEM in combination with a CEM or BPM, no chemical input (except water) was required to increase the pH, which is not only interesting for terrestrial applications, where chemical storage and dosing are a nuisance, but is crucial in RLSS, where the use of consumables is restricted by payload limitations. Moreover, electrochemical alkalization decreased the salinity of the urine (by anion migration across the AEM) whereas NaOH addition

increased the sodium concentration with a factor of 3, which can negatively affect the fertilizer potential of the urine. NaOH addition or electrochemical OH⁻ addition both yielded ~80-90% of calcium and magnesium removal. About 30% (Chapter 2, 20% urine+80% demineralized water, pH 11 with NaOH) to 78% (Chapter 5, 33% urine+67% tap water, pH 12 with electrochemical OH⁻ addition) of the phosphate was captured in the precipitates, which could be valorized as a slow-release P fertilizer in agriculture or as a resource for the phosphate industry. While downstream precipitation is limited by the low calcium and magnesium concentrations, it can still occur since the ion product approximates the solubility product. Concentration, for instance, can increase the ion product and thus trigger further precipitation. To reduce the risk for scaling, the pH should be lowered again to decrease the ion product, which was accomplished in the subsequent nitrification step. No excessive scaling was observed in the electrodialysis (ED) unit used in Chapter 2 or in the electrochemical cell of Chapter 5, demonstrating that the combination of alkalization and nitrification effectively prevented scaling. Chapter 4 also investigated the stability of the alkalized urine by monitoring the pH, electrical conductivity and total ammonia nitrogen (TAN) concentration over time. At pH 11, urine could be stabilized for only one week, while an increase to pH 12 allowed urine storage without urea hydrolysis for >18 months. The same electrochemical stabilization technology was applied as a pre-treatment in **Chapter 5**, with similar results as in Chapter 4. Yet, urine is only temporarily stabilized by increasing the pH and still contains urea, which can easily hydrolyse when the pH is lowered or urease is added, and organics, which can cause biofouling. Therefore, the urine was further processed using bacteria, oxidizing COD and urea into CO₂ and nitrate.

Chapter 3 evaluated COD removal in a microbial electrolysis cell (MEC). Up to 85% of the COD was removed at a COD loading rate of ~30 g COD m⁻² d⁻¹ in the MEC, which was dominated by (strictly) anaerobic genera, such as *Geobacter* (electroactive bacteria), *Thiopseudomonas*, a *Lentimicrobiaceae* member, *Alcaligenes* and *Proteiniphilum*. Electroactive bacteria transferred the electrons obtained by COD oxidation to the anode, generating an electric current of 0.5 and 2 A m⁻², which was about 27-46% of the current that was expected based on the observed COD removal. Apart from COD removal, urea hydrolysis took place in the MEC, increasing the TAN/TN ratio from <10% (influent) to ~100% (effluent). TAN diffusion and migration to the cathodic compartment resulted in a N loss of 11-41%. By directing the anodic effluent through the cathodic compartment, all TAN could be captured again in the effluent. Moreover, this also increased the alkalinity of the urine as the OH⁻ produced at the cathode was recovered. Overall, MEC treatment reduces the oxygen demand and limits biomass production in subsequent aerobic treatment, increases the urine alkalinity and can recover some energy from the organics. The latter should be further optimized because, despite the high COD removal efficiencies, a low current output was achieved.

A nitrification bioreactor was used to convert urea and/or TAN into nitrate in **Chapter 2, 3 and 5**. Treatment in the aerobic bioreactor also yielded urea hydrolysis and ~90%

COD removal in Chapter 2 and 5, whereas almost all biodegradable COD had been removed by a MEC prior to nitrification in Chapter 3. Three different reactors were employed: a pilot scale MBBR (Chapter 2), a bench scale MABR (Chapter 3) and a bench scale MBBR (Chapter 5) (Table 7.1). MABR reactors have a high oxygen utilization efficiency, compact design and are compatible with the reduced gravity conditions in space, but, due to their counter-diffusional biofilm, there is a higher risk for denitrification. Indeed, feeding the MABR directly with raw urine in Chapter 3 resulted in N loss (18%) due to denitrification, whereas bio-electrochemical COD removal prior to nitrification allowed to recover all N in the MABR. Full urine nitrification (conversion of all TAN into nitrate) is preferred over partial nitrification because of the higher process stability and safety, but requires additional alkalinity to compensate for the proton release by nitrification. The alkalization step provided some additional alkalinity, but this was not sufficient to obtain complete TAN conversion (Chapter 5). Therefore, the nitrification reactors in Chapter 2 and 3 were equipped with NaOH control. In Chapter 5, the nitrification reactor was coupled to a dynamically controlled electrochemical cell to study in-situ electrochemical hydroxide production as an alternative to NaOH addition, enabling full nitrification while avoiding the use of NaOH, the logistics associated with base storage and dosing, and the associated increase in salinity. Similar to the electrochemical cell used in Chapter 4, the bioreactor content was recirculated over the cathodic compartment of the electrochemical cell, where water and/or oxygen reduction produced hydroxide ions, which compensated for the acidification caused by nitrification. Overall, stable, full urine nitrification was obtained in all nitrification reactors at urine concentrations of 17% to 40% (i.e., urine dilution factors of 6 to 2.5) and maximum loading rates between 200 and 300 mg N L⁻¹ d⁻¹ without substantial N loss. TAN and/or nitrite accumulation only occurred in case of technical issues (such as pH control failure or influent dosing problems). All reactors showed robustness against fluctuating influent N concentrations, loading rates and operational conditions.

Nitrified urine can be applied as a fertilizer, but the nutrient concentrations are relatively low compared to synthetic fertilizers. Hence, for terrestrial applications, a concentration step is preferred in order to reduce the storage and transportation volumes. **Chapter 2** explored the feasibility of ED to concentrate nutrients. About 70% of the ions were captured in 15% of the initial volume when the pilot installation was operated using a 20% urine solution at a volumetric salt loading rate of 240 mmol NaCl-eq L⁻¹ d⁻¹. Nitrate, phosphate and potassium were concentrated by factors 4.3, 2.6 and 4.6, respectively. Doubling the urine concentration from 20% to 40% further increased the ED recovery efficiency by ~10% and decreased the volume ratio of diluate to concentrate from 5.8 to 4.

Table 7.1: Overview of some key parameters of the nitrification reactors studied in Chapter 2, 3 and 5.

	Chapter 2	Chapter 3 ^a	PN ^b	Chapter 5 FN-NaOH	FN-EC ^c
Purpose	nitrification & COD removal	nitrification		nitrification & COD removal	
Reactor type	MBBR	MABR		MBBR	
Reactor volume [L]	30.7	0.5		3.2	
pH control strategy	NaOH addition	NaOH addition	-	NaOH addition	electrochemical OH ⁻ addition
Pre-treatment	alkalinization (pH 11)	alkalinization (pH 11-12) & MEC treatment		alkalinization (pH 12)	
Influent [vol%urine]	20 or 40	33	33	33	33
N loading rate [$mg\ N\ L^{-1}\ d^{-1}$]	214 ± 85	198 ± 16	251 ± 18	289 ± 33	277 ± 25
COD loading rate [$mg\ COD\ L^{-1}\ d^{-1}$]	154 ± 40	35 ± 3	210 ± 9	292 ± 28	196 ± 13
HRT [d]	5 (20%) - 8.6 (40%)	8.8 ± 0.5	7.0 ± 0.3	6.1 ± 0.2	7.1 ± 0.3
DO [$mg\ O_2\ L^{-1}$]	>5	0.10 ± 0.12	>5	>5	>5
EC [$mS\ cm^{-1}$]	10.5 ± 1.2 (20%) 17.3 ± 1.1 (40%)	17.4 ± 0.3	10.4 ± 1.1	15.7 ± 1.6	5.3 ± 1.3 ^d

^a results from phase MEC IV are shown

^b results from phase PN-I on electrochemically stabilized urine (pH 12)

^c results from configuration 1, pH set-point 7.5

^d low EC caused by anion migration across the AEM of the electrochemical cell

Besides providing alkalinity to enable full nitrification, the electrochemical cell installed in the bioreactor in **Chapter 5** functioned as concentration technology, yielding a clean acidic nitrate-rich side stream and a nitrate-depleted urine stream. Configuration 2 enabled anion extraction and concentration, whereas in configuration 3 both anions and cations were extracted. Similar to ED, ~70% of the nitrate could be recovered and a concentration factor of ~3 was obtained. In contrast to ED which yielded a concentrate with a neutral pH, the concentrate of the electrochemical cell had a pH below 2 due to proton migration from the anolyte.

Alternatively, nitrified urine can be valorized as culture medium for microalgae. **Chapter 6** provided a proof of concept of *Limnospira indica* cultivation on the nitrified urine produced in Chapter 5. Dilution proved to be important to obtain high N utilization efficiencies, as the N uptake is limited by the biomass concentration which is in turn limited by the light availability. Furthermore, supplementation with limiting elements was required to obtain a high yield and N uptake. Nitrified urine supplemented with phosphorus, magnesium, calcium, iron, EDTA and trace elements was as effective as standard synthetic medium in terms of biomass production, nutrient uptake and protein yield. Urine precipitates harvested in the alkalization step could potentially supply enough phosphorus, calcium and magnesium, requiring only external addition of iron, EDTA and (possibly) trace elements. Carbon dioxide (in the atmosphere or in flue gases) can be used as inorganic carbon source, rendering CO₂ sequestration.

7.2 Strengths, challenges and potential bottlenecks for technology development and implementation

7.2.1 Strengths

The process configuration can be tailored, offering versatility for applications on Earth and in space.

The urine treatment trains consist of a sequence of multiple interchangeable building blocks, that can be exchanged or omitted depending on the application, resulting in different levels of complexity. In principle, a nitrification bioreactor can be used as standalone technology with only air or oxygen gas as an external input. Yet, without alkalization step, urea hydrolysis would occur in the urine collection system, resulting in scaling, clogging, odor nuisance and reducing the recovery potential (due to P loss by uncontrolled precipitation and N loss by ammonia volatilization). Without additional alkalinity, partial nitrification would be obtained, which is more prone to process failure, because of the suboptimal pH and high TAN fraction. Moreover, without concentration step, storage and transportation of the (partially) nitrified urine to arable land would be extremely costly and unsustainable. Hence, to circumvent these issues, it is recommended to add an alkalization and concentration step. Depending on the scenario, a certain set of technologies can be chosen.

Many of the explored (bio)electrochemical technologies could also function as standalone technology or be combined with other urine treatment technologies. Bio-electrochemical cells for instance can be used to generate electricity from urine (e.g., Pee Power urinal developed by the Bristol Robotics Laboratory and Oxfam which is used on festivals or in refugee camps), while the on-site electrochemical urine alkalization is a promising new concept to facilitate urine collection and storage and can be combined with e.g., urea recovery technologies.

The versatility of electrochemical systems enables to tweak the make-up and quality of the end product. Some treatment train configurations enable recovery of almost all valuable urine compounds, whereas other combinations only target specific compounds (e.g., nitrate). The integration with microalgae cultivation yields microbial biomass, which can be used as a food ingredient for humans, a feed ingredient for livestock production, a biofuel feedstock for energy production or as an organic fertilizer for plant nutrition.

(Bio)-electrochemical systems are keystone technologies for resource efficient urine recycling using nitrification

Chapter 2, 3, 4 and 5 demonstrated the feasibility and added value of several (bio)-electrochemical systems in achieving resource efficient urine recycling with maximum nutrient recovery and minimal energy expenditure and use of consumables.

Electrolysis cells enable in-situ production of acids and bases, which are needed in several stages of the urine treatment train and represent a nuisance (because they are costly, require storage capacity and safety measures). For deep-space missions, the use of consumables is restricted because of payload limitations. Base is required for alkalization of the urine (to prevent urea hydrolysis during storage and to decrease the scaling potential of urine) and to obtain full nitrification. The acids generated at the anode could be used to periodically rinse the urine diverting toilet to remove scaling and to hygienize and suppress microbial activity. In RLSS, acids could be dosed to a hydroponic plant cultivation system to compensate for the release of OH^- ions that accompanies nitrate uptake by most plants. Besides OH^- and H^+ , hydrogen gas and oxygen gas are produced at the cathode and anode, respectively. Hydrogen gas can be recovered and valorized as an energy source, whereas oxygen gas can be directed to the nitrification reactor where it is required for TAN and nitrite oxidation by nitrifying bacteria and COD oxidation by heterotrophic bacteria.

The electrolysis cell studied in Chapter 5 additionally extracted nitrate from the nitrification reactor, yielding a refined and concentrated nitrate-rich product. Alternatively, ED can be used to concentrate the nutrients in nitrified urine to decrease the storage and transportation volumes.

Removing the COD in a microbial electrolysis cell prior to membrane aerated nitrification proved to be key in preventing N losses through denitrification and allowed MABR operation at a high urine loading rate, reducing the required reactor volume. Incorporating a MEC offers many advantages including i) energy efficient COD removal

since no aeration is required to remove the COD and some energy can be recovered from the organics, and ii) OH^- production at the cathode, which increases the alkalinity of the urine, thereby reducing the OH^- demand for full nitrification.

7.2.2 Practical considerations and potential bottlenecks

The need for a highly robust system

Robustness and safety are two critical determinants for the success of a technology. In the first place, the urine treatment train must meet a very high level of robustness and reliability, be highly automated and require minimal maintenance, especially in space, where the time of astronauts is limited and where there is no or very limited access to spare equipment. Also for on-site or decentralized treatment on Earth, a high level of automation and minimal maintenance is important, as operator costs and maintenance costs can significantly increase the overall cost and thus affect the economic feasibility.

A first challenge is the biology involved in several steps of the urine treatment train (i.e., in the MEC, nitrification reactor and photobioreactor), as biological systems require a certain start-up time (i.e., for biofilm formation on electrodes or carriers) and continuous (not interrupted) operation.

The complexity of the developed multistage urine treatment trains presents another challenge. The more units, the higher the risk for failure and, unfortunately, failure in one unit can affect the operation of the downstream units. A problem in the MEC unit, for instance, can result in a higher COD input in the MABR, leading to oxygen depletion, which causes a loss of nitrogen through denitrification and TAN or nitrite accumulation. High levels of TAN or nitrate can inhibit nitrification, and nitrite could cause inhibition in the subsequent microalgae cultivation reactor [90, 113].

This illustrates the need for careful process monitoring and control, a detailed risk assessment and mitigation strategies. To deal with the increased oxygen demand in the MABR in the previous example, an additional hollow fiber membrane unit could be installed and switched on to temporarily increase the oxygen transfer, while attempting to restore the MEC performance.

Currently, most of the technologies are only tested at lab scale (except for the pilot scale installation used in Chapter 2). The integration and real time control over the different processes is a hurdle still to overcome. The robustness of the treatment trains should be evaluated in long-term tests, in which operational parameters are varied to mimic failures (e.g., a temperature or pH control failure resulting in a sub/superoptimal temperature or pH).

Safety concerns

When producing fertilizers or food from urine, particular attention needs to be directed towards safety with respect to pathogens and micropollutants (e.g., pharmaceuticals) [151, 231, 289]. According to literature, pathogens and micropollutants might be partially

removed or inactivated by alkalization and nitrification [22, 231]. If membrane based technologies (ED/electrolysis cell) are included in the treatment train, the residual pathogens and micropollutants are retained by the ion-exchange membranes, although breakthrough might occur over time [82, 229, 231]. Hence, to ensure that the ED concentrate and middle compartment of the electrolysis cell are free of contaminants, an additional treatment step such as activated carbon adsorption, UV or ozone treatment is recommended [151, 231, 233, 289]. In combination with microalgae production, this step should be introduced between the nitrification reactor and photobioreactor. Interestingly, disinfectants could be produced in the anodic compartment of the electrochemical cell. Depending on the type of electrode, chlorine or reactive oxygen species (ROS, i.e., peroxide, superoxide and hydroxyl radicals) could be generated at the anode. Further research is required to investigate how this affects the fertilizer potential of urine (e.g., due to formation of chlorinated by-products) and whether it is compatible with subsequent plant or microalgae cultivation.

Biological treatment can furthermore introduce harmful microorganisms in urine. The use of open, mixed microbial communities consisting of unknown species, which might be pathogenic, presents a health hazard to the operators or crew members, especially in confined space cabins [48, 52]. Moreover, complex microbial communities and interactions might be more difficult to understand and to capture in a mechanistic mathematical model [48]. Therefore, in MELiSSA, axenic synthetic cultures are preferred to eliminate the risk for pathogen spreading and to facilitate mechanistic modeling. Within MELiSSA, nitrification is envisaged to be carried out by a coculture of *Nitrosomonas europaea* (AOB) and *Nitrobacter winogradskyi* (NOB) and *Limnospira indica* is the selected microalga [105]. The microbial community analysis of the MEC and nitrification reactors in Chapter 2 and 3 can be useful to identify suitable candidates to engineer a synthetic MEC community and to find strains capable of urea hydrolysis. For terrestrial applications, reactors with open communities are probably more convenient, due to the complexity of axenic reactor construction and operation. Furthermore, open mixed communities usually achieve higher conversion rates (thus requiring lower reactor volumes) and display a larger robustness. Open microbial communities are self-organizing and diverse, and can better cope with changing conditions and microbial invasions due to functional redundancy (all niches are covered by multiple community members) [48]. Membrane filtration and post-treatment can be implemented to produce a sterile end-product.

Furthermore, hydrogen and oxygen gas production in the electrolysis cells presents a safety risk. Without proper separator (e.g., gas-impermeable ion exchange membrane), a flammable, potentially explosive mixture of H₂ and O₂ could be formed due to convection or diffusion of the gasses across the membrane [320]. Hydrogen has a very wide flammability range (from 4 to 75% in air) and very low ignition energy, so a proper risk management of the system is required for applying this technology on a large scale. Likely the introduction of an open air cathode with gas diffusion layer can alleviate

this concern by avoiding hydrogen production besides minimizing energy requirements. Space agencies have developed extensive experience in the safe handling of hydrogen and operation of alkaline or PEM electrolyzers and fuel cells on-board the ISS [118]. PEM electrolyzers (i.e., with proton exchange membrane/polymer) are used to generate oxygen for breathing and hydrogen from water [30]. The hydrogen is recombined with exhaled CO_2 to water and CH_4 (Sabatier process). PEM fuel cells generate electricity and water using hydrogen and oxygen as the fuel and oxidant [30].

Technology-specific challenges

Challenges and potential bottlenecks for implementation and recommendations for future research and optimization are identified and discussed for each technology below.

Electrochemical urine alkalization

- Installation of the electrochemical cell near the toilet:
It is important to minimize the time between urine collection and alkalization, as urea hydrolysis already starts in urine collection systems due to the ubiquity of urease-positive bacteria. Ideally, the electrochemical cell for urine stabilization is installed near the toilet or even integrated into the toilet, requiring a very compact and robust system. Periodically rinsing or flushing of the toilet with the acid produced in the middle compartment of the electrochemical cell could hygienize or suppress microbial activity in the toilet and piping between the toilet and alkalization unit.
- Preventing scaling in the electrochemical cell:
Urine alkalization promotes precipitation, thereby reducing the calcium and magnesium concentration in urine and thus decreasing the risk for scaling in downstream treatment steps, but this comes with a high risk for scaling in the alkalization unit. A proper design of the crystallizer and electrochemical cell is crucial so that precipitation mainly occurs in the crystallizer and not inside the cathodic chamber or pipes. In Chapter 4, the setup was operated as a batch system in which the pH of consecutive batches of urine was gradually increased from ~ 7 to 11-12. A high recirculation rate was applied to efficiently distribute the alkalinity generated in the vicinity of the electrode throughout the cathodic compartment and crystallizer to minimize scaling on the electrode. Alternatively, urine could be semi-continuously fed into the crystallizer, containing alkalized urine at pH 12. This way, the pH of the freshly added urine will instantaneously increase (by mixing with the alkaline urine), promoting precipitation in the crystallizer. The pH in the crystallizer can be maintained at 12 by recirculation over the cathodic compartment of a dynamically controlled electrochemical cell. Periodic cleaning in place using the acidic middle compartment fluid could remove the precipitates accumulated on the electrode surface and/or membrane.

- Precipitate collection:

An efficient precipitate collection system should be designed and installed to harvest the urine precipitates, which contain a considerable part of the P present in urine and can be valorized as slow-release fertilizers or redissolved in nitrified urine prior to microalgae cultivation, minimizing external chemical input. Even when recovery is not envisaged, precipitate collection is important as precipitates will accumulate and eventually clog the system.

- Future research and optimization:

The design of the electrochemical cell could be improved in order to minimize the energy consumption. The cell resistance could, for instance, be decreased by reducing the distance between the electrodes, which would result in a lower cell voltage. Also membrane fouling has a significant impact on the energy consumption. The AEM turned brown, probably due to the adsorption of organics to the positively charged functional groups of the AEM. It is not known whether this can affect the performance of the electrochemical cell during long-term operation. Different membranes could be tested and compared in terms of resistance (affects the energy consumption), fouling tendency and lifespan. Also the fertilizer potential of the precipitates should be further assessed.

Microbial Electrolysis cell

- Scale up of MEC:

One of the limitations of bio-electrochemical systems (BES) is the scalability [35, 167]. It is well established that large BES are less efficient due to the increased internal resistance (resulting from the larger distance between the electrodes and the larger distance electrons need to travel through the material) and the pressure drop [138, 327]. Yet, this issue can be circumvented by using multiple separate modules or by stacking multiple units in parallel or in series, which increases the voltage or current output, respectively [4, 35]. The use of multiple units can furthermore largely sustain reactor performance, when one of the units is impaired by inhibition or toxicity or affected by technical failure.

- Future research: improve energy output:

MEC operation should be further optimized in order to increase the coulombic efficiency. Only about 25-45% of the removed COD was converted into current. Other electron sinks should be identified in order to elucidate the COD gap and to improve the conversion of chemical energy into electrical energy. Analysing the different COD compounds in the influent and effluent could also gain new insights.

Nitrification

- The unique properties of urine, such as the fluctuations in composition, the high N concentration and low alkalinity, present particular challenges for nitrification. Nevertheless, stable urine nitrification could be achieved by providing additional alkalinity (NaOH or electrochemical OH⁻ addition), without major problems.
- Future research:
Future research could focus on decreasing the start-up time and investigating N₂O emissions.

Concentration with electrolysis cell or electrodialysis

- Nutrient losses are inevitable:
It is practically impossible to capture all nutrients in the concentrate of the ED unit or electrolysis cell. As a result of the equilibrium established between the diluate and concentrate stream, part of the nutrients remain in the diluate. The overall nutrient recovery could be improved by feeding the diluate to a second ED unit to recover a part of the remaining nutrients. This would, however, greatly increase the costs and energy consumption (because of the lower conductivity of the streams in the second ED unit).
- Concentration is limited by osmotic and electro-osmotic water transport and back diffusion:
Relatively low concentration factors present a second limitation inherent to the ED and electrolysis cell due to the osmotic and electro-osmotic water transport. A high concentration gradient between the diluate and the concentrate leads to increased osmotic water transport from diluate to concentrate and back diffusion of ions from concentrate to diluate, which in turn limits the maximum achievable concentration factor. Decreasing the concentrate volume by means of distillation is an option to concentrate the nutrients in a smaller volume. In contrast to ED or the electrolysis cell, distillation can remove almost all water, but the high energy demand presents a major drawback of the process. However, when combined with ED or the electrolysis cell, ~60-80% of the water can be removed prior to distillation, reducing the overall energy demand. Thus, a combination of ED or the electrolysis cell and distillation could offer a maximal concentration of nutrients with a minimal input of energy.

Microalgae cultivation

- Light requirement results in a relatively large land-use:
Microalgae production has a relatively large land-use compared to other sources of microbial protein (i.e., bacteria) because of the light requirement and lower growth

rates. The biomass concentration is limited to several grams per liter due to light limitation (self-shading). Depending on the application and the availability of local resources (e.g., waste stream rich in organics), other types of microorganisms might be more appropriate for microbial protein production. Aerobic heterotrophic bacteria, for instance, grow on organics as carbon and energy source and have higher growth rates compared to microalgae [206]. High biomass concentrations can be reached as they do not depend on light, resulting in a lower land-use. For space applications, microalgae likely remain the best option, as, besides being a source of food for the astronauts, they are important for atmosphere revitalization.

- Quality of the microalgal biomass:

Further research is required to assess the quality and safety of microalgal biomass cultivated on urine. A potential concern is the presence of heavy metals in urine, since microalgae tend to accumulate heavy metals [257]. Microbial protein also contains high levels of nucleic acids (mostly RNA, but also DNA), of which overconsumption can increase the level of uric acid in the blood, causing gout and kidney stone formation [76, 206]. Compared to other sources of microbial protein, *Spirulina* has a relatively low nucleic acid concentration (4-6%). Moreover, chemical or enzymatic post-treatment can further reduce the levels [206, 221]. Furthermore, culturing and harvesting conditions can affect the quality and safety of the produced biomass, pinpointing the need to regularly monitor the biomass composition [253]. Although *Spirulina* is believed not to produce any toxic compounds, contamination with other species might lead to the production of cyanotoxins [253]. Moreover, harvesting methods can introduce toxic elements (i.e., the use of $AlCl_3$ as a flocculant can increase the aluminum content of the biomass) [253].

7.3 On a mission to Mars

7.3.1 Optimal urine treatment train

The optimal degree of mass loop closure and the optimal design of a life support system (LSS) depend on the mission duration, as demonstrated in Figure 7.2 adapted from Wieland (1994) [312]. Besides the duration, distance is an important aspect. Due to the short distance to the ISS (two days) regular resupply remains possible, whereas deep-space missions cannot be frequently resupplied due to the long distance. For short space missions, it is advisable to take all the life support consumables on board or to resupply the mission (i.e., open LSS using nonregenerable techniques) as the mass of a RLSS is higher compared to the total mass of the required life support consumables. Nonregenerable physicochemical techniques are used, e.g., cartridges to remove CO_2 from the cabin atmosphere, and waste can be stored or vented [312]. The cumulative mass of the life support consumables linearly increases with the mission duration (Figure 7.2, Nonregenerable P/C). Therefore, as mission duration increases, a RLSS with an

increased level of closure becomes profitable as it has a lower total system/mission mass. Water is the first target to recover, as it represents about 90% of the total mass of life support consumables [74]. Physicochemical systems are the best option for space missions with an intermediate duration or distance. Longer missions or planetary bases require a hybrid-biological system, as, including biological steps in the process permits to reduce the energy requirements, to increase the overall recovery efficiency and enables food production [74, 192, 312]. Olson et al. (1984) [217] estimated that the cumulative cost and mass savings for a LSS with 50-97% food production compared to a LSS with only in-situ water recycling and O₂ production start to pay off between 1 and 12.9 years depending on the mission scenario.

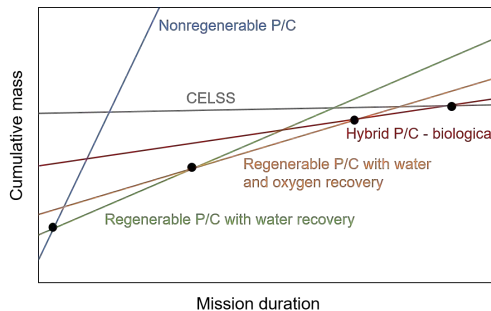


Figure 7.2: **Cumulative mass versus mission duration, based on Wieland (1994) [312].** Break-even points are indicated with black dots, whereas the initial mass of each system can be inferred from the intersection with the y-axis. P/C: physicochemical system, CELSS: controlled ecological LSS (exclusively biological processes).

The optimal urine processing method thus depends on the mission scenario.

- On short-term missions, urine can be vented or stored on-board. When urine is stored on-board, measures need to be taken to prevent ammonia volatilization (caused by urea hydrolysis). Alkalinization (with base or electrochemical OH⁻ addition) could be used to inhibit urea hydrolysis.
- On medium-term missions where water recovery is targeted, urine is an important input of the water reclamation system as it presents one of the main wastewater streams. Currently, at the ISS, water is recycled from urine, flush water, Sabatier product water and humidity condensate in the Water Recovery and Management System [38]. This physicochemical system highly depends on hazardous chemicals and is challenged by scaling. Alternatively, the urine treatment train studied in Chapter 2 could be combined with nanofiltration (NF) and reverse osmosis (RO) to recover water from urine, condensate and grey water, as demonstrated by Lindeboom et al. (under review) (Figure 7.3). Alkalinization and nitrification can stabilize urine, obviating the need for toxic chemicals (i.e., CrO₃). ED separates the

water from the nutrients, thereby decreasing the osmotic load to the subsequent membrane systems. The ED diluate is mixed with grey water and treated with NF and RO to recover water.

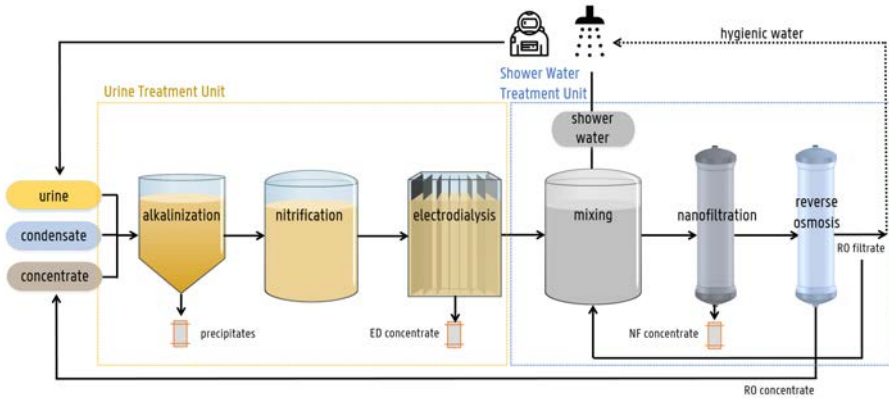


Figure 7.3: **Water recovery from urine through alkalization, nitrification, electro dialysis, nanofiltration and reverse osmosis.**

- On medium-term missions, besides water, inert nitrogen gas, the primary component of the cabin atmosphere, could be recovered from urine. Leakage overboard during cargo resupply or extra vehicular activities (EVA, e.g., space walks) accounts for a significant usage of N₂ to repressurize the space cabin. In-situ production of N₂ from urine could reduce the need for N₂ resupply. N₂ can be produced by means of nitrification/anammox in an MABR. The optimal treatment train in this case (enabling N₂ and water recovery) consists of: alkalization, nitrification-anammox MABR, ED, NF and RO.
- For long duration missions (e.g., a crewed planetary base), nutrient recovery from urine becomes important as a significant fraction of the nutrients in a RLSS ends up in urine. The optimal urine treatment train consists of electrochemical stabilization, a MEC and MABR with in-situ electrochemical OH⁻ addition in order to minimize the use of consumables and maximize the recovery. In contrast to terrestrial applications, a concentration step does not present an added value in space. Figure 7.4 shows how this urine treatment train could be integrated within MELiSSA. After collection, urine is immediately treated in an electrochemical alkalization unit (C1B) in order to prevent urea hydrolysis, while other waste streams (faeces, toilet paper, non edible parts of plants...) are processed in a thermophilic anaerobic fermenter (C1A). Urine is not added to the fermenter to prevent inhibition by the high TAN concentration (resulting from urea hydrolysis). Subsequently, the fermenter effluent is mixed with the alkalized urine and treated in a bio-electrochemical system (MEC or MFC) to convert volatile

fatty acids (in the fermenter effluent) and urine organics into CO_2 . The dilution resulting from mixing the urine with fermenter effluent will facilitate MEC treatment (lower anolyte pH) and subsequent MABR treatment (lower N concentration). In the next compartment, the MEC effluent is nitrified in an MABR coupled to an electrochemical cell to enable full nitrification. The urine precipitates harvested in the stabilization unit are added to the effluent of the MABR before feeding to the hydroponic unit and photobioreactor.

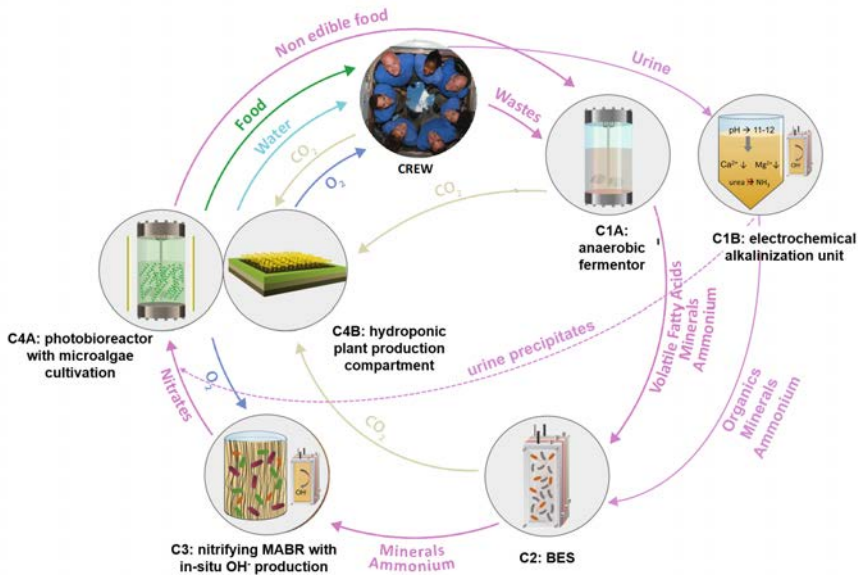


Figure 7.4: **Modified MELiSSA loop.**

7.3.2 Design of a urine treatment train for deep-space missions

Based on the results obtained in Chapter 2-6, a urine treatment train was designed for a space mission with 6 crew members (Figure 7.5, Table 7.2). Urine is collected in a storage tank in which the pH is kept at 12 by recirculation over a dynamically controlled electrolysis cell. The size of the storage tank is estimated at 9 L, which corresponds to an average HRT of 1 day to homogenize the urine. The electrode surface of the electrochemical cell was estimated at 400 cm^2 (considering a safety factor of 5 to handle pulse loadings resulting from the discontinuous urine influx) to guarantee a sufficiently high pH in the storage tank. Alkalinized urine is subsequently fed into a MEC with was dimensioned with a surface of about 2.16 m^2 based on the COD loading obtained in Chapter 3. The real surface can probably be reduced as the MEC in Chapter 3 was not pushed to its limits (probably the MEC could handle higher loading rates). Moreover, the required surface depends on the type of electrode and design of the cell (e.g., flat sheets

versus granules). Ideally, multiple MEC units are used as large MEC are less efficient and the reactor performance can be largely sustained when one unit fails. An MABR with a total volume of 120 L is required to nitrify all urine. Similar to the MEC, it is advisable to work with multiple MABR modules to ensure sufficient capacity upon failure of one unit. Biomass management in the MABR can be achieved by periodically replacing one of the modules by a new module, preventing biomass accumulation and allowing for the development of a new biofilm. The electrolysis cell used for in-situ hydroxide production to enable full nitrification should have an electrode surface of about 300 cm². The photobioreactor for *Limnospira* cultivation is the biggest reactor of the urine treatment train. A volume of 580L is required, considering the N uptake rates obtained in Chapter 6. The volume could be reduced by using a short-path photobioreactor, as light is the main limiting factor. Another option would be to redirect a part of the nitrified urine to a hydroponic unit to cultivate plants.

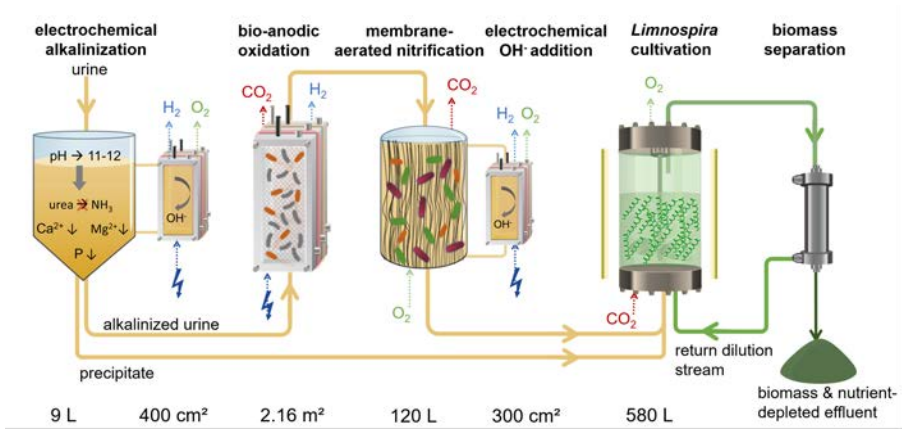


Figure 7.5: **Design of a urine treatment train for a space mission with 6 crew members.**

Table 7.2: **Design of a urine treatment train for a space mission with 6 crew members.**

Urine production	$[L \text{ urine } IE^{-1} d^{-1}]$	1.5
Storage tank		
Size (HRT=1d) ^a	$[L IE^{-1}]$	1.5
Electrochemical cell for alkalinization		
Electric charge to reach pH 12 (Chapter 4)	$[C L^{-1} \text{ urine}]$	7000
Current density	$[A m^{-2}]$	100
Required electrode surface area (safety factor of 5) ^b	$[m^2 IE^{-1}]$	0.0061

Electrochemical energy consumption (Chapter 4)	$[Wh_{el} L^{-1} urine]$	14.5
	$[Wh_{el} IE^{-1} d^{-1}]$	21.75
Cathodically generated H_2	$[mol H_2 IE^{-1} d^{-1}]$	0.05
	$[g H_2 IE^{-1} d^{-1}]$	0.11
Anodically generated O_2	$[mol O_2 IE^{-1} d^{-1}]$	0.03
	$[g O_2 IE^{-1} d^{-1}]$	0.87
Microbial electrolysis cell (MEC)		
Average COD load ^c	$[g COD IE^{-1} d^{-1}]$	9
COD loading achieved in Chapter 3	$[g COD m^{-2} d^{-1}]$	30
MEC size	$[m^2 IE^{-1}]$	0.3
MEC size with safety margin (+20%) ^d	$[m^2 IE^{-1}]$	0.36
Electric charge generated with 100% RE and CE	$[C L^{-1} urine]$	72364
	$[C IE^{-1} d^{-1}]$	108546
Cathodically generated H_2	$[mol H_2 L^{-1} urine]$	0.375
Membrane-aerated biofilm reactor (MABR)		
N load	$[g N IE^{-1} d^{-1}]$	9
N loading achieved in Chapter 3 (active volume)	$[g N L^{-1} d^{-1}]$	0.56
MABR size	$[m^3 IE^{-1}]$	0.016
MABR size with safety margin (+20%) ^d	$[m^3 IE^{-1}]$	0.019
Nitrogenous oxygen demand (NOD)	$[g O_2 g^{-1} N]$	4.33
	$[g O_2 IE^{-1} d^{-1}]$	38.97
Electrochemical cell for in-situ hydroxide production to enable full nitrification		
Electric charge to counteract acidification (Chapter 5)	$[C L^{-1} urine]$	28829
Current density	$[A m^{-2}]$	100
Required electrode surface area ^e	$[m^2 IE^{-1}]$	0.005
Electrochemical energy consumption (Chapter 5)	$[Wh_{el} L^{-1} urine]$	23.4
	$[Wh_{el} IE^{-1} d^{-1}]$	35.1
Cathodically generated H_2	$[mol H_2 IE^{-1} d^{-1}]$	0.22
	$[g H_2 IE^{-1} d^{-1}]$	0.45
Anodically generated O_2	$[mol O_2 IE^{-1} d^{-1}]$	0.11
	$[g O_2 IE^{-1} d^{-1}]$	3.59
Photobioreactor with <i>Limnospira</i> cultivation		
N load	$[g N IE^{-1} d^{-1}]$	9
Volumetric N uptake rate achieved in Chapter 6	$[g N L^{-1} d^{-1}]$	0.112
PBR size (to achieve near 100% N utilization)	$[m^3 IE^{-1}]$	0.080

PBR size with safety margin (+20%) ^d	$[m^3 IE^{-1}]$	0.096
Biomass production (Chapter 6)	$[g N g^{-1} VSS]$	0.11
Daily biomass production	$[g VSS IE^{-1} d^{-1}]$	82

^a A HRT of 1d should be sufficient to obtain a rather stable influent flow for the MEC

^b A relatively high safety factor was considered due to the discontinuous urine supply

^c Assuming an average COD and N concentration of 6 g COD L⁻¹ and 6 g N L⁻¹

^d A safety margin of 20% was added to ensure that the reactor can handle a temporary increase in load

^e No safety margin was added since the current density can be increased in case of an increased OH⁻ demand

7.3.3 Readiness towards space

Space is a resource-scarce, harsh and hostile environment, in which living organisms are subjected to broad ranges of gravity and ionizing radiation. As microorganisms play a key role in the urine treatment trains, in depth research on the long-term effects of radiation and microgravity on these key players is pivotal. Within MELiSSA, the capacity of nitrifiers and microalgae to survive in microgravity and increased radiation conditions has been established in LEO flight experiments (BISTRO, NITRIMEL and ArtemISS). The urea hydrolysis, nitritation and nitratation activity of both axenic cultures as well as mixed nitrifying communities could be restored after a LEO flight experiment [134, 175]. The next development step would be to test their activity in a nitrification MABR in space conditions. The activity of microalgae has already been demonstrated in a photobioreactor on board the ISS (ArtemISS project). Further research is needed to investigate whether a synthetic community can be developed for the MEC and to assess the survival and activity of this community in space. Moreover, to enable deep-space missions, the activity of all key players should be demonstrated beyond LEO, where they are confronted with higher levels of radiation (including cosmic galactic radiation and solar particle events). The Lunar Gateway could be a good testing platform for this.

The reduced gravity in space also affects the operation of (bio)reactors, by impeding gas/liquid/solid interactions. The MABR is already fit for application in space, but the design of the electrolysis cells, MEC and photobioreactor should be adapted to enable operation in a reduced gravity environment. In the MEC, a gas diffusion air cathode could be used for instance to prevent the production of hydrogen gas, which would be difficult to separate from the liquid in reduced gravity. Furthermore, the urine treatment train should be evaluated by the Advanced Life Support System Evaluator (ALiSSE), a multi-criteria tool developed by ESA to assess the volume and mass, energy input, workload on the crew and efficiency, reliability and safety.

7.4 Implementation of urine recycling on Earth

7.4.1 Optimal urine treatment train

Urine source separation and recycling gains attention on Earth to shorten the terrestrial nutrient cycles, to facilitate wastewater treatment, to save water and/or to reduce environmental pollution. In contrast to space applications where high recovery efficiencies are critical and concentration does not present an added value, terrestrial applications do require a concentration step (to facilitate transportation and use) and a trade-off should be made between high recovery efficiencies and other factors such as cost effectiveness, energy consumption and footprint. Other differences include i) the gravity on Earth which facilitates bioreactor design and operation (e.g., no need for membrane aeration) and ii) the economic feasibility, as urine diversion will only be implemented on a large scale when economically viable.

Urine treatment can occur on-site or in a decentralized treatment facility. The latter benefits from the economies of scale (the cost per volume of urine decreases as the total volume of treated urine increases), but requires transportation to the facility. For small scale scenarios, decentralized treatment in a nearby facility is probably the best option. E.g., in a building where 100 people work, about 15-20 m³ of urine can be collected per year in a storage tank, which has to be emptied and transported to the treatment facility only one or two times a year. For large buildings (universities, schools, airports...), on the other hand, on-site treatment might be more competitive. A third option is the use of a mobile treatment facility, such as the Vuna-mobile [305].

To prevent malodor, scaling and blockages in urine diverting toilets and pipes, urine stabilization is recommended, which has to be done on-site as urea hydrolysis already starts in collection systems [160]. Electrochemically induced stabilization and precipitation, developed and studied in Chapter 4, is a promising new concept to inhibit urea hydrolysis. A disadvantage is the need for pumps and an advanced control system to dynamically control the electrochemical cell. A more 'low-tech' alternative, not requiring any pumps or control/dosing systems, is Ca(OH)₂ addition, as demonstrated by Randall et al. (2016) [240] and used in the Autarky toilet, the on-site resource recovery toilet under development in the Blue Diversion Autarky project. Disadvantages of this approach include i) the chemical input and ii) the fact that the scaling potential is not reduced (due to calcium addition).

Since the energy recovery from the MEC is currently limited by the low coulombic efficiency and N losses in the nitrification reactor are less detrimental on Earth, it is likely more convenient to remove COD in a nitrification reactor instead of a MEC. This way, only one bioreactor is required, but it results in a slightly higher oxygen demand in the nitrification reactor.

Nitrification can occur on-site or in the decentralized treatment facility. In principle, any reactor design can be used, but biofilm-based systems are usually preferred for urine nitrification since relatively long SRT are required. MABR can achieve higher

oxygen utilization efficiencies (thereby reducing the energy consumption) compared to MBBR, but have a higher capital cost and biofilm management is more challenging.

Nitrification should be followed by a concentration step. The electrolysis cell achieved similar recovery efficiencies and concentration factors as electrodialysis, while concomitantly enabling full nitrification. Hence, an electrolysis cell seems the best option. In large installations, microalgae production can be implemented (e.g., in raceway ponds).

To conclude, a urine treatment train composed of an electrochemical cell for alkalization, a bioreactor for nitrification and COD removal equipped with an electrochemical cell for in-situ pH control and concentration is proposed as the best option for terrestrial urine recycling. A design is presented in the following section for different scenarios.

7.4.2 Design of a urine treatment train

The dimensions of the individual reactors in the urine treatment train for a single household with 4 people and a workplace with 25 to 1000 people were extrapolated from the results in Chapter 3, 4 and 5 (Table 7.3).

Table 7.3: Size of the electrochemical cell for alkalization, nitrification reactor and electrochemical cell for concentration and an estimation of the amount of N and P that can be recovered in different situations (household with 4 people or workplace with 25, 100, 200, 500 or 1000 people). The same methodology as in Table 7.2 was used. RE: recovery efficiency.

		Household		Workplace			
		4	25	100	200	500	1000
Number of inhabitants/workers		4	25	100	200	500	1000
% of urine collected per person	[%]	60	30	30	30	30	30
Urine production	[$L d^{-1}$]	3.6	11	45	90	225	450
Electrochemical cell for alkalization	[m^2]	0.01	0.05	0.18	0.36	0.91	1.82
Nitrification reactor	[m^3]	0.04	0.12	0.48	0.96	2.41	4.82
Electrochemical cell for in-situ hydroxide production and concentration	[m^2]	0.01	0.0	0.2	0.3	0.8	1.5
N recovered (70% RE)	[$kg N year^{-1}$]	5.5	17	69	138	345	690
P recovered (70% RE)	[$kg P year^{-1}$]	0.7	2.2	8.6	17.2	43.1	86.2

7.4.3 Barriers for terrestrial urine recycling

Economic prospect of urine treatment and recycling

Producing and selling urine-derived fertilizers does not seem to be lucrative due to the low market value of nutrients (e.g., €430 ton⁻¹ N, €950 ton⁻¹ P and €380 ton⁻¹ K). Derese et al. (in preparation) estimated the total value of urine nutrients at €5.11 m⁻³, of which the majority comes from N (up to 67%). Currently, P only adds €0.8 m⁻³ urine, however, due to the rapidly shrinking P reserves, the market price is expected to rise in the future which can make P the highest value compound in urine and can increase the total value of urine. Still, it is clear that nutrient recovery from urine at current market prices has to be very cost-effective (<€4 m⁻³) to generate profit from urine-based fertilizer sales. Moreover, impurities might decrease the value of urine-derived fertilizers.

Besides the sale of urine-derived fertilizers, urine diversion and separate treatment can raise revenues by lowering water bills (due to water savings by the use of low-flush toilets), and by reducing operational costs of WWTP (due to the reduced nutrient load) and pollution-related costs. The latter two, however, present downstream benefits which are hard to cash, unless specific agreements with water treatment companies and the government are made to reward sustainable urine diversion and treatment initiatives. At present, converting nutrients recovered from urine into value-added products, such as microbial protein, is possibly the easiest way to make profit from urine diversion.

Due to the large infrastructural needs (multiple treatment train modules and auxiliary equipment including pumps, sensors and control systems), it is probably not economically viable to install the complete urine treatment train at small scale (households or small buildings). Therefore, it might be better to target sites where large volumes of urine can be collected and treated on-site (e.g., university buildings, schools, office buildings...).

User acceptance and legislation

Besides economic viability, social acceptance by consumers and farmers might present a barrier for widespread implementation of urine diversion and treatment. In general, urine source separation is a well-accepted idea [160]. In user surveys, most people indicate to be satisfied about urine diverting toilets (e.g., NoMix) and to accept reuse of human urine as fertilizer [171]. Also farmers are willing to apply urine fertilizers as long as they are safe, cost-competitive and convenient [160].

Furthermore, urine-based fertilizers should be legally approved before they can be commercialised and applied. Regulatory frameworks regarding the use of human excreta and quality standards for the produced fertilizers are still lacking in many countries [246].

7.5 Outlook

7.5.1 'A journey of a thousand miles begins with a single step' - Chinese proverb

A journey to Mars, on average 140 million miles away from Earth, presents many challenges, including the development of a robust and efficient 'next generation' regenerative life support system for in-situ oxygen, water and food production and waste management. In this PhD thesis, a resource efficient bio-physico-chemical urine treatment train was developed, which could be integrated in a regenerative life support system such as MELiSSA. Promising results were obtained, but there is still a long way to go. The integration and real time control of the different processes and a long-term evaluation of the safety, stability and robustness of the system, are hurdles to overcome before the system could be tested in real space conditions. The adaptation to the microgravity and reduced gravity conditions to enable operation on transit vehicles and Lunar or Martian bases is expected to be the major obstacle to application in space, as most of the processes involve liquid-gas-solid interactions.

7.5.2 Urine source separation can contribute to a more sustainable, circular future on Earth

Scientific and technological advancements from research into regenerative life support systems can drive technological innovation on Earth in many areas such as bioprocessing, circular technology, cleantech and life sciences [2, 53]. The urine recycling technologies developed in this PhD open opportunities for efficient urine collection and nutrient recovery from urine on Earth, thereby reducing the need for energy intensive ammonia production using the Haber-Bosch process and mining of non-renewable phosphorus and potassium. Yet, nutrient recovery from urine could only replace a small fraction of the current fertilizer production, as major nutrient losses occur in agriculture or in other steps of the food production chain. Hence, minimizing these losses in agriculture will be pivotal for a more sustainable future. Besides, other nutrient-rich streams should be targeted to further close nutrient cycles on Earth. Nutrient recovery from animal manure deserves prime attention, as about five times more nutrients end up in animal manure compared to human waste [313]. Microbial protein production (to partially substitute plant and animal protein) could also significantly reduce the need for nutrients due to higher nutrient conversion efficiencies, leading to a more sustainable food production chain. Other benefits from microbial protein production include the lower fresh water consumption, land usage and greenhouse gas emissions.

Besides nutrient recovery, water scarcity and wastewater management are other important drivers for terrestrial urine source separation. The use of low-flush toilets can significantly reduce domestic water consumption. There is a need for a paradigm shift in urban wastewater management from the end-of-pipe approach toward a resource-

oriented approach, as currently large amounts of nutrients and energy are wasted. Unfortunately, the water sector is quite reluctant to major innovations, hampering the widespread implementation of urine source separation [161]. Developing countries have great potential to implement urine diversion and reuse. Urine diversion could boost the sanitation coverage, without the need to install expensive sewer systems and centralized WWTP, in addition to providing a cheap source of fertilizer and reducing environmental pollution [241].

During the past decade, numerous recovery technologies have been proposed and evaluated, but there is no 'one-size-fits-all' solution. Hence, case by case, the best available technology that fits the purpose will need to be determined and implemented. Despite the large interest for urine diversion in the academic world, urine source separation is only scarcely put into practice thus far [188].

The major obstacle to application on Earth is expected to be the economic feasibility, as the value of nutrients is low. Hence, to be economically viable, technologies should be very cost-effective or the recovered resources should be converted into value-added products, such as microbial protein. Moreover, urine source separation could be promoted through subsidies or by introducing sustainability targets and goals to bridge the gap between economy and the environment. To quote Wangari Maathai: '*The environment and the economy are really both two sides of the same coin. If we cannot sustain the environment, we cannot sustain ourselves*'.

Bibliography

- [1] Abey Suriya, K., Fam, D., and Mitchell, C. Trialling urine diversion in Australia: technical and social learnings. *Water Science & Technology* 68, 10 (2013), 2186–2194.
- [2] Adams, C., Andersson, I., and Feighery, J. Water for two worlds: Designing terrestrial applications for exploration-class sanitation systems. SAE technical paper 2004-01-2269 (2004).
- [3] Adamsson, M. Potential use of human urine by greenhouse culturing of microalgae (*Scenedesmus acuminatus*), zooplankton (*Daphnia magna*) and tomatoes (*Lycopersicon*). *Ecological Engineering* 16, 2 (2000), 243–254.
- [4] Aelterman, P., Rabaey, K., Pham, H. T., Boon, N., and Verstraete, W. Continuous electricity generation at high voltages and currents using stacked microbial fuel cells. *Environmental Science & Technology* 40, 10 (2006), 3388–3394.
- [5] Andersen, S. J., Candry, P., Basadre, T., Khor, W. C., Roume, H., Hernandez-Sanabria, E., Coma, M., and Rabaey, K. Electrolytic extraction drives volatile fatty acid chain elongation through lactic acid and replaces chemical pH control in thin stillage fermentation. *Biotechnology for Biofuels* 8, 1 (2015), 221.
- [6] Anderson, M. J., Ellingsen, K. E., and McArdle, B. H. Multivariate dispersion as a measure of beta diversity. *Ecology Letters* 9, 6 (2006), 683–693.
- [7] Andersson, E. Turning waste into value: using human urine to enrich soils for sustainable food production in Uganda. *Journal of Cleaner Production* 96 (2015), 290–298.
- [8] Antonini, S., Paris, S., Eichert, T., and Clemens, J. Nitrogen and phosphorus recovery from human urine by struvite precipitation and air stripping in vietnam. *CLEAN Soil, Air, Water* 39, 12 (2011), 1099–1104.
- [9] Anupama, and Ravindra, P. Value-added food: single cell protein. *Biotechnology Advances* 18, 6 (2000), 459–479.
- [10] Aponte, V. M., and Colon, G. Sodium chloride removal from urine via a six-compartment ED cell for use in advanced life support systems (part 1: Salt removal as a function of applied voltage and fluid velocity). *Desalination* 140, 2 (2001), 121–132.
- [11] Aponte, V. M., and Colon, G. Sodium chloride removal from urine via a six-compartment ED cell for use in advanced life support systems (part 2: Limiting current density behavior). *Desalination* 140, 2 (2001), 133–144.
- [12] Barbosa, S. G., Peixoto, L., Soares, O. S. G. P., Pereira, M. F. R., Ter Heijne, A., Kuntke, P., Alves, M. M., and Pereira, M. A. Influence of carbon anode properties on performance and microbiome of microbial electrolysis cells operated on urine. *Electrochimica Acta* 267 (2018), 122–132.
- [13] Barbosa, S. G., Peixoto, L., Ter Heijne, A., Kuntke, P., Alves, M. M., and Pereira, M. A. Investigating bacterial community changes and organic substrate degradation in microbial fuel cells operating on real human urine. *Environmental Science: Water Research & Technology* 3, 5 (2017), 897–904.
- [14] Barbosa, S. G., Rodrigues, T., Peixoto, L., Kuntke, P., Alves, M. M., Pereira, M. A., and Ter Heijne, A. Anaerobic biological fermentation of urine as a strategy to enhance the performance of a microbial electrolysis cell (MEC). *Renewable Energy* 139 (2019), 936–943.
- [15] Bassin, J. P., Kleerebezem, R., Muyzer, G., Rosado, A. S., van Loosdrecht, M. C. M., and Dezotti, M. Effect of different salt adaptation strategies on the microbial diversity, activity, and settling of nitrifying sludge in sequencing batch reactors. *Applied Microbiology and Biotechnology* 93, 3 (2012), 1281–1294.
- [16] Bassin, J. P., Pronk, M., Muyzer, G., Kleerebezem, R., Dezotti, M., and van Loosdrecht, M. C. M. Effect of elevated salt concentrations on the aerobic granular sludge process: Linking microbial activity with microbial community structure. *Applied and Environmental Microbiology* 77, 22 (2011), 7942–7953.
- [17] Becker, E. W. Micro-algae as a source of protein. *Biotechnology Advances* 25, 2 (2007), 207–210.
- [18] Behrendt, J., Arevalo, E., Gulyas, H., Niederste-Hollenberg, J., Niemlec, A., Zhou, J., and Otterpohl, R. Production of value added products from separately collected urine. *Water Science & Technology* 46, 6-7 (2002), 341–346.
- [19] Benoit, M. R., and Klaus, D. M. Microgravity, bacteria, and the influence of motility. *Advances in Space Research* 39, 7 (2007), 1225–1232.
- [20] Berkovich, Y. A., Chetirkin, P. V., Wheeler, R. M., and Sager, J. C. Evaluating and optimizing horticultural regimes in space plant growth facilities. *Advances in Space Research* 34, 7 (2004), 1612–1618.
- [21] Bischel, H. N., Duygan, B. D. O., Strande, L., McArdell, C. S., Udert, K. M., and Kohn, T. Pathogens and pharmaceuticals in source-separated urine in eThekweni, South Africa. *Water Research* 85 (2015), 57–65.
- [22] Bischel, H. N., Schertenleib, A., Fumasoli, A., Udert, K. M., and Kohn, T. Inactivation kinetics and mechanisms of viral and bacterial pathogen surrogates during urine nitrification. *Environmental Science-Water Research & Technology* 1, 1 (2015), 65–76.

- [23] Blume, S., and Winker, M. Three years of operation of the urine diversion system at GTZ headquarters in Germany: user opinions and maintenance challenges. *Water Science & Technology* 64, 3 (2011), 579–586.
- [24] Bolan, N. S., Hedley, M. J., and White, R. E. Processes of soil acidification during nitrogen cycling with emphasis on legume based pastures. *Plant and Soil* 134, 1 (1991), 53–63.
- [25] Boland, M. J., Rae, A. N., Vereijken, J. M., Meuwissen, M. P. M., Fischer, A. R. H., van Boekel, M. A. J. S., Rutherford, S. M., Gruppen, H., Moughan, P. J., and Hendriks, W. H. The future supply of animal-derived protein for human consumption. *Trends in Food Science & Technology* 29, 1 (2013), 62–73.
- [26] Bond, D. R., Holmes, D. E., Tender, L. M., and Lovley, D. R. Electrode-reducing microorganisms that harvest energy from marine sediments. *Science* 295, 5554 (2002), 483–485.
- [27] Bonvin, C., Etter, B., Udert, K. M., Frossard, E., Nanzer, S., Tamburini, F., and Oberson, A. Plant uptake of phosphorus and nitrogen recycled from synthetic source-separated urine. *Ambio* 44 (2015), S217–S227.
- [28] Boyer, T. H., Taylor, K., Reed, A., and Smith, D. Ion-exchange softening of human urine to control precipitation. *Environmental Progress & Sustainable Energy* 33, 2 (2014), 564–571.
- [29] Bracken, P., Wachtler, A., Panesar, A., and Lange, J. The road not taken: how traditional excreta and greywater management may point the way to a sustainable future. *Water Supply* 7, 1 (2007), 219–227.
- [30] Brey, J., Munoz, D., Mesa, V., and Guerrero, T. Use of fuel cells and electrolyzers in space applications: From energy storage to propulsion/deorbitation. E3S web of conferences 16, ESPC 2016.
- [31] Brown, D., Lindstrom, R., and Smith, J. The recovery of water from urine by membrane electrodialysis. *U.S. Air Force Medical Research Laboratory, AMRL-TDR-63* (1963), 56.
- [32] Bucur, B., Icardo, M. C., and Calatayud, J. M. Spectrophotometric determination of ammonium by an rFIA assembly. *Revue Roumaine De Chimie* 51, 2 (2006), 101–108.
- [33] Buffle, J., Zhang, Z., and Startchev, K. Metal flux and dynamic speciation at (bio)interfaces. Part 1: Critical evaluation and compilation of physicochemical parameters for complexes with simple ligands and fulvic/humic substances. *Environmental Science & Technology* 41, 22 (2007), 7609–7620.
- [34] Cailliez, F. The analytical solution of the additive constant problem. *Psychometrika* 48, 2 (1983), 305–308.
- [35] Caizán-Juanarena, L., Borsje, C., Sleutels, T., Yntema, D., Santoro, C., Ieropoulos, I., Soavi, F., and ter Heijne, A. Combination of bioelectrochemical systems and electrochemical capacitors: Principles, analysis and opportunities. *Biotechnology Advances* 39 (2020), 107456.
- [36] Campanella, L., Crescentini, G., Avino, P., and Moauro, A. Determination of macrominerals and trace elements in the alga *Spirulina platensis*. *Analisis* 26, 5 (1998), 210–214.
- [37] Caranto, J. D., and Lancaster, K. M. Nitric oxide is an obligate bacterial nitrification intermediate produced by hydroxylamine oxidoreductase. *Proceedings of the National Academy of Sciences of the United States of America* 114, 31 (2017), 8217–8222.
- [38] Carter, D. L. Status of the regenerative ECLSS water recovery system. SAE Technical Paper 2009-01-2352 (2009).
- [39] Carter, D. L., Williamson, J., Brown, C. A., Bazley, J., Gazda, D., Schaezler, R., and Thomas, F. Status of ISS water management and recovery. 48th International Conference on Environmental Systems, Albuquerque, New Mexico (2017).
- [40] Casey, E., Glennon, B., and Hamer, G. Review of membrane aerated biofilm reactors. *Resources, Conservation and Recycling* 27, 1 (1999), 203–215.
- [41] Chang, Y., Wu, Z., Bian, L., Feng, D., and Leung, D. Y. C. Cultivation of *Spirulina platensis* for biomass production and nutrient removal from synthetic human urine. *Applied Energy* 102 (2013), 427–431.
- [42] Chatterjee, P., Granatier, M., Ramasamy, P., Kokko, M., Lakaniemi, A.-M., and Rintala, J. Microalgae grow on source separated human urine in Nordic climate: Outdoor pilot-scale cultivation. *Journal of environmental management* 237 (2019), 119–127.
- [43] Cheah, W. Y., Show, P. L., Chang, J.-S., Ling, T. C., and Juan, J. C. Biosequestration of atmospheric CO₂ and flue gas-containing CO₂ by microalgae. *Bioresource Technology* 184 (2015), 190–201.
- [44] Chen, L. P., Yang, X. X., Tian, X. J., Yao, S., Li, J. Y., Wang, A. M., Yao, Q. A., and Peng, D. C. Partial nitrification of stored source-separated urine by granular activated sludge in a sequencing batch reactor. *AMB Express* 7 (2017), 1–10.
- [45] Chen, R. D., Semmens, M. J., and LaPara, T. M. Biological treatment of a synthetic space mission wastewater using a membrane-aerated, membrane-coupled bioreactor (M2BR). *Journal of Industrial Microbiology & Biotechnology* 35, 6 (2008), 465–473.
- [46] Chen, W., Zhang, C. K., Cheng, Y. M., Zhang, S. W., and Zhao, H. Y. A comparison of methods for clustering 16S rRNA sequences into OTUs. *Plos One* 8, 8 (2013), 10.
- [47] Christenson, D., Sevanthi, R., Morse, A., and Jackson, A. Assessment of membrane-aerated biological reactors (MABRs) for integration into space-based water recycling system architectures. *Gravitational and Space Research* 6 (2018), 12–27.
- [48] Christiaens, M. E. R., De Paepe, J., Ilgrande, C., De Vrieze, J., Barys, J., Teirlinck, P., Meerbergen, K., Lievens, B., Boon, N., Clauwaert, P., and Vlaeminck, S. E. Urine nitrification with a synthetic microbial community. *Systematic and Applied Microbiology* (2019), 126021.

- [49] Christiaens, M. E. R., Gildemyn, S., Matassa, S., Ysebaert, T., De Vrieze, J., and Rabaey, K. Electrochemical ammonia recovery from source-separated urine for microbial protein production. *Environmental Science & Technology* 51, 22 (2017), 13143–13150.
- [50] Cid, C. A., Stinchcombe, A., Ieropoulos, I., and Hoffmann, M. R. Urine microbial fuel cells in a semi-controlled environment for onsite urine pre-treatment and electricity production. *Journal of Power Sources* 400 (2018), 441–448.
- [51] Clauwaert, P., De Paepe, J., Jiang, F., Alonso-Fariñas, B., Vaiopoulou, E., Verliefe, A., and Rabaey, K. Electrochemical tap water softening: A zero chemical input approach. *Water Research* (2019), 115263.
- [52] Clauwaert, P., Muys, M., Alloul, A., De Paepe, J., Luther, A., Sun, X. Y., Ilgrande, C., Christiaens, M. E. R., Hu, X. N., Zhang, D. D., Lindeboom, R. E. F., Sas, B., Rabaey, K., Boon, N., Ronsse, F., Geelen, D., and Vlaeminck, S. E. Nitrogen cycling in bioregenerative life support systems: Challenges for waste refinery and food production processes. *Progress in Aerospace Sciences* 91 (2017), 87–98.
- [53] Clément, G., and Slenzak, K. *Fundamentals of Space Biology: Research on Cells, Animals, and Plants in Space*. Springer New York, 2006.
- [54] Cogne, G., Lehmann, B., Dussap, C.-G., and Gros, J.-B. Uptake of macrominerals and trace elements by the cyanobacterium *Spirulina platensis* (*Arthrospira platensis* PCC 8005) under photoautotrophic conditions: Culture medium optimization. *Biotechnology and Bioengineering* 81, 5 (2003), 588–593.
- [55] Cole, J. R., Wang, Q., Fish, J. A., Chai, B. L., McGarrell, D. M., Sun, Y. N., Brown, C. T., Porras-Alfaro, A., Kuske, C. R., and Tiedje, J. M. Ribosomal database project: data and tools for high throughput rRNA analysis. *Nucleic Acids Research* 42, D1 (2014), D633–D642.
- [56] Coppens, J., Lindeboom, R., Muys, M., Coessens, W., Alloul, A., Meerbergen, K., Lievens, B., Clauwaert, P., Boon, N., and Vlaeminck, S. E. Nitrification and microalgae cultivation for two-stage biological nutrient valorization from source separated urine. *Bioresource Technology* 211 (2016), 41–50.
- [57] Cordell, D. Chapter 3: Peak phosphorus and the role of P recovery in achieving food security. In *Source Separation and Decentralization for Wastewater Management. Chapter 3: Peak phosphorus and the role of P recovery in achieving food security*. IWA Publishing, London, UK, 2013.
- [58] Cordell, D., Drangert, J.-O., and White, S. The story of phosphorus: Global food security and food for thought. *Global Environmental Change* 19, 2 (2009), 292–305.
- [59] Cordell, D., Rosemarin, A., Schröder, J. J., and Smit, A. L. Towards global phosphorus security: A systems framework for phosphorus recovery and reuse options. *Chemosphere* 84, 6 (2011), 747–758.
- [60] Cortes-Lorenzo, C., Rodriguez-Diaz, M., Sipkema, D., Juarez-Jimenez, B., Rodelas, B., Smidt, H., and Gonzalez-Lopez, J. Effect of salinity on nitrification efficiency and structure of ammonia-oxidizing bacterial communities in a submerged fixed bed bioreactor. *Chemical Engineering Journal* 266 (2015), 233–240.
- [61] Council, N. R. *Microgravity Research in Support of Technologies for the Human Exploration and Development of Space and Planetary Bodies*. The National Academies Press, Washington, DC, 2000.
- [62] Cox, T. F. Multidimensional scaling used in multivariate statistical process control. *Journal of Applied Statistics* 28, 3-4 (2001), 365–378.
- [63] Côté, P., Bersillon, J.-L., Huyard, A., and Faup, G. Bubble-free aeration using membranes: Process analysis. *Journal (Water Pollution Control Federation)* 60, 11 (1988), 1986–1992.
- [64] Cui, Y. W., Peng, C. Y., Peng, Y. Z., and Ye, L. Effects of salt on microbial populations and treatment performance in purifying saline sewage using the MUCT process. *Clean-Soil Air Water* 37, 8 (2009), 649–656.
- [65] De Paepe, J., De Pryck, L., Verliefe, A. R. D., Rabaey, K., and Clauwaert, P. Electrochemically induced precipitation enables fresh urine stabilization and facilitates source separation. *Environmental Science & Technology* (2020).
- [66] De Paepe, J., Lindeboom, R. E. F., Vanoppen, M., De Paepe, K., Demey, D., Coessens, W., Lamaze, B., Verliefe, A. R. D., Clauwaert, P., and Vlaeminck, S. E. Refinery and concentration of nutrients from urine with electrodialysis enabled by upstream precipitation and nitrification. *Water Research* 144 (2018), 76–86.
- [67] De Paepe, K., Kerckhof, F.-M., Verspreet, J., Courtin, C. M., and Van de Wiele, T. Inter-individual differences determine the outcome of wheat bran colonization by the human gut microbiome. *Environmental Microbiology* 19, 8 (2017), 3251–3267.
- [68] Defoirdt, T., Vlaeminck, S. E., Sun, X. Y., Boon, N., and Clauwaert, P. Ureolytic activity and its regulation in *Vibrio campbellii* and *Vibrio harveyi* in relation to nitrogen recovery from human urine. *Environmental Science & Technology* 51, 22 (2017), 13335–13343.
- [69] Delrue, F., Alaux, E., Moudjaoui, L., Gaignard, C., Fleury, G., Perilhou, A., Richaud, P., Petitjean, M., and Sassi, J. F. Optimization of *Arthrospira platensis* (*Spirulina*) growth: From laboratory scale to pilot scale. *Fermentation-Basel* 3, 4 (2017), 14.
- [70] Deng, S., Xie, B., and Liu, H. The recycle of water and nitrogen from urine in bioregenerative life support system. *Acta Astronautica* 123 (2016), 86–90.
- [71] Derese, S., and Verliefe, A. R. D. Full nitrogen recovery and potable water production from human urine by membrane distillation. AMTA/AWWA Membrane Technology Conference, San Antonio, TX (2016).
- [72] Dincer, A. R., and Kargi, F. Salt inhibition of nitrification and denitrification in saline wastewater. *Environmental Technology* 20, 11 (1999), 1147–1153.

- [73] Dodd, M. C., Zuleeg, S., Von Gunten, U., and Pronk, W. Ozonation of source-separated urine for resource recovery and waste minimization: Process modeling, reaction chemistry, and operational considerations. *Environmental Science & Technology* 42, 24 (2008), 9329–9337.
- [74] Eckart, E. *Spaceflight Life Support and Biospherics*, 1 ed. Space Technology Library. Springer, Netherlands, 1996.
- [75] Edgar, R. C., Haas, B. J., Clemente, J. C., Quince, C., and Knight, R. UCHIME improves sensitivity and speed of chimera detection. *Bioinformatics* 27, 16 (2011), 2194–2200.
- [76] Edozien, J. C., Udo, U. U., Young, V. R., and Scrimshaw, N. S. Effects of high levels of yeast feeding on uric acid metabolism of young men. *Nature* 228, 5267 (1970), 180–180.
- [77] Encarnação, T., Burrows, H., Pais, A., Campos, M., and Kremer, A. Effect of N and P on the uptake of magnesium and iron and on the production of carotenoids and chlorophyll by the microalgae *Nannochloropsis sp.* *Journal of Agricultural Science and Technology* (2012), 824–832.
- [78] Encyclopaedia Britannica. Nitrogen cycle. <https://www.britannica.com/science/nitrogen-cycle/images-videos/media/1/416271/118424>. Access date: 1/06/2020, 2020.
- [79] Erisman, J. W., Galloway, J., Seitzinger, S., Bleeker, A., and Butterbach-Bahl, K. Reactive nitrogen in the environment and its effect on climate change. *Current Opinion in Environmental Sustainability* 3, 5 (2011), 281–290.
- [80] Erisman, J. W., Sutton, M. A., Galloway, J. N., Klimont, Z., and Winiwarter, W. How a century of ammonia synthesis changed the world. *Nature Geoscience* 1 (2008).
- [81] Ermis, H., Guven-Gulhan, U., Cakir, T., and Altinbas, M. Effect of iron and magnesium addition on population dynamics and high value product of microalgae grown in anaerobic liquid digestate. *Scientific Reports* 10, 1 (2020), 3510.
- [82] Escher, B. I., Pronk, W., Suter, M. J. F., and Maurer, M. Monitoring the removal efficiency of pharmaceuticals and hormones in different treatment processes of source-separated urine with bioassays. *Environmental Science & Technology* 40, 16 (2006), 5095–5101.
- [83] Etter, B., Hug, A., and Udert, K. M. Total nutrient recovery from urine - operation of a pilot-scale nitrification reactor. WEF/IWA International Conference on Nutrient Removal and Recovery, Vancouver, Canada (2013).
- [84] Etter, B., Tilley, E., Khadka, R., and Udert, K. M. Low-cost struvite production using source-separated urine in Nepal. *Water Research* 45, 2 (2011), 852–862.
- [85] Etter, B., and Udert, K. VUNA handbook on urine treatment. Tech. rep., Eawag, Dübendorf, Switzerland, 2015.
- [86] Eyal, A., and Kedem, O. Nitrate-selective anion-exchange membranes. *Journal of Membrane Science* 38, 2 (1988), 101–111.
- [87] Fabregas, J., Herrero, C., Abalde, J., Liaño, R., and Cabezas, B. Biomass production and biochemical variability of the marine microalga *Dunaliella tertiolecta* (butcher) with high nutrient concentrations. *Aquaculture* 53, 3 (1986), 187–199.
- [88] Fan, X. H., Tang, C., and Rengel, Z. Nitrate uptake, nitrate reductase distribution and their relation to proton release in five nodulated grain legumes. *Annals of Botany* 90, 3 (2002), 315–323.
- [89] Feng, D.-l., and Wu, Z.-c. Culture of *Spirulina platensis* in human urine for biomass production and O₂ evolution. *Journal of Zhejiang University SCIENCE B* 7, 1 (2006), 34–37.
- [90] Feng, D. L., Wu, Z. C., and Wang, D. H. Effects of N source and nitrification pretreatment on growth of *Arthrospira platensis* in human urine. *Journal of Zhejiang University-Science A* 8, 11 (2007), 1846–1852.
- [91] Feng, D. L., Wu, Z. C., and Xu, S. H. Nitrification of human urine for its stabilization and nutrient recycling. *Bioresource Technology* 99, 14 (2008), 6299–6304.
- [92] Fixen, P. E., and Johnston, A. M. World fertilizer nutrient reserves: a view to the future. *Journal of the Science of Food and Agriculture* 92, 5 (2012), 1001–1005.
- [93] Food and Agricultural Organization of the United Nations (FAO). FAOSTAT (food and agriculture organization statistics, 2020).
- [94] Fowler, D., Coyle, M., Skiba, U., Sutton, M. A., Cape, J. N., Reis, S., Sheppard, L. J., Jenkins, A., Grizzetti, B., Galloway, J. N., Vitousek, P., Leach, A., Bouwman, A. F., Butterbach-Bahl, K., Dentener, F., Stevenson, D., Amann, M., and Voss, M. The global nitrogen cycle in the twenty-first century. *Philosophical Transactions of the Royal Society B: Biological Sciences* 368, 1621 (2013), 20130164.
- [95] Freguia, S., Logrieco, M. E., Monetti, J., Ledezma, P., Virdis, B., and Tsujimura, S. Self-powered bioelectrochemical nutrient recovery for fertilizer generation from human urine. *Sustainability* 11, 19 (2019), 10.
- [96] Fumasoli, A., Bürgmann, H., Weissbrodt, D. G., Wells, G. F., Beck, K., Mohn, J., Morgenroth, E., and Udert, K. M. Growth of *Nitrosococcus*-related ammonia oxidizing bacteria coincides with extremely low pH values in wastewater with high ammonia content. *Environmental science & technology* 51, 12 (2017), 6857–6866.
- [97] Fumasoli, A., Etter, B., Sterkele, B., Morgenroth, E., and Udert, K. M. Operating a pilot-scale nitrification/distillation plant for complete nutrient recovery from urine. *Water Science & Technology* 73, 1 (2016), 215–222.

- [98] Fumasoli, A., Morgenroth, E., and Udert, K. M. Modeling the low pH limit of *Nitrosomonas europaea* in high-strength nitrogen wastewaters. *Water Research* 49 (2015), 161–170.
- [99] Gabrielli, C., Maurin, G., Francy-Chausson, H., They, P., Tran, T. T. M., and Tlili, M. Electrochemical water softening: principle and application. *Desalination* 201, 1-3 (2006), 150–163.
- [100] Gajda, I., Greenman, J., Santoro, C., Serov, A., Atanassov, P., Melhuish, C., and Ieropoulos, I. A. Multi-functional microbial fuel cells for power, treatment and electro-osmotic purification of urine. *Journal of Chemical Technology & Biotechnology* 94, 7 (2019), 2098–2106.
- [101] Galloway, J. N., Aber, J. D., Erisman, J. W., Seitzinger, S. P., Howarth, R. W., Cowling, E. B., and Cosby, B. J. The nitrogen cascade. *BioScience* 53, 4 (2003), 341–356.
- [102] Galloway, J. N., Dentener, F. J., Capone, D. G., Boyer, E. W., Howarth, R. W., Seitzinger, S. P., Asner, G. P., Cleveland, C. C., Green, P. A., Holland, E. A., Karl, D. M., Michaels, A. F., Porter, J. H., Townsend, A. R., and Vöösmary, C. J. Nitrogen cycles: Past, present, and future. *Biogeochemistry* 70, 2 (2004), 153–226.
- [103] Galloway, J. N., Winiwarter, W., Leip, A., Leach, A. M., Bleeker, A., and Erisman, J. W. Nitrogen footprints: past, present and future. *Environmental Research Letters* 9, 11 (2014), 115003.
- [104] Gao, Y., Sun, D., Wang, H., Lu, L., Ma, H., Wang, L., Ren, Z. J., Liang, P., Zhang, X., Chen, X., and Huang, X. Urine-powered synergy of nutrient recovery and urine purification in a microbial electrochemical system. *Environmental Science: Water Research & Technology* 4, 10 (2018), 1427–1438.
- [105] Gòdia, F., Albiol, J., Montesinos, J. L., Pérez, J., Creus, N., Cabello, F., Mengual, X., Montras, A., and Lasseur, C. MELISSA: a loop of interconnected bioreactors to develop life support in space. *Journal of Biotechnology* 99, 3 (2002), 319–330.
- [106] Gòdia, F., Albiol, J., Perez, J., Creus, N., Cabello, F., Montras, A., Masot, A., and Lasseur, C. The MELISSA pilot plant facility as an integration test-bed for advanced life support systems. In *Space Life Sciences: Life Support Systems and Biological Systems under Influence of Physical Factors*, D. L. Henninger, A. E. Drysdale, and A. V. Kondyurin, Eds., vol. 34 of *Advances in Space Research*. Pergamon-Elsevier Science Ltd, Kidlington, 2004, pp. 1483–1493.
- [107] Geise, G. M., Paul, D. R., and Freeman, B. D. Fundamental water and salt transport properties of polymeric materials. *Progress in Polymer Science* 39, 1 (2014), 1–42.
- [108] Gerringa, L. J. A., de Baar, H. J. W., and Timmermans, K. R. A comparison of iron limitation of phytoplankton in natural oceanic waters and laboratory media conditioned with EDTA. *Marine Chemistry* 68, 4 (2000), 335–346.
- [109] Güler, E., van Baak, W., Saakes, M., and Nijmeijer, K. Monovalent-ion-selective membranes for reverse electrodialysis. *Journal of Membrane Science* 455 (2014), 254–270.
- [110] Godfray, H. C. J., Beddington, J. R., Crute, I. R., Haddad, L., Lawrence, D., Muir, J. F., Pretty, J., Robinson, S., Thomas, S. M., and Toulmin, C. Food security: The challenge of feeding 9 billion people. *Science* 327, 5967 (2010), 812–818.
- [111] Gong, Z., Yang, F., Liu, S., Bao, H., Hu, S., and Furukawa, K. Feasibility of a membrane-aerated biofilm reactor to achieve single-stage autotrophic nitrogen removal based on anammox. *Chemosphere* 69, 5 (2007), 776–784.
- [112] Gonzalez-Silva, B. M. *Salinity as a driver for microbial community structure in reactors for nitrification and anammox. Thesis for the Degree of Philosophiae Doctor, Norwegian University of Science and Technology-Trondheim, Norway.* PhD thesis, 2016.
- [113] González-Camejo, J., Montero, P., Aparicio, S., Ruano, M. V., Borrás, L., Seco, A., and Barat, R. Nitrite inhibition of microalgae induced by the competition between microalgae and nitrifying bacteria. *Water Research* 172 (2020), 115499.
- [114] Gower, J. C. Some distance properties of latent root and vector methods used in multivariate analysis. *Biometrika* 53 (1966), 325–338.
- [115] Greenberg, A.E., C. L., and Eaton, A. Standard methods for the examination of water and wastewater. 18th edition. American Public Health Association (APHA) / American Water Works Association (AWWA) / Water Environment Federation. Washington DC, USA.
- [116] Gruber, N., and Galloway, J. N. An Earth-system perspective of the global nitrogen cycle. *Nature* 451, 7176 (2008), 293–296.
- [117] Guo, K., Freguia, S., Dennis, P. G., Chen, X., Donose, B. C., Keller, J., Gooding, J. J., and Rabaey, K. Effects of surface charge and hydrophobicity on anodic biofilm formation, community composition, and current generation in bioelectrochemical systems. *Environmental Science & Technology* 47, 13 (2013), 7563–7570.
- [118] Guo, Q., Ye, F., Guo, H., and Ma, C. F. Gas/water and heat management of PEM-based fuel cell and electrolyzer systems for space applications. *Microgravity Science and Technology* 29, 1 (2017), 49–63.
- [119] Hamed, I. The evolution and versatility of microalgal biotechnology: A review. *Comprehensive Reviews in Food Science and Food Safety* 15, 6 (2016), 1104–1123.
- [120] Hanifzadeh, M., Garcia, E. C., and Viamajala, S. Production of lipid and carbohydrate from microalgae without compromising biomass productivities: Role of Ca and Mg. *Renewable Energy* 127 (2018), 989–997.
- [121] Harms, C., Schleicher, A., Collins, M. D., and Andreesen, J. R. *Tissierella creatinophila* sp. nov., a gram-positive, anaerobic, non-spore-forming, creatinine-fermenting organism. *International journal of systematic bacteriology* 48 Pt 3 (1998), 983–93.

- [122] Harper, L. D., Neal, C. R., Poynter, J., Schalkwyk, J. D., and Wingo, D. R. Life support for a low-cost lunar settlement: No showstoppers. *New Space* 4 (2016), 40.
- [123] Hasson, D., Sidorenko, G., and Semiat, R. Calcium carbonate hardness removal by a novel electrochemical seeds system. *Desalination* 263, 1-3 (2010), 285–289.
- [124] Heinonen-Tanski, H., and van Wijk-Sijbesma, C. Human excreta for plant production. *Bioresource Technology* 96, 4 (2005), 403–411.
- [125] Hellström, D., Johannsson, E., and Grennberg, K. Storage of human urine: acidification as a method to inhibit decomposition of urea. *Ecological Engineering* 12, 3-4 (1999), 253–269.
- [126] Höglund, C., Stenström, T. A., and Ashbolt, N. Microbial risk assessment of source-separated urine used in agriculture. *Waste Management & Research* 20, 2 (2002), 150–61.
- [127] Horneck, G., Klaus, D. M., and Mancinelli, R. L. Space microbiology. *Microbiology and Molecular Biology Reviews* 74, 1 (2010), 121–156.
- [128] Hug, A., and Udert, K. M. Struvite precipitation from urine with electrochemical magnesium dosage. *Water Research* 47, 1 (2013), 289–299.
- [129] Ieropoulos, I., Greenman, J., and Melhuish, C. Urine utilisation by microbial fuel cells: energy fuel for the future. *Physical Chemistry Chemical Physics* 14, 1 (2012), 94–98.
- [130] Ieropoulos, I. A., Stinchcombe, A., Gajda, I., Forbes, S., Merino-Jimenez, I., Pasternak, G., Sanchez-Herranz, D., and Greenman, J. Pee power urinal - microbial fuel cell technology field trials in the context of sanitation. *Environmental Science: Water Research & Technology* 2, 2 (2016), 336–343.
- [131] Igos, E., Besson, M., Navarrete Gutierrez, T., Bisinella de Faria, A. B., Benetto, E., Barna, L., Ahmadi, A., and Sperandio, M. Assessment of environmental impacts and operational costs of the implementation of an innovative source-separated urine treatment. *Water Research* 126 (2017), 50–59.
- [132] Ikematsu, M., Kaneda, K., Iseki, M., and Yasuda, M. Electrochemical treatment of human urine for its storage and reuse as flush water. *Science of the Total Environment* 382, 1 (2007), 159–164.
- [133] Ikuma, K., D. A. W. L. B. L. The extracellular bastions of bacteria - a biofilm way of life. *Nature Education Knowledge* 4(2):2 (2013).
- [134] Ilgrande, C., Mastroleo, F., Christiaens, M. E. R., Lindeboom, R. E. F., Prat, D., Van Hoey, O., Ambrozova, I., Coninx, I., Heylen, W., Pommereney-Roser, A., Spieck, E., Boon, N., Vlaeminck, S. E., Leys, N., and Clauwaert, P. Reactivation of microbial strains and synthetic communities after a spaceflight to the International Space Station: Corroborating the feasibility of essential conversions in the MELiSSA loop. *Astrobiology* 19, 9 (2019), 1167–1176.
- [135] International Space Exploration Coordination Group (ISECG). The global exploration roadmap. Tech. rep., 2018.
- [136] Jaatinen, S., Lakaniemi, A.-M., and Rintala, J. Use of diluted urine for cultivation of *Chlorella vulgaris*. *Environmental Technology* 37, 9 (2016), 1159–1170.
- [137] Jackson, W. A., Morse, A., McLamore, E., Wiesner, T., and Xia, S. Nitrification-denitrification biological treatment of a high-nitrogen waste stream for water-reuse applications. *Water Environment Research* 81, 4 (2009), 423–431.
- [138] Janicek, A., Fan, Y., and Liu, H. Design of microbial fuel cells for practical application: a review and analysis of scale-up studies. *Biofuels* 5, 1 (2014), 79–92.
- [139] Jiang, F., Chen, Y., Mackey, H. R., Chen, G. H., and van Loosdrecht, M. C. M. Urine nitrification and sewer discharge to realize in-sewer denitrification to simplify sewage treatment in Hong Kong. *Water Science & Technology* 64, 3 (2011), 618–626.
- [140] Jönsson, H., Richert Stintzing, A., Vinneras, B., and Salomon, E. Guidelines on the use of urine and faeces in crop production. Tech. rep., Stockholm Environment Institute, Sweden, 2004.
- [141] Johnson, P. E. Accumulation of mercury and other elements by *Spirulina* (Cyanophyceae). *Nutrition reports international v. 34*, no. 6 (1986), pp. 1063–1070–1986 v.34 no.6.
- [142] Kabdaşlı, I., and Tünay, O. Nutrient recovery by struvite precipitation, ion exchange and adsorption from source-separated human urine - a review. *Environmental Technology Reviews* 7, 1 (2018), 106–138.
- [143] Kay, R. A. Microalgae as food and supplement. *Crit Rev Food Sci Nutr* 30, 6 (1991), 555–573.
- [144] Kikhavani, T., Ashrafzadeh, S. N., and Van der Bruggen, B. Nitrate selectivity and transport properties of a novel anion exchange membrane in electrodialysis. *Electrochimica Acta* 144 (2014), 341–351.
- [145] Kirkby, E. A., and Mengel, K. The role of magnesium in plant nutrition. *Zeitschrift für Pflanzenernährung und Bodenkunde* 139, 2 (1976), 209–222.
- [146] Klaus, D., Simske, S., Todd, P., and Stodieck, L. Investigation of space flight effects on *Escherichia coli* and a proposed model of underlying physical mechanisms. *Microbiology* 143 (1997), 449–455.
- [147] Klindworth, A., Pruesse, E., Schweer, T., Peplies, J., Quast, C., Horn, M., and Glockner, F. O. Evaluation of general 16S ribosomal RNA gene PCR primers for classical and next-generation sequencing-based diversity studies. *Nucleic Acids Res* 41, 1 (2013), e1.
- [148] Könneke, M., Schubert, D. M., Brown, P. C., Hügl, M., Standfest, S., Schwander, T., Schada von Borzyskowski, L., Erb, T. J., Stahl, D. A., and Berg, I. A. Ammonia-oxidizing archaea use the most energy-efficient aerobic pathway for CO₂ fixation. *Proceedings of the National Academy of Sciences of the United States of America* 111, 22 (2014), 8239–8244.

- [149] Koops, H. P., Bottcher, B., Moller, U. C., Pommereningroser, A., and Stehr, G. Classification of 8 new species of ammonia-oxidizing bacteria - *Nitrosomonas communis* sp. nov., *Nitrosomonas ureae* sp. nov., *Nitrosomonas aestuarii* sp. nov., *Nitrosomonas marina* sp. nov., *Nitrosomonas nitrosa* sp. nov., *Nitrosomonas eutropha* sp. nov., *Nitrosomonas oligotropha* sp. nov. and *Nitrosomonas halophila* sp. nov. *Journal of General Microbiology* 137 (1991), 1689–1699.
- [150] Kozich, J. J., Westcott, S. L., Baxter, N. T., Highlander, S. K., and Schloss, P. D. Development of a dual-index sequencing strategy and curation pipeline for analyzing amplicon sequence data on the MiSeq Illumina Sequencing Platform. *Applied and Environmental Microbiology* 79, 17 (2013), 5112–5120.
- [151] Köpping, I., McArdell, C. S., Borowska, E., Böhler, M. A., and Udert, K. M. Removal of pharmaceuticals from nitrified urine by adsorption on granular activated carbon. *Water Research X* (2020), 100057.
- [152] Kumar, M. From gunpowder to teeth whitener: the science behind historic uses of urine. *Smithsonian Magazine* (2013).
- [153] Kuntke, P. *Nutrient and energy recovery from urine*. PhD thesis, Wageningen University, Wageningen, The Netherlands, 2013.
- [154] Kuntke, P., Asmiech, K. M., Bruning, H., Zeeman, G., Saakes, M., Sleutels, T. H. J. A., Hamelers, H. V. M., and Buisman, C. J. N. Ammonium recovery and energy production from urine by a microbial fuel cell. *Water Research* 46, 8 (2012), 2627–2636.
- [155] Kuntke, P., Rodríguez Arredondo, M., Widyakristi, L., ter Heijne, A., Sleutels, T. H. J. A., Hamelers, H. V. M., and Buisman, C. J. N. Hydrogen gas recycling for energy efficient ammonia recovery in electrochemical systems. *Environmental Science & Technology* 51, 5 (2017), 3110–3116.
- [156] Kuntke, P., Rodrigues, M., Sleutels, T., Saakes, M., Hamelers, H. V. M., and Buisman, C. J. N. Energy-efficient ammonia recovery in an up-scaled hydrogen gas recycling electrochemical system. *ACS Sustainable Chemistry & Engineering* 6, 6 (2018), 7638–7644.
- [157] Kuntke, P., Sleutels, T. H. J. A., Rodríguez Arredondo, M., Georg, S., Barbosa, S. G., ter Heijne, A., Hamelers, H. V. M., and Buisman, C. J. N. (Bio)electrochemical ammonia recovery: progress and perspectives. *Applied Microbiology and Biotechnology* 102, 9 (2018), 3865–3878.
- [158] Kuntke, P., Sleutels, T. H. J. A., Saakes, M., and Buisman, C. J. N. Hydrogen production and ammonium recovery from urine by a microbial electrolysis cell. *International Journal of Hydrogen Energy* 39, 10 (2014), 4771–4778.
- [159] Kuntke, P., Zamora, P., Saakes, M., Buisman, C. J. N., and Hamelers, H. V. M. Gas-permeable hydrophobic tubular membranes for ammonia recovery in bio-electrochemical systems. *Environmental Science: Water Research & Technology* 2, 2 (2016), 261–265.
- [160] Larsen, T. A., Alder, A. C., Eggen, R. I. L., Maurer, M., and Lienert, J. Source separation: Will we see a paradigm shift in wastewater handling? *Environmental Science & Technology* 43, 16 (2009), 6121–6125.
- [161] Larsen, T. A., Hoffmann, S., Lüthi, C., Truffer, B., and Maurer, M. Emerging solutions to the water challenges of an urbanizing world. *Science* 352, 6288 (2016), 928–933.
- [162] Larsen, T. A., Udert, K. M., and Lienert, J. *Source Separation and Decentralization for Wastewater Management*. IWA Publishing, London, UK, 2013.
- [163] Lasseur, C., Brunet, J., de Weever, H., Dixon, M., Dussap, G., Gòdia, F., Leys, N., Mergeay, M., and Van Der Straeten, D. MELISSA: the european project of closed life support systems. *Gravitational and Space Biology* 23 (2010), 3–12.
- [164] Lasseur, C., Verstraete, W., Gros, J. B., Dubertret, G., and Rogalla, F. MELISSA: A potential experiment for a precursor mission to the moon. *Advances in Space Research* 18, 11 (1996), 111–117.
- [165] Launius, R. *The Smithsonian history of space exploration: from the ancient world to the extraterrestrial future*. Philip Cooper, Washington DC, 2018.
- [166] Ledezma, P., Jermakka, J., Keller, J., and Freguia, S. Recovering nitrogen as a solid without chemical dosing: Bio-electroconcentration for recovery of nutrients from urine. *Environmental Science & Technology Letters* 4, 3 (2017), 119–124.
- [167] Ledezma, P., Kuntke, P., Buisman, C. J. N., Keller, J., and Freguia, S. Source-separated urine opens golden opportunities for microbial electrochemical technologies. *Trends in Biotechnology* 33, 4 (2015), 214–220.
- [168] Lee, H. S., Parameswaran, P., Kato-Marcus, A., Torres, C. I., and Rittmann, B. E. Evaluation of energy-conversion efficiencies in microbial fuel cells (MFCs) utilizing fermentable and non-fermentable substrates. *Water Research* 42, 6-7 (2008), 1501–1510.
- [169] Lee, H.-S., and Rittmann, B. E. Significance of biological hydrogen oxidation in a continuous single-chamber microbial electrolysis cell. *Environmental Science & Technology* 44, 3 (2010), 948–954.
- [170] Leys, N., Hendrickx, L., De Boever, P., Baatout, S., and Mergeay, M. Space flight effects on bacterial physiology. *Journal of Biological Regulators and Homeostatic Agents* 18, 2 (2004), 193–199.
- [171] Lienert, J., and Larsen, T. A. Soft paths in wastewater management - the pros and cons of urine source separation. *GAI: Ecological Perspectives for Science and Society* 16(4) (2007), 280–288.
- [172] Lind, B. B., Ban, Z., and Byden, S. Volume reduction and concentration of nutrients in human urine. *Ecological Engineering* 16, 4 (2001), 561–566.
- [173] Lind, B.-B., Ban, Z., and Bydén, S. Nutrient recovery from human urine by struvite crystallization with ammonia adsorption on zeolite and wollastonite. *Bioresource Technology* 73, 2 (2000), 169–174.

- [174] Lindeboom, R., Alonso Farinas, B., Clauwaert, P., Vanoppen, M., Christiaens, M., Abbas, A., W., C., De Paepe, J., Beckers, H., Dotremont, C., Rabaey, K., Verliefe, A., B., L., Demey, D., and Vlaeminck, S. Water and nutrient recovery from urine and grey water in space. Abstract, 1st IWA Resource Recovery Conference, Ghent, Belgium.
- [175] Lindeboom, R. E. F., Ilgrande, C., Carvajal-Arroyo, J. M., Coninx, I., Van Hoey, O., Roume, H., Morozova, J., Udert, K. M., Sas, B., Paille, C., Lasseur, C., Ilyin, V., Clauwaert, P., Leys, N., and Vlaeminck, S. E. Nitrogen cycle microorganisms can be reactivated after space exposure. *Scientific Reports* 8, 1 (2018), 13783.
- [176] Logan, B. E., Hamelers, B., Rozendal, R., Schröder, U., Keller, J., Freguia, S., Aelterman, P., Verstraete, W., and Rabaey, K. Microbial fuel cells: Methodology and technology. *Environmental Science & Technology* 40, 17 (2006), 5181–5192.
- [177] Logan, B. E., Rossi, R., Ragab, A., and Saikaly, P. E. Electroactive microorganisms in bioelectrochemical systems. *Nature Reviews Microbiology* 17, 5 (2019), 307–319.
- [178] Luther, A. K., Desloover, J., Fennell, D. E., and Rabaey, K. Electrochemically driven extraction and recovery of ammonia from human urine. *Water Research* 87 (2015), 367–377.
- [179] Lynch, S., and Matin, A. Travails of microgravity: man and microbes in space. *Biologist* 52, 2 (2005).
- [180] Mackey, H. R., Morito, G. R., Hao, T., and Chen, G. H. Pursuit of urine nitrifying granular sludge for decentralised nitrite production and sewer gas control. *Chemical Engineering Journal* 289 (2016), 17–27.
- [181] Madigan, M., Martinko, J., Dunlap, P., and Clark, D. *Brock Biology of Micro-organisms*. Pearson International Edition. 2009.
- [182] Marschner, H. *Mineral nutrition of higher plants*. 2nd edition. London : Academic, 1995.
- [183] Martin, K. J., and Nerenberg, R. The membrane biofilm reactor (MBfR) for water and wastewater treatment: Principles, applications, and recent developments. *Bioresource Technology* 122 (2012), 83–94.
- [184] Matassa, S., Batstone, D. J., Hülsen, T., Schnoor, J., and Verstraete, W. Can direct conversion of used nitrogen to new feed and protein help feed the world? *Environmental Science & Technology* 49, 9 (2015), 5247–5254.
- [185] Matula, E. E., and Nability, J. A. Failure modes, causes, and effects of algal photobioreactors used to control a spacecraft environment. *Life Sciences in Space Research* 20 (2019), 35–52.
- [186] Maurer, M., Pronk, W., and Larsen, T. A. Treatment processes for source-separated urine. *Water Research* 40, 17 (2006), 3151–3166.
- [187] Maurer, M., Schwegler, P., and Larsen, T. A. Nutrients in urine: energetic aspects of removal and recovery. *Water Science & Technology* 48, 1 (2003), 37–46.
- [188] McConville, J. R., Kvarnström, E., Jönsson, H., Kärrman, E., and Johansson, M. Source separation: Challenges & opportunities for transition in the swedish wastewater sector. *Resources, Conservation and Recycling* 120 (2017), 144–156.
- [189] McMurdie, P. J., and Holmes, S. Waste not, want not: Why rarefying microbiome data is inadmissible. *Plos Computational Biology* 10, 4 (2014), 12.
- [190] MELISSA Foundation. <https://www.melissafoundation.org/> (access date: 10/04/2020), 2020.
- [191] Merino-Jimenez, I., Celorrio, V., Fermin, D. J., Greenman, J., and Ieropoulos, I. Enhanced MFC power production and struvite recovery by the addition of sea salts to urine. *Water Research* 109 (2017), 46–53.
- [192] Meyer, C., Pensinger, S., Pickering, K., Barta, D., Shull, S., Vega, L., Christenson, D., and Jackson, W. Rapid start-up and loading of an attached growth, simultaneous nitrification/denitrification membrane aerated bioreactor. In *45th International Conference on Environmental Systems* (Washington, 2015).
- [193] Mihelcic, J. R., Fry, L. M., and Shaw, R. Global potential of phosphorus recovery from human urine and feces. *Chemosphere* 84, 6 (2011), 832–839.
- [194] Mikhaylin, S., and Bazinet, L. Fouling on ion-exchange membranes: Classification, characterization and strategies of prevention and control. *Advances in Colloid and Interface Science* 229 (2016), 34–56.
- [195] Millero, F. J., and Roy, R. N. A chemical equilibrium model for the carbonate system in natural waters. *Croatica Chemica Acta* 70, 1 (1997), 1–38.
- [196] Mkeni, P. N., Kutu, F. R., Muchaonyerwa, P., and Austin, L. M. Evaluation of human urine as a source of nutrients for selected vegetables and maize under tunnel house conditions in the Eastern Cape, South Africa. *Waste Management & Research* 26, 2 (2008), 132–139.
- [197] Mobley, H. L., and Hausinger, R. P. Microbial ureases: significance, regulation, and molecular characterization. *Microbiological reviews* 53, 1 (1989), 85–108.
- [198] Montgomery, H., and Dymock, J. The determination of nitrite in water. *Analyst* 86 (1961), 414–416.
- [199] Morgan, J. L., Zwart, S. R., Heer, M., Ploutz-Snyder, R., Ericson, K., and Smith, S. M. Bone metabolism and nutritional status during 30-day head-down-tilt bed rest. *Journal of Applied Physiology* 113, 10 (2012), 1519–1529.
- [200] Moussa, M. S., Sumanasekera, D. U., Ibrahim, S. H., Lubberding, H. J., Hooijmans, C. M., Gijzen, H. J., and van Loosdrecht, M. C. M. Long term effects of salt on activity, population structure and floc characteristics in enriched bacterial cultures of nitrifiers. *Water Research* 40, 7 (2006), 1377–1388.
- [201] Muirhead, D., Carter, D. L., and Williamson, J. Preventing precipitation in the ISS urine processor. 48th International Conference on Environmental Systems, Albuquerque, New Mexico , 2018.

- [202] Mulder, M. *Basic Principles of Membrane Technology. Second edition, Kluwer Academic Publishers, the Netherlands.* 1996.
- [203] Mulyati, S., Takagi, R., Fujii, A., Ohmukai, Y., and Matsuyama, H. Simultaneous improvement of the monovalent anion selectivity and antifouling properties of an anion exchange membrane in an electrodialysis process, using polyelectrolyte multilayer deposition. *Journal of Membrane Science* 431 (2013), 113–120.
- [204] Munns, R., and Tester, M. Mechanisms of salinity tolerance. *Annu Rev Plant Biol* 59 (2008), 651–681.
- [205] Muralikrishna, I. V., and Manickam, V. Chapter eighteen - analytical methods for monitoring environmental pollution. In *Environmental Management*, I. V. Muralikrishna and V. Manickam, Eds. Butterworth-Heinemann, 2017, pp. 495–570.
- [206] Muys, M. *Microbial protein as sustainable feed and food ingredient: Production and nutritional quality of phototrophs and aerobic heterotrophs.* PhD thesis, Universiteit Antwerpen, 2019.
- [207] Muys, M., Coppens, J., Boon, N., and Vlaeminck, S. E. Photosynthetic oxygenation for urine nitrification. *Water Science & Technology* 78, 1 (2018), 183–194.
- [208] Muys, M., Sui, Y., Schwaiger, B., Lesueur, C., Vandenheuvel, D., Vermeir, P., and Vlaeminck, S. E. High variability in nutritional value and safety of commercially available *Chlorella* and *Spirulina* biomass indicates the need for smart production strategies. *Bioresource Technology* 275 (2019), 247–257.
- [209] Nagarajan, D., Lee, D.-J., Chen, C.-Y., and Chang, J.-S. Resource recovery from wastewaters using microalgae-based approaches: A circular bioeconomy perspective. *Bioresource Technology* 302 (2020), 122817.
- [210] Nasser, A., Rasoul-Amini, S., Morowvat, M., and Ghasemi, Y. Single cell protein: Production and process. *American Journal of Food Technology* 6 (2011), 103–116.
- [211] National Aeronautics and Space Administration (NASA). National space exploration campaign report. Tech. rep., 2018.
- [212] National Research Council (US). *Committee on Acute Exposure Guideline Levels. Acute Exposure Guideline Levels for Selected Airborne Chemicals: Volume 6. Washington (DC): National Academies Press (US); 2008. 2. Ammonia Acute Exposure Guideline Levels. Available from: <https://www.ncbi.nlm.nih.gov/books/NBK207883/>.* 2008.
- [213] Nerenberg, R. The membrane-biofilm reactor (MBfR) as a counter-diffusional biofilm process. *Current Opinion in Biotechnology* 38 (2016), 131–136.
- [214] Nickerson, C. A., Ott, C. M., Wilson, J. W., Ramamurthy, R., and Pierson, D. L. Microbial responses to microgravity and other low-shear environments. *Microbiology and Molecular Biology Reviews* 68, 2 (2004), 345–361.
- [215] Oksanen, J., Blanchet, G., Friendly, M., Kindt, R., Legendre, P., McGlenn, D., Minchin, P., O'Hara, R., Simpson, G., Solymos, P., Stevens, H., Szoecs, E., and Wagner, H. vegan: Community Ecology Package. R package version 2.4-0. <https://CRAN.R-project.org/package=vegan>.
- [216] Oliveira, M. A. C. L. d., Monteiro, M. P. C., Robbs, P. G., and Leite, S. G. F. Growth and chemical composition of *Spirulina Maxima* and *Spirulina Platensis* biomass at different temperatures. *Aquaculture International* 7, 4 (1999), 261–275.
- [217] Olson, R. L., Gustan, E. A., and Vinopal, T. J. CELSS transportation analysis. *Advances in Space Research* 4, 12 (1984), 241–250.
- [218] O'Neal, J. A., and Boyer, T. H. Phosphate recovery using hybrid anion exchange: Applications to source-separated urine and combined wastewater streams. *Water Research* 47, 14 (2013), 5003–5017.
- [219] Oosterhuis, M., and van Loosdrecht, M. Nitrification of urine for H₂S control in pressure sewers. *Water Practice and Technology* 4, 3 (2009).
- [220] Oren, A. Bioenergetic aspects of halophilism. *Microbiology and Molecular Biology Reviews* 63, 2 (1999), 334–348.
- [221] Ortega-Calvo, J. J., Mazuelos, C., Hermosin, B., and Saiz-Jimenez, C. Chemical composition of *Spirulina* and eukaryotic algae food products marketed in Spain. *Journal of Applied Phycology* 5, 4 (1993), 425–435.
- [222] Pahore, M. M., Ushijima, K., Ito, R., and Funamizu, N. Fate of nitrogen during volume reduction of human urine using an on-site volume reduction system. *Environmental Technology* 33, 1-3 (2012), 229–235.
- [223] Parida, A. K., and Das, A. B. Salt tolerance and salinity effects on plants: a review. *Ecotoxicology and Environmental Safety* 60, 3 (2005), 324–349.
- [224] Pellicer-Nàcher, C., Sun, S., Lackner, S., Terada, A., Schreiber, F., Zhou, Q., and Smets, B. F. Sequential aeration of membrane-aerated biofilm reactors for high-rate autotrophic nitrogen removal: Experimental demonstration. *Environmental Science & Technology* 44, 19 (2010), 7628–7634.
- [225] Pikaar, I., de Vrieze, J., Rabaey, K., Herrero, M., Smith, P., and Verstraete, W. Carbon emission avoidance and capture by producing in-reactor microbial biomass based food, feed and slow release fertilizer: Potentials and limitations. *Science of the Total Environment* 644 (2018), 1525–1530.
- [226] Pikaar, I., Matassa, S., Rabaey, K., Bodirsky, B. L., Popp, A., Herrero, M., and Verstraete, W. Microbes and the next nitrogen revolution. *Environmental Science & Technology* 51, 13 (2017), 7297–7303.
- [227] Pillai, M. G., Simha, P., and Gugalia, A. Recovering urea from human urine by bio-sorption onto microwave activated carbonized coconut shells: Equilibrium, kinetics, optimization and field studies. *Journal of Environmental Chemical Engineering* 2, 1 (2014), 46–55.

- [228] Poulet, L., Fontaine, J. P., and Dussap, C. G. Plant's response to space environment: a comprehensive review including mechanistic modelling for future space gardeners. *Acta Botanica Gallica* 163, 3 (2016), 337–347.
- [229] Pronk, W., Biebow, M., and Boller, M. Electrodialysis for recovering salts from a urine solution containing micropollutants. *Environmental Science & Technology* 40, 7 (2006), 2414–2420.
- [230] Pronk, W., Biebow, M., and Boller, P. Treatment of source-separated urine by a combination of bipolar electrodialysis and a gas transfer membrane. *Water Science & Technology* 53, 3 (2006), 139–146.
- [231] Pronk, W., and Kone, D. Options for urine treatment in developing countries. *Desalination* 248, 1-3 (2009), 360–368.
- [232] Pronk, W., Palmquist, H., Biebow, M., and Boller, M. Nanofiltration for the separation of pharmaceuticals from nutrients in source-separated urine. *Water Research* 40, 7 (2006), 1405–1412.
- [233] Pronk, W., Zuleeg, S., Lienert, J., Escher, B., Koller, M., Berner, A., Koch, G., and Boller, M. Pilot experiments with electrodialysis and ozonation for the production of a fertiliser from urine. *Water Science & Technology* 56, 5 (2007), 219–227.
- [234] Putnam, D. *Composition and concentrative properties of human urine*. National Aeronautics and Space Administration; distributed by National Technical Information Service, Springfield, Va., 1971.
- [235] Quast, C., Pruesse, E., Yilmaz, P., Gerken, J., Schweer, T., Yarza, P., Peplies, J., and Glockner, F. O. The SILVA ribosomal RNA gene database project: improved data processing and web-based tools. *Nucleic Acids Research* 41, D1 (2013), D590–D596.
- [236] R Core Team. R: A language and environment for statistical computing. *R Foundation for Statistical Computing, Vienna, Austria*. <https://www.R-project.org/>. (2016).
- [237] Rabaey, K., Boon, N., Siciliano, S. D., Verhaege, M., and Verstraete, W. Biofuel cells select for microbial consortia that self-mediate electron transfer. *Applied and Environmental Microbiology* 70, 9 (2004), 5373–5382.
- [238] Rabaey, K., and Rozendal, R. A. Microbial electrosynthesis - revisiting the electrical route for microbial production. *Nature Reviews Microbiology* 8, 10 (2010), 706–716.
- [239] Ramette, A. Multivariate analyses in microbial ecology. *Fems Microbiology Ecology* 62, 2 (2007), 142–160.
- [240] Randall, D. G., Krahenbuhl, M., Köpping, I., Larsen, T. A., and Udert, K. M. A novel approach for stabilizing fresh urine by calcium hydroxide addition. *Water Research* 95 (2016), 361–369.
- [241] Randall, D. G., and Naidoo, V. Urine: The liquid gold of wastewater. *Journal of Environmental Chemical Engineering* 6, 2 (2018), 2627–2635.
- [242] Ray, H., Perreault, F., and Boyer, T. H. Urea recovery from fresh human urine by forward osmosis and membrane distillation (FO-MD). *Environmental Science: Water Research & Technology* 5, 11 (2019), 1993–2003.
- [243] Ray, H., Saetta, D., and Boyer, T. H. Characterization of urea hydrolysis in fresh human urine and inhibition by chemical addition. *Environmental Science-Water Research & Technology* 4, 1 (2018), 87–98.
- [244] Rector, T. J., Garland, J. L., and Starr, S. O. Dispersion characteristics of a rotating hollow fiber membrane bioreactor: Effects of module packing density and rotational frequency. *Journal of Membrane Science* 278, 1-2 (2006), 144–150.
- [245] Ren, H.-Y., Liu, B.-F., Kong, F., Zhao, L., Xie, G.-J., and Ren, N.-Q. Enhanced lipid accumulation of green microalga *Scenedesmus* sp. by metal ions and EDTA addition. *Bioresource Technology* 169 (2014), 763–767.
- [246] Richert, A., Gensch, R., Jönsson, H., Stenstrom, T. A., and Dagerskog, L. Practical guidance on the use of urine in crop production. stockholm environment institute, EcoSanRes Series, 2010-1. Tech. rep., 2010.
- [247] Richmond, A. *Handbook of Microalgal Culture: Biotechnology and Applied Phycology*. Blackwell Publishing Ltd, Oxford, UK, 2004.
- [248] Rittmann, B. E., Mayer, B., Westerhoff, P., and Edwards, M. Capturing the lost phosphorus. *Chemosphere* 84, 6 (2011), 846–853.
- [249] Rockström, J., Steffen, W., Noone, K., Persson, A., Chapin, F. S., Lambin, E. F., Lenton, T. M., Scheffer, M., Folke, C., Schellnhuber, H. J., Nykvist, B., de Wit, C. A., Hughes, T., van der Leeuw, S., Rodhe, H., Sörlin, S., Snyder, P. K., Costanza, R., Svedin, U., Falkenmark, M., Karlberg, L., Corell, R. W., Fabry, V. J., Hansen, J., Walker, B., Liverman, D., Richardson, K., Crutzen, P., and Foley, J. A. A safe operating space for humanity. *Nature* 461, 7263 (2009), 472–475.
- [250] Ronteltap, M., Maurer, M., and Gujer, W. The behaviour of pharmaceuticals and heavy metals during struvite precipitation in urine. *Water Research* 41, 9 (2007), 1859–1868.
- [251] Ronteltap, M., Maurer, M., Hausherr, R., and Gujer, W. Struvite precipitation from urine - influencing factors on particle size. *Water Research* 44, 6 (2010), 2038–2046.
- [252] Rose, C., Parker, A., Jefferson, B., and Cartmell, E. The characterization of feces and urine: A review of the literature to inform advanced treatment technology. *Critical Reviews in Environmental Science and Technology* 45, 17 (2015), 1827–1879.
- [253] Rzymiski, P., Budzulak, J., Niedzielski, P., Klimaszuk, P., Proch, J., Kozak, L., and Poniedzialek, B. Essential and toxic elements in commercial microalgal food supplements. *Journal of Applied Phycology* 31, 6 (2019), 3567–3579.

- [254] Saetta, D., and Boyer, T. H. Mimicking and inhibiting urea hydrolysis in nonwater urinals. *Environmental Science & Technology* 51, 23 (2017), 13850–13858.
- [255] Salama, E.-S., Kurade, M. B., Abou-Shanab, R. A. I., El-Dalatony, M. M., Yang, I.-S., Min, B., and Jeon, B.-H. Recent progress in microalgal biomass production coupled with wastewater treatment for biofuel generation. *Renewable and Sustainable Energy Reviews* 79 (2017), 1189–1211.
- [256] Salar-García, M. J., Ortiz-Martínez, V. M., Gajda, I., Greenman, J., Hernández-Fernández, F. J., and Ieropoulos, I. A. Electricity production from human urine in ceramic microbial fuel cells with alternative non-fluorinated polymer binders for cathode construction. *Separation and Purification Technology* 187 (2017), 436–442.
- [257] Sandau, E., Sandau, P., and Pulz, O. Heavy metal sorption by microalgae. *Acta Biotechnologica* 16, 4 (1996), 227–235.
- [258] Schloss, P. D., and Westcott, S. L. Assessing and improving methods used in operational taxonomic unit-based approaches for 16S rRNA gene sequence analysis. *Applied and Environmental Microbiology* 77, 10 (2011), 3219–3226.
- [259] Schloss, P. D., Westcott, S. L., Ryabin, T., Hall, J. R., Hartmann, M., Hollister, E. B., Lesniewski, R. A., Oakley, B. B., Parks, D. H., Robinson, C. J., Sahl, J. W., Stres, B., Thallinger, G. G., Van Horn, D. J., and Weber, C. F. Introducing mothur: Open-source, platform-independent, community-supported software for describing and comparing microbial communities. *Applied and Environmental Microbiology* 75, 23 (2009), 7537–7541.
- [260] Schwartzkopf, S. Electrochemical control of pH in a hydroponic nutrient solution. available at: <https://ntrs.nasa.gov/archive/nasa/casi.ntrs.nasa.gov/19860010447.pdf>. Tech. rep., 1986.
- [261] Sedlak, D. *Water 4.0 The Past, Present, and Future of the World's Most Vital Resource*. Yale University Press, 2014.
- [262] Senecal, J., and Vinneras, B. Urea stabilisation and concentration for urine-diverting dry toilets: Urine dehydration in ash. *Science of the Total Environment* 586 (2017), 650–657.
- [263] Simha, P., Senecal, J., Nordin, A., Lalander, C., and Vinneras, B. Alkaline dehydration of anion-exchanged human urine: Volume reduction, nutrient recovery and process optimisation. *Water Research* 142 (2018), 325–336.
- [264] SpaceX, 2020.
- [265] Spanoghe, J., Grunert, O., Wambacq, E., Sakarika, M., Papini, G., Alloul, A., Spiller, M., Derycke, V., Stragier, L., Verstraete, H., Fauconnier, K., Verstraete, W., Haesaert, G., and Vlaeminck, S. E. Storage, fertilization and cost properties highlight the potential of dried microbial biomass as organic fertilizer. *Microbial Biotechnology* n/a, n/a (2020).
- [266] Spinu, V. C., Langhans, R. W., and Albright, L. D. Electrochemical pH control in hydroponic systems. International Society for Horticultural Science (ISHS), Leuven, Belgium, pp. 275–282.
- [267] Spolaore, P., Joannis-Cassan, C., Duran, E., and Isambert, A. Commercial applications of microalgae. *Journal of Bioscience and Bioengineering* 101, 2 (2006), 87–96.
- [268] Sprott, G. D., and Patel, G. B. Ammonia toxicity in pure cultures of methanogenic bacteria. *Systematic and Applied Microbiology* 7, 2 (1986), 358–363.
- [269] Stamatakis, A. RAxML version 8: a tool for phylogenetic analysis and post-analysis of large phylogenies. *Bioinformatics* 30, 9 (2014), 1312–1313.
- [270] Steffen, W., Richardson, K., Rockström, J., Cornell, S. E., Fetzer, I., Bennett, E. M., Biggs, R., Carpenter, S. R., de Vries, W., de Wit, C. A., Folke, C., Gerten, D., Heinke, J., Mace, G. M., Persson, L. M., Ramanathan, V., Reyers, B., and Sörlin, S. Planetary boundaries: Guiding human development on a changing planet. *Science* 347, 6223 (2015), 1259855.
- [271] Strathmann, H. Electrodialysis, a mature technology with a multitude of new applications. *Desalination* 264, 3 (2010), 268–288.
- [272] Sudarno, U., Bathe, S., Winter, J., and Gallert, C. Nitrification in fixed-bed reactors treating saline wastewater. *Applied Microbiology and Biotechnology* 85, 6 (2010), 2017–2030.
- [273] Sui, Y., and Vlaeminck, S. E. Dunaliella microalgae for nutritional protein: An undervalued asset. *Trends in Biotechnology* 38, 1 (2020), 10–12.
- [274] Sun, F. Y., Dong, W. Y., Shao, M. F., Li, J., and Peng, L. Y. Stabilization of source-separated urine by biological nitrification process: treatment performance and nitrite accumulation. *Water Science and Technology* 66, 7 (2012), 1491–1497.
- [275] Sun, F. Y., Yang, Y. J., Dong, W. Y., and Li, J. Granulation of nitrifying bacteria in a sequencing batch reactor for biological stabilisation of source-separated urine. *Applied Biochemistry and Biotechnology* 166, 8 (2012), 2114–2126.
- [276] Sutton, M. A., and Bleeker, A. The shape of nitrogen to come. *Nature* 494, 7438 (2013), 435–437.
- [277] Tamponnet, C., and Savage, C. Closed ecological systems. *Journal of Biological Education* 28, 3 (1994), 167–174.
- [278] Tansel, B. Significance of thermodynamic and physical characteristics on permeation of ions during membrane separation: Hydrated radius, hydration free energy and viscous effects. *Separation and Purification Technology* 86 (2012), 119–126.

- [279] Tansel, B., Sager, J., Rector, T., Garland, J., Strayer, R. F., Levine, L., Roberts, M., Hummerick, M., and Bauer, J. Integrated evaluation of a sequential membrane filtration system for recovery of bioreactor effluent during long space missions. *Journal of Membrane Science* 255, 1 (2005), 117–124.
- [280] Tao, R., Bair, R., Lakaniemi, A.-M., van Hullebusch, E. D., and Rintala, J. A. Use of factorial experimental design to study the effects of iron and sulfur on growth of *Scenedesmus acuminatus* with different nitrogen sources. *Journal of Applied Phycology* 32, 1 (2020), 221–231.
- [281] Tarpeh, W. A., Udert, K. M., and Nelson, K. L. Comparing ion exchange adsorbents for nitrogen recovery from source-separated urine. *Environmental Science & Technology* 51, 4 (2017), 2373–2381.
- [282] Tellier, L. *Urban World History: An Economic and Geographical Perspective*. Presses de l'Université du Québec, 2009.
- [283] Tice, R. C., and Kim, Y. Energy efficient reconcentration of diluted human urine using ion exchange membranes in bioelectrochemical systems. *Water Research* 64 (2014), 61–72.
- [284] Tuantet, K., Janssen, M., Temmink, H., Zeeman, G., Wijffels, R. H., and Buisman, C. J. N. Microalgae growth on concentrated human urine. *Journal of Applied Phycology* 26, 1 (2014), 287–297.
- [285] Tuantet, K., Temmink, H., Zeeman, G., Janssen, M., Wijffels, R. H., and Buisman, C. J. N. Nutrient removal and microalgal biomass production on urine in a short light-path photobioreactor. *Water Research* 55 (2014), 162–174.
- [286] Tuantet, K., Temmink, H., Zeeman, G., Wijffels, R. H., Buisman, C. J. N., and Janssen, M. Optimization of algae production on urine. *Algal Research* 44 (2019), 101667.
- [287] Tun, L. L., Jeong, D., Jeong, S., Cho, K., Lee, S., and Bae, H. Dewatering of source-separated human urine for nitrogen recovery by membrane distillation. *Journal of Membrane Science* 512 (2016), 13–20.
- [288] Udert, K., Larsen, T., and Gujer, W. Biologically induced precipitation in urine-collecting systems. *Water Science and Technology: Water Supply* 3, 3 (2003), 71–78.
- [289] Udert, K. M., Buckley, C. A., Wachter, M., McArdell, C. S., Kohn, T., Strande, L., Zolig, H., Fumasoli, A., Oberson, A., and Etter, B. Technologies for the treatment of source-separated urine in the eThekweni municipality. *Water Sa* 41, 2 (2015), 212–221.
- [290] Udert, K. M., Etter, B., and Gounden, T. Promoting sanitation in South Africa through nutrient recovery from urine. *Gaia-Ecological Perspectives for Science and Society* 25, 3 (2016), 194–196.
- [291] Udert, K. M., Fux, C., Munster, M., Larsen, T. A., Siegrist, H., and Gujer, W. Nitrification and autotrophic denitrification of source-separated urine. *Water Science and Technology* 48, 1 (2003), 119–130.
- [292] Udert, K. M., Larsen, T. A., Biebow, M., and Gujer, W. Urea hydrolysis and precipitation dynamics in a urine-collecting system. *Water Research* 37, 11 (2003), 2571–2582.
- [293] Udert, K. M., Larsen, T. A., and Gujer, W. Estimating the precipitation potential in urine-collecting systems. *Water Research* 37, 11 (2003), 2667–2677.
- [294] Udert, K. M., Larsen, T. A., and Gujer, W. Fate of major compounds in source-separated urine. *Water Science & Technology* 54, 11-12 (2006), 413–420.
- [295] Udert, K. M., and Wächter, M. Complete nutrient recovery from source-separated urine by nitrification and distillation. *Water Research* 46, 2 (2012), 453–464.
- [296] UNICEF and World Health Organization (WHO). Progress on household drinking water, sanitation and hygiene 2000-2017: Special focus on inequalities. Tech. rep., 2019.
- [297] United Nations - Department of Economic and Social Affairs - Population Division. World population prospects 2019. highlights. Tech. rep., 2019.
- [298] Van Drecht, G., Bouwman, A. F., Harrison, J., and Knoop, J. M. Global nitrogen and phosphate in urban wastewater for the period 1970 to 2050. *Global Biogeochemical Cycles* 23, 4 (2009).
- [299] Vandenbrink, J. P., and Kiss, J. Z. Space, the final frontier: A critical review of recent experiments performed in microgravity. *Plant Science* 243 (2016), 115–119.
- [300] Verstraete, W., Clauwaert, P., and Vlaeminck, S. E. Used water and nutrients: Recovery perspectives in a 'panta rhei' context. *Bioresource Technology* 215 (2016), 199–208.
- [301] Vinnerås, B., Palmquist, H., Balmér, P., and Jönsson, H. The characteristics of household wastewater and biodegradable solid waste - a proposal for new Swedish design values. *Urban Water Journal* 3, 1 (2006), 3–11.
- [302] Vlaamse Milieumaatschappij (VMM). Riolerings- en zuiveringsgraden. <https://www.vmm.be/data/riolerings-en-zuiveringsgraden> (accessed on 10/04/2020), 2020.
- [303] Volpin, F., Chekli, L., Phuntsho, S., Ghaffour, N., Vrouwenvelder, J. S., and Shon, H. K. Optimisation of a forward osmosis and membrane distillation hybrid system for the treatment of source-separated urine. *Separation and Purification Technology* 212 (2019), 368–375.
- [304] von Münch, E., Winker, M., and GIZ, S. s. e. Technology review of urine diversion components. overview of urine diversion components such as waterless urinals, urine diversion toilets, urine storage and reuse systems. Tech. rep., 2011.
- [305] VUNA. http://www.vuna.ch/aurin/index_en.html, 2020.
- [306] Walter, X. A., Merino-Jiménez, I., Greenman, J., and Ieropoulos, I. PEE POWER urinal II - urinal scale-up with microbial fuel cell scale-down for improved lighting. *Journal of Power Sources* 392 (2018), 150–158.

- [307] Walther, I., van der Schoot, B. H., Jeanneret, S., Arquint, P., de Rooij, N. F., Gass, V., Bechler, B., Lorenzi, G., and Cogoli, A. Development of a miniature bioreactor for continuous culture in a space laboratory. *Journal of Biotechnology* 38, 1 (1994), 21–32.
- [308] Wang, Q., Garrity, G. M., Tiedje, J. M., and Cole, J. R. Naive bayesian classifier for rapid assignment of rRNA sequences into the new bacterial taxonomy. *Applied and Environmental Microbiology* 73, 16 (2007), 5261–5267.
- [309] Wang, X., Cai, Y., Sun, Y., Knight, R., and Mai, V. Secondary structure information does not improve OTU assignment for partial 16S rRNA sequences. *Isme j* 6, 7 (2012), 1277–80.
- [310] Wheeler, R. M. Agriculture for space: People and places paving the way. 14.
- [311] Whitsen, P. A., Pietrzyk, R. A., and Pak, C. Y. Renal stone risk assessment during space shuttle flights. *The Journal of Urology* 158, 6 (1997), 2305–10.
- [312] Wieland, P. Designing for human presence in space: An introduction to environmental control and life support systems. Tech. rep., NASA, 1994.
- [313] Wilsenach, J., and van Loosdrecht, M. Impact of separate urine collection on wastewater treatment systems. *Water Science & Technology* 48, 1 (2003), 103–110.
- [314] Wilsenach, J. A., Maurer, M., Larsen, T. A., and van Loosdrecht, M. C. M. From waste treatment to integrated resource management. *Water Science & Technology* 48, 1 (2003), 1–9.
- [315] Wilsenach, J. A., Schuurbijs, C. A. H., and van Loosdrecht, M. C. M. Phosphate and potassium recovery from source separated urine through struvite precipitation. *Water Research* 41, 2 (2007), 458–466.
- [316] Wohlsager, S., Clemens, J., Nguyet, P. T., Rechenburg, A., and Arnold, U. Urine - a valuable fertilizer with low risk after storage in the tropics. *Water Environ Res* 82, 9 (2010), 840–847.
- [317] Wolff, S. A., Coelho, L. H., Karoliussen, I., and Jost, A. I. Effects of the extraterrestrial environment on plants: Recommendations for future space experiments for the MELISSA higher plant compartment. *Life (Basel)* 4, 2 (2014), 189–204.
- [318] World Health Organization (WHO). Guidelines for the safe use of wastewater, excreta and greywater. Tech. rep., 2006.
- [319] World Health Organization (WHO). Sanitation. <https://www.who.int/news-room/fact-sheets/detail/sanitation> (Access date: 26/03/2020), 2019.
- [320] Xiang, C., Papadantonakis, K. M., and Lewis, N. S. Principles and implementations of electrolysis systems for water splitting. *Materials Horizons* 3, 3 (2016), 169–173.
- [321] Xing, D., Cheng, S., Logan, B. E., and Regan, J. M. Isolation of the exoelectrogenic denitrifying bacterium *Comamonas denitrificans* based on dilution to extinction. *Applied Microbial and Cell Physiology* 85, 5 (2010), 1575–1587.
- [322] Xu, K., Qu, D., Zheng, M., Guo, X., and Wang, C. Water reduction and nutrient reconcentration of hydrolyzed urine via direct-contact membrane distillation: Ammonia loss and its control. *Journal of Environmental Engineering* 145, 3 (2019), 04018144.
- [323] Yang, C., Liu, H., Li, M., Yu, C., and Yu, G. Treating urine by *Spirulina platensis*. *Acta Astronautica* 63, 7 (2008), 1049–1054.
- [324] Yang, L., Li, H., Liu, T., Zhong, Y., Ji, C., Lu, Q., Fan, L., Li, J., Leng, L., Li, K., and Zhou, W. Microalgae biotechnology as an attempt for bioregenerative life support systems: problems and prospects. *Journal of Chemical Technology & Biotechnology* 94, 10 (2019), 3039–3048.
- [325] Yenigün, O., and Demirel, B. Ammonia inhibition in anaerobic digestion: A review. *Process Biochemistry* 48, 5 (2013), 901–911.
- [326] You, J., Greenman, J., Melhuish, C., and Ieropoulos, I. Electricity generation and struvite recovery from human urine using microbial fuel cells. *Journal of Chemical Technology & Biotechnology* 91, 3 (2016), 647–654.
- [327] Zamora, P., Georgieva, T., Ter Heijne, A., Sleutels, T. H. J. A., Jeremiasse, A. W., Saakes, M., Buisman, C. J. N., and Kuntke, P. Ammonia recovery from urine in a scaled-up microbial electrolysis cell. *Journal of Power Sources* 356 (2017), 491–499.
- [328] Zang, G. L., Sheng, G. P., Li, W. W., Tong, Z. H., Zeng, R. J., Shi, C., and Yu, H. Q. Nutrient removal and energy production in a urine treatment process using magnesium ammonium phosphate precipitation and a microbial fuel cell technique. *Physical Chemistry Chemical Physics* 14, 6 (2012), 1978–1984.
- [329] Zarrouk, C. *Contribution à l'étude d'une cyanophycée. Influence de divers facteurs physiques et chimiques sur la croissance et la photosynthèse de Spirulina maxima Geiliter*. PhD thesis, Université de Paris, Paris, France. 1966.
- [330] Zaslavski, I., Shemer, H., Hasson, D., and Semiat, R. Electrochemical CaCO₃ scale removal with a bipolar membrane system. *Journal of Membrane Science* 445 (2013), 88–95.
- [331] Zhang, J., Giannis, A., Chang, V. W., Ng, B. J., and Wang, J. Y. Adaptation of urine source separation in tropical cities: Process optimization and odor mitigation. *Journal of the Air and Waste Management Association* 63, 4 (2013), 472–481.
- [332] Zhang, J., She, Q., Chang, V. W., Tang, C. Y., and Webster, R. D. Mining nutrients (N, K, P) from urban source-separated urine by forward osmosis dewatering. *Environmental Science & Technology* 48, 6 (2014), 3386–3894.

- [333] Zhang, Y., Li, Z. F., Zhao, Y., Chen, S. L., and Mahmood, I. B. Stabilization of source-separated human urine by chemical oxidation. *Water Science & Technology* 67, 9 (2013), 1901–1907.
- [334] Zhao, J., Zhu, L., Fan, C., Wu, Y., and Xiang, S. Structure and function of urea amidolyase. *Bioscience reports* 38, 1 (2018), BSR20171617.
- [335] Zheng, H. Q., Han, F., and Le, J. Higher plants in space: Microgravity perception, response, and adaptation. *Microgravity Science and Technology* 27, 6 (2015), 377–386.
- [336] Zhou, X. Q., Li, Y. J., Li, Z. F., Xi, Y., Uddin, S. M. N., and Zhang, Y. Investigation on microbial inactivation and urea decomposition in human urine during thermal storage. *Journal of Water Sanitation and Hygiene for Development* 7, 3 (2017), 378–386.

Copyright attribution

- Figure 1.1: Image has been released publicly from ISECG. Permission to reprint this image was obtained from ISECG ESA on 01/06/2020.
- Figure 1.4: This image is free to use in publications, scientific or otherwise, describing the planetary boundaries concept. Credit: J. Lokrantz/Azote based on Steffen et al. 2015, <https://www.stockholmresilience.org/research/planetary-boundaries.html>
- Figure 1.6: From Larsen et al. (2016) [161]. Reprinted with permission from AAAS.
- Figure 1.7: As co-author of the publication, permission to reprint this image is not required.
- Figure 1.9: Image courtesy NASA Glenn Research Center (no copyright).
- Figure 1.10: Credit: Madigan, Michael T., Martinko, John M., Dunlap, Paul V., Clark, David P., Brock Biology of Microorganisms: International Edition, 12th ©2009. Reprinted by permission of Pearson Education, Inc., New York, New York.

Curriculum Vitae

Personal information

Name Jolien De Paepe
Date and place of birth 24th of February 1993, Ghent, Belgium
Nationality Belgian
Email Jolien.DePaepe@UGent.be
joliendepaepe@hotmail.com
Phone +32 499 10 46 98
Affiliation Ghent University - Faculty of Bioscience Engineering
Center for Microbial Ecology and Technology
(CMET, www.cmet.ugent.be)
Universitat Autònoma de Barcelona
MELiSSA Pilot Plant - Claude-Chipaux Laboratory
Workplace address Coupure Links 653, 9000 Gent, Belgium

Education

2016 - 2020 **PhD Candidate in Bioscience engineering**
Ghent University
PhD Candidate in Biotechnology
Universitat Autònoma de Barcelona
Supervisors: Prof. dr. ir. Korneel Rabaey
Prof. dr. ir. Siegfried E. Vlaeminck
Dr. ir. Peter Clauwaert
Prof. dr. Francesc Gòdia Casablanca
PhD thesis: Urine recycling technologies for a circular future
within and beyond terrestrial boundaries
Scholarship: POMP I program MELiSSA Foundation

2014 - 2016 **Master of Science in Bioscience Engineering,
Environmental technology**
Ghent University. Graduated with greatest distinction.
Master thesis: Water recycling in Space: from urine to

- August-September 2014 hygienic water.
Internship Avecom NV
Subject: Resource recovery from wastewater:
immobilisation of nitrogen.
- 2011 - 2014 **Bachelor of Science in Bioscience Engineering,
Environmental Technology**
Ghent University. Graduated with greatest distinction.
Bachelor thesis: Socio-economische effecten en milieu-impact
van genetisch gewijzigde *Phytophthora*-resistente aardappelen

International peer reviewed publications (A1)

Jolien De Paepe, Laurens De Pryck, Arne R.D. Verliefde, Korneel Rabaey, and Peter Clauwaert. Electrochemically induced precipitation enables fresh urine stabilization and facilitates source separation. *Environmental Science & Technology*, 54 (2020), 3618-3627

Peter Clauwaert*, **Jolien De Paepe***, Fu Jiang, Bernabé Alonso-Fariñas, Eleni Vaiopoulou, Arne Verliefde, and Korneel Rabaey. Electrochemical tap water softening: A zero chemical input approach. *Water Research*, 169 (2020). * *equally contributed*

Marlies E.R. Christiaens, **Jolien De Paepe**, Chiara Ilgrande, Jo De Vrieze, Justyna Barys, Pieter Teirlinck, Ken Meerbergen, Bart Lieven, Nico Boon, Peter Clauwaert, and Siegfried E. Vlaeminck. Urine nitrification with a synthetic microbial community. *Systematic and Applied Microbiology* 42 (2019), 126021.

Jolien De Paepe, Ralph E.F. Lindeboom, Marjolein Vanoppen, Kim De Paepe, Dries Demey, Wout Coessens, Brigitte Lamaze, Arne Verliefde, Peter Clauwaert, and Siegfried E. Vlaeminck. Refinery and concentration of nutrients from urine with electrodialysis enabled by upstream precipitation and nitrification. *Water Research*, 144 (2018), 76-86.

Peter Clauwaert, Maarten Muys, Abbas Alloul, **Jolien De Paepe**, Amanda Luther, Xiaoyan Sun, Chiara Ilgrande, Marlies E.R. Christiaens, Xiaona Hu, Dongdong Zhang, Ralph E.F. Lindeboom, Benedikt Sas, Korneel Rabaey, Nico Boon, Frederik Ronsse, Danny Geelen, and Siegfried E. Vlaeminck. Nitrogen cycling in Bio-regenerative Life Support Systems: Challenges for waste refinery and food production processes. *Progress in aerospace sciences*, 91 (2017), 87-98.

Publications in preparation or under review

Jolien De Paepe, Kim De Paepe, Francesc Gòdia, Korneel Rabaey, Siegfried E. Vlaeminck and Peter Clauwaert. Bio-electrochemical COD removal for energy-efficient, maximum and robust nitrogen recovery from urine through membrane aerated nitrification. Under review (*Water Research*)

Ralph E.F., Lindeboom, **Jolien De Paepe**, Marjolein Vanoppen, Bernabé Alonso-Fariñas, Wout Coessens, Abbas Alloul, Marlies E.R. Christiaens, Chris Dotremont, Herman Beckers, Brigitte Lamaze, Dries Demey, Peter Clauwaert, Arne R.D. Verliefde, and Siegfried E. Vlaeminck. A five-stage treatment train for water recovery from urine and shower water for long-term human Space missions. Under review (*Desalination*)

Jolien De Paepe, Peter Clauwaert, Maria Celeste Gritti, Ramon Ganigué, Siegfried E. Vlaeminck, and Korneel Rabaey. Electrochemical in-situ pH control enables chemical-free full urine nitrification with concomitant nitrate extraction. (in preparation)

Jolien De Paepe, David Garcia Gragera, Carolina Arnau Jimenez, Korneel Rabaey, Siegfried E. Vlaeminck, and Francesc Gòdia. Limited supplementation maximizes nitrogen recovery from nitrified urine through continuous cultivation of microalgae. (in preparation)

Participation at (inter)national conferences and symposia

Oral presentations

Jolien De Paepe, Maria Celeste Gritti, Kim De Paepe, Francesc Gòdia, Korneel Rabaey, Siegfried E. Vlaeminck, and Peter Clauwaert. Combining (bio)electrochemical processes and nitrification for urine recycling in Space. Will be presented at the MELiSSA Conference (Ghent, November 2020)

Jolien De Paepe, Kim De Paepe, Francesc Gòdia, Korneel Rabaey, Siegfried E. Vlaeminck, and Peter Clauwaert. Membrane aerated nitrification preceded by bio-anodic COD removal yields maximum nitrogen recovery from urine. Will be presented at IWA Nutrient Removal and Recovery Conference (virtual conference, September 2020)

Jolien De Paepe, Ralph E.F. Lindeboom, Marjolein Vanoppen, Kim De Paepe, Wout Coessens, Dries Demey, Brigitte Lamaze, Arne Verliefde, Peter Clauwaert,

and Siegfried E. Vlaeminck. Breadboard verification of a novel technology train to recycle nutrients and water from urine for human spaceflight. Presented at: 42nd COSPAR Scientific Assembly (Pasadena, US, July 2018)

Peter Clauwaert, Maarten Muys, Abbas Alloul, **Jolien De Paepe**, Amanda Luther, Xiaoyan Sun, Chiara Ilgrande, Marlies E.R. Christiaens, Xiaona Hu, Dongdong Zhang, Ralph E.F. Lindeboom, Benedikt Sas, Korneel Rabaey, Nico Boon, Frederik Ronsse, Danny Geelen, and Siegfried E. Vlaeminck. Nitrogen cycling in Bio-regenerative Life Support Systems: Challenges for waste refinery and food production processes. Presented at: 42nd COSPAR Scientific Assembly (Pasadena, US, July 2018)

Siegfried E. Vlaeminck*, Ralph E.F. Lindeboom*, **Jolien De Paepe***, Dries Demey, Marjolein Vanoppen, Bernabé Alonso Fariñas, Wout Coessens, Marlies E.R. Christiaens, Chiara Ilgrande, Kim De Paepe, Benedikt Sas, Abbas Alloul, Chris Dotremont, Herman Beckers et al. Water cycling for regenerative life support systems: MELiSSA's development of an integrated biophysicochemical approach. Presented at: 42nd COSPAR Scientific Assembly (Pasadena, US, July 2018)
**equally contributed*

Jolien De Paepe, Siegfried E. Vlaeminck, Korneel Rabaey, Francesc Gòdia, and Peter Clauwaert. Bio-electrochemical pre-treatment and membrane aeration to intensify full nitrogen recovery for Spaceflight urine nitrification. Presented at: 1st Joint AgroSpace-MELiSSA workshop (Rome, Italy, May 2018)

Chiara Ilgrande, Marlies E.R. Christiaens, **Jolien De Paepe**, Ralph E.F. Lindeboom, Felice Mastroleo, Tom Defoirdt, Benedikt Sas, Nico Boon, Natalie Leys, Siegfried E. Vlaeminck, and Peter Clauwaert. Nitrogen recovery from urine in Space: a case for nitrification. Presented at: 1st Joint AgroSpace-MELiSSA workshop (Rome, Italy, May 2018)

Chiara Ilgrande, Ralph E.F. Lindeboom, Felice Mastroleo, Marlies E.R. Christiaens, Xiaoyan Sun, Tom Defoirdt, **Jolien De Paepe**, Benedikt Sas, Nico Boon, Siegfried E. Vlaeminck, Natalie Leys, and Peter Clauwaert. Nitrogen recovery from urine in Space: a case for nitrification. Presented at: 51st ESLAB Symposium: Extreme Habitable Worlds (Noordwijk, The Netherlands, December 6th, 2017)

Jolien De Paepe*, Ralph E.F., Lindeboom*, Marjolein Vanoppen, Bernabé Alonso Fariñas, Wout Coessens, Abbas Alloul, Marlies E.R. Christiaens, Chris Dotremont, Herman Beckers, Brigitte Lamaze, Dries Demey, Korneel Rabaey, Peter Clauwaert, Arne R.D. Verliefe and Siegfried E. Vlaeminck. Water Treatment Unit Breadboard: Ground test facility for the recycling of urine and shower water for one astronaut. Presented at: 5th Benelux Young Water Professionals Regional Conference (Ghent, Belgium, July 6th, 2017) **equally contributed*

Poster Presentations

Jolien De Paepe, Ralph E.F., Lindeboom, Marjolein Vanoppen, Bernabé Alonso Fariñas, Wout Coessens, Laurens De Pryck, Dries Demey, Chris Dotremont, Herman Beckers, Brigitte Lamaze, Peter Clauwaert, Arne R.D. Verliefde, and Siegfried E., Vlaeminck. An integrated bio-physicochemical water recovery system for future Space missions. MELiSSA mini-symposium (Antwerp, Belgium, March 30th, 2017)

Symposium Presentations

Jolien De Paepe, Siegfried E. Vlaeminck, Francesc Gòdia, Korneel Rabaey, and Peter Clauwaert. Combining (bio)electrochemical processes and nitrification for urine recycling in Space. Symposium Innovative routes for recovery of nitrogen (Ghent, Belgium, December 3rd, 2018)

Teaching and scientific communication

Supervising practical exercises for the course 'Microbieel Ecologische Processen' (Prof. Nico Boon) (2017-2018)

Tutor of 5 master and 2 bachelor students (2016-2020)

Contribution for the 'Dag Van De Wetenschap' (Ghent, November, 2018)

Participation in IGLUNA 2020 - A Space Habitat - Remote operations (Swiss Space Center), virtual field campaign, July 2020

Awards

Odissea-prize 2016. Belgian Senate, March 7th, 2016

Master thesis competition winner, awarded by EITRawMaterials, iSUP conference 2016, Antwerp

ArcelorMittal Indaver Thesisprijs 2015-2016, Environmental Science and Technology

First price in the contest for scientific presentations by the journal of 'Natuur en Wetenschap' (May 11th, 2011). Thesis: Bijensterfte, wat zijn de oorzaken en mogelijke oplossingen voor de recente bijensterfte?, (Possible causes and consequences of the bee Colony Collapse Disorder)

